INTERNATIONAL JOURNAL OF ENGLISH: LITERATURE, LANGUAGE & SKILLS

Volume 10 Issue 2 / July 2021
ISSN 2278-0742 / www.ijells.com

~Contents~

Cover Page Image "Monsoon 2021"
Racharla Bhargava Ram, +91-9581953939
#maortmsy7

A Study of Hindu Hegemony, Spiritualism and Dalits in Narendra Jadhav's *Outcaste: A Memoir*

Ghansham S Baviskar

Abstract

Conservative religions and the spurious religious books trap Dalits in the Varna system. The religious exclusion and marginal space lead Dalits to explore alternative identities. The untouchables in India were always in search of new religions at various historical junctures as there was no scope for growth and emancipation in Hindu society. Buddhism and Jainism in ancient India, Islam in the medieval period and Christianity in the modern era attracted Dalits. Dr BR Ambedkar's liberation movement turned Dalits to Buddhism for their emancipation. This paper is an attempt to present the struggle of Dalits who have been protesting against the Varna system for their natural rights.

Key words: Caste, Hegemony, Atrocities, Rights, Identity, Secular, Humanity

Introduction

Narendra Jadhav, a renowned Marathi writer projects Dalit life and struggle in his works. In *Outcaste: A Memoir*, he puts forth the challenges before the Dalit liberation movement and highlights the need to change the present conditions to empower Dalits in India. His protagonists thus fight the Varna system and embrace Buddhism to instil the basic human values freedom, fraternity, equality and social justice which were uprooted by the fundamentalists for centuries.

Suppression of Dalits and their Conversion

It is a universal truth that the Varna system still exists in India and it is difficult to change the mindset of the traditionalists and fanatics as it has been sown and perpetuated in the barren minds of the people. As a result of this, the followers of Manu have succeeded in keeping their hold over the minds of people through Gods and scriptures to maintain hegemony and their place and position in society. Though, all the people are equal before law in India as per the Indian Constitution, the caste system has been deeply rooted in people and therefore, they do not want the social change and oppose any such change in practical. Suppression of Dalits and the denial of their natural rights in the Varna system turn Dalits to explore the alternative religious identities, so that they can live freely as human beings and not as lesser human beings.

By laws of the Indian Constitution, any person can profess and practice any religion he or she selects of likes to follow in India. The right to life and the space to growth which was denied to them in Hindu religion, they exercise in Buddhism. But the questions which remain unanswered are- why the conversion was required in past? Why is it required today and why it will be required in future? Why do people convert to other religions? Do people blindly convert to other religions? What is Parent Religion? Does one know the history of his or her parent Religion? Why does a Hindu Dalit call Hinduism as his or her parent religion? And the last, do the historically oppressed understand how they have been quarantined in the Varna system? Moreover, why does he or she want to remain in the Varna system? If any studious person goes through the religious history of the nation, he shall find the people converting themselves to other religions. In Muslim Regime, the people feared the rule and embraced Muslim Religion while some other wanted an escape from the tortures of the

exclusion enforced upon them. In British rule, thousands of the people coming from the suppressed castes embraced Christianity for their emancipation. Did these conversions really bring change in their life? Even in the 21st century, people have been embracing Buddhism, the religion that attracted those most. Did the conversion in Muslim, Christian, and the Buddhism make any difference to the lives of the people who were slaves in the Varna system? The answer is, when the people are deprived of their natural rights, they protest against the orthodoxy and fanaticism and turn to the alternative religions. Are there really ideal conditions for growth and rational ideas?

In Muslim and Christian religions, there is the idea of salvation i.e. *moksha* which is attained through the mediator who is no other than the *Preshit* or God. Muslim and Christian religions project the idea of heavenly world and salvation from the pains of rebirth. In Hindu religion, salvation can be sought through one's *karma* in the caste, he or she is born into. How does one should obtain this salvation in Hinduism? The answer to this question is, 'accepts the lost in the caste system and carry the work allotted by the Varna system, is a way to salvation. Buddhism does not claim any salvation through the mediator or *preshit* and does not create the imaginative heavenly world with the idea of salvation of deliverance. Buddhism has its base in reason which is merely the other name for science. Still the spiritual mysticism in Hinduism keeps its firm grip or hold over the mental psyche of the people and they are not ready to lose the firm faith or belief that they had in its spirituality. In "The Buddha and His Dhamma", Dr. Ambedkar explores Hindu spiritualism and Mysticism as:

1. Belief in the infallibility of the Vedas;
2. Belief in Moksha or Salvation of the soul, i.e., its ceasing to be born again;
3. Belief in the efficacy of rites, ceremonies and sacrifices as means of obtaining moksha;
4. Belief in Chaturvarna as the ideal for social organization;
5. Belief in Iswara as the creator of and in Brahmana as the principle underlying the universe.
6. Belief in Atmana, or the soul.
7. Belief in Karma, i.e., the determination of man's position in present life by deeds done by him in his past life." (103)

Belief in all the above eight is Hindu Spiritualism and Mysticism which is above science. Therefore, it is the trained mindset of the fundamentalists opposes science in the name of God and the Holy Scriptures. In other way, they have been trying to project the same as science which one can term 'pseudo-science'.

Conversion to Buddhism in Narendra Jadhav's *Outcaste: A Memoir,* a Way to Protest and Claim Natural Rights:

In Outcaste: A Memoir, Damu, the protagonist is very much influenced by the ideology of Dr. B. R. Ambedkar and hence he converts himself and his wife to Buddhism and registers his protest against the Varna system. But while he adopts this change, he does nowhere think if his wife is ready for this conversion. His wife, Sonu is not ready for this conversion but he does so without taking her consent. She resists the move and questions the change of the religion. D. Murli Manohar in his paper, "Who is 'Brahman', not Brahmana/Brahmin? A Personal Narrative of Mala Dasari" states, "She argues that how can she give up her Gods and worship new Gods.'. He further questions: Is change of religion like change of clothes we wear? It means in D. Manohar Murali's words: Damu blindly converts himself and makes his wife to convert. Thus, Murali's mysticism is in line with Gandhi's mysticism. According

to D. Murli, Sonu's conversion to Buddhism is blind act as she, he thinks, is forced to do so. However, the fact is something different that D. Murli is ignorant about or trying to overlook it. In fact, Damu is inspired by Dr. B. R. Ambedkar's liberation movement which demands for freedom, fraternity, equality and social justice in society. He is aware of his suppression and oppression and hence decides to embrace Buddhism to find space for growth and emancipation. On the other hand, Sonu is unaware of her exploitation as a Dalit and again a woman. It is this ignorance which turns her to resist her husband and his decision to embrace Buddhism." Her words, "I would never stop worshipping my Hindu Gods" prove the fact that she has been enslaved in Hindu society and therefore not ready to accept Buddhist principles wholly. (Jadhav, 192) Here Sonu's resistance to conversion is just an argument between the husband and wife; it is an attempt to prove her individuality that she too is a human being and hence she cannot be forced to accept the conversion. She asserts her individuality and denies acting puppet or agent to it. Therefore, a researcher must examine her argument with her husband from the feminist point of view as well and not from the spectacle of an upper caste historian taking undue advantage of the ignorance of women like Sonu. Here the argument is a strong attempt on her side to assert the point she is raising that she too is a human being and is equal to husband and therefore, cannot be forced. So, D. Murli's statement; Damu's and his wife's conversion to Buddhism is blindly done act proves to be wrong.

Damu's wife's act of continuing worship Hindu Gods at the same time embracing Buddhism seems to be her complete ignorance. Therefore, it is true that the Dalits still follow D. Murli's parent religion which is full of mysticism. Such class of Dalits still exists in India and it is a great challenge before all the Ambedkarite movements, as they have to tackle with the trained psyche of the Hindu Dalits, shaped by Hindu Spiritualism, which is nothing but the medium to make Dalits slaves in the Varna system. Thus, Damu's protest against it is a way to free oneself from Manu's laws which deny natural rights to Dalits.

What is a Parent Religion? A Counter Argument to D. Murli's Staunch on Buddhism as Outside Religion:

In the article, "Who is 'Brahman', not Brahmana /Brahmin?" D Murli writes: "By reading all these (things on conversion) and listening to speeches on Dalits converting into Buddhism following by Ambedkar's logic, I was put in a conflict. However, those conflicts and storms vanished with my strong spirituality in Hinduism." (5) Thus, he concludes that the "conversion is not a solution to Dalits." He stresses, "In fact, it makes them outsiders whether to go to Christianity or Buddhism or Islam or Sikhism. Why should the Dalits move from their parent religion to outside religion? (8) Here, D Murli's knowledge about Buddhism is vague. Buddhism does deny the myth or idea of God, nor does it make any claim of Moksha or salvation through the mediator, it follows the Reason i.e. the scientific truth. Secondly, his question: "Is change of Religion like the change of clothes we wear?" makes it clear that the Clothes and religion are two entirely different things. D Murli seems to be ignoring the very fact that the clothes, he is talking about even were denied to the untouchables and they had to live in utter poverty and the world of ignorance. Untouchability even followed to the shop when they were going to buy the new clothes.

Maybe, the stalwart like D Murli is intentionally overlooking the facts and propagating the Varna system and its mysticism which denies natural rights to Dalits in this country. Thirdly, his conclusion, 'Conversion is not a solution for the dalits' is a message for the Dalits, if he might have stated Conversion is not a solution for him, then it was quite alright but he is not talking about an individual here but giving the message to Dalits. D Murli Manohar regards Hindu religion, as the "Parent religion" and he puts Buddhism in the list of "outside religion". (8) It seems here that his knowledge of religions is vague or he does not

seem to acknowledge the fact that Buddha founded Buddhism in India and emancipated all the suppressed and oppressed people who were denied equal rights. It is Murli's faith in Hindu Spiritualism and Mysticism thus, forces him to change the parent religion and call it outside. Even the Ambedkar logic, he is talking about is not the simple logic, but the ocean of knowledge, the light of sun that erased the darkness of Hindu spirituality in the lives of Untouchables. The poem, "When Darkness Encountered the Sun" cited by Rangrao Bhongle, in the article, "A Semiotic Study of Dalit Poetry in Marathi" puts forth Namdev Dhasal's realistic view of Dalit life in the Varna system:

When Darkness encountered the sun
Words thundered
How long shall we remain trapped
Suffocating in the prison-hole of Hell
(172)

Here Damu's act of embracing Buddhism is the rejection of Varna system which obliterated the existence of Dalits for centuries. Hence, this acceptance of new life is for growth and emancipation.

Conclusion:

To conclude, Damu's protest against the Varna system and his resolution to embrace Buddhism is his denial to be a victim and suffer in the prison hole of hell. He rejects Hindu Mysticism and embraces Buddhism to enlighten and empower his life and therefore, he sets an ideal example for the upcoming generations to follow in future. Hindu Spiritualism is the prison hole of Hell that trapped Untouchables and is still trapping them in it. Damu's act of embracing Buddhism makes it clear that he is aware of Dr. B. R. Ambedkar and his liberation movement that made Dalits to raise their voice reject the Varna system and demand for egalitarian society to turn this planet into a paradise.

Works cited

- Ambedkar, Babasaheb. "Dr. B. R. Ambedkar Writings and Speeches", Vol. 11, *The Buddha And His Dhamma*. Pune, Government Potozinco Press, 1992.
- Bhongle, Rangrao. "A Semiotic Study of Dalit Poetry in Marathi", Indian Literature, Vol.50, No.3, June 2006.
- Jadhav, Narendra. *Outcaste: A Memoir*..Viking, Penguin Books India, 2003.
- Manohar, Murli. "Who is "Brahman", not Brahmana / Brahmin?" *Dalits and Religion ed.* New Delhi: Atlantic Publishers and Distributors Pvt., 2009.

Journal Homepage: -www.journalijar.com

INTERNATIONAL JOURNAL OF ADVANCED RESEARCH (IJAR)

Article DOI:10.21474/IJAR01/13191
DOI URL: http://dx.doi.org/10.21474/IJAR01/13191

RESEARCH ARTICLE

MARGINAL VOICES IN ALICE WALKER'S STRONG HORSE TEA

Ghansham S. Baviskar
Associate Professor & Head, Department of English RNC Arts, JDB Commerce & NSC Science College, Nashik.

Manuscript Info

Manuscript History
Received: 20 May 2021
Final Accepted: 24 June 2021
Published: July 2021

Key words:-
Hegemony, Patriarchy, Oppression, Education, Reason, Solidarity Humanist

Abstract

The dominant forces, the torchbearers of civilizations in America, have always silenced marginal voices.Thereligious books have always been the instrumental foundationsfor the whites to retaindominance across the world. Ruthlesswhites like the Aryansdefeated the nativesand enslaved them in their trap. They enforced slavery and imbibed the superstitious notions and outdated religious rituals that never allowed the oppressed to question its authorityon the base of reason and science. In the twentieth century, the emergence of revolutions and the movements for the human rights of the African Americans forced the imperialists to accept democratic values, implement, and administer them in the countries. Under the influence of the dominant oppressive forces, thewhiteskept the downtrodden and oppressed people ignorant about it. The pains and problems of the people did not end with the abolition of slavery and untouchability in both the countries but continuedhorribly in racist, classist, and sexist society. The vintages of slavery resulted from the race and caste are still on display in the slums.The humble dwellers in the slumsstruggle never ending problems caused by the elite dominated industrialism and capitalism in the metropolitan citieswhere there is hardly any room and scope for their growth and emancipation. Alice Walker's "Strong Horse Tea" voicesthe margins who were rejected and dejected for ages. This paper is an attempt to throw light on the margins within the margins and voice the miserable livesof the oppressed, those who struggle against the oppressionandare silenced meticulously by the hypocritical ruthless masters.

Introduction:-

Alice Walker a renowned writer deals with the women's issues in racist and sexist America where the literary giants of her time in white literary circle miserably failed in their presentation of the African Americans in America and even if they projectedthe people of color, they were presented from the whites' point of views and not the humanists' worldview.Walker deals with the several issues that concern black women's identity, voice, human rights and their exploitation in racist and sexist society. The entire race of the black raised their voice against their discrimination and remained silent towards the pains and problems faced by the black women in patriarchal construct of race and sex. In her exploration of the African American society, Walker finds black males and the whites more responsible for the status quo in society in regard to women's pains,problems and identity issues that they failed to identify, recognize and address in the whites'race and gender-based society.

Corresponding Author:- Ghansham S. Baviskar
Address:-Associate Professor & Head, Department of English, RNC Arts, JDB Commerce & NSC Science College, Nashik

Black women's voices are not only silenced meticulously by the whites but they are also dominated forcibly by the black men who regarded them sexual beings and imposed single parenthood forcibly on them without any sense of duty and responsibility on their part towards their women and children, they fathered. Rannie Toomer represents such women. The way, the whites administered racism to administer their sovereignty; the same way mendevised patriarchy to control women in their reign and quiet their voice by marginalizing their position in society. In *In Search of Our Mothers' Gardens Womanist Prose,* Alice Walker highlights black women's plight in the racist and sexist conformist order that has regarded women the "mule of the world" and handed them the burdens that "everyone else-everyone else-refused to carry." (237) Rannie Toomer, the protagonist of *Strong Horse Tea* is a representative of black women who are in love and trouble of various predicaments. She is imposed motherhood without marriage and the man who is responsible to bring the child in the world is nowhere seen shouldering father's responsibilities and his complete absence marks the deterioration in the entire black community and the lack of solidarity between men and women to work towards the emancipation of entire African American society.

In ***Strong Horse Tea***, Walker projects the marginal world of African American mother, Rannie Toomer who is trapped in racial imperialism and notgranted freedom in any form to exercise her abilities and faith in science. She is condemned to live in slum as the black women's world is ruled and dominated by the racial and imperial authority of the whitesand the irresponsiblebehaviour of the black men who imposed motherhood on black women and left them. Rannie Toomer, the protagonist raises her voice against the injustice done to her by the racistwhite communityand the black male ideology those who do not regard black women as human beings and victimize them in the name of God and religion.The story beings with a description of her son's critical health condition and details her plight. Her plight is due to theracism and sexism perpetuated in theimperial world in which black women are trapped in ugly relations and burdened with themotherhood. The narrator recalls, "Rannie Toomer's little baby boy Snooks was dying from double pneumonia and whooping cough. She sat away from him, gazing into the low fire, her long crusty bottom lip hanging. She was not married. Was not pretty. Was not anybody much. And he was all she had." (Walker,*The Complete..., 80*)The narrator's description of RannieToomer's plight displays the deprived world of the black community in which the mothers and children suffered due to the incapacity of the black men to understand their responsibility towards women and also the children, they fathered.

Rannie Toomer raises her voice stronglyagainst the dominant forces with her faith in science and medicine but she isinnocent enough not to understand that it is ruled by the whites who do not care for the blacks and their children. She voices strong rejection of the swamp magic in her remark, "I don't believe in none of that swamp magic."The white mailman shatters her faith in science and medicine when he should assist her in calling doctor, he directs her to the "swamp magic" in a mocking tone, "Magic that if it didn't work on whites probably would on blacks." (Walker,*The Complete..., 83*-84)His attitude towards her appeal is a manifestation of the white race mentality towards the entire black community. Her voice is silenced and she is condemned to poverty, ignorance and the set norms of imperialism that the sexist male dominated patriarchy rules through the conformist religious authoritarian dogmathat has been imbibed and instilled methodically in society.

In *An Essay on Alice Walker* Mary H. Washington's comments,"…struggling to get a doctor for her dying child, is handicapped by poverty and ignorance as well as by the racism of the southern rural area she lives in." (Christian:93) Rannie Toomer fails to understand the entrenched pattern of discrimination. Unable to realize her marginalized position as a black and a black woman, she puts her faith in a white doctor and appeals the white mailman to send one to treat her only child Snooks. Her failure to understand her racial positions displays her limited understanding of colonialism and imperialism. In *Racism and Feminism: The Issue of Accountability*, Hell Books rightly comments,"…the American woman's understanding of racism as a political tool of colonialism and imperialism is severely limited." (119)Rannie Toomer's voice is muffled and the black women like her are rejected their right to life and relegated to a worse level than animals. She is denied the basic needs in life she requires to live with dignity and respect in society. She receives the advertising circulars often, the ones, the white mailman delivers. Her ignorance about the advertisement law that sends circulars makes her to consider the issue seriously, and question the mailman, if "She couldn't ever buy any of the things in the pictures - so why did the stores keep sending them to her?"(Walker,*The Complete…,* 82)It is a mockery to the humanity, that the white capitalists mock the poor by sending their advertising circulars even when the blacks are not in position to buy any one item from the list of the circulars and are in the dire need of basic demands of food, cloth and shelter in their life. The medical facilities remained a distance reality in their life which they could not afford for centuries and remained deprived of everything, they deserved as human beings. African Americans were deprived of education that critically affected their lives and controlled their beings through the literature they provided through the advertising circulars. In

*Reanimating the Trope of the Talking Book*Deborah Anne Hooker's observation in this regard throws light on the pathetic conditions to which the blacks were conditioned, "… the appearance of printed texts to illiterate auditors whose amazement reveals both a simple lack of literacy and a profound unfamiliarity with the dominant forces shaping and controlling their world." (Bloom, 189) Although Rannie puts her trust in science and a doctor, she fails to recognize the dynamic forces behind her oppression in the world of science and technology that is controlled by the whites to exploit and gain more profit. Deborah further rightly points, "Despite failing to grasp why she repeatedly receives the pictures of all the objects she "couldn't buy," Rannie paradoxically invests her trust in the world from which these texts emerge." (Bloom, 192)

The white imperialist world denied the blacks education and threw them permanently in the dark wholes of ignorance and superstition. Rannie, left with no alternative is forced to seek Sarah's adviceto save her only child Snooks who is dying of phenominaia and cough. The white mailman's advice to seek the help of black root maker and the swamp magic throws light on the mentality of the white people and the conspiracy of nigger magic and the white racist society that deny the blacks the basic needs of food, health and education. Snooks' death symbolizes the irresponsiblebehaviour and racist entrenched pattern of discrimination to maintain the blacks under the threshold of the white hegemony.In *An Essay on Alice Walker*, Mary Helen Washington comments on Snook's death, a great tragedy that struck Rannie, "In his death, all the elements seem to have conspired- the earth, the "nigger" magic of Aunt Sarah, the public and private racism of the south. One wonders what desperate hysteria allowed Rannie Toomer to stomach the taste and smell of horse urine." (Christian, 93)

Rannie Toomer's critical condition is presented through the use of circulars she makes in protecting herself and her child from utter cold. The narrator states, "Cold wind was shooting all around her from the cracks in the window framing, faded circulars blew inward from the walls." (Walker, *The Complete…,*85) She plastered the circulars as use value futilely to protest from the wild cold Georgia weather.Rannie's is forced to fetch strong horse tea, the only remedy to save her dying child in a shoe that leaks and has to put her tongue against it to offer warm strong horse tea to her son, highlights her tragedy caused by the lack of the fundamental opportunities, education provides. Rannie Toomer's plight and Snooks death is not incidental, it is caused by the entrenched pattern of racism and sexism, and she is victim of. In *Strong Horse Tea by Alice Walker: A Review*Taskeen, Samiya and AbidaTaskeen rightly comment on the root cause of the blacks' suppression and oppression that has resulted in denying the equal rights to them. In their opinion,Rannie's plight and her son's death are the results of the whites' cruelty, brutality and savagery and the ignorance of their own equal rights in racist orthodox society. (59)

To conclude,racial prejudice instilled in the white class not only relegated the blacks to poverty and deprived them of basic needs in life but italso critically affected black women. Denial of the basic needs was a great disaster that left the blacks at the mercy of conventions and rituals, left them with no other alternative except the swamp magic to save their dear ones. Racism and classism compelled men to reject their duty as fathers and burdened women with a single parenthood. Rannie is a representative of the black women who carried the burden of childrenwith paramount feelings of love and affection for them. Snooks' tragic death in racist and sexist America is the ultimate end ofhumanity.Racism not only destroyed the blacks but critically affected women's relations with the black men who becameirresponsible, unaccountable toward their duties as a companion, husband and father, and overall a human being.Race, Sex and Class prejudice and inequitysuppress Rannie's voice and strong faith in science and reason, cause a disaster in her life,and leave her with no alternative except to catch a *strong horse tea* in stormy rain to save her dying child, Snooks. Walker's *Strong Horse Tea*demands the human beings to raise their strong voice against all the kinds of discriminations, oppressions and subjugations wherever they are and force the governments to act according the law and democracy to sustain humanity in materialistic imperialistic world that adheres race, class and sex distinctions in the age of science and technology.

Works Cited:-

1. Bloom, Harold. Edit. Alice Walker. United States of America: New York, 2007.
2. Christian, Barbara. Everyday Use. New Jersey: Rutgers University Press, 1994.
3. Hooks, Bell. *Ain't A Woman: Black Women and Feminism*. London: Pluto Press, 1990.
4. **Taskeen, Samiya and AbidaTaskeen. "Strong Horse Tea by Alice Walker: A Review"** Stem Cell. 2010; 1 (1).
5. Walker, Alice. The Complete Stories. London: Phoenix, 2005.
6. In Search of Our Mothers' Gardens. London: Phoenix, 2000.

Journal Homepage: -www.journalijar.com

INTERNATIONAL JOURNAL OF ADVANCED RESEARCH (IJAR)

Article DOI:10.21474/IJAR01/13158
DOI URL: http://dx.doi.org/10.21474/IJAR01/13158

RESEARCH ARTICLE

SUPPRESSION TO PROTEST: A JOURNEY OF STRUGGLE OF A DALIT WOMAN IN BABURAO BAGUL'S NOVEL *SOOD*

Ghansham S. Baviskar
Associate Professor and Head, Department of English, RNC Arts, JDB Commerce & NSC Science College, Nasik.

Manuscript Info

Manuscript History
Received: 15 May 2021
Final Accepted: 18 June 2021
Published: July 2021

Key words:-
Caste, Hegemony,Atrocities, Rights, Identity, Secular, Humanity

Abstract

Gender violence in any form is a punishable crime in India but still it is prevailing in society. Indian constitution safeguards women's rights and guarantees them equal status. Despite the strong measures taken by the constitution makers, the loopholes in the entire system of the law implementing authority and the government machineries do not act responsible and consider the atrocities on women seriously.The largenumber of atrocity cases registered in the police station and pending in the courts makes it clear.Though Hindu society worships women and regards them'goddesses,'they areperceivedsexual beings, play things, commodities and men's possession in reality.This paper is an attempt to present this reality and highlight the plight of women in caste gender-based society that Baburao Bagul projects in his Marathi novel, ***Sood***. Janki, the protagonistis a victim of gender violence perpetuated in the caste prejudiced society. Her rebel against the caste and gender discrimination proves to be a milestone in her struggles with the upper caste mentalities those ones who subjugate and oppress women. Her voice is the voice of entire Dalit community that that she raises to assert her resistance for asserting the identities of entire community and demands for a more open and equal egalitarian society for the welfare of entire humanity on this beautiful planet that has already been turned into a hell by the conformist religious ideologies of the priests.

Introduction:-

Baburao Bagul, a renowned prolific Marathi writer dealt with women's issuesin his works.His protagonists are confined in theVarna system that has beenadhered and administeredby the so-called pundit classwhich has always been regarded the torch bearerof civilization.Baburao Bagul'sprotagonists makethe people conscious of the age-oldcustoms and rituals which need to be uprooted completely to form an ideal secular societythat has its roots in the basicuniversal human values - freedom, fraternity, equality, and social justice.

Women in India are equal to men, but the constitutional measures taken for their welfares have not been taken seriously and ignored intentionally by all the fundamentalists in the governments who were in power since the first Independence of the country.Rape, murder, dowry deaths, female foeticides and exploitations are routine matters in *shining*and *clean* India. Although the law promises safety and security for women, the law-abidingimplementing authority does not implement the law and punish the culprits accordingly.It has resulted in certain threats to the safety and security of women and a serious menace to the identity of nation across the entire globe.Dalit women are

Corresponding Author:- Ghansham S. Baviskar
Address:- Associate Professor and Head, Department of English, RNC Arts, JDB Commerce & NSC Science College, Nasik.

not safe at all in the country as the number of rape cases have tremendously increased and the Atrocity Act made by the central government has miserably failed to safeguard the rights of Dalit women and guarantee security and safety to their life and existence. The large numbers of cases are filed under Atrocity Act and the victims arestill waitingfor justice. It is shocking that many atrocities complaintsare not filed and registered as the officer-in-charge under the influence of upper caste politicians never register such atrocities and even if they get registered, the loopholes are maintained to favour the culprits. The culprits with caste based mentalities are never punished due to the lacunas in the technicalities in the entire system starting with the governing parliamentary systemto the implementing authorities in many states, those who strongly believe and secretly follow the Varna system which has already been abolished and uprooted by the constitution makers in the country by administering Democracy as a way of living life and the ideal secular culture to be followed in every day, public sphere of the nation to ascertainthe nationality of the people: 'proud to beIndian first and Indian last' but the fact is something different that people in India live with multiple identitiesimposedand imbibed on them by the laws of Manu and his spurious book Manusmruti.

Since the ages women have always been more prone to the exploitations promoted by the elite caste politics administered by the mainstreamof the society. Jankiand her mother arethe representatives of Dalit women who suffer in such unequal society. As a daughter of *Murali* and a Dalit woman, she becomes aprey to the caste discrimination and conventions that forcibly victimize her.In "StritvachiAdimSahajprerna: *Sood*", M.N.Wankhede rightly comments on Janki's tragedy. He states, "She is a daughter of *Murali*. One of theDalits, her language testifies her low status. How can a daughter of *Murali* be chaste and pious? It is this question that her mother and the world around deliver her." (22) He further continues,"Janki is a heroine of Dalit people. Who else would bear such infernal atrocities? Dalit women are anybody's possession." (23): (Trans.by Researcher). ***Sood***, published in 1970, after twenty years of the republic day, it comments on the striking reality of the caste, class, and gender politics in India. Despite the constitutional measures incorporated in constitution, the governments failed to protect the human rights of the Dalit women. It is nothing but the denial of women's existence and their rights to their being as the subjects in the secular nation.It is a disgrace to the nation.

While returning from the floor mill, a crew of ruffian chaseJanki, abuse and attack her to violate her chastity. The conversation that follows among them throws light on the disaster that she is going to become a victim of. Their conversation follows as:
"Consume her."
"How would people retort?"
"She is not from a decent lineage. She is *Murali*'s daughter. Who would trust her?"(Bagul,18) (Translated by the researcher)

It is her caste and low status in society,victimizes her and makes her a rapevictim. Later, Gangu, her mother propels her into her profession that she must abide by the laws of *Murali* imposed on her. Her profession as a prostitute has its origin in *Devdashi* and *Murali* traditions which wereinducted in the social order of the day to maintain the hegemony of Aryans to disgracewomen and the downtrodden.The so-called *pundit* class and the other elite classes viewed *Devdashi*and *Murali*traditions a pious service to gods, goddesses, and Earth Gods in which mostly all the women victims were from the *bahujan*community.Vasant Rajas in his "*Devdashi*: Shodh ani Bodh," points out that theorigin of inhuman traditions is in the religious scriptures written by the Pope and the Aryan Brahmin. He elucidates, "Since the ancient time, all the inhuman conventions and traditions came to be formed in the name of gods and religions. The Aryan Brahmins and the Christian priests inscribed the myths and the rituals to their benefit" So, in his view all the outdated traditions do have their origins in religious scriptures made to dupe the common mass in the country. He further continues, "In order not to question the authority of Vedas, Verna ani Smruti, the Brahmins proclaimed that these books were"*apaurushaiya*" meaning, not written by men but by the gods and to doubt its authenticity is a sin." (21): (Trans. by the Researcher)

In Baburao Bagul's *Sood*, Jankiisavictim of *Murali* convention.In the patriarchal set up of the society, the upper castes and her own mother that follows a *Murali* tradition forcibly put her in prostitution.She is forced to live a life of a prostitute. Her mother who too is a victim of such tradition continues her ways of life and she too is regarded 'sex object' than a human being. She is made to believe in preordained state sanctioned in the name of gods and religion.When she should protect *Janki* and oppose her exploitation, she herself contributes in administering violence on her and gives permission to Dagadu, her lover to consume her.*Janki*'s mother works here as an agent to such an order and proves helpful in sustaining masculinity and patriarchy that regard women as 'sex objects' than human beings. She too like many other women whose psyche is trained to accept *Murali* tradition as her lot and

preordained destiny, goes for it without questioning it that propagates subjugation and exploitation. Her mother does not regard her own existence of any worth and respect. Gangu and Janki live their life in utter poverty that is caused by their low status designated to them in caste set up by the elite hegemony that imposed traditions and outdated rituals to annihilate their existence permanently. It is a mockery tohumanity that the orthodox social order relegates women to mere bodiesthanhuman beings.Gangu is made to accept her life as preordained destiny. Instead to fight the oppressive forces, she accepts it as her lot and inflicts the same on her daughter. Her mental psyche is thus, the result of conventions strongly instilled in her mind by the descendantsof *Manu* those who exploitthousands of women even today in the entire republic andthe Maharashtra and Karnataka states where *Devadasis* and *Murali* traditions still exist.

Later, Janki is handed over to the custody of her husband and mother-in-law. Her plight does not end with her marriage, rather it continues in more horrible ways. Her mother-in-lawfails to pay off the money to Rasul, a butcher and sells her to him. Rasul too regards heras *body* and humiliates her for two years and sells her to Naikin, the woman who puts Janki in prostitution and starts earning money. Janki is thus also becomes a victim of convention-based caste and gender discrimination. The cycle of her exploitation gets renewed in more inhuman form, the moment she is handed over from one hand to the other.The crew of vagabonds violently rape her. Her mother forcibly wants to put her in her prostitution.Her mother's lover, Dagadu views her as a play thing and forcibly rapes her.Gangumixes drugs in her food to make her fast asleep, so that Dagadu can get an opportunity to consume her. The writer narrates,

> She forcibly put her down. Pressed her both arms hard with her feet and sat on her bosom. Shut her mouth fast with her hands, so that she cannot scream aloud and signalledDagadu to proceed. He started taking off her clothes. She came in her conscious the moment, he started consuming her. She strived hard with her legs. He summoned all his strength and tried to lock her legs under his own. She kept struggling under his heavy body. Fiery with rage for getting money from Dagadu, Gangu started showering her with blows. And soon both initiated heating her brutally till the moment a sharp weaponwas thrustin his back; he fell downand cried aloud in pain. (39): (Trans. by the Researcher)

When she gets married, her husband and her father-in-law regard her as commodity and sell her to a butcher.Rasul too after using her for two years sells her to Naikin, the owner of brothel house who puts her in prostitution.Janki resists all the forces but all her attempts against these dominant oppressive forces fail. It is the disgrace to humanity that women are not viewed as human beings but as play things.Janki survives the inhuman brutal forms of oppressions and exploitations and thus begins to rebel and revolt against the hegemony that caused her plight and denied her birth right and existence as a human being.In *Baburao Bagul YanchyaSahityachaChikitsakAbhyas*,Nazarethamiskita states, "In *Sood*, Bagurao Bagul has presented the story about a Dalit woman's plight"(117): (trans. by the researcher) How long can such a woman withstand the brutalatrocities and rapes with no intervention of laws anywhere in any form to safeguard their existential rights? She must break the religious conformist barricades that have constrained her. She plans to kill herself and goes to a river side to commit a suicide and while attempting it, a sadhu wants to rape her. She fights with him and kills him. Her exploitation continues even when she tries to put an end to her life.SubhashPulavale's rightly points at the reality of *Sood*. He terms it a fiction with "a naked reality of Dalit woman who is regarded any man's possession and a play thing to appease male hungers." (127): (trans., by the Researcher)It is here, she disguises herself Jwalaprasad, a *sannyashi*, a man. She does so to hide her identity as a woman as she thinks that her being a woman has caused all her troubles. She starts despising her body and considers it the cause of all her sufferings. In *Dalit Katha: Nirmiti ani Samiksha*, Chaya Nikam substantiates the prime cause of her sufferings is her caste and then the body. In her view, the cause of Janki's despising her body is"Being a daughter of *murali*, she is not respected. The upper caste Hindus exploit her sexually. Her exploitation begins, the day she enters puberty(97). (Translated by the researcher) It is on her way to Himalaya, she happens to meet *Swami*,a Sadhu, the guiding principle in her life who brings change in her attitude towards life at the end, but her story leads to the diagnosis of religious scriptures to find out the truth of this kind of double slavery inflicted on women who have to bear it unquestioned. In Vasant Rajas' opinion, "it is due to the ignorance and superstitions, people even in the world of science believe gods and desire for heavenly salvation." (15) (trans. by the Researcher)It is a stunning reality to see that the people even in the twenty first century believe traditions, conventions and outdated rituals organized systematically for their exploitation and oppression.

Janki's rebel comes in the form of revenge by killing a *sadhu* who tries to rape her. In orthodox religion, a woman is viewed aplay thing.It makes her to hate her womanhood and desire for a man's substance. In *Baburao BagulanchyaKadambaraya*, Subhash Pulavale rightly comments, "Dalit woman rejects her body as it is regarded a play thing and the offspring of all the pains, sufferings and exploitation but when awoman's body is perceived with the dignity and respect, she accepts her womanhood whole heartedly" (128) (trans., by the Researcher)In her journey to Himalaya with Swami in a disguise of a sadhu, sheoutshinesVidyacharanin her journey with Swami. She hides her identity and reveals it to Swami, the moment; he makes her realize her folly for desiring a man's body and despising her own.He guides her and stands with her in her fight with the caste and gender biased society, but before she could begin her struggle in future, she and Swami stand prey to the wild forces and die in an attackof the wolfs.

To conclude, no doubt, gender discrimination in caste-based conformist society has posed serious threats to societybut it would not be too late to realize its seriousness and work towards it. It is the right time to wake to the call and give a proper response to the serious issues concerningcaste and gender discrimination to stop violence in society.Janki's rebel against the religion is rendering example of the worse treatment women get in society, so as nation, the intellectual people of the country must have to raise the strong voice against such discrimination and violence, if not then it would not take much time to disturb the peace of entire nation. Each act of atrocity and violence must have to be condemned and punishedwith severity accordingly by the law machineries,and then only the nation can hope for the best of entire society, otherwise, it would pose serious threat to the nation in the coming years. In *Sood*, Dagadu, Rasul,Vidyacharan, a crew of ruffian, and a sadhu who tries to rape Janki are the representatives of male dominated society who do mock at women by disgracing them.It is a mockery to Hindu society that on one hand it worships women as goddesses and the other regards them *sex objects* and forcibly puts them in *Devdashi* and *Murali* traditions. It exposes the duality of society that on one side it supports women and the other it degrades their identity and character in the name of God and religion.Janki's voice and rebel that ends with her death, is the real beginning and the state of consciousness she reached for her rights is the state of consciousness the entire Dalit community has reached and started questioning the unquestioned authority and hegemony of the religious scriptures produced by the Aryan Brahmins. So, the government machineries and the implementing authorities whoever is there in the power today must have to abide towards their constitutional responsibilities and duties and act accordingly to set an ideal before the society that the constitutional law is supreme, the parliament is supreme, and it can encroach in any religious body and any scripture for the broader interest of the entire

Works Cited:-

1. Bagul, Baburao. *Sood.* Mumbai: LokwangmayGruha, 2014.
2. Miskita, Nazareth. *Baburao Bagul YanchyaSahityachaChikitsakAbhyas*. Thane: DimplePublication, 2006.
3. Nikam, Chaya. *Dalit Katha: Nirmiti ani Samiksha*. Pune, SuvidhyaPrakashan, 2006.
4. Wankhede, M.N. *Sood. StritvachiAdimSahajprerna:Sood*Gaikwad, Gangarao. (Edit.), Nasik: Disha Prakashan, 2005
5. Pulavale, Subhash. *Baburao BagulanchyaKadambaraya*. Aurangabad, ChinmaiPrakashan, 2004.
6. Rajas, Vasant. *Devdashi: Shodh ani Bodh*.Pune: SugawaPrakashan, 2012.

Kanpur Philosophers
ISSN 2348-8301
International Journal of humanities, Law and Social Sciences
Published biannually by New Archaeological & Genological Society
Kanpur India

Vol. VIII, Issue III : 2021

CLASS EXPLOITATION IN ALICE WALKER'S NOVEL, *THE THIRD LIFE OF GRANGE COPELAND*

Dr. Ghansham Sardar Baviskar Associate Professor & Head, Department of English, RNC Arts, JDB Commerce & NSC Science College, Nashik

Abstract
The racist capitalist white people control the economy and the political powers to exploit the African Americans. The rich white people trapped the black labourers and menial workers in the brutal cycle of the labour mechanism and paid them low wages and manipulated their labour. The origin of poverty and economic destitution depicted by Walker is in the slavery which relegated the blacks' existence to the mere cheap labourers and did not provide any scope for their liberation and emancipation. Devoid of education, the blacks remained ignorant about their exploitation and failed miserably to upgrade their socio-economic conditions. The dominant rich white class became rich after entrapping the blacks in the brutal cycle of manual labour work and denied them their fundamental right to live with pride and dignity. In the present paper, an attempt has been done to explore the life and plight of African Americans who suffered from the racial inequalities and class exploitation.
Keywords- Racism, exploitation, capitalist, Class oppression, sharecropping

Introduction:

The trinity of the race, gender and class degraded the positions of African Americans and entrapped them in the brutal cycle of exploitation. The capitalist white American society exploits the labour of African American people and degrades their positions in society. The imposition of menial labour works on the African American people results in utter poverty and the economic destitution. It ultimately denies their right to live with dignity and pride. Deprived of opportunities in the industrialist capitalist society, the African Americans suffered miserably and tried to survive in debilitating conditions in white America.

Sharecropping, a Brutal way to Exploit African Americans:

The blacks who were brought as the slave owners were forced to do the menial works for the white masters and rejected their existence as human beings. Though, the slavery ended in America, it continued in the evilest form of the sharecropping system. After the abolition of slavery, the blacks had no opportunity to survive in the capitalist society and poverty forced them to work on the cotton farms of the white masters. Even after working for years together, they could not earn much to meet the basic requirements and necessities in their lives. To solve their economic problems, they borrowed money from the white landlords and continued to work and repay the amount which they could not make as the white masters took undue advantages of their ignorance of education and compelled them to work for years together on their farms as labourers. Geeta Bindal rightly observes, "The voices of the oppressed are not those of race and gender alone. Class exploitation is the greatest source of oppression of blacks in white America." (162)

Class Exploitation in Racist Industrialist World:

Grange Copeland, Margaret, Brownfield, and Mem represent the poor African Americans. They are the symbols of poverty. In the racist capitalist society, they are forced to do the menial

works and paid less in the South. Grange and Brownfield remain sharecroppers. Margaret and Mem are compelled to carry out the works of maids. They represent the victims of the capitalist racist order. They get low and irregular incomes and struggle to survive in the oppressive conditions. "To be a poor man is hard, but to be a poor race in a land of dollars is the very bottom of hardships," says E. B. Du Bois and this is true of Grange, Margaret, Brownfield, Mem, and the child workers in Walker's *The Third Life of Grange Copeland*. (13) Alice Walker does not only project the dark aspect of African American life but also presents the critique of the capitalist society to free the nation from the bloody agenda of the rich racist capitalist society.

Copeland Family, a Victim of Race-Based Class Oppression:

Grange Copeland represents the plight of the labourers in the plantation system. He works for Shipley and fails to pay off the debt he had taken from him. He is overworked by the white landlord. Even his wife Margaret becomes the victim of the white master's lust. She is overworked in the cotton field and paid meagre amount. To pay off the money, her husband borrowed from him, she is compelled to trade her body. She gives birth to a white baby and suffers miserably after Grange Copeland deserts her. She commits suicide and leaves her son, Brownfield orphaned. After Grange Copeland deserts his family, Brownfield is left alone. To survive in the hostile world without parents, he continues the work of sharecropper and suffers endless miseries humiliations and tortures from his white masters. He marries Mem, a schoolteacher and further tries to change the prospects in their lives. His trap in the brutal cycle of sharecropping system and the exploitation inherent in it fails him miserably to deliver his promises to his family. In case of Grange, the white landlord, Shipley creates such circumstances that the other white landlords do not offer him job and he is forced to work for Shipley, but Brownfield is not allowed to settle at one place by the white landowners. At each place, he is overworked and paid less. He reveals, "I don't make much money... the white folks don't give us decent houses to live in." He is even often fired from his job without any reason and compelled to search for the work at the place of other white landlords. As he is propelled to move from place to place, his family suffers endless. Mem Copeland finds it unendurable as she is forced to move from one shabby place to the other. At each new place, she must begin everything a new and also to remake every dirty shack worth to live for her children. These hardships break her spirit and make her suffer the depression which the millions of the African American women experienced in America. The omniscient narrator observes,

> Each time she stepped into a new place, with its new, and usually bigger rat holes, she wept. Each time she had to clean cow manure out of a room to make it habitable for her children, she looked as if she had been dealt a death blow. Each time she was forced to live in a house that was enclosed in a pasture with cows and animals eager to eat her flowers before they were planted, she became like a woman walking through a dream, but a woman who had forgotten what it is to wake up. She logged along, ploddingly, like a cow herself, for the sake of the children. (*Walker* 77-78)

It is not Mem who suffers from this moving but also her children. After her husband is constantly forced to move from one place to the other, she fails to provide education to her children. So, the poverty and the sharecropping system brutally victimises African American women and children in the brutal cycle of exploitation. Even though, Mem works as a schoolteacher, she too is paid very less. It is her husband's insensitivity towards her teaching profession, she stops teaching. Like Grange, Brownfield too fails to realise the worth and importance of education and does not support Mem in her endeavour to continue her teaching profession and even offer higher education to his daughters.

Even they are not in condition to afford fruits to children. While the white landlords and their families enjoyed the luxuries of nutritious food and fruits, the Grange Copeland family fails to provide it to Brownfield. Later, Brownfield too fails to offer fruits to his children. His children could only have fruits at Christmas. After Grange brings the bags of fruits to his grandchildren, Brownfield feels jealous of his children. The omniscient narrator observes, "It was only at Christmas that Brownfield's children got apples and oranges and grapes. As a child Brownfield had never seen a

grape. He clutched the bags in a confusion of feeling. He was hungry, he was suffering from a malaise of the spirit, he was jealous of his children's good fortune. He wishes he did not have children down whose gullets the good fruit would go; he wished he were a child himself." (*Walker* 90)

The whites lived in the cosy, posh and comfortable cottages whereas the blacks lived in the poor houses and suffered from the deadly cold. Brownfield, Mem and their daughters Daphne and Ornette lived in a small shack and slept in one small room and struggled to survive in the bitter cold:

> "In winter, usually they all slept in the same room. Brownfield, Mem, Daphne, and Ornette; because it was impossible to heat two rooms in such a hole-filled house. It was impossible, really to heat one room; but when four people slept together in one small room and kept a fire going they could manage not to freeze to death before summer." (*Walker* 90-91)

It is not the food and fruits, but also the medical facilities, the blacks suffered. The white landowners could afford the expensive medical facilities whereas the blacks could not. They lived poverty-stricken lives and suffered the agonies resulting from it. Brownfield and Mem Copeland are too poor, that they cannot afford the medical facilities for themselves and children. At the time of Mem's delivery, he watches her helplessly and tries to avoid the children to witness the sight of childbirth. Mem undergoes the labour pains at home and delivers baby at night in rainy season:

> Brownfield looked over his shoulder at his wife's folded pallet. Not wanting the children to see the blood she had folded it as neatly as a newspaper and had tied it with string. There was a sheet hanging before Mem's bed. It formed a curtain which would have protected her children from the sight of childbirth. Brownfield thought what a blessing it must have been to Mem that the baby was born at night while Daphne and Ornette Slept and wind and rain muffled her sounds of struggle. (*Walker* 92)

The child labour is another crucial problem highlighted by Walker. All the child workers help their parents in the cotton field. They assist in loading the sacks in the truck. The omniscient narrator records, "The children's job was to go over the rows their parents had gone over the week before-"scrapping cotton" it was called. When the children saw their parents puts down their sacks they came and stood beside them at the edge of the field as all of them waited for the truck to come." (Walker 8) Similarly, Brownfield too assists his parents in the cotton field. He is over worked for hours together and paid very less. As the extreme poverty in his family forces him to work as a child labourer, he does not get the opportunity to go to school and learn. Grange's failure to send Brownfield to school, Even though Margaret strongly desires for it, ultimately leads to the life of a menial worker. He starts working in the cotton field at the age of six. Like the other child labourers, he too does not get opportunity to education and continues to work in the cotton field even in his youth. After Brownfield marries Mem, a schoolteacher, like his father, he too fails to see the worth and importance of education in changing the prospects in their lives. He too does not take his three daughters' education seriously. Like him, his daughters too become the victim of child labour in their childhood. His daughters are forced to work in the cotton field and exploited brutally.

Conclusion:

African Americans are brutally exploited in the capitalist society. They are not offered the better job opportunities in the white America. While white women get the job opportunities to work as receptionists, employees and nurses, African American women are destined to the low paid jobs and the works of maids, cooks, and nannies. This is very much a reality which Ruth notices when she happens to witness the cruelty of the capitalist industries which ruthlessly launch in the newspaper advertisements. Extreme poverty and the economic destitution too propel them to surrender to the whims of the rich landlords and even to prostitute to themselves to fill their stomach. Margaret, Mem and Josie suffer due to extreme poverty. After Grange fails to return the loan, the white landlord victimises Margaret. She trades her body to compensate for the loan her husband had taken from the landlord. Mem is too forced to do the work of maid at the houses of the whites and paid meagre amount. Ultimately, the trinity of the race, gender and class degrades the positions of African Americans and entraps them in the brutal cycle of exploitation in racist classist society.

ORIGINAL ARTICLE e-ISSN: 2349-0659 p-ISSN; 2350-0964

Epidemiological Characteristics of COVID-19 among the Individuals from Nasik District, Maharashtra

Dhumal Kishori Tukaram*

Abstract

Background: Coronavirus Disease 2019 (COVID 19) pandemic has created havoc around the world. All states of India, including Maharashtra, are severely affected by this viral infection. In Maharashtra, various regions including Mumbai, Pune and Nasik are largely affected due to this pandemic. **Objectives:** To study the epidemiological characteristic of COVID-19 Individuals from the Nasik district. **Materials and Methods:** A cross-sectional e-survey was conducted to study the epidemiological characteristics of COVID-19 individuals from and around Nasik. A random sampling method was adopted. Information from the individuals was collected in the form of a questionnaire, which was shared among 300 individuals, out of these 253 responses were received. Data analysis was done using Chi-square method. **Results:** Of 253 individuals, 90 (35.57%) were found to be COVID positive. Majority (50%) of them belonged to the age group 40–60 years. Among those tested positive, 83 (92.2%) individuals were symptomatic while, 7 (7.8%) were asymptomatic. Of 90 COVID positive individuals, 39 (43.3%) individuals with pre-COVID comorbidities showed severe symptoms and were hospitalized, while those without any comorbidity showed mild symptoms and were home quarantined, (Odds ratio = 15.88,95% confidence interval = 5.6–44.95, $P < 0.0001$). Post COVID symptoms, particularly diabetes and Mucormycosis, were developed among 8.8% and 1.1% individuals, respectively. **Conclusion:** Severity of illness was associated with comorbidity, among majority of the patients.

Key words: Comorbidity, Epidemiology, Pandemic, Post-COVID symptoms

Asian Pac. J. Health Sci., (2022); DOI: 10.21276/apjhs.2022.9.2.02

Introduction

Coronaviruses are a large family of viruses that cause illnesses ranging from the common cold to more severe diseases, in animals and humans. A novel coronavirus, also named as Coronavirus Disease 2019 (COVID-19) virus, is a new strain that is newly identified in humans. COVID-19 outbreak was declared as a global pandemic by the World Health Organization on March 11, 2020. This disease known to originate from Wuhan city of China, and has become a major health problem all over the world.[1] It is highly infectious and its human to human transmission occurs if aerosols or droplets containing the virus are inhaled or if virus comes in contact with the eyes, nose, or mouth of an individual, through contaminated surfaces. Clinical symptoms of this viral infection include fever, cold, sore throat, dry cough, pain in bones and muscles, breathing problems ultimately leading to pneumonia.[2] COVID-19 pandemic has severe impact on every field of life, including health of individuals. The virus is causing mild diseases in many individuals. The course of illness may be severe leading to hospitalization and even death in elderly or those with comorbidities.[3] The present survey was done to study the pre and post COVID comorbidities among the COVID positive patients from and around Nasik.

Materials and Methods

A cross-sectional e-survey was performed using social media platform, in July 2021. Informed consent was obtained from the subjects for their willingness to participate in the study. Participation in the study was voluntary and during the study, anonymity and confidentiality of the participants was maintained, as personal information such as name, contact number or email id was not inquired. The study population consisted of individuals who themselves were COVID positive or had at least one family member who was COVID positive.

Department of Zoology, RNC Arts JDB Commerce and NSC Science College, Nashik, Maharashtra, India

Corresponding Author: Dr. Dhumal Kishori Tukaram, Department of Zoology, RNC Arts JDB Commerce and NSC Science College, Nashik, Maharashtra, India. E-mail: kishoritdhumal@gmail.com

How to cite this article: Tukaram DK. Epidemiological Characteristics of COVID-19 among the Individuals from Nasik District, Maharashtra. Asian Pac. J. Health Sci., 2022;9(2):5-7.

Source of support: Nil.

Conflicts of interest: None.

Received: 18/11/21 **Revised:** 10/12/21 **Accepted:** 29/12/21

Sample Size

The sample size for the study was estimated by using the formula for estimating proportion: $n = Z\alpha 2\ P\ (1 - P)/d2$, where $Z\alpha = 1.96$; $P = 90\%$ of the response rate of the online survey, and $d = 5\%$.[3] Sample size calculated for the study was 253. A simple random sampling method was used to select the individuals of the population.

Regular exercise enhances immunity and reduces the risk of infection but reduction in physical activity during lockdown period might have affected the physiological processes of the body such as cardiovascular function, insulin sensitivity, cholesterol level, obesity and hypertension.[4]

Research Instrument

A self-designed questionnaire was prepared, both, in English and Marathi (vernacular Language). The questionnaire was pre-tested for validity and reliability. Only one response was accepted per subject. The questionnaire was divided into three sections. Section I-consisted of informed consent. Section II comprised

Demographic details of the individuals, while section three included eleven questions related to corona information.

The demography questions included name of the individual (which was not mandatory), age group, gender, area of residence (urban or rural), and district. While the questions related to corona infection included comorbidity questions and the genes of coronavirus that were detected during the reverse transcription-polymerase chain reaction (RT-PCR) test. The RT-PCR report was demanded from those individuals who were found to be positive. The survey questionnaire was sent to 300 individuals belonging to the Nasik district of Maharashtra, out of which 253 responses were received. A time span of 30 days was given to the participants to submit their responses. Deceased individuals were not reported.

Data Analysis

The data were analyzed by IBM Statistical Package for the Social Sciences 28.0.0 version. Descriptive statistics was done, using Chi-square tests and significance of the test was decided at $P = 0.05$

Results

Of total 253 individuals, 90 (35.57%) were found to be COVID positive. Slight male predominance (54.4%) was observed among the positive individuals. About 74.4% individuals were inhabitants of urban area, whereas 25.6% were inhabitants of rural area. Majority, i.e, 45 (50%) of them belonged to age group 40–60 years [Table 1]. 82.2% of the individuals were detected corona positive in 2021 while 17.8% were positive in 2020 [Table 2].

This shows the severity of the pandemic in 2021 than in first wave, i. e, in the year 2020. During the first wave of pandemic, the severity was more in the month of September 2020 (11.9%) and in the second wave, during March (14.3%) and in April (52.4%) 2021.

Among the 90 individuals confirmed as COVID-19 positive, 93.4% individuals had done the RT-PCR testing and had received the laboratory report, whereas 6.6% individuals had done rapid antigen test. Among the remaining 163 individuals who were not detected corona positive, 56 (34%) individuals had done rapid antigen test and were detected negative but showed mild symptoms such as cold and/or cough.

Among those tested positive, Corona symptoms were observed in 83 (92.2%) individuals while 7 (7.8%) were asymptomatic [Table 3].

Symptoms of these individuals are described in Figure 1. The most common symptom was fever 58 (64.4%), followed by breathlessness 47 (52.2%). Other symptoms include, Cough 39 (43.3%), body ache 28 (31.1%), Muscle weakness 25 (27.7%), headache 23 (25.5%), Loss of appetite 15 (16.6%), Diarrhea 9 (10%), and Conjunctivitis (Redness of eyes) 7 (7.8%).

The association of comorbidity diseases, such as diabetes and hypertension with the severity of COVID-19 has been assessed repeatedly.[5] In the present study, 43.3% of individuals who were hospitalized showed comorbidities of either one or more diseases. The remaining (56.7%), who were home quarantined, showed mild symptoms and cured themselves either by allopathic or ayurvedic or a combination of the therapy medicines (Odds Ratio = 15.88, 95% confidence interval = 5.6–44.95, $P < 0.0001$) [Table 4]. Out of 90 COVID-19 positive individuals, 62 (79.5%) individuals were not vaccinated, 13 (16.7%) had taken the first dose of vaccine (Covishield or Covaxin), and hardly 3 (3.8%) individuals had taken both the doses of vaccine [Table 5].

Out of 90 individuals, 50 (55.5%) had no history of any comorbidity, while remaining 40 (44.5%) reported one or more comorbidities, among them hypertension was the most common, followed by diabetes. Of 40 reported cases of COVID-19, 10 (11.11%) had only diabetes, 15 (16.6%) had only hypertension, 9 (10%) had dual comorbidity of hypertension and diabetes, 3 (3.3%) had respiratory disorders such as asthma or bronchitis, 2 (2.2%) had dual comorbidity of diabetes and kidney disorders [Table 6].

Post-COVID symptoms in the recovering patients are becoming a cause of concern. Among health conditions plaguing

Table 1: Frequency distribution and percent of age group of COVID-19 positive individuals

Year of infection	*Frequency*	*Percent*
2020	16	17.8
2021	74	82.2
Total	90	100.0

Table 2: Frequency and percent of COVID Infections in 2020-2021

Age group	*Frequency*	*Percent*
Below 20	4	4.4
Between 20 and 40	35	38.9
Between 40 and 60	45	50.0
Above 60	6	6.7
Total	90	100.0

Table 3: Percent COVID-19 symptomatic and asymptomatic individuals

Whether symptomatic or asymptomatic	*n*	*%*
Asymptomatic	7	7.8
Symptomatic	83	92.2

Table 4: Percent of individuals hospitalized or home quarantined

Whether Hospitalized or Home quarantined	*n*	*%*
Home quarantined	51	56.7
Hospitalized	39	43.3

Table 5: Frequency of individuals vaccinated before turning COVID positive

Vaccination Status	*n*	*%*
Not vaccinated before viral infection	67	74.44
Only first dose of Vaccine was taken	18	20
Both the doses of vaccine were taken	05	5.5

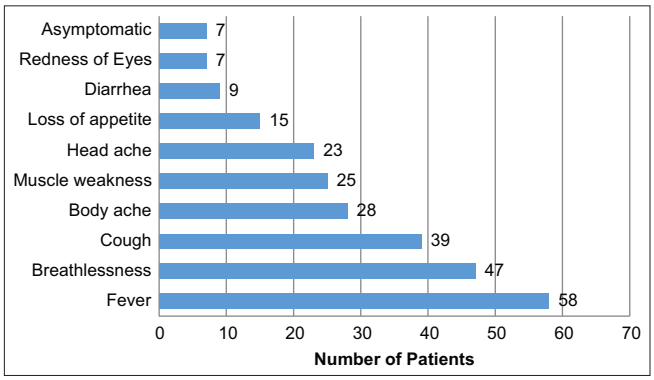

Figure 1: Symptoms of COVID-19 patients

Table 6: Pre-COVID diseases among COVID positive individuals

Pre-COVID diseases	*n*	*%*
Diabetes	10	11.11
Diabetes, hypertension	9	10
Hypertension	15	16.6
Diabetes, kidney disorders	2	2.2
None	50	55.5

Table 7: Post COVID diseases among COVID positive individuals

Post COVID diseases	*Frequency*	*Percent*
Diabetes	8	8.8
Diabetes, hypertension	0	0.0
Mucor-mycosis	1	0.0
Hypertension	0	0.0
Psychological disorder	0	0.0
None	81	91.1
Total	90	100.0

the COVID-recovered patients, diabetes has emerged as a prominent health concern. 8 (8.8%) have developed diabetes after recovering from COVID-19. Mucor mycosis was not significant (1.1%). Remaining 81 (91.1%) have not developed any post-COVID disorders [Table 7].

Discussion

The present survey was undertaken to study the epidemiological characteristics of COVID-19 patients from and around Nasik. The results of the survey showed that there was a slight predominance of male infected individuals. Most of these males belonged to age group 40–60 years and had got infected to coronavirus either at their workplace, during travel, or at market place. Similar results were also observed in a study conducted in Sassoon hospital Pune.[3]

COVID-19 is reported to be a mild disease for those aged <50 years.[6] Results of the present study also reflect the same. 56.7% of the individuals showed mild symptoms and were home quarantined. Most of these individuals belonged to age group 40–60 years and had either none or less comorbidities. They responded to the treatment properly, that increased their chances of survival. The most common symptom observed among the COVID-19 infected individuals was Fever (64.4%), followed by breathlessness (52.2%). These findings are at par with those reported by Gupta *et al*.,[7] but the findings are in contrast to the findings reported by Tambe *et al*.[2] This may be because of the fact that the individuals were asked to mention all the symptoms right from the day of early infection till the day of complete cure, while hospital study recorded only those symptoms observed in the patients at the time of hospitalization.

The most common Post COVID-19 symptom among the hospital discharged individuals was diabetes. According to Doctors, the mental and physical stress of COVID-19 infection on the pancreas has affected the production of insulin in the bodies of many patients. Some patients with moderate or severe COVID symptoms are administered steroids such as dexamethasone, which can also increase blood sugar.[8]

Conclusion

The present study reports that the COVID-19 has affected males more than females. Those with one or more pre-COVID comorbidities had severe COVID symptoms and had to be hospitalized, but those with mild symptoms were home quarantined. Post COVID diseases such as diabetes has developed in some of individuals due to the side effects of certain drugs.

References

1. Backer JA, Klinkenberg D, Wallinga J. Incubation period of 2019 novel coronavirus (2019-nCoV) infections among travellers from Wuhan, China, 20-28 January 2020. Euro Surveill 2020;25:2000062.
2. World Health Organization. (n.d.). Coronavirus. World Health Organization. Available from: https://www.who.int/health-topics/coronavirus [Last accessed on 2021 Dec 27].
3. Tambe MP, Parande MA, Tapare VS, Borle PS, Lakde RN, Shelke SC, *et al*. An epidemiological study of laboratory confirmed COVID19 cases admitted in a tertiary care hospital of Pune, Maharashtra. J Public Health 2020;64:S183-7.
4. Rathod VJ. Impact of coronavirus disease 19 lockdown on physical activity and energy expenditure among middle adolescence: A cross sectional E-survey. Arch Med Health Sci 2021;9:35-8.
5. Sanyaolu A, Okorie C, Marinkovic A, Patidar R, Younis K, Desai P, *et al*. Comorbidity and its impact on patients with COVID-19. SN Compr Clin Med 2020;1-8. doi: 10.1007/s42399-020-00363-4
6. Muliyil JP. A science-based response to COVID-19. Indian J Public Health 2020;64:S90.
7. Gupta N, Agrawal S, Ish P, Mishra S, Gaind R, Usha G, *et al*. Clinical and epidemiologic profile of the initial COVID19 patients at a tertiary care centre in India. Monaldi Arch Chest Dis 2020;901:193-6.
8. Alessi J, de Oliveira GB, Schaan BD, Telo GH. Dexamethasone in the era of COVID-19: Friend or foe? An essay on the effects of dexamethasone and the potential risks of its inadvertent use in patients with diabetes. Diabetol Metab Syndr 2020;12:80.

A STUDY OF GLOBALIZATION AND ITS IMPACT ON INDIA

Dr. VIDYULLATA R. HANDE

Head and Associate Professor, Department of Cost and Works Accounting, R.N.C. Arts, J.D.B. Commerce and N.S.C. Science College, Nasik-road, Nasik (Maharashtra)

Abstract

Globalization can be defined as integration of economies and countries through cross country flow of foreign trade, investment, ideas, technologies, capital, finance, goods, services and people. The process of globalization can be explained as a gradual removal of hurdles of the investment among the countries. It is the fully-free economic operations across the borders of the countries. It also benefits to the region, who have skill and technology. In India, the economic reforms of early 1990's, has witnessed a rapid rise in the economic growth. It also helped in reducing the unemployment, and poverty. Due to globalization, foreign companies brought highly advanced technology with them. After 30 years of Globalization, i.e. in 2021, it is significant to study the impact of Globalization on India. This paper tries to capture the globalization concept, study of GDP growth rate, Foreign Direct Investment trends, export-import and balance of payment etc. It is an attempt to study the globalization and its impact on Indian economy.

Keywords: Liberalization, Privatization, Globalization (LPG), India's Foreign Trade, Foreign Direct Investment (FDI).

Introduction

Globalization can be defined as integration of economies and countries through cross country flow of foreign trade, investment, ideas, technologies, capital, finance, goods, services and people. Globalization can be described as a process by which regional economies, societies, and cultures have become integrated through a global network of communication, transportation and trade. The process of globalization can be explained as a gradual removal of hurdles of the investment among the countries. It is the fully-free economic operations across the borders of the countries. It also benefits to the region, who have skill and technology. In India, the economic reforms of early 1990's, has witnessed a rapid rise in the economic growth. It also helped in reducing the unemployment, improvement in standard of living, better purchasing power and reduction in poverty. With a step of 'Liberalization Privatization and Globalization', in 1991 a new chapter was opened in Indian economic history and Indian economy was become opened for foreign investors. Foreign investors were got attracted to India after liberalization decision. . Foreign companies invest in India to take advantage of comparatively cheap wages, special privileges for investment such as tax exemptions. Due to globalization, foreign companies brought highly advanced technology with them. The main aim is to study and understand the globalization and its impact on GDP growth, foreign trade, export – import, foreign investment inflows to India.

The basic objectives of the present study are:

1. To study and understand India's journey towards globalization.

2. To study sectorial GDP growth rate.
3. To study the trends in Foreign Direct Investment inflows to India.
4. To study and understand India's Foreign Trade.

Methodology:

The present study is based on secondary data. The information and data was obtained from books, published papers, periodicals, journals, websites, internet, RBI annual reports and RBI Bulletin, Monthly statistics of Foreign Trade of India- DGCI & S, GOVT. of India, CMIE, Union Budget, Economic Survey of India, Ministry of Commerce and Industry data, online database of Indian economy, articles, newspaper etc. various relevant statistical tools were used to analyze the data.

Review of Literature:

In early 1990's, Globalization was the sizzling topic for a long time in India. The LPG program me has witnessed a rapid rise in the economic growth. Various researchers, committees, economists has studied it through various angles. Here we refer few studies for the purpose of review of literature. MathurVibha reveals in her book that, foreign investment in India has grown substantially in last decade following the liberalization of Indian economy in 1991. Certain booming sectors of our economy, especially the infrastructure have attracted considerable attention'. 'Foreign investment is the investment made by an investor of one country in another country. It is also named as cross border investment. FDI is an investment directly in the trade of manufacture of growth of providing services in some other country as described by Dr. Govilkar V.M. 'Flowing with globalization, India is shining in nearly every perspective. GDP growth has helped to improve India's global position. It also effected India's international trade positively as concluded by Agarwal Rinku in her article. M.Yuvaprasanna&Kannappan elaborated impact of globalization as 'Rural sector is the backbone of the rural Indian economy and globalization has helped it in raising expectations for everyday comforts, mollifying status, reassuring sustenance security, generating light commercial center for growth of business and administrations, and making significant commitment to the national procedure.' Goyal K.A reveals in his article that, how the process of globalization, liberalization and privatization has boosted economy of the developing countries.'

India's Journey towards Globalization:

As the Indian economy had suffered huge financial and economic crisis, the then Finance Minister of India Dr. Man Mohan Singh brought a new policy also known as New Economic Policy,1991 or LPG Policy. The policy was a measure to come out of the crisis that was going on at that time. The significant measures taken to liberalize and globalize the Indian economy was as follows:

1. Devaluation: To solve the balance of payment problem Indian currency were devaluated by 18 to 19 %
2. Disinvestment: To make the LPG model smooth many of the public sectors were sold to the private sector.
3. Allowing FDI: FDI was allowed in a wide range sectors such as Insurance (26%).
4. NRI Scheme: the facilities which were available to foreign investors were also give to NRI's.

5. Throwing open industries reserved for the public sector to private sector.
6. Abolition of MRTP Act.
7. Wide ranging financial sector reforms in banking, capital markets and insurance sectors.

The new economic policy 1991 introduced changes in the areas like trade policies, monetary and financial policies, fiscal and budgetary policies and pricing and institutional reforms. Now after thirty years, i.e. in 2021, it is significant to study the impact of Globalization on India. There are many implications of globalization on Indian economy. It can be discussed through the study of GDP growth, India's foreign trade, and foreign direct investments inflows to India.

Sectorial Composition of GDP of India:

After Globalization, Indian economy has developed rapidly during last two decades and significant features of this growth performance has been the strength of the service sector. The GDP growth rate is the percent increase in GDP from quarter to quarter. It tells us exactly how fast a country's economy is growing in various sectors.

Table 1.1: Sectorial Growth: (Pre and Post-Globalization)

(Percent per annum)

Sector	1951-80	1981-90	1991-2000	1992-97	1997-2002	2002-2007	2007-2012	2011-2012	2012-2013	2013-2014
Agriculture	2.1	4.4	3.1	4.8	2.5	2.4	4.1	5.0	1.4	4.6
Industry	5.3	6.8	5.8	7.3	4.3	9.2	7.7	7.8	1.0	0.7
Services	4.5	6.6	7.5	73	7.9	8.8	9.4	6.6	7.0	6.9
GDP at factor cost	3.5	5.8	5.8	6.6	5.5	7.6	8.0	6.7	4.5	4.9

Source: Compiled from Indian Economy: V.K.Puri, S.K.Mishra (2014) Himalaya publishing House, New Delhi.

Table 1.1, shows that, services grew slower than industry from 1950 to 1990. Services grew in 1980 and get accelerated in 1990 when it averaged 7.5 percent per annum. The slowdown of ninth plan (1997-2002) was confined to Agriculture and Industry sector, Service sector was not affected and had developed with 7.9 percent per annum rate of growth. The Tenth plan period (2002-2007) service sector grew at a rate of 8.8 percent and that of 9.4 percent in eleventh plan. In 2011-12 the growth rate was slipped to 6.6 percent per annum and 7.0 percent per annum in2012-13. In 2013-14, services growth rate was recorded at 6.9 percent per annum. The above discussion clears that, the Indian economy had witnessed a services led growth, especially post 1991 period. It reveals that, due to globalization not only the GDP has increased but also the composition of the sectors has also changed. Beforeglobalization maximum part of the GDP in the economy was from agriculture and industry sector. After globalization the service sector consistently remains on the top position of economy.

India's Foreign Trade:

Foreign trade in India is all about imports and exports to and from India. India exports nearabout eight thousand commodities to 190 countries and imports about six thousand commodities from 140

countries. The difference between export and import is known as balance of trade or trade balance. Following table is the statistics of export, import and trade balance of India in last fifty years.

Table 1.2: Exports, Imports and Trade Balance

Year	Exports (including re-exports US $ Million)	Imports (US $ Million)	Trade Balance (US $ Million)
1971-72	2153	2443	-290
1981-82	8704	15174	-6470
1991-92	17865	19411	-1546
2001-02	43827	51413	-7587
2011-12	305964	489319	-183356
2020-21(April-Nov Provisional)	174116	218874	-44758

Source. Economic Survey, Ministry of Finance, Govt. of India, 2020-21, p.no. A-96,A-97.

The statistics of above table indicates that, globalization has major impact on India's foreign trade. The exports increased from 17865 US $ Million in 1991-92 to 174116 US $ Million in 2020-21 and imports continuously increased from19411 US $ Million in 1991-92 to 218874 US $ Million in 2020-21. The rate of import was always high, as a result of which the trade balance was always negative throughout the period.

Trends in FDI inflows to India:

Foreign Direct Investment (FDI) means the investment from one country into another (generally by companies) that involves installing operations of acquiring assets etc. Foreign Direct Investment (FDI) plays significant role in the process of economic development of any country. FDI can brought tremendous economic growth and development. Many countries have used FDI as a catalytic agent for stimulating economic growth and development. With a step of 'Liberalization Privatization and Globalization', in 1991 a new chapter was opened in Indian economic history and Indian economy was become opened for foreign investors. Foreign investors were got attracted to India afterliberalization decision. Foreign companies invest in India to take advantage of comparatively cheap wages, special privileges for investment such as tax exemptions.The trends in FDI inflows to India can be observed from the following table. It is classified in pre-globalization and post-globalization inflows to India.

Table 1.3: FDI Inflows to India: (From 1970 to 2015)

Pre-Globalization Period(before 1991)		Post- Globalization period (after 1991)	
Year	FDI Inflows to India (US$ 000 million)	Year	FDI Inflows to India (US$ 000 million)
1970	0.05	1992	0.25
1971	0.05	1993	0.55
1972	0.02	1994	0.97
1973	0.04	1995	2.15
1974	0.06	1996	2.53
1975	0.09	1997	3.62

1976	0.05	1998	2.63
1977	0.04	1999	2.17
1978	0.02	2000	3.59
1979	0.05	2001	5.48
1980	0.08	2002	5.63
1981	0.09	2003	4.32
1982	0.07	2004	5.78
1983	0.01	2005	7.62
1984	0.02	2006	20.33
1985	0.11	2007	25.35
1986	0.12	2008	47.10
1987	0.21	2009	35.63
1988	0.09	2010	27.42
1989	0.25	2011	36.19
1990	0.24	2012	24.20
1991	0.08	2013	28.20
-	-	2014	34.58
-	-	2015	44.21

Source: UNCTAD Data Centre

During pre-globalization period, the FDI inflow was increased from $ 0.05 thousand million in 1970 to $ 0.24 thousand million in 1990. The flow of FDI registered wide fluctuations during the period from 1977 to 1989. During post-globalization period, the FDI inflow to India was increased from $ 0.25 thousand million in 1992 to $ 44.21 thousand million in 2015. The trend of FDI inflows in pre and post – globalization period together (i.e. from 1970 to 2015) was a rising trend. FDI increased significantly after 2001. The global economic recession also reflects in FDI inflow figures from the year 2009 to 2013. It reveals that the globalization had accelerated the FDI inflows to India.

Conclusion

Indian economy has developed rapidly during last two decades i.e.after Globalization.It had witnessed a services led growth, especially post 1991 period. It reveals from table 1.1 that, due to globalization not only the GDP has increased but also the composition of the sectors has also changed. Before globalization maximum part of the GDP in the economy was from agriculture and industry sector. After globalization the service sector consistently remains on the top position of economy.The exports increased from17865 US $ Million in 1991-92 to 174116 US $ Million in 2020-21 and imports continuously increased from19411 US $ Million in 1991-92 to 218874 US $ Million in 2020-21.Export and import was continuously increasedin last three decades. During post-globalization period, the FDI inflow to India was increased from $ 0.25 thousand million in 1992 to $ 44.21 thousand million in 2015.The trend of FDI inflows in pre and post – globalization period together (i.e. from 1970 to 2015) was a rising trend. Hence we can say that globalization affected Indian economy positively.

References:

1. MathurVibha (2001),'Trade Liberalization and Foreign Investment in India', New Century Publication Delhi, pp.206.
2. Govilkar Dr. V.M.(2012),'FDI in Retail', Think line, Guru Gaurav Nyasa Publication, Nasik,pp.5

Peer Reviewed Refereed
and UGC Listed Journal

An International Multidisciplinary
Half Yearly Research Journal

GALAXY LINK

ISO 9001:2008 QMS
ISBN / ISSN

ISSN - 2319 - 8508
Volume - IX, Issue – II, May - October - 2021
Impact Factor 2019 - 6.571 (www.sjifactor.com)

Is Hereby Awarding This Certificate To

Dr. Vidyullata Rahul Hande

In Recognition of the Publication of the Paper Titled

A Study of Performance of Khadi and Village Industries Commission in India

Editor : Vinay S. Hatole

Ajanta Prakashan,
Jaisingpura, Near University Gate, Aurangabad. (M.S.) 431 004
Mob. No. 9579260877, 9822620877 Tel. No.: (0240) 2400877,
ajanta6060@gmail.com, www.ajantaprakashan.com

24. A Study of Performance of Khadi and Village Industries Commission in India

Dr. Vidyullata Rahul Hande
Associate Professor and Head, Department of Cost and Works Accounting, R.N.C. Arts, J.D.B. Commerce and N.S.C. Science College, Nasik-Road, Nasik, (Maharashtra).

Abstract

Under the Khadi and Village Industries Commission (KVIC) Act, 1956, Khadi and Village Industries Commission (KVIC), was established as a statutory organization under the Ministry of MSME's. The main objective was to promote and develop khadi and village industries for providing employment opportunity to rural population, to gear up rural economy by producing saleable articles and creating self-reliance amongst people and building up a strong community spirit. For last near about 65 years KVIC is actively working. It has implemented various schemes to provide employment to rural youth and artisans and to make their products saleable and marketable. The employment generation intensity of KVIC sector is remarkable.

The present paper is an attempt to study performance of Khadi and Village Industries Commission in India. The performance is studied on the basis of three variables namely, production, sales and employment. It also covers study of initiatives taken by KVIC in promoting Khadi and village industries.

Keywords: MSME's, KVIC, Khadi, Village Industry, Employment.

1. Introduction

The Micro, Small and Medium Enterprises sector is a dynamic and vibrant sector of Indian economy. For last five decades, it had contributed in the economic and social development of India. It has enhanced entrepreneurship and generated employment in a large scale at comparatively low capital cost. It was established under KVIC Act, 1956 (61 of 1956). The main objective of KVIC is to promote and develop khadi and village industries and to provide employment opportunities in rural area. To achieve these objectives KVIC was working actively, for last 65 years. Near about 2731 khadi institutions vast network implements the program of KVIC in India. 4.97 lakh people are engaged in these programs, out of which 80 percent are women artisans. Today KVIC have a vast network of 8 Departmental Sales outlets

(entitled as Khadi India), its 15 branches and 8035 sales outlets of khadi institutions across the country. The goods produced by khadi and village industries, are sold through these outlets. KVIC is performing for last six decades. Hence researcher has decided, to evaluate the performance of KVIC in India.

2. Objectives

1. To study fundamentals of KVIC.
2. To study and understand performance of Khadi and Village Industries.

3. Methodology

The present study is based on secondary data. The data was obtained from books, published papers, periodicals, journals, websites, MSME's annual reports, KVIC's official website. portals, GOVT. of India, Economic Survey of India, online database of Indian economy, articles, newspaper etc. various relevant statistical tools were used to analyze the data.

4. Review of Literature

M. Alaguraja, Dr. G. Nedumaran, and M. Manida stated in their article that, KVIC is charged with the dependability of hopeful and promoting research in the production techniques and equipment employed in the Khadi and Village industry sector and provided that facilities for the revision of the problems relating to it, including the use of non-conventional energy and emotional influence with a view to increasing productivity.' Dr. Dey Sanjeeb Kumar,(2014) conclude his article with , 'SMSE's contribute to economic development in various ways such as creating employment opportunities for rural and urban population, providing goods and services at affordable costs by offering innovative solutions and sustainable development to the economy as whole.' Garg Bhoomika (2014) concluded in the article as, MSME's is the major constituent sector in employment generation, production system, enhancing exports and GDP. But there is a need to carefully nurture and support this sector. Joint effort is needed from the Govt. and MSME's to acquire technological effectiveness.'

5. Khadi and Village Industries Commission (KVIC)

As per No. 61 of Khadi and Village Industries Commission Act, 1956, this commission was established, which is a statutory organization under the Ministry of Micro, Small and Medium Enterprises. The main objective was to promote and develop khadi and village industries for providing employment opportunity to rural population, to gear up rural economy by producing saleable articles and creating self-reliance amongst people and building up a strong

community spirit. KVIC provides training facility through its 35 Departmental and Non-Departmental Training Centers. KVIC also helps Khadi institutions by making available quality raw material.

KVI Commission's head office is located at Mumbai and it works through its six zonal offices located at New Delhi, Bhopal, Bengaluru, Kolkata, Mumbai and Guwahati and 44 field offices all over the country. There are two major constituents of KVIC, which are as follows:

1. Khadi sector
2. Village Industries Sector

6. Khadi Sector

Khadi: (Section 2(d)) of Khadi and Village Industries Commission Act, 1956, defined khadi as "khadi, means any cloth woven on handlooms in India from cotton, silk or woolen, yarn hand spun in India or from a mixture of any two or all of such yarns."

Khadi also called as khaddar, it is a hand spun and woven natural fiber cloth originates from eastern India and Indian subcontinent. In 1918, Mahatma Gandhi has started a movement for 'Khadi' as self-employment generation program for the population of rural India. After independence khadi became grand symbol of nationalism. Afterwards Khadi was popular not just as a piece of cloth, but as a symbol of freedom and self-reliance. There are more than 2737 khadi institutions, implementing various programs of KVIC all over the country and near about 4.97 lakh people engaged in this activity, out of which 80 percent are female artisans. Khadi products produced by the industries, institutions and units etc. are marketed by 'Khadi Gramodyog Bhandar and Bhavans', run by KVI institutions. There are 8 Departmental Sales Outlets (entitled as Khadi India) and 15 branches and 8035 sales outlet of khadi institutions throughout the India. From following table we can observe performance of khadi sector in last four years.

Table 1.1

Performance of Khadi Sector

Production, Sales and Employment

Sr. No.	Year	Production (in Crores)	Sales (in Crores)	Employment (in Lakhs)
1	2016-17 @	1520.83	2146.60	4.56
2	2017-18 #	1626.66	2510.21	4.65
3	2018-19 #	1963.30	3215.13	4.96

4	2019-20 #	2324.24	4211.26	4.97
5	2020-21# (up to 31-12-2020)	1344.69	1877.19	4.97
6	2020-21# (projected up to 31-3-2021)	2104.01	3856.50	5.00

Source: compiled from Annual Report of MSME 2020-21, Government of India.

@-including polyvastra # - including polyvastra and solarvastra

From Table 1.1, it reveals that, khadi sector has grown in last few years. Production of Khadi was increased every year from Rs. 1520.83 Crores in 2016-17 to Rs. 2324.24 crores in 2019-20 i.e 52 percent increase. Now a days, trend and demand of khadi cloths is on hike. Hence sale of khadi products is also increased. Increase in sales can also be observed from year 2016-17 Rs.2146.60 crores to year 2019-20 Rs 4211.26 crores i.e. 96 percent increase in four years. The basic social objective of KVIC is to provide employment in rural areas and to organize training programs for persons desirous of seeking employment in khadi and village industries. For last many years khadi was proved as a significant tool for employment creation in rural area.

7. Village Industries

Village Industries: Section 2(h) of Khadi and Village Industries Commission Act, 1956, defined Village Industry as, "Village Industry means,-

i. Any industry located in a rural area which produces any goods or renders any service with or without the use of power and in which the fixed capital investment per head of an artisan or a worker does not exceed (one lakh rupees) or such other sum as may, by notification in the official Gazette, be specified from time to time by the Central Government

Provided that any industry specified in the schedule and located in an area other than a rural area and recognized as a village industry at any time before the commencement of the Khadi and Village Industries Commission (Amendment) Act, 1987 (12 of 1987), shall notwithstanding anything contained in this sub-clause, continue to be a village industry under this Act:

Provided further that in the case of any industry located in a hilly area, the provisions of this sub-clause shall have effect as if for the words "one lakh rupees", the words "one lakh and fifty thousand rupees".

ii. Any other non-manufacturing unit established for the sole purpose of promoting, maintaining, assisting, servicing (including mother units) or managing any village industry."

The basic objective behind village industries is to enhance self-employment and self-reliance amongst rural people. For last near about 65 years KVIC is actively working to build up active rural and social community, to provide employment to rural youth and artisans, to make their products saleable and marketable, to uplift economically weaker section by providing opportunity of self-employment. The performance of village industries can also observed from following table.

Table 1.2

Performance of Village Industries

Production, Sales and Employment

Sr. No.	Year	Production (in Crores)	Sales (in Crores)	Employment (in Lakhs)
1	2016-17	41110.26	49991.61	131.84
2	2017-18	46454.75	56672.22	135.71
3	2018-19	56167.04	71076.96	142.03
4	2019-20	65343.07	84664.28	147.76
5	2020-21 (up to 31-12-2020)	53705.04	70454.28	150.31
6	2020-21 (projected up to 31-3-2021)	76582.43	101306.87	154.12

Source: compiled from Annual Report of MSME 2020-21, Government of India.

Table states that, the level of production of village industries is increasing from year 2016-17 Rs.41110.26 crores to year 2019-20 Rs. 65343.07 crores i.e. 59 percent increase in four years. Sales of products of village industries is also showing increasing trend. From year 2016-17 Rs. 49991.61 crores to year 2019-20 Rs. 84664.28 crores i.e. 69 percent increase in last four years. The performance of village industries employment is also satisfactory. Table shows that, employment level was increased from 131.84 lakhs in the year 2016-17 to 147.76 lakhs in 2019-20 i.e. 13 percent increase in last four years.

8. Conclusion

Performance of khadi sector and village industries can be observed from few percentages. Khadi sector shows increasing trend as, production increased by 52 percent. Sales increased

by96 percent, Employment is also increased from 2016-17 to 2019-20. Now a days, trend and demand of khadi cloths is on hike. Hence sale of khadi products is also increased. Village industries sector shows increasing trend as, the level of production increased by 59 percent, Sales increased by 69 percent and Employment also increased from year 2016-17 to year 2019-20. There is annual increase in khadi production, sales and employment. With this one can conclude that khadi and village industries performance is remarkable. In future, in the era of artificial intelligence KVIC have to face technological challenges. Hence for sustainable employment generation, KVIC should implement its scheme more dynamically.

9. References

1. Dr. Dey Sanjeeb Kumar (2014), 'An Assessment of Performance of MSME's in India: with special reference to Odisha', Siddhant-Journal of decision making, Dec 2014 issue, pp.1-8.
2. Annual Report 2020-21, Government of India, Ministry of Micro, Small and Medium Enterprises.
3. Bhuyan Ujjal (2016), 'A Study on the Performance of Micro, Small and Medium Enterprises in India', Global Journal of Management and Business Research: A Administration and Management, Vol.16, Issue 9, Version 1.0 pp.34-36
4. M. Alaguraja, Dr. G. Nedumaran, and M. Manida (2020), 'Performance of Khadi and Village Industries commission through Micro, Small, and Medium Enterprises', AEGAEUM JOURNAL, Vol. 8,Issue 3, pp.667-684.

Websites

1. www.mkgandhi.org
2. www.kvic.gov.in
3. www.legislative.gov.in
4. www.kviconline.gov.in

Peer Reviewed Refereed
and UGC Listed Journal

An International Multidisciplinary
Half Yearly Research Journal

ISO 9001:2008 QMS
ISBN / ISSN

ROYAL

ISSN - 2278 - 8158
Volume - X, Issue – I, June - November - 2021

Impact Factor 2019 - 5.756 (www.sjifactor.com)

Is Hereby Awarding This Certificate To

Dr. Vidyullata Rahul Hande

In Recognition of the Publication of the Paper Titled

Online Marketing: An Emerging Opportunity in Covid-19 Pandemic Period

Ajanta Prakashan,
Jaisingpura, Near University Gate, Aurangabad. (M.S.) 431 004
Mob. No. 9579260877, 9822620877 Tel. No.: (0240) 2400877,
ajanta6060@gmail.com, www.ajantaprakashan.com

Editor : Vinay S. Hatole

12. Online Marketing: An Emerging Opportunity in Covid-19 Pandemic Period

Dr. Vidyullata Rahul Hande
Associate Professor and Head, Department of Cost and Works Accounting, R.N.C. Arts, J.D.B. Commerce and N.S.C. Science College, Nasik-Road, Nasik, (Maharashtra).

Abstract

The waves of corona pandemic has devastated India economically as well as socially. It had impacted almost all segments of the economy. The industry sector across India witnessed a significant decline in growth rate due to impact of corona. Difficult time always create new opportunities and one can turn such bad time into opportunity. For marketers, online marketing is emerged as an opportunity in pandemic period. Through online and digital media, marketers can be in touch with their prospective buyer. The article focuses on concept of online marketing, channels or tools of online marketing, effect of pandemic on business sector, how online mode work as a good option of marketing. The article talks about online marketing and its significance in present pandemic scenario.

Keywords: Online marketing, offline marketing Industry sector, Covid-19, Pandemic period.

1. Introduction

The first and second wave of Covid-19 pandemic has devastated India economically as well as socially. It had impacted almost all segments of the economy. The industry sector across India witnessed a significant decline in growth rate compared to 2018-19 due to impact of corona. A huge population had lost their employment. Industrial workers were migrated to their hometowns in fear of pandemic. Everyone is in fear with the increasing cases, increasing deaths across the country. After reporting the first case in late Jan 2020 in the southern Kerala, today we are facing horrible picture of this pandemic. In second wave, India has passed 200000 deaths mark, which is about one in 16 of all Corona deaths across the world. But, world never ends, never stops. Everyday sun rises with new hope. Difficult time always create new opportunities for us and one can turn such bad time into opportunity. Though we are locked in our homes and finding it difficult to fulfill our daily needs, but online purchasing is the way to satisfy customer's needs. For industries online marketing is emerged as an opportunity in pandemic period. Through online, they can be in touch with their prospective buyer. The main objective of

this article is to study concept of online marketing, and how it is emerged as an opportunity in pandemic period and to study various channels of online marketing. This study also describes advantages of online marketing.

Objectives

1. To study online marketing concept, its challenges and tools.
2. To study the effects of pandemic on business sector.
3. To understand how online marketing can act as an opportunity in pandemic period.

2. Literature Review

Dr. Singh S.N. concluded his article as 'There is a need to change the marketing strategy of various companies from traditional marketing to digital marketing. If the companies does not use the digital platforms to market their products and services then they will lack the competition that exist in a perfect competition market and hence the future of the company cannot be assured and it will go in loss.' Atshaya s. & Sristy Rungta, quoted in their article, 'it refers to marketing or promotion of products, services or brands using digital media, or electronic media through various channels both online and offline like social media marketing, pay per click, search engine optimization, email marketing, content marketing, phone marketing, print ads, banners, digital advertising, television marketing radio advertising, gaming advertising etc.'

3. Online Marketing

Online Marketing is a set of tools and methodologies used for promoting products and services through internet. It includes a wide range of marketing elements than traditional marketing due to extra channels and mechanisms available on internet. It is also known as Web Marketing, Digital Marketing, and Internet Marketing. As the name suggests, it is the act of promoting goods and services through internet. It includes various concepts like, Social Media Marketing (SMM), Search Engine Optimization (SEO), Pay-per-Click Advertising (PPC), Search Engine Marketing (SEM). In online marketing, various channels, media and electrical gadgets are used for marketing and promotion of products or services. Online marketing is the use of digital channels to promote or market products and services to consumers and businesses. The significant advantage is, it reaches to large number of customers in very less time and it is also cheaper, thus it is time and cost efficient one. It helps in analyzing the effectiveness of campaign, as it provides a complete record of number of views, duration of views of any particular advertisement, feedback etc. Online marketing also helps in analyzing, buyers behavior.

4. Challenges of Online Marketing

There are many advantages of using online marketing tools to advertise products or services but there are some challenges that the marketer has to face. During this pandemic period these challenges are increased. Marketers has to identify the right viewers, develop a dynamic website, maintain consistency , should be active on social media, should maintain hygiene in supply chain, maintain two-way communication, getting customers trust, Manage Customers relationship.

5. Online Marketing Tools

Online marketing involves search engine marketing, email marketing, social media marketing and many other types of display advertising. There are multiple online marketing tools available namely, Social Network, Social Network Application, Social News, Online Favorites and bookmarking, Blogging, Email Marketing, SMS Marketing, Search Engines, Pay per Click Advertising, Press Release, Automated Inbound Marketing.

6. Pandemic's Effect on Business Sector

The waves of Covid-19 pandemic has disrupted India's business sector economically. It had impacted almost all segments of the economy. The industry sector across India witnessed a significant decline in growth rate compared to 2018-19 due to impact of corona. A huge population had lost their employment. A large population have seen their income cut and find it difficult to meet their daily needs. The International Monetary Fund (IMF) estimates that, the world economy was shrunk by 4.4 percent in 2020. It also added that the decline was as the worst since the depression of 1930's. Everyone is in fear with the increasing cases, increasing deaths across the country. In India, MSME's(Micro, Small, Medium Enterprises) creates more than 90 percent of the jobs, employing near about 114 million people and it has 30 percent contribution in GDP, is today at the stage of severe cash crunch. Many of these MSME's are bankrupt and facing financial crisis. If such situation continued for some time, many small industries will disappeared due to disturbance in cash flow. Hospitality sector had faced severe damages and had shut its doors worldwide. Tourism industry had lost billions of dollars in 2020-21. Travel industry is still far away from taking off due to lockdown. As the customers are staying at home, retail industry is also facing great fall. Though the customers are anxious to return to stores, but the lockdown stops them. Only pharmaceutical sector is on the winning position.

As per the report of Research Department of statista website, published on 11th June 2021, estimated cost of full lockdown is 26 billion USD, estimated impact on GDP (from Oct 2020 to Dec 2020) is 0.4 percent, Manufacturing sector shows -39.3 percent decrease (April

2020 to June 2020). Industrial workers were migrated to their hometowns in fear of pandemic. Due to migration of labor, manufacturing industry is at high risk of financial crisis. Small businesses are struggling with increasing cost of raw material, non-availability of labor .These few examples are alarming for industrial sector. Hence, to overcome from such situation, the manufacturers as well as service sector has to change their marketing strategy. Online marketing is a good way to gear up and channelize the business. Today near about 60-70 percent population have smart phones and they are connected on internet through various applications. So companies can approach the customers through net, advertise and sale their products, listen customers voice, solve their problems. Hence, in this pandemic scenario online marketing is an emerging opportunity.

7. Online Marketing as an Emerging Opportunity

In this pandemic scenario, online marketing is emerging as an opportunity to approach to customers. We can summarize the significance of online marketing to marketers as follows:

Online marketing is more affordable than traditional offline marketing methods. A social media campaign or an e-mail can forward marketing message to customers. It is cost saving marketing option than the TV advertisement. It provides quickly the market data, customer's response, rating is easy, easy market survey and research data. Marketers can monitor the frequency of viewers, what was viewed, how often and for how long, which products works which not, guess customers liking, can suggest, can recommend, offer discount or combo pack, can motivate to purchase. In online marketing, customers get thousand number of options, brands, sizes, colors, which is not possible in offline mode. Its customer's psychology, they spend more on online mode as compared to cash payment in offline mode. Spending cash in hand is a sad feeling for customer. So online shopping motivates them to purchase. Now a days, maintaining hygiene at outlet, preventing staff from infection, avoiding unnecessary crowd, sanitizing the environment, are very costly, time consuming and tedious task for marketers. Online marketing is a safe option in pandemic. Online marketing allows 24 hours and 7 days of service to the customers to purchase

8. Conclusion

In last one and half year the waves of Covid-19 pandemic has devastated India. It had impacted almost all segments of the economy. The industry sector across India witnessed a significant decline in growth rate compared to 2018-19[1] due to impact of corona. Hospitality sector had faced severe damages, travel and tourism industry had lost billions of dollars, the customers are confined at home retail industry is also facing great fall. Only pharmaceutical sector is on the winning position. In Covid-19 pandemic scenario, online marketing is emerging

as an opportunity to approach to customers. Through online and digital media, marketers can be in touch with their prospective buyer. Online marketing means promotion of services or products by using electronic media. There are various online marketing channels such as social media marketing, search engine optimization, email, phone, print media, television, radio, internet etc. As the world is rapidly transforming from traditional to digital. Customers are consuming more and more digital content. Corporates also have recognized this trend and have adapted online marketing strategies. Through online marketing, retailers and marketers can increase awareness about product or services. Online marketing is also helpful in analyzing the effectiveness of campaign, sale, demand etc. it also provides detail record of number of views, feedback, duration of views of any particular product and buyer behavior.

References

1. Yasmin,Tasneem, Fatema, "Effectiveness of Digital Marketing in Challenging Age : An Empirical Study", International Journal of Management, Science and Business Administration, Vol 1, Issue 5, April 2015,pp.69-80.
2. Soheila Bostanshirin, (Sept. 2014)'Online Marketing: Challenges and Opportunities', proceedings of SOCIOINT14-International conference on social science and humanities, Istambul , Turkey,pp.783-792
3. P. Sathya, "A Study of Digital Marketing and its Impact", International Journal of Science and Research, Vol 6, Issue 2, Feb 2017, pp.866-868.
4. Atshaya and Sristy Rungta, "Digital Marketing vs Internet Marketing: A detailed Study", International Journal of Novel Research in Marketing, Management & Economics, Vol-3, Issue 1 pp.29-33.
5. Dr.Singh, Pawan Kumar and Kumar Dubey, "Digital Marketing: Necessity and Key Strategies to Suceed in Current Era" pp. 14-19.

Websites

1. http://www.statista.com
2. http://www.business-standard.com
3. www.iec.edu.in
4. www.academia.edu.in

Sustainability, Agri, Food and Environmental Research, (ISSN: 0719-3726), 12(X), 2023: http://dx.doi.org/10.7770/safer-V12N1-art2802

The technique of writing a review article: Understanding the past for the management of future knowledge.

La técnica de escribir un artículo de revisión: Comprender el pasado para la gestión del conocimiento futuro.

Dr. Meenakshi V. Rathi *
P. G. Department of Chemistry, RNC Arts, JDB Commerce, NSC Science College, Nashik Road, Nashik. (Maharashtra) India
Affiliated to Savitribai Phule Pune University, e-mail: meenakship2@gmail.com
Phone No. +91 9403510314

ABSTRACT

A study of past, relevant material is a vital component of every academic research. In the era of rising numbers of research papers, review articles of good standard are often needed. A literature review aims to critically evaluate existing research data. Academic writing should not be shaped by technical jargon or limited to a series of tips and tactics aimed at a quick publishing. This brief contribution does not impose stringent regulations on academic publications, but rather helps potential authors prepare and improve their review papers to the advantage of a wide audience .Review articles might suggest new study directions and draw fresh conclusions from current data. Because reviews are important for evaluating results, the value of one is related to the results that have been discovered, as well as how these findings are presented. The issue of "why" is most crucial when writing a review, not "how." One of the primary and essential reasons for composing a review is to assemble an informative synthesis of the most superior resources.

Key Words: Scientific review, Academic research, Analysis of literature, Research papers.

RESUMEN

Un estudio del material relevante del pasado es un componente vital de toda investigación académica. En la era del creciente número de trabajos de investigación, a menudo se necesitan artículos de revisión de buen nivel. Una revisión de la literatura tiene como objetivo evaluar críticamente los datos de investigación existentes. La escritura académica no debe estar moldeada por una jerga técnica o limitada a una serie de consejos y tácticas destinadas a una publicación rápida. Esta breve contribución no impone normas estrictas a las publicaciones académicas, sino que ayuda a los autores potenciales a

preparar y mejorar sus artículos de revisión en beneficio de una amplia audiencia. Los artículos de revisión pueden sugerir nuevas direcciones de estudio y sacar nuevas conclusiones a partir de los datos actuales. Debido a que las revisiones son importantes para evaluar los resultados, el valor de una está relacionado con los resultados que se han descubierto, así como con la forma en que se presentan estos hallazgos. El tema del "por qué" es más crucial al escribir una reseña, no el "cómo". Una de las razones principales y esenciales para componer una revisión es reunir una síntesis informativa de los recursos más superiores.

Palabras clave: Revisión científica, Investigación académica, Análisis de literatura, Trabajos de investigación.

INTRODUCTION

A review article is a survey of previously published research on a topic. A good review is thorough and focused on ideas. The primary goal of writing a review is to generate a legible summary of the best materials available.in the literature for a critical research question or a hot topic in the field.(Conn & Coon Sells, 2014) Unlike an original research article, it will not present new experimental data. Reorganisation of existing facts, rather than the review article may be seen as an original publication, by some. A study scientist's "not-original" attitude is understandable.(Wright et al., 2007) Review studies do not provide new data to the literature. It has a topic, a beginning, a logical development of the theme, and an end. A good literature review can convey a tale. It must start with a key idea and then take the reader on a journey, detailing it from basics to advanced concepts.(Short, 2009) Review articles are similar to class notes combined into one enormous file - but the author must never take the reader for granted and must start with the basics, progressively unravelling the intricacies. They give us new perspectives on old issues. They innovate and increase novel knowledge in this way.

Chapter 1

Strategies of writing the review article:

- Writing an article may be done primarily to emphasise one's own or others' scholarly efforts.
- This is fine as long as it is stated explicitly.
- For each article in the references, the data supporting the reported conclusion should be scrutinised.

- It should be determined if there is an alternate interpretation consistent with the data presented or other data that differs from the authors' interpretation.(Siwek et al., 2002)
- Reconsiderations of data are particularly relevant in light of subsequent changes.
- Each section, and even each paragraph, should convey a key point to the article's ultimate goal.
- he field's conceptual framework and the review article's contribution to its advancement should always be clear.
- Controversies should be highlighted, with an emphasis on their origins and resolutions.
- Ultimately, the analysis should assist the synthesis of data and concepts reflected in the model given.(Sanders, 2020)
- No one research approach, journal, or geographic area is covered in a comprehensive assessment.
- What has been done, what has been discovered, and how these findings are presented determine the usefulness of a review? When starting to write a review, the question of "why" comes first and then "How". (Gülpinar & Güçlü, 2013).

Chapter 2

Troubleshooting Guidelines for the authors:

A good review builds a solid basis for learning. It helps build theories, solves research gaps, and exposes research needs. A scientific review article should be viewed as a scientific endeavour employing scientific procedures.(Taylor, 2012) A summary of the criteria for including and excluding non-cited articles should be supplied. Authors and editors should include a section explaining how the review's sources were found. A modern literature review may include an Internet survey. (Sasson et al., 2021) Provide a list of databases and search phrases used. There is an abundance of scientific material available, and it might be intimidating to examine it systematically. Understanding motivation in scientific review writing is critical. You should not claim authorship unless you believe that publishing the article would result in a better understanding of a discipline and an original contribution to the literature based on your own informed perspective. Other factors exist, but if they dominate, the review article is likely to be flawed.(Wright et al., 2007). Readers would then perceive that the article is more of a promotional advertisement than a review.

Potential authors are also scholars who have conducted a literature review before to starting a project and built theoretical models based on this review. (García-Granda, 2013) There are two categories of reviews. First, authors could tackle a mature issue requiring

analysis and synthesis of existing research. They would then provide a conceptual model that synthesises and extends prior research. Second, authors could address a new subject that would benefit from theoretical grounding. The literature review on the emerging issue would have to be shorter here. The author's contribution would be to build new theoretical underpinnings for a conceptual model.

Chapter 3

Meticulous writing techniques:

As a reviewer, organise the material so that your review functions as a useful ‘guidebook'. Creating schematic maps and classifications might help readers visualise a field's evolution and discover relevant papers. A review paper should have a solid plot to engage the reader. Introduce the topic with a compelling problem statement that piques the reader's curiosity. Then take the reader on a journey that gently reveals the problem's origin. Always start with the essentials. Use visuals and words to illustrate ideas. Schematic charts and diagrams help illustrate difficult-to-understand theories, keeping the reader involved and helping them grasp the theory. Analyse the literature as a scientist, you must integrate data from various sources and comprehend its broader implications.(Paul & Criado, 2020) Comparing and contrasting research often reveals hidden scientific paths. No single study can reveal these patterns. These minor writing techniques are identified and interpreted in a literature review report to generate new research ideas and hypotheses.

Chapter 4

Scientific Steps for drafting a review article:

A literature review is not simply a summary of published research because every study is unique and the findings and interpretations may vary. Rather, a review can point out gaps or contradictions in the literature. So, attempt to produce a review that conveys what is ‘clear' and what is still ‘mysterious'.

To write flawless review article, the scientific steps are (Mondal, H., & Mondal, 2019)

1 .Keep it simple. Assume your audience isn't an expert.

2. Use referencing software - no article is perfect on the first draught. Learn this skill to make life easier.

3. Get the review outline correct — your review will likely require numerous iterations, and a good outline can help.

4. Always provide the finest quality pictures and design the schematics as best you can

5. The opportunity to write a literature review is serious.

6. When conducting a literature review, differentiating good research from bad research and relying on the outcomes of the better studies is an important aspect of the review process.(Sharma & Singh, 2011) This strategy decreases the workload.

This is a great way to start your study as well as get your article published. Having a thorough grasp of the field you will be working on beforehand greatly speeds up your development. This can help keep the article as a living document. It would organise the periodic updating of the article with fresh content and revisiting older facts.

Chapter 5

Approaches to writing reviews:

Review articles come in many forms. We all know the traditional types. Systematic reviews and Chronological reviews are the two main categories of review papers. A Chronological review offers the facts and statistics in an easy-to-follow format, so we can comprehensively assess the subject matter. While it is correct to say that systematic reviews are done on a specific topic, it is incorrect to say that such studies are carried out on selected issues. A systematic review is formed by including both qualitative and quantitative reviews. As well, considerable literature study is performed in both cases. The collection and statistical analysis of study data are commonly used in quantitative reviews (eg. in a meta-analysis). .

Systematic reviews of relevant studies can provide the best information for not only academicians but also clinicians.(Pautasso, 2013).This includes: (1) summarising a large amount of literature; (2) resolving literature conflicts; (3) evaluating the need for a large clinical trial; and (6) increasing the statistical power of smaller studies.(Harris et al., 2014)

Chapter 6

Significance of writing the review article:

Writing a literature review,

- Explain the current level of knowledge ,
- Identify gaps in existing studies for prospective future research ,
- Highlight the primary methodology and research strategies and
- Also allows you to critically evaluate and arrange current research.(Harris et al., 2014)

Many publications, including some of the most prominent, publish review articles routinely, if you write a meaningful, well-organized essay in good English. The fact that

almost every magazine publishes reviews helps the new author. , if you keep seeking publication, you should ultimately see it in print.(Mulrow, 1987) People who have finished or made significant progress on a research stream are well positioned to tell their colleagues what they have learned and where the field can most profitably focus its efforts.(Riordan, 2012).

Good review methods are important since they give the reader an unbiased perspective on the subject.(Ogunsolu et al., 2004) A review should be prepared in a systematic manner, according to popular beliefis commonly observed. The research methodologies must be clearly stated in a systematic review with a focused question. The best way for determining the optimum working style for a research project is to use a 'methodological filter.' Finally, when writing a review, it is best to be concise, to keep a firm focus on fixed concepts, to approach the literature in a procedural and analytical manner, and to articulate your self-discoveries in an appealing manner.(Lexchin et al., 2003)

Chapter 7

Adversity and Endurance in review writing:

While the prospect of writing a review is appealing, it is critical to devote time to identifying the most important issues. It has been observed that the act of beginning to write an article and getting right to it appears to be quite attractive, but identifying the challenging points in your review won't be a waste of time. Despite having agreed upon a systematic review design, it was determined that the majority of the studies that were expected to follow this design failed to meet this agreement. (Carver et al., 2011) .One out of every four studies that were assessed did not apply suitable procedures of describing, evaluating, or synthesising evidence.(Daldrup-Link, 2018). Non-systematic reviews utilise old research that has been gathering dust for years, along with your colleagues' recommendations. Reviews, in contrast, take into consideration the time and effort required to identify and review the best possible research.(Cargill, M., & O'Connor, 2021).The question that must be answered requires an array of techniques and delivers the most effective outcomes when multiple approaches are employed. (Lorés-Sanz, 2011) Some yet slightly distinct studies can be synthesised to better answer critical concerns. Set aside time to come up with a solution to a problem that interests your peers in the same field. As we are drawing on research in order to resolve specific challenges, we can potentially deal with two issues at once.

As conclusions, with the foregoing, it may reasonably conclude that reading, reviewing, and writing for imaging literature are all worthwhile endeavours.(Beyea & Nicoll, 1998) As a critical reader and reviewer, it is crucial to remember to read selectively and critically.(Ng, K. H., & Peh, 2010) .With regard to producing a review article, you

should be able to indicate the steps to be achieved as follows: see the matter from a large perspective, and get rid of entrenched notions and obsessions from your head. A critical approach, along with a methodological attitude, should be taken when researching papers in the literature. (Pautasso, 2013) Data should be conveyed in an interesting way. Presents conclusions and implications for researchers and managers. To produce findings based on the best available scientific data and evidence, a systematic review is done. To lift the standard for non-systematic narrative expert opinion evaluations, a systematic method to a critical review of all the relevant evidence will be employed.

REFERENCES

Beyea, S. C., & Nicoll, L. H. (1998). Writing an integrative review. *AORN Journal*, *67*(4), 877–880. https://doi.org/10.1016/S0001-2092(06)62653-7

Cargill, M., & O'Connor, P. 2. (2021). *Writing scientific research articles: Strategy and steps.* John Wiley & Sons.

Carver, J., Dellva, B., Emmanuel, P., & Parchure, R. (2011). Ethical considerations in scientific writing. *Indian Journal of Sexually Transmitted Diseases and AIDS*, *32*(2), 124. https://doi.org/10.4103/2589-0557.85425

Conn, V. S., & Coon Sells, T. G. (2014). Is It Time to Write a Review Article? *Western Journal of Nursing Research*, *36*(4), 435–439. https://doi.org/10.1177/0193945913519060

Daldrup-Link, H. E. (2018). Writing a review article - Are you making these mistakes? *Nanotheranostics*, *2*(2), 197. https://doi.org/10.7150/NTNO.24793

García-Granda, S. (2013). Writing science: how to write papers that get cited and proposals that get funded. *Crystallography Reviews*, *19*(1), 53–54. https://doi.org/10.1080/0889311x.2013.769529

Gülpinar, Ö., & Güçlü, A. G. (2013). Derleme makalesi nasil yazilir? *Turk Uroloji Dergisi*, *39*(SUPPL. 1), 44–48. https://doi.org/10.5152/tud.2013.054

Harris, J. D., Quatman, C. E., Manring, M. M., Siston, R. A., & Flanigan, D. C. (2014). How to write a systematic review. *American Journal of Sports Medicine*, *42*(11), 2761–2768. https://doi.org/10.1177/0363546513497567

Lexchin, J., Bero, L. A., Djulbegovic, B., & Clark, O. (2003). Pharmaceutical industry sponsorship and research outcome and quality: Systematic review. In *British Medical Journal* (Vol. 326, Issue 7400, pp. 1167–1170). BMJ Publishing Group.

https://doi.org/10.1136/bmj.326.7400.1167

Lorés-Sanz, R. (2011). The construction of the author's voice in academic writing: The interplay of cultural and disciplinary factors. *Text and Talk*, *31*(2), 173–193. https://doi.org/10.1515/TEXT.2011.008

Mondal, H., & Mondal, S. (2019). Strategy to improve English language in scientific writing. *Medical Journal of Dr. DY Patil Vidyapeeth*, *12*(5), 475.

Mulrow, C. D. (1987). The medical review article: state of the science. *Annals of Internal Medicine*, *106*(3), 485–488. https://doi.org/10.7326/0003-4819-106-3-485

Ng, K. H., & Peh, W. C. (2010). Writing a systematic review. *Singapore Medical Journal*, *51*(5), 362-366.

Ogunsolu, O. O., Wang, J. C., & Hanson, K. (2004). *Writing a Review Article: A Graduate Level Writing Class*. https://doi.org/10.1021/acs.jchemed.7b00838

Paul, J., & Criado, A. R. (2020). The art of writing literature review: What do we know and what do we need to know? *International Business Review*, *29*(4), 101717. https://doi.org/10.1016/j.ibusrev.2020.101717

Pautasso, M. (2013). Ten Simple Rules for Writing a Literature Review. In *PLoS Computational Biology* (Vol. 9, Issue 7, p. e1003149). Public Library of Science. https://doi.org/10.1371/journal.pcbi.1003149

Riordan, L. (2012). Modern-day considerations for references in scientific writing. *Journal of the American Osteopathic Association*, *112*(8), 567–569. https://doi.org/10.7556/JAOA.2012.112.8.567/XML

Sanders, D. A. (2020). How to write (and how not to write) a scientific review article. *Clinical Biochemistry*, *81*(November 2019), 65–68. https://doi.org/10.1016/j.clinbiochem.2020.04.006

Sasson, A., Okojie, O., Verano, R., Moshiri, M., Patlas, M. N., Hoffmann, J. C., Hines, J. J., & Katz, D. S. (2021). How to Read, Write, and Review the Imaging Literature. *Current Problems in Diagnostic Radiology*, *50*(2), 109–114. https://doi.org/10.1067/j.cpradiol.2020.01.002

Sharma, B. B., & Singh, V. (2011). Ethics in writing: Learning to stay away from plagiarism and scientific misconduct. *Lung India : Official Organ of Indian Chest Society*, *28*(2), 148. https://doi.org/10.4103/0970-2113.80337

Short, J. (2009). The art of writing a review article. In *Journal of Management* (Vol. 35, Issue 6, pp. 1312–1317). https://doi.org/10.1177/0149206309337489

Siwek, J., Gourlay, M. L., Slawson, D. C., & Shaughnessy, A. F. (2002). How to write an evidence-based clinical review article. *American Family Physician*, *65*(2), 251–258.

Taylor, R. B. (2012). How to Write a Review Article. *Medical Writing*, 143–159. https://doi.org/10.1007/978-1-4419-8234-6_6

Wright, R. W., Brand, R. A., Dunn, W., & Spindler, K. P. (2007). How to write a systematic review. *Clinical Orthopaedics and Related Research*, *455*, 23–29.

Received: 23th January 2022; Accepted: 12th April 2022; First distribution: 12th May 2022.

IMPACT OF COVID-19 PANDEMIC IN INDIAN ECONOMY*

BY

Dr. Govardhane Sachin Ranu♣
Asst. Prof. Dept. of Geography V. V. Mandal's S. G. Patil Arts, Science & Comm. College, Sakri, Dhule, Maharashtra'sachingovardhane@gmail.com

Dr. Borase Sudhakar Jagannath♣
Asst. Prof. Dept. of Geography, G. E. Society's RNC Arts, JDB Comm. & NSC Sci. College Nashik Road, Maharashtra. borasesudha@gmail.com

Abstract:
The epidemic of Covid – 19 has spread not only across the country but all over the world and its outbreak is an unprecedented blow to the Indian economy. The Government of India has announced a number of measures to address the situation, ranging from additional funding for food, security and healthcare to sector-related incentives and tax extensions. The long-term nationwide lockdown, the global economic downturn, and the relative disruption of supply and demand chains have left the economy facing a long period of recession and are likely to continue to do so. This study has shown the potential impact of the shock on various sectors such as the manufacturing sector. This research paper seeks to present a set of policy recommendations for financial services, banking, infrastructure, Indian agriculture, real estate, other services and specific sectors.

Keywords: Covid – 19, Indian Economy, Varies sectors.

Received 06 June 2021, Accepted 20 June 2021, Published 26 June 2021
♣Correspondence Author: Dr. Govardhane Sachin Ranu

1. Introduction:

Outbreaks of the corona virus pose a serious threat to billions of people worldwide. In addition to being detrimental to human health, global trade is affecting the entire economic system and trade and commerce worldwide. The first outbreak of the disease occurred in December 2012 in Wuhan, China. The World Health Organization (WHO) is fully monitoring its global threat and thus it is declaring 30 January 2020 as a public health emergency of international concern. The virus began to spread at an unprecedented rate in various countries around the world on March 11, 2020, forcing the WHO to declare it an epidemic, now the whole world is facing this useless and harmful enemy. Many countries are under lockdown and everything has come to a standstill, including normal life, social and social conditions. The first case of corona virus was reported in Kerala on January 30, 2020. As many patients were found in different cities of India, on 24th March 2020, the Government of India declared

a lockdown in every corner of the country and took necessary action. The metropolises of Delhi, Mumbai, Ahmadabad Kolkata, Chennai are densely populated which has given rise to a spurt in cases of covid-19 and these cities are the engines for growth and development of Indian Economy

2. Objectives:

The entire business world is in the cycle of the corona virus. As the virus is having a severe and rapid effect, companies need to come up with appropriate strategies to deal with this difficult situation. Therefore, the objectives of this study are as follows.

1. To understand the impact of Covid – 19 on the Indian economy.
2. To find out the challenges for different sectors in Indian economy
3. To create awareness among the people about impact of Indian economy due to Covid – 19.

3. Sources of Research Papers:

The study is descriptive nature. Secondary Sources such as Books, Research Journals Magazines, Internet and Daily News papers.

4. Impact of COVID-19 in Various Indian Sectors:

Covid-19 has set foot in India and has taken the country into a major crisis. Corona virus disease has become a world-changing phenomenon and is not only a humanitarian crisis but also an economic and social crisis. This affects the business environment and it grows worldwide and many times over. Due to the rapid spread of the corona virus, a number of factors are bound to limit their business operations, which hinders the economic functioning of many industries that contribute to growth. The impact on different sectors of the economy is highlighted below.

4.1 Primary Sector:

Primary sector includes information and manufacturing and raw material related industries. The sector employs about 43.21% of India's population and contributes about 16.1% of Indian GDP. It supplies raw materials to the secondary sector and provides the basic necessities of human life.

4.1.1. Agricultural industry:

Travel restrictions for lockdowns in the agricultural sector have led to a shortage of agricultural workers, leading to a decline in production. Also, the lockdown period (epidemic) all over the country (or across the continent) is consistent with the harvest season of the "Rabi" crop, but due to the shortage of labor, the crop remained in the field without any problems. The markets for the raw materials used

for this have gone down and so have the complaints of the farmers. The revenue of tea-based industries has declined significantly as most of their production is now being exported.

4.1.2. Mining Industry:

Outbreaks appear to be exacerbated by the overall demand for metals and minerals all over the country (or continents), which has led to lower rates. Mining firms have also seen their share prices fall sharply.

4.2 Secondary sector:

The secondary sector employs about 24.89% of the population and accounts for 29.6% of Indian GDP. It embraces industries engaged in the production and distribution of manufactured goods or construction activism, which provides support to both the primary and service sectors.

4.2.1. Manufacturing Industries:

The manufacturing industries are picking up the brunt of the corona virus as they discontinue their production in a short time. The value of the goods in the production center or warehouse of these industries has come down and the machines have been idle for a long time. The biggest hurdles that industries faces are cash flow disruptions and supply chain disruptions.

4.2.2 Automobile Industry:

With almost all plants shut and imports being sealed up, there is a steep decline n production and sales of the automobile companies impelling them to declare pay cuts The situation will be awful even during post lockdown period due to fall in income levels

4.2.3 Textile and Apparel Industry:

This industry is workplace for over 45 million people in the country but temporary closure of production units has increased their hurdles leading to lay-offs. The terminations of exports and imports have adverse impact on the spinning mills in India as the exports of fabne, yam and other materials have disrupted.

4.2.4. Pharmaceutical and Chemical Industries:

These industries are heavily dependent on imports of large quantities of drugs and raw materials from China. Import restrictions also affect these industries.

4.2.5. Electronic Industry:

The finished goods and raw materials used in this industry are mainly supplied to China. The spread of the corona virus has reduced the good production and sales of electronics and also disrupted the supply chain.

4.2.6. Solar Power Industry:

Solar power project builders depend on Chinese imports. About 80% of the solar modules and solar cells used in India are from Chinese manufacturers. Thus Indian solar project developers began to face a shortage of raw materials and their stocks were limited.

4.3 Service Sector:

About 31.9% of the population is employed in the service sector which accounts for 54.3% of Indian GDP.

4.3.1. Tourism and Hospitality Industries:

Tourism and hospitality is the biggest industry in the corona virus crisis and the most important industry to resume this initiative. The lockdown has hampered the flow of tourists, hitting the tourism and hospitality industries.

4. 3.2. Transportation Segment:

Outbreaks appear to be exacerbated during this time of year. Airlines, cruise and road cargo operators have been hit hard by border closures and travel restrictions. Some airlines are not even in a position to refund their customers for flights canceled due to lockdown.

4.3.4. Healthcare Segment:

According to FIICCI, the healthcare department is at the center of this global test. Demand for this specialty has grown significantly as a result of recent corporate scandals. Private hospitals are available to provide the government with all the help it needs.

4.3.5. IT Segment:

IT segment is reeling under corona virus crisis as there is immense dwindle in global deal activities as well as growth rate. They are downsizing their work force to tussle with the presence scenario.

4.3.6. BFSI Segment:

- S.J. Borase and S. K. Shelar (2017) Environmental Impact on Human Health-A study in Medical Geography Research paper
- S.J. Borase and S.K. Shelar (2019) Comparative study of infected patients with malaria and dengue in Nashik District Research paper. Electronic Interdisciplinary International Research Journal (EIIRJ) Volume – VII, Special Issue – XIV pp.11 -21
- S.J. Borase (2020) Impact of Covid -19 on the Rural Life Research Paper AJANTA Prakashan. Volume – IX, Issue III, July- sep, pp 36-40
- V.J Kamble & S.J. Borase (2020) State wise Depiction of Covid – 19 in India Research Paper AJANTA Prakashan Volume – IX, Issue III, July- sep, pp 59-64
- Daily News paper- Times of India, Lokmat Times, Divya Marathi

AFFECTED PEOPLE OF DENGUE IN NASHIK DISTRICT*

BY

Dr. Nigale Chintaman Bhaguji♣
Asst. Prof. & Head ,Dept. of Geography, KGDM Arts, Commerce & Science College, Niphad, Nashik. Email Id- chintamannigale2010@gmail.com

Dr. Shelar Suresh Kautik♣
Asst. Prof. & Head. PG Dept. & Research centre of Geography, G.E.T. Arts, Comm. & Sci. College, Nagaon, Dhule. Email Id- dr.skshelar@rediffmail.com

Dr. Borase Sudhakar Jagannath♣
Asst. Prof. Dept. of Geography, RNC Arts, JDB Comm. & NSC Sci. College Nashik Road, Maharashtra. Email Id- borasesudha@gmail.com

Abstract:
In India the highest dengue cases in the year 2015 total 99913 and 220 second highest deaths have been reported. During 2012, 50222 cases and 242 deaths and during 2013, 75808 cases and 193 deaths were reported. And lowest during 2002, 2139 cases and 35 deaths were reported Highest number of deaths were reported by Kerala in 2003 (68) followed by Tamil Nadu in 2012 (66). Delhi 65 in 2006 and 60 in 2015 then Maharashtra 59 in 2012, 56 in 2005 and in 2014, 54 deaths have been reported. In Maharashtra has recorded 54 Dengue positive cases in 2001 and 4936 positive cases in 2015 and total Dengue deaths 2 and 23 respectively. The highest positive cases were reported in the year 2014 were 8573 and lowest were 54 in 2001. Then there was a growing number of Dengue positive cases from 2001 to 2015, 370 in year 2002, 772, in 2003, 856 in 2004 In 2005, however, it stabilized to a low of 349 and later again it increased in 2006 ,were 736, 2007, were 830 , in year 2007 were 910, After that the number of Dengue cases was more than 1000 in all the years from 2009 to 2015 e.g. 1224, 1489, 1138 2931, 5610 8573 and 4936 respectively Nashik reported the 11 positive cases in 2001, after that Thane district reported 86 Dengue positive cases in 2002, again Thane and Nashik district was highest cases reported in 2004, there were 88 Dengue positive cases in Thane district. In 2006, there were 115 Dengue positive cases in Thane district and 112 in Nashik district,

Keywords: Dengue favor, positive cases, total deaths

Received 02May 2021, Accepted 11May 2021, Published 17May 2021
♣ Correspondence Author: Dr. Nigale Chintaman Bhaguji

INTRODUCTION:

In this research paper I have tried to get the information about The Affected People of Dengue in Nashik District. In the last few years, many positive cases and people died due to dengue favor in the Nashik district, and according to reports and Taluka Wise of blood sample test and positive cases of Dengue in Nashik district during 2011-2017. As well as Dengue high risk villages, total positive cases and total deaths due to Dengue had shown in this paper.

METHODOLOGY:

The methodology of present work will includes primary and secondary data the collection of data regarding the Dengue various methods will be adopted. I visited some government and private Hospitals continuously to know the information from hospitals staff and patients through the dialogues and interviews through the questionnaires methods, and observations. And the secondary data collected through health department, medical bulletins, such as District malaria office and Government hospital in Nashik.

OBJECTIVES:

- To identify the situation and existing knowledge of Dengue in Nashik District.
- To assess the awareness regarding Dengue among people in Nashik district.

STUDY AREA:

Nashik district lying between 19°35’18” North latitude to 20°53’07” North latitude and 73°16’07” East longitude to 74°56’27” East longitude, with an area 15530 sq.km The total population of the district was 6107187 as per the census of 2011. Nashik is bounded on the North-West by the Dangs and Surat districts of Gujarat state, on the North by the Dhulia district, on the East by the Jalgaon and Aurangabad district, on the south by the Ahmadnagar district and towards South-West by the Thane district. The district comprises 15 talukas like Nashik, Peth, Surgana, Trimbak, Igatpuri, Sinner, Niphad, Dindori, Kalvan, Satana, Malegaon, Devla, Chandwad, Nandgaon and Yeola. Nashik district covers 5.05% area of Maharashtra

Study area Map:

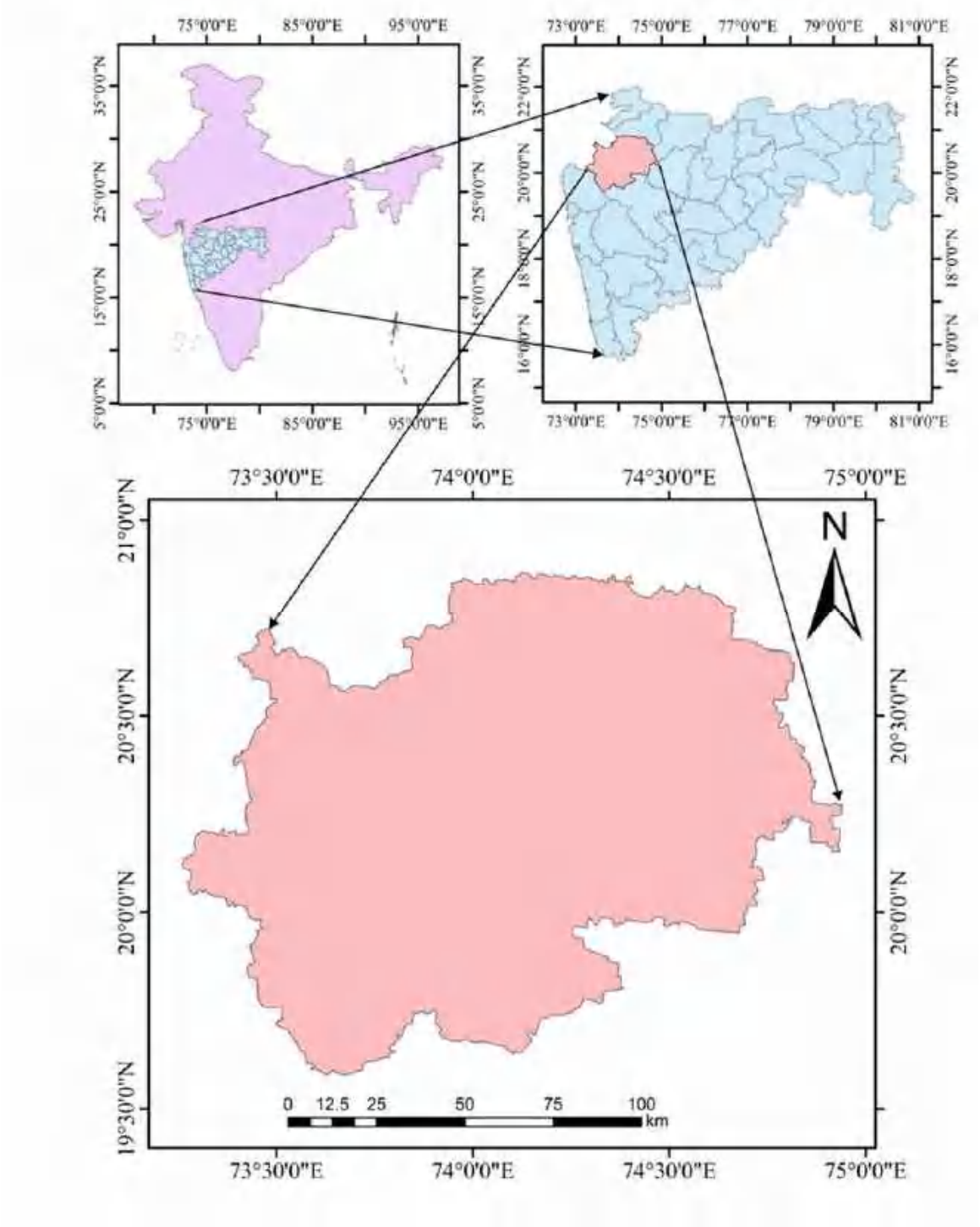
75°0'0"E
85°0'0"E
95°0'0"E
35°0'0"N
25°0'0"N
15°0'0"N
5°0'0"N
73°0'0"E
75°0'0"E
77°0'0"E
79°0'0"E
81°0'0"E
22°0'0"N
20°0'0"N
18°0'0"N
16°0'0"N
73°30'0"E
74°0'0"E
74°30'0"E
75°0'0"E
21°0'0"N
20°30'0"N
20°0'0"N
19°30'0"N
N
0 12.5 25 50 75 100
km

DENGUE SITUATION IN NASHIK DISTRICT:

Table No.1 Nashik District Dengue Outbreak Information from 2001 to 2017

Year	Positive	Death
2001	106	04
2002	68	02
2003	88	10
2004	43	01
2005	38	07
2006	94	04
2007	301	00
2008	87	03
2009	75	00
2010	67	01
2011	34	03
2012	313	11
2013	458	06
2014	698	09
2015	425	00
2016	1216	06
2017	1043	01

Source: District Government Hospital Nashik

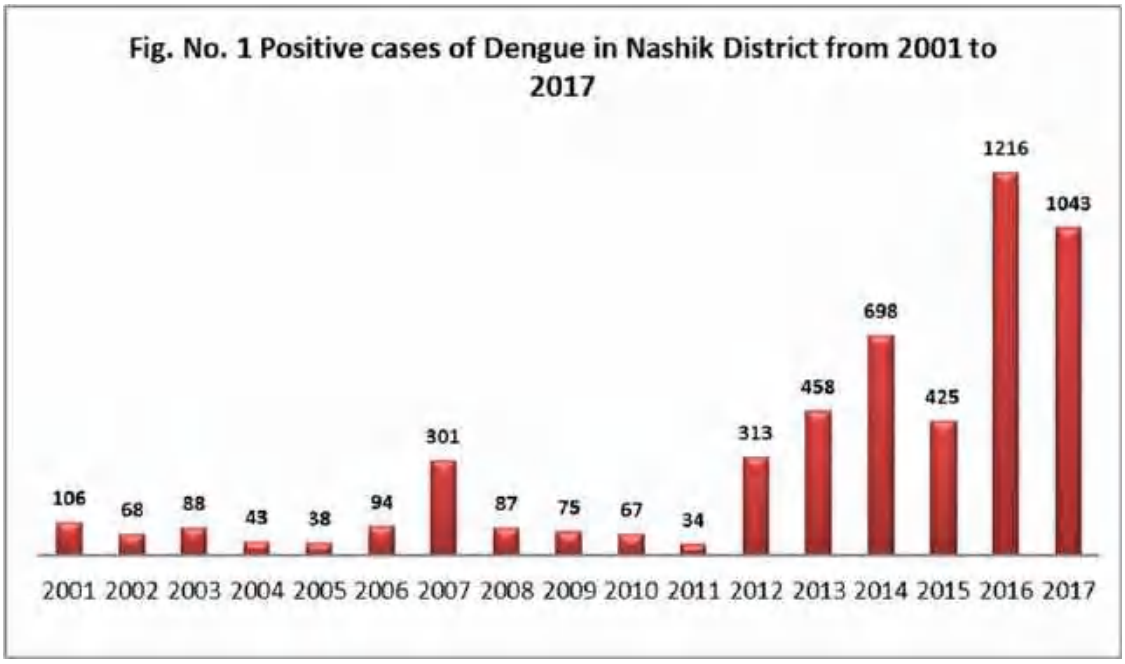

Above the figure No 1. shows the Nashik District Positive cases of Dengue information from 2001to 2017. In the year 2016 and the year 2017 the highest numbers of cases were positive and it was 1216 and 1043 respectively. As per the descending order of 698 in 2014, 458 in 2013, 425 in 2015 and there were 313 Dengue positive cases in year 2012. The lowest in 2001, there were only eleven positive cases in Dengue from 2002 to 2011, the Dengue positive cases were below 100. In 2006 alone, there were potentially over 112 cases of Dengue.

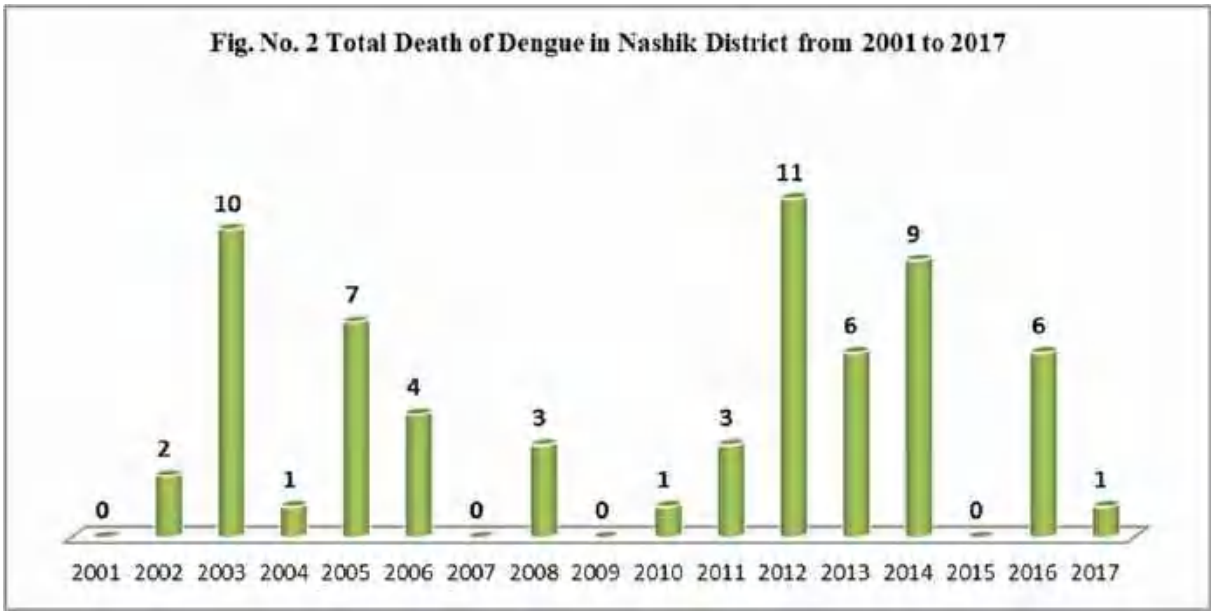

Figure No. 2 shows the Nashik District Total deaths of Dengue year 2001 to 2017. In 2012, the highest numbers of death were recorded and it was eleven. After that, in the year 2003 and 2014 there were ten and nine deaths respectively due to Dengue. In the year 2005 seven deaths in the year 2013 and 2016, 6 deaths each were due to Dengue. Four persons in 2006, three person's death 2008 and 2011. And only one person died due to Dengue in the year 2004, 2010 and 2017. And the years 2001, 2004, 2009 and 2015 even there was a Dengue infected persons but there was no deaths in this period due to Dengue.

Sr. No	Taluka	2001	2002	2003	2004	2005	2006	2007	2008	2009	2010	2011	2012	2013	2014	2015	2016	2017
1	Chandwad	10	6	8	5	3	4	18	8	7	5	3	33	41	48	23	78	58
2	Niphad	5	3	4	4	1	3	19	5	4	6	2	12	25	33	22	52	42
3	Nandgaon	8	4	8	4	3	9	24	6	6	4	3	38	40	58	33	105	88
4	Yeola	8	4	7	4	4	6	21	8	7	7	2	41	46	68	51	102	98
5	Malegaon	12	8	11	5	5	10	41	11	9	8	4	44	52	82	54	184	147
6	Sinnar	11	7	6	6	4	9	30	8	7	7	3	29	49	68	41	156	145
7	Satana	3	2	3	1	1	3	10	3	3	3	3	12	21	38	33	72	66
8	Peth	3	3	3	3	2	4	12	2	2	1	0	6	15	22	12	30	30
9	Surgana	2	2	3	0	2	4	10	3	3	2	0	5	16	28	14	44	28
10	Trimbak	5	5	5	1	1	4	14	3	3	4	2	7	18	28	21	38	33
11	Deola	4	4	4	1	1	4	18	5	4	4	2	9	12	33	28	44	38
12	Dindori	9	5	6	2	2	4	13	4	3	2	2	9	18	27	12	42	38
13	Igatpuri	3	3	4	1	2	5	11	3	3	2	1	14	23	32	9	38	33
14	Kalwan	2	2	4	0	1	7	12	4	3	4	2	8	18	26	11	30	31
15	Nashik	21	10	12	6	6	18	48	14	11	8	5	46	64	107	61	201	168
	Total	**106**	**68**	**88**	**43**	**38**	**94**	**301**	**87**	**75**	**67**	**34**	**313**	**458**	**698**	**425**	**1216**	**1043**

Table No. 2 Positive Cases of Dengue in Nashik District from 2001 to 2017
Source: District Government Hospital Nashik

Table no. 2 shows statistics of positive Dengue cases in Nashik district for the 17 year period from 2001 to 2017. The highest number was 1216 in 2016 and 1014 positive cases were recorded in 2017. In 2011, only 34 positive cases were reported in the entire Nashik district. And in particular, of all the talukas, Nashik Taluka has more Dengue patients than other talukas.

In the year 2001, 21 of 106 Nashik and two of the lowest Surgana, ten in 68 positive cases in 2002 and two in Satana, Surgana respectively. In 2003, the maximum number of twelve in Nashik

Taluka, followed by Malegaon eleven and the lowest three were Satana, Surgana and Peth. In 2004, no more than 43 Nashik cases and no Dengue positive cases were found in Surgana and Kalwan. In 2005, six Dengue positive cases were reported again in Nashik Taluka of the total 94 Dengue positive cases in 2006, eight were in Nashik. In 2007, 48 out of 301 Nashik 48 cases were registered following Malegaon 41 and 30 Dengue positive cases in Sinnar Taluka. In 2008, Dengue positive cases dropped to 87 out of which 14 in Nashik. And only two Dengue positive cases were reported in Peth Taluka. Total 75 cases in 2009, Nashik Eleven In the year 2010, there were 34 Dengue positive cases in the district in the year 67, 2011, out of which five positive cases were not reported in Nashik but five in Surgana Taluka. Thereafter, there was a sharp increase in Dengue positive cases again in the district e.g. in 2012, out of 313 Nashik 46, Malegaon 44, Yeola 41, Nandgaon 38. In the year 2013, 458 Dengue positive cases were reported in Nashik 64, Malegaon 52, Sinnar 49, and Yeola 46. Dengue positive cases were recorded in the lowest in Deola Taluka. In 2014, there was a slight increase in Dengue positive cases, with Nashik Taluka crossing 100 and reporting 107 Dengue positive cases. Thereafter, Malegaon Taluka also increased to 82. Similarly, Sinnar and Yeola Taluka recorded 68 and Peth Taluka recorded the lowest. In 2015, Dengue positive cases dropped slightly to 425. In 2016, however, the Dengue positive cases increased tremendously, surpassing the number of 1000 and reaching 1246. The maximum numbers of Dengue positive cases were reported in Nashik 201, Malegaon 184, Sinnar 156, Nandgaon 105 and Yeola 102. In 2017, however, Dengue positive cases declined slightly to 1043 in comparison to 2016, but Nashik Taluka increased and it recorded 168, Malegaon 147, Sinnar 145 Yeola 98 and Nandgaon 88 thus maximum Dengue positive cases were reported.

Sr. No	Taluka	2001	2002	2003	2004	2005	2006	2007	2008	2009	2010	2011	2012	2013	2014	2015	2016	2017
1	Chandwad	1	0	1	0	0	0	0	0	0	0	1	1	0	1	0	1	0
2	Niphad	0	0	0	0	0	0	0	0	0	0	0	0	0	0	0	1	0
3	Nandgaon	0	0	1	0	1	0	0	1	0	0	0	0	1	1	0	0	0
4	Yeola	0	0	1	0	1	1	0	0	0	0	1	0	1	1	0	0	0
5	Malegaon	1	1	2	0	1	1	0	1	0	0	0	2	2	2	0	1	1
6	Sinnar	1	0	1	1	1	0	0	0	0	1	1	1	1	1	0	0	0
7	Satana	0	0	1	0	0	0	0	0	0	0	0	1	0	0	0	0	0
8	Peth	0	1	1	0	1	0	0	0	0	0	0	1	0	0	0	0	0
9	Surgana	0	0	0	0	0	0	0	0	0	0	0	1	0	0	0	0	0
10	Trimbak	0	0	0	0	0	0	0	0	0	0	0	0	0	0	0	0	0
11	Deola	0	0	0	0	0	0	0	0	0	0	0	0	0	0	0	0	0
12	Dindori	0	0	0	0	1	0	0	0	0	0	0	0	0	0	0	0	0
13	Igatpuri	0	0	0	0	0	0	0	0	0	0	0	1	0	0	0	0	0
14	Kalwan	0	0	0	0	0	1	0	0	0	0	0	1	0	1	0	0	0
15	Nashik	1	0	2	0	1	1	0	1	0	0	0	2	1	2	0	3	0
	Total	**4**	**2**	**10**	**1**	**7**	**4**	**0**	**3**	**0**	**1**	**3**	**11**	**6**	**9**	**0**	**6**	**1**

Table No. 3 Nashik District Taluka-Wise Deaths of Dengue from 2001 to 2017
Source: District Government hospital Nashik

In the above table no. 3 In the Nashik district, the total and Taluka-Wise Dengue deaths were reported from 2001 to 2017. During this entire 17-year period, 68 people died of Dengue in Nashik district. In Malegaon Taluka, the highest number of fifteen, followed by Nashik fourteen, Sinnar nine, Chandwad and Yeola six each, Nandgaon five, Peth four, Kalvan three, Satana two, Igatpuri, Dindori and one each in Niphad Taluka. In Deola, Trimbak and Surgana Taluka, however, no one died due to Dengue. Considering the entire district, eleven people died of Dengue in 2012, ten in 2003, and nine in 2009, while in 2004, 2010 and 2017, only one person died of Dengue in the entire district. In 2007, 2009 and

2015, there were no recorded cases of Dengue deaths. All the above data indicate that Malaria and Dengue positive cases and total deaths have been reported in Nashik, followed by Malegaon, Sinnar, Yeola and Nandgaon Taluka. However, cases of Malaria and Dengue positive cases and deaths in the districts of Igatpuri, Peth, Surgana Trimbak, Kalvan, Niphad etc. are very small. In the remaining Deola, Satana, Chandwad and Dindori talukas, the number of Malaria and Dengue positive cases is moderate and the number of deaths is low.

CONCLUSION:

The only way to get rid of Aedes Aegypti mosquito is by itself due to the diagnosis and treatment of the patient and the treatment of symptoms, the mortality rate can be greatly reduced. However, various types of remedies can be managed to get control over Dengue. Actually there is no drug or vaccine available for DHF treatment, so be careful not only to treat it but also to get better. There is no specific treatment for Dengue but in the year 2019, Denguexia (Dengue vaccine) was approved, but the World Health Organization vaccine will be given only to the confirmed person due to Dengue infection.

1. Personal Remedial Treatment

- Whole sleeves with shirts and full pants with socks
- Dosage killer creams, liquefied, hands, legs, to the naked body
- To set up coils, mats, etc., to avoid being enslaved
- Using mosquito nets for children and younger does not mean mosquito bites

2. Biological Control

- In ornamental tanks, fishes such as mosquito larvae, such as gappi fish
- Use biological pesticides to slaughter or escape

3. Chemical Control

- Use chemical insecticides if there is reproduction in large tanks
- Using aerosol spray during the day is so sure to burn.

4. Environmental Management System

- Finding and destroying mosquito breeding sites

- Management of Roof, Vertical and Shadow Wings of the house
- Suitable cover over the stored water
- Sure water supply
- Keeping a dry day in a week
- Separate the wet and dry waste in the house.

5. Health Education

To inform common people about this disease and the mosquito causing mosquitoes, such as TV, radio, newspapers, graffiti cinema slides, medical bulletins, magazines etc.

6. Community Participation

Sensitize people to find and destroy Mosquitos breeding sites and participate in various social institutions, schools, colleges. In addition to this, one day in a month, in various public places such as Garden, market River banks, roads, various government

REFERENCES:

1. Aluoch, J. R. (1997): Higher resistance to Plasmodium falciparum infection in patients with homozygous sickle cell disease in western Kenya. Trop. Med. Int. Health. 2: 568-571.
2. Borease S.J (2021) "Geographical Study of Epidemic Duiseases in Nashik District of Maharashtra With Special reference to malaria and Dengue Ph.D. Thesis
3. Borease S.J. and Shelar S.K. (2016): Environmental Impact on Human Health- A study in Medical Geography. Global Environment: Issues, Challenges and Solutions
4. Borease S.J. and Shelar S.K. (2018): "A Cross sectional study of awareness in Malaria and Dengue –A case study of Nashik city (Maharashtra)" International Multidisciplinary E-Research Journal 98-104
5. Borease S.J. and Shelar S.K. (2018): "Comparative study of Infected Patients with Malaria and Dengue Nashik District", Electronic Interdisciplinary International Research Journal, 11-21
6. Nilofar Izhar (2011) "Geography and Health A Study in Medical Geography. A.P.H. Publishing Corporation New Delhi.

7. Shelar S.K. (2012) “Introduction to Medical Geography”. Chandralok Prakashan. Kanpur-208021(India)

ISSN: P-2455-0515
E- 2394-8450

OPEN ACCESS

erj

EDUCREATOR RESEARCH JOURNAL

A PEER REVIEWED REFERRED JOURNAL

"Population, Society, Development and Environmental Sustainability"

VOLUME-IX, SPECIAL ISSUES-I
MARCH- APRIL 2022
SJIF IMPACT FACTOR: 7.717

ISSN: P-2455-0515
E- 2394-8450

Educreator Research Journal

A Peer Reviewed Referred Journal

OPEN ACCESS

Volume–IX, Special Issues–I
March– April 2022

Original Research Article

INDEX

ISSN: P-2455-0515
E- 2394-8450

Educreator Research Journal

A Peer Reviewed Refereed Journal

Volume-IX, Special Issues-1
March – April 2022

Original Research Article

EFFECT OF SPACE POLLUTION ON ENVIRONMENT AND HUMAN HEALTH

*Dr. Sudhakar Jagannath Borase

*Assistant Professor, Department of Geography, RNC Arts, JDB Commerce & NSC Science College, Nashik , Maharashtra.

Abstract

The problem of waste is now being felt in space as well as on earth. There is so much rubbish growing around the earth in space that a mission has to be launched for it. Scientists estimate that there is 7600 tons of space waste around the earth. If a small piece of debris hits a satellite in space, it could split into thousands of pieces. Not only is that, but the speed of the satellite in danger of increasing to 25000 kilometers per hour. Fragments of satellites orbiting in space at this speed can be dangerous to other satellites. It is better not to think about what will happen if these pieces hit a human spacecraft. In the current age of science and technology, the rate of launching satellites into space has increased rapidly. Private companies have also started sending satellites. Rockets and their components needed to launch a satellite into space do not usually return to Earth. They revolve around the earth. So naturally, the more rockets go into space, the more waste there will be. It usually lasts 10 to 15 years after launching a satellite into space. After that it fails. But it keeps moving in space. Moreover, some satellites fail after going into space. So they are also moving. So the more satellites go into space, the greater the risk. For this, the whole world needs to think of the future and take concrete steps

Keywords: *Space Pollution, Fragmentation Debris, Satellite.*

Introduction:

Debris in space is any man-made object in orbit that no longer serves a useful purpose, including the failed satellites, discarded equipment and rocket phases, and fragments of satellites and rocket phases. This is a matter of concern because - due to the very high speed in orbit - even relatively small pieces can damage or destroy satellites in a collision. High-altitude mounds can remain in orbit for decades or more, so they accumulate during high production and increase the risk of collisions with satellites. Since there is currently no effective way to remove large amounts of debris from the orbit, it is important to control scrap production in order to maintain long-term use of space. Today, as of January 1, 2021, there are approximately 6,542 satellites orbiting the Earth. Of these, 3,372 satellites are active and 3,170 are inactive.

There are about 34,000 pieces of space junk larger than 10 centimetres, and millions of smaller pieces that can still be devastating if they collide with another object.

Methodology:

The methodology of present work includes secondary data. The secondary data collected through varies books and internet.

Objectives:

- To identify the situation of Space pollution.
- To assess the awareness regarding Space pollution.

Causes of space pollution:

Space is generally polluted for all the following reasons or its various sources are as follows.

- Defunct satellites. Satellites have a limited useful life and, when their batteries are spent or they break down, they are left drifting about in space. ...
- Missing equipment. Astronauts sometimes drop tools or other objects during space walks.
- Rocket stages. ...
- Weapons.

Table No. 1: No. of Satellites by various Countries and Organizations 2021

Sr. No.	Country/Organization Name	Satellites in Orbit	Sr. No.	Country/Organization Name	Satellites in Orbit
1	Algeria	06	47	Malaysia	07
2	Arab Satellite Communications org.	14	48	Mauritius	01
3	Argentina	39	49	Mexico	15
4	Asia Satellite Communications org.	08	50	Morocco	02
5	Australia	31	51	Netherlands	11
6	Azerbaijan	31	52	New Ico	01
7	Bangladesh	01	53	New Zealand	05
8	Belarus	02	54	Nigeria	06
9	Boliva	01	55	North Atlantic Treaty Organization	08
10	Brazil	19	56	North Korea	02
11	Bulgaria	03	57	Norway	11
12	Canada	73	58	O3B Networks	20
13	Chile	03	59	Orbcomm	41
14	China/Brazil	03	60	Pakistan	06
15	Commonwealth of Independent states (Former USSR)	1534	61	Peoples Republic of China	519
16	Czech Republic (Former Vzechoslovakia)	03	62	Peru	02
17	Czechia	03	63	Philippines (Republic of the Philippines)	04
18	Denmark	09	64	Poland	10
19	Ecuador	02	65	Portugal	02
20	Egypt	07	66	Qatar	01
21	Estonia	02	67	Regional African Satellite Com. Org.	02
22	European Org. for the Exploration of Metrological Satellite	09	68	Republic of Rwanda	02
23	European Space Agency	93	69	Republic of Slovenia	02
24	European Telecomm. Satellite Org.	55	70	Republic of Tunisia	01
25	France	86	71	Saudi Arabia	15
26	France/Germany	02	72	Sea launch	01
27	France/Italy	02	73	Singapore	10
28	Germany	75	74	Singapore/Taiwan	02
29	Global star	84	75	Slovakia	01
30	Greece	03	76	Societe Europeenne des satellites	57
31	Hungary	01	77	South Africa	08
32	India	103	78	South Korea	25
33	Indonesia	17	79	Spain	40
34	International Mob. Satellite Organization (Inmarsat)	19	80	Sweden	11
35	International Space Station	05	81	Taiwan (republic of China)	19
36	International Telecommunication Satellite Organization	86	82	Thailand	13
37	Iran	03	83	Turkey	15
38	Iraq	01	84	Turkmenistan/Monaco	01

39	Israel	23	85	United Arab Emirates	16
40	Italy	36	86	United Kingdom	438
41	Japan	209	87	United States	4321
42	Kazakhstan	08	88	United States/Brazil	01
43	Laos	01	89	Uruguay	01
44	Latvia	01	90	Venezuela	03
45	Lithuania	08	91	Vietnam	03
46	Luxembourg	12			

Source: https://www.statista.com

The table above lists the number of satellites launched by different countries and organizations in space so far. Most satellites launched by Commonwealth of Independent States (Former USSR) (1534). It is followed by United States (4321). Almost all countries in the world, with a few exceptions, are responsible for space pollution. This is evident from the statistics.

The contamination of space from non-working and decommissioned satellites, abandoned rocket stages and other debris. An estimated 20,000 objects considered "space junk" have been tracked; however, more than a million smaller pieces are estimated. Starting with Russia's Sputnik I in 1957, the ever-increasing rocket launches and number of satellites in orbit all contribute to space pollution. In 2020, there were approximately 2,500 satellites with plans by companies such as Amazon and Space to launch thousands more

In the most general sense, the term space pollution includes both the natural micrometeoroid and man-made orbital debris components of the space environment; however, as "pollution" is generally considered to indicate a despoiling of the natural environment, space pollution here refers to only man-made orbital debris. Orbital debris poses a threat to both manned and unmanned spacecraft as well as the earth's inhabitants.

Environmental and health impact:

Effects of debris on other spacecraft range from surface abrasion due to repeated small-particle impact to a catastrophic fragmentation due to a collision with a large object. The relative velocities of orbital objects (10 km/s on average, but ranging from meters per second up to 15.5 km/s allow even very small objects such as a paint flake to damage spacecraft components and surfaces . For example, a 3mm aluminum particle traveling at 10 km / s is equivalent in energy to a bowling ball traveling at 38 Km/h. In this case, all the energy Contamination of space due to inactive and decommissioned satellites, launched rocket stages and other debris. Approximately 20,000 objects are considered "space junk"; however, more than a million smaller pieces are estimated. Beginning with Russia's Sputnik 1 in 1957, the ever-increasing number of rocket launches and the number of satellites in orbit all contribute to space pollution. By 2020, companies like Amazon and Space have approximately 2,500 satellites with plans to launch thousands more

In the most general sense, the term space pollution includes both natural micrometeoroids and man-made orbital debris in the space environment; however, "pollution" is generally considered to indicate the degradation of the natural environment, here the reference to space pollution is only man-made orbital debris. Orbital debris poses a threat to unmanned and unmanned spacecraft as well as to Earth's inhabitants.

The impact of piles on other spacecraft is often due to the effects of small-particles, from surface friction to catastrophic fractures due to collisions with large objects. The relative speed of orbiting objects averages 10 kilometres per second, but meters per second to 15.5 km/s. For example, a 3 mm aluminium particle traveling at a speed of 10 km/s is equivalent to the energy of a bowling ball traveling at a speed of 37.5 km/h.

Table No. 2: Various sources that pollute the space

	Payloads	Rocket bodies	Operational debris	Breakup debris	Anomalous debris	Totals
Leo	1612	758	651	3232	119	6372

Meo	126	28	2	0	0	156
Geo	587	116	1	2	0	706
Elliptical	249	515	135	167	0	1066
Unknown	171	120	185	0	0	476
Totals	2745	1537	974	3401	119	8776

Source: Anz-meador, p.d., "history of on-orbit satellite fragmentations", 12th ed., NASA Johnson space centre report

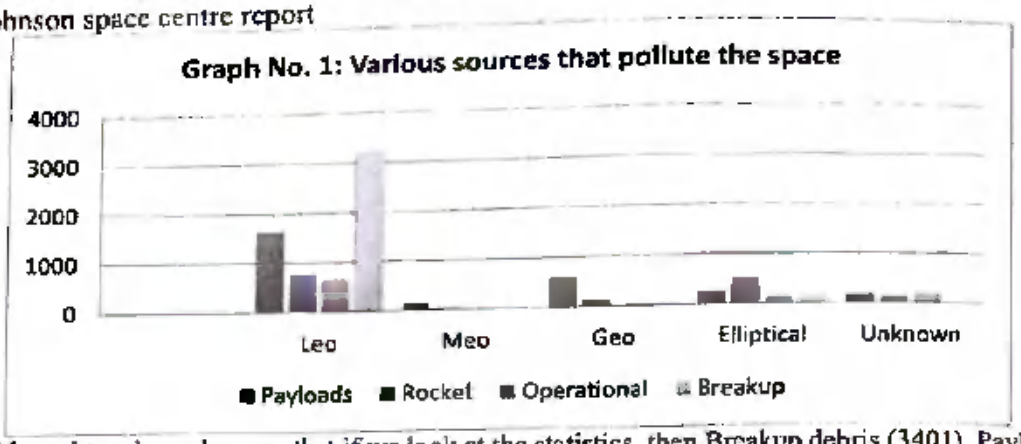

Above the table and graph can be seen that if we look at the statistics, then Breakup debris (3401), Payloads (2745), Rocket bodies (1537), Operational debris (974), and Anomalons debris (119) are generated in this way. So much waste has been created.

Fragmentation breakdown:

The particles will be distributed over an area of equal size, causing cracking or penetration, depending on the thickness and physical properties of the surface being affected. There has been an accidental collision between objects catalogued to date, but surfaces returned from space and examined in a laboratory confirm regular bombings by small particles. Due to this type of damage while in orbit, the components of the space shuttle vehicle with windows are regularly replaced. Garbage also poses a threat to the earth's surface. High-melting-point materials such as titanium, steel, ceramics, or large or densely constructed objects can withstand re-entry into the atmosphere to strike the Earth's surface. Although no casualties or serious injuries have been reported from the piles, re-entry items are routinely inspected, and occasional found debris is generally divided into three sizes, depending on the damage caused: 1 cm, less than 1 to 10 cm, And larger than 10 cm. Objects less than 1 cm in size can be protected, but they still have the potential to damage most satellites. Piles in the range of 1 to 10 cm are not protected; they are not easily seen and can destroy satellites. Finally, collisions with objects larger than 10 cm can cause the satellite to break. Of these sizes, only 10 cm and larger objects are regularly tracked and catalogued by surveillance networks in the United States and the former Soviet Union. Other populations are estimated statistically by analysis of the returned surface by special measurement operations with sensitive radar (size greater than 3 mm). Approximately 30 million piles of approximately 1 mm and 1 cm for a population, more than 100,000 debris between 1 and 10 cm, and 8,800 objects larger than 10 cm provided the number, nature and location of objects larger than 10 cm. In the fragmentation debris table and the image of the mounds in space around the earth. Low Earth Orbit (LEO) is defined as the orbital altitude of 2,000 km below the Earth's surface and is the subject of the image of clusters in space around the Earth. Middle Earth Orbit (MEO) is the territory of the Global Positioning System (GPS) and the Russian Navigation Satellite System and is located at an altitude of approximately 20,000-km, while the Geosynchronous Earth Orbit (GEO) "belt" is dominated by communications and Earth. - Observation payload about 35,800 km. Most of the objects in these orbits are in a circular or near-spherical orbit around the earth. In contrast, the elliptical orbital range includes MEO and GEO, as well as rocket bodies released into their transfer orbits in scientific, communications and Earth-

observation payloads. Of all the objects listed in the fragmentation debris table, the majorities are "debris" - only 5 percent of the objects in orbit represent operational payloads or spacecraft. Also, of the approximately 28,000 objects tracked since the launch of Sputnik 1 in October 1957, items not included in the fragmented debris table have either re-entered Earth's atmosphere or escaped Earth's influence (to land on Mars, for example). The distribution of piles smaller than 10 cm is assumed to be in the orbit of the original object and is assumed to be similar to the distribution presented in the image of the piles in space around the Earth.

Solution plan:

Measures take two courses: protection and mitigation. The defense seeks to protect the spacecraft and uses intelligent design methods to minimize the impact of piles. Mitigation efforts to prevent debris from forming. Active mitigation techniques include the avoidance of collisions between traceable and manipulative objects and the deliberate re-entry of objects into the oceans. Passive techniques include the removal of residual fuel or pressure vessels from rockets and spacecraft, retention of operational debris, and the disposal of spacecraft at the end of the mission. Space salvage or recovery, while an option, is currently very expensive to hire on a regular basis.

The United States and the International Atomic Energy Agency (IAEA) have identified the threat and are working to limit its environmental and health risks. The Inter-Agency Space Debris Coordination Committee (IADC), originally sponsored by the National Aeronautics and Space Administration (NASA), includes all major space-traveling nations. The IADC Charter covers the coordination and dissemination of solution research, and policies based on research findings are being adopted by the space community around the world.

Although the overall population is growing, the rate of growth has slowed down in the 1990s due to policies to improve growth. However, continuous work is needed to reduce the risk of orbital debris for future generations and to continue to use space safely, economically.

Conclusion:

A collision with a mound larger than 1 cm will disable the working spacecraft and may cause a disintegrated spacecraft or rocket body to explode. The impact of the millimetre-sized pile could cause local damage or disable the subsystem of the operational spacecraft. Therefore, it is necessary to make arrangements in such a way that all the waste products will be burnt to ashes. So that the risk is reduced

References:

Committee on Space Debris, Aeronautics and Space Engineering Board, Commission on Engineering and Technical Systems, National Research Council. (1995).

"Orbital Debris: A Technical Assessment." Washington, D.C.: National Academy Press. Johnson, Nicholas L. (1998). "Monitoring and Controlling Debris in Space." Scientific American 279(2):62–67.

http://www.iadc-online.org.

http://pompeii.nap.edu/books/0309051258/html/index.html

https://www.statista.com

Daily Lokmat News paper

Cite This Article:

****Dr. Sudhakar Jagannath Borase, (2022). Effect of Space Pollution on Environment and Human Health, Educreator Research Journal IX (Special Issues - I), March –April, 7-11.***

भारतीय योद्धा

योगदान, युद्धनीति एवं सामरिक विचार

संपादक

प्रो. (डॉ.) सी. बी. भांगे

प्रोफेसर एवं विभागाध्यक्ष, सैनिक शास्त्र विभाग
श्री शिवाजी महाविद्यालय, परभणी, महाराष्ट्र

देविदास विजय भोसले

सहायक प्रोफेसर और विभागाध्यक्ष, रक्षा और सामरिक अध्ययन विभाग तुलजाराम चतुरचंद कॉलेज, बारामती, महाराष्ट्र

भारती पब्लिकेशंस

नई दिल्ली 110002

शीर्षक: भारतीय योद्धाः योगदान, युद्धनीति एवं सामरिक विचार

संपादक: प्रो. (डॉ.) सी. बी. भांगे एवं देविदास विजय भोसले

प्रथम संस्करण: 2021

ISBN : 978-93-90818-95-2

प्रकाशक:

भारती पब्लिकेशन्स

4819 / 24, तीसरी मंजिल, अंसारी रोड

फोन नं.: 011–23247537, 9899897381

ई–मेल: bhartipublications@gmail.com

Website : www.bhartipublications.com

मुद्रक : एस. पी. कौशिक एंटरप्राइजेज, दिल्ली

35

बिरसा मुंडा आदिवासी क्रांतिकारी योद्धा

डॉ. शशिकांत गोकुळ साबळे

इतिहास विभाग प्रमुख, आर .एन .सी.आर्ट्स,
जे.डी..बी.कॉम.एन.एस.सी.सायन्स वरिष्ठ
महाविद्यालय नाशिकरोड, नाशिक

सार :

किसी भी क्षेत्र के विकास उस क्षेत्र में काम करने वाले मेहनती लोगों के कार्यपर निर्भर रहा है। इस अवधि में विकास प्रक्रिया की दिशामें विभिन्न समस्याएं आती हैं। आदिवासियों के बारे में आम लोगों का विचार है कि वे जंगल की घाटियों में रहने वाले जंगली, एक समान संस्कृती, एक भाषा समूह मी रहनेवाले शिकार भेड बकरी चराकर खेती पशुपालन कर आपणा जीवन व्यतीत करणे वाला समुदाय, सभ्य समाज से दूर रहकर अपनी स्वयंनिर्मित संस्कृती को जतन करनेवाले आदिवासी । वास्तव में, आदिवासी इस देश के मूल निवासी हैं। देश

निष्कर्ष :

ब्रिटीश शासन कि स्थापना के पश्चात अर्थव्यवस्था.कानून प्रशासन ओर जीवन के अन्य क्षेत्रो में जो परिवर्तन हुआ उसीका विरोध करणे हेतुसे बिरसा के नेतृत्व के माध्यमसें विरोध हुआ अग्रेजोने अन्य शोषक वर्ग कि सहायता से आदिवासिको दबा दिया लेकीन इस विद्रोह् से जनजातीय लोगो को आपने हको के लिये संघर्ष के लिये प्रेरणा प्रदान कि बिरसा को नेता मानकर अंग्रेजोके खिलाफ खडे हुए । बिरसा का नाम आते ही 'उलगुलान' शब्द भी सामने आ जाता है। बिरसा और उलगुलान के बीच का संबंध मनुष्य और उसकी छाया है। 'उलगुलान' मुंडारी भाषा का एक शब्द है। इसका सीधा सा मतलब है कि 'सभी स्तरों पर एक बार उठो'। उलुगुलान एक व्यापक लड़ाई है जो एक बार में न्याय के लिए लड़ी जाती है। यह बिरसा के मानवीय संघर्ष का नाम है।

संदर्भ :

1. K-Suresh Singh]Birsa Munda Aur Unka Andolan] N-Delhi]1979-
2. K-Suresh Singh]Tribal Movement in India Vol-I & Vol-II] N-Delhi]1982-
3. समीर एम. ए,भगवान बिरसा मुंडा,मनोज पब्लिकेशन,दिल्ली,२०११
4. गारे गोविंद ,आदिवासी विकासाचे शिल्पकार,श्री विद्या प्रकाशन पुणे १९९७.
5. गारे गोविंद,आदिवासी वीर पुरुष, श्री विद्या प्रकाशन पुणे १९९४.
6. गारे गोविंद,स्वातंत्रलढ्यातील आदिवासी क्रांतिकारक, श्री विद्या प्रकाशन पुणे २०१८.
7. Daink Bhaskar 2019–11–18 अभिगमन तिथी 2020–06–09.
8. Dainik Jagran vfl-Ikxeu frlkh 2020&06&09-https%@@hi-wikipedia-org@@ Js.kh%lckYVuZ&vè;u-

WFL Publisher
Science and Technology
P L Box 48, FI-00981
Helsinki, Finland
e-mail: contact@wflpublisher.com

Journal of Food, Agriculture & Environment Vol.19 (2):131-136. 2022 *www.wflpublisher.com*

Effects of wastewater irrigation on soil physical and chemical properties

Sudesh Bhaskar Ghoderao[1] and Sarita Gajbhiye Meshram [2]*

Department of Chemistry, RNC Arts, JDB Commerce and NSC Science College, Nasik Road, Nasik, Maharastra, 422101, India.
Department for Management of Science and Technology Development, Ton Duc Thang University, Ho Chi Minh City, Vietnam.
**email: gajbhiyesarita@gmail.com, sudeshghoderao@gmail.com*

Received 3 February 2022, accepted 28 March 2022.

Abstract

A growing number of scientists believe that using wastewater to irrigate crops is an effective way to reduce soil deterioration and restore soil nutrient content. Following long-term irrigation with wastewater, this study examined soil and ground water composition. Organic carbon (OC), manganese (Mn), iron (Fe), sodium (Na), copper (Cu), total alkalinity (TA) and zinc (Zn) were found in soil samples collected at the surface and 30 cm below the surface. Due to salt and poisonous metal concentrations from wastewater application to soil, it is vital to study the long-term impacts of wastewater concentration on soil salinity and toxic metal concentrations.

***Key words**:* Irrigation, soil properties, wastewater, water quality.

Introduction

As the global population continues to rise, industrial and agricultural activities to increase food supplies, as well as a string of droughts in recent years have pushed water resources in arid and semi-arid countries to their limits. This is why it is important to explore any sources of water that can be used economically and effectively.

Worldwide, wastewater is used to irrigate agricultural land. Developing countries, whose water treatment expenses are prohibitive, are particularly susceptible to this [1]. Enhanced living standards in industrialized societies have resulted in a rise in waste items that may lead to contamination of the environment. Even though pollution prevention is costly, recycling trash is a particularly effective way to combat it [2]. A more cost-effective option to wastewater disposal is to use it on agricultural lands, where it improves nutrient cycling while also posing a risk to soil quality and production in the long run [1].

Since it contains so many different nutrients, wastewater irrigation is a great way to add a variety of essential macro- and micronutrients to the soil. These include nitrogen, phosphorus, potassium, zinc, iron, manganese, and copper (Cu) [3]. Wastewater may include a significant amount of organic matter, making it a valuable source of organic matter for soils and a stimulant for plant growth [4].

Soil type, wastewater properties, and the irrigated soil's vegetation all influence how wastewater application affects the environment. Water irrigation may alter soil qualities, including physical and chemical as well as biological properties. Applied wastewater contains nutrients that can be transformed by soil qualities [5]. Wastewater application to farmland and forestland is an attractive option for disposal since it can improve soil physical and nutritional qualities [6, 7]. There is a concern regarding the accumulation of potentially harmful metals such as Cd, Cu, Mn, Pb, and Zn from both home and industrial sources in the soils that are irrigated with wastewater. The amount of these elements in wastewater is the most important factor in determining how much of it can be used. As far as public concern goes, the uptake of trace elements by plants cultivated in wastewater-irrigated land is a major one [8]. The possible absorption by grazing animals of these components from soil under wastewater irrigation is also a cause for worry in terms of toxicity. As a result, it is imperative that the buildup of certain hazardous metals in plants and the consumption of contaminated water by farm animals be thoroughly investigated [9].

Reducing the demand for costly inorganic fertilizers and enhancing soil fertility and crop yield can be achieved by using wastewaters [10]. Reusing agricultural waste water to reduce pressure on freshwater supplies has been a common practice for centuries [11]. Wastewater use, regardless of its benefits, may have an impact on soil physical and chemical qualities and, ultimately, agricultural yields [12-15]. Soil salinization (an increase in sodium ions relative to other cations) and the accumulation of heavy metals in the soil and crops can result from the use of wastewater in agriculture. This can pose a long-term health risk to humans. On the basis of the source of the wastewater, treatment methods used, and the soil's natural properties, this may or may not happen[3, 16].

An investigation into how industrial wastewater irrigation affects soil and groundwater quality was the goal of this project (macro and micronutrients, heavy metal content).

Materials and Methods

Location: For this investigation, the city of Jabalpur was chosen. The experiment is based on industrial waste as a point source (Vehicle factory nala). Jabalpur has a sub-tropical, sub-humid

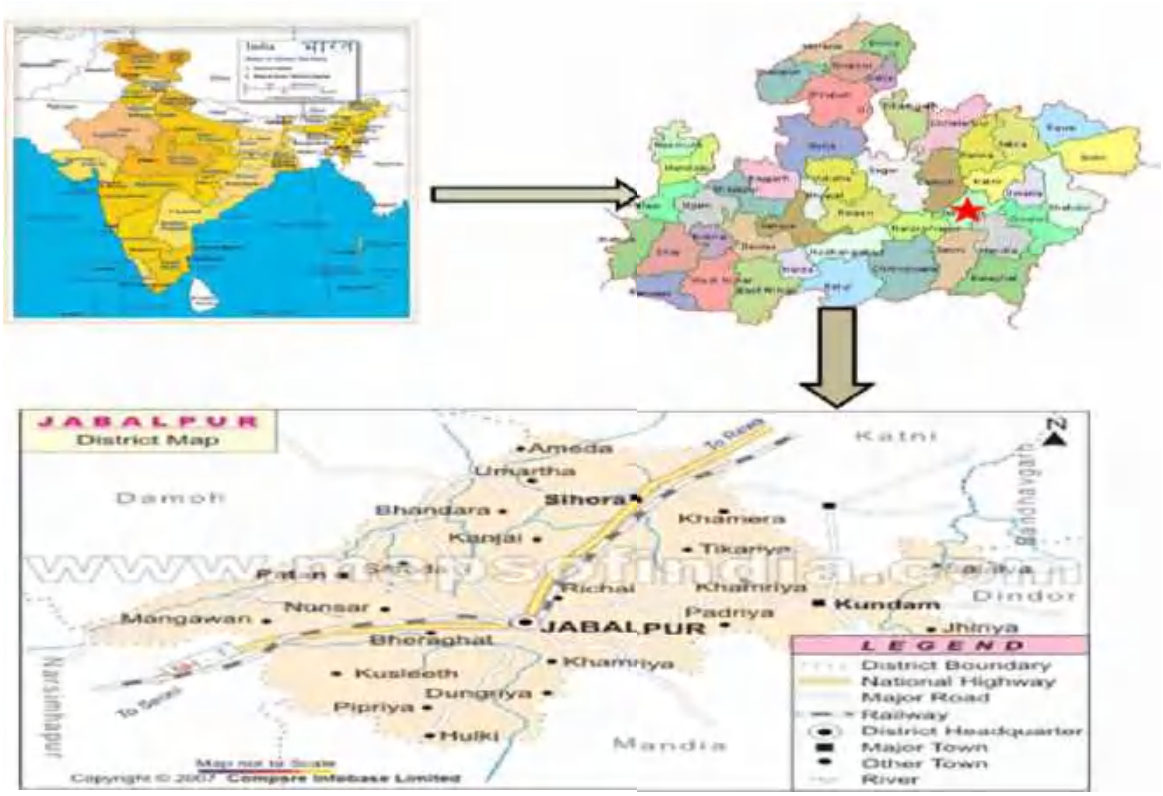

Figure 1. Location map of the study area.

climate and is located on the Kymore plateau and Satpura hills in the agro-climatic area at 2309" latitude and 79058" E longitude, at an altitude of 411.78 m above mean sea level, with hot, dry summers and chilly, rainy winters. The temperature drops below freezing point in the winter and reaches as high as 460 degrees in the summer, making the environment of this location rather harsh. The study area's location map is depicted in Fig. 1.

Sampling: During the pre-monsoon season of 2018, water samples from industrial waste (vehicle nala) were collected from open wells, bore wells, and tube wells. In a plastic container, a sample of water was collected. As specified in Standard Methods for the Examination of Water and Wastewater, all samples were collected, maintained, and stored for analysis [17]. Before seeding, a 30 cm deep soil sample was taken from the research area with a hand auger.

Analytical methods: Wastewater samples were processed for examination using a temperature programme based on the Milestones Cookbook of microwave application notes for MDR technology and an acid digestion beforehand. Na and K contents were determined using the atomic emission method, Fe, Al, Cu, and Mn contents were determined using the atomic absorption spectroscopy method, and chloride (Cl), sulphate (SO_4), nitrite, and nitrate contents were determined using the ionic chromatography method in wastewater and drinking water samples. The APHAAWWA-WPCF method [17] was used to determine N-Kjeldahl, total P, BOD5, COD, electrical conductivity, carbonate and bicarbonate, IC (inorganic carbon), and TOC (total organic carbon).

The pH and electrical conductivity (EC) in saturation extract (1:2.5 suspension of solid in water), pH with a previously calibrated pH meter [18], EC with a previously calibrated conductive meter [19], organic matter content with the Walkley and Black method [20], total nitrogen (N) by the Kjeldahl procedure, and available phosphorus (P) by the Kjeldahl procedure [21] were determined. According to Milestones Cookbook of microwave application notes for MDR technology, the soil was acid digested for various parameters and metal measurements. Na and K were afterwards determined using atomic emission spectroscopy in an atomic absorption spectrometer, while Ca, Mg, Fe, Zn, Mn, Cu, Ni, Cr, Cd, As, Hg, and Pb were determined using atomic absorption spectroscopy in an atomic absorption spectrometer [22].

Results and Discussion

Physical properties of water at source: Physical properties of waste water obtained from industrial waste (Nala near Vehicle factory) were evaluated for pH and electrical conductivity (Table 1).

The pH scale measures the acidity or alkalinity of water as well as the concentration of hydrogen ions. The pH has no direct negative impact on one's health. Trihalomethanes, which are poisonous, are formed when the pH is too high. Corrosion begins in pipes when the pH falls below 6.5, releasing hazardous metals such as Zn, Pb, Cd, and Cu. The pH value of water sample of the Vehicle Nala is 7.42. This value is within the prescribed limit of WHO and also in safe range of pH for irrigation water i.e 6.5-8.5.

Electrical conductivity (EC) is a quick way to figure out how much ionized stuff is in a given amount of water. The water recovered from the Vehicle Factory Nala has an average EC of 1.11 dS/m, which is in the High category according to USSSL but suitable for irrigation.

Table 1. Physico-chemical properties of waste water at surface and ground water.

Parameters	Units	At Source	Ground water	Percentage Change
pH		7.42	7.47	-0.66
EC	(dS/m)	1.11	1.11	0.26
Cu	(mg/l)	0.4	0.18	55
Cr	(mg/l)	0.08	0.03	62.5
SO_4	(mg/l)	47	31.57	32.89
Fe	(mg/l)	0.52	0.18	65.38
NO_3	(mg/l)	0.45	0.27	40
Chloride	(mg/l)	75	44.71	40.38
TH	(mg/l)	280	232.85	16.83
TA	(mg/l)	710	530.85	25.23
Na	(mg/l)	130	109	16.15
Cl	(mg/l)	0.67	0.53	20.89
Br	(mg/l)	2.01	1.68	16.41
Iodine	(mg/l)	1.08	1.01	6.48
NH_4-N	(mg/l)	4.12	2.57	37.62
PO_4	(mg/l)	3.16	1.42	55.06
Si	(mg/l)	4.26	3.04	28.63
NO_2-N	(mg/l)	0.01	0.001	90
Su	(mg/l)	0.02	0.02	0
Zn	(mg/l)	0.86	0.38	55.81
RSC	(me/l)	4.3	2.98	30.69
SAR	millmole/l	1.09	1.01	7.92

Chemical properties of waste water: Chemical properties of waste water obtained from Industrial waste (Nala near Vehicle factory) are presented in Table 1.

Copper (Cu): The higher concentration of Cu can be related to anemia, digestive disturbance, liver and kidney damage, bitter and metallic taste, blue green or plumbing fixture diseases. The copper in Vehicle Factory is 0.40 mg/l. The copper is within the permissible limit as per WHO.

Chromium (Cr): Cr causes skin irritation, ulcers, lung tumors, gastrointestinal consequences, nervous system damage, and circulatory system harm. In the water recovered from the Vehicle Nala, a value of Cr (0.08 mg/l) was detected.

Sulphate: Drinking water with a sulphate level of more than 400 mg/l has a bitter, medicinal flavor and can produce gastric discomfort and catharsis. The SO_4 value of the Vehicle Nala's water sample (Table 1) is 47 mg/l. This SO_4 level is within the WHO's recommended range.

Iron (Fe): Fe occurs in water either as ferrous Fe or as ferric Fe. Plant growth, especially vegetable growth, benefits from a tiny amount of Fe. Large quantities cause unpleasant, metallic, bitter taste and favour the slimy growth of iron bacteria. The value of Fe (0.52 mg/l) was recorded (Table 1) in the water obtained from the Vehicle Factory. The iron concentration of water sample is within the permissible limit as per WHO.

Nitrate (NO_3): Nitrate is a contaminant found in ground water as a result of sewage percolation under the surface. Organic sources of nitrate, as well as industrial and agricultural pollutants, are found in natural water. Nitrate encourages growth of organism like algae that cause undesirable taste and odour. The nitrate concentration in excess of 45 ppm may cause methenoglobinemia in infants (blue babies). The highest value of NO_3 is 0.45 mg/l for Vehicle Factory. The nitrate concentration is within permissible limits as per WHO. Presence of nitrate in water indicates the final stage of mineralization. The increase in nitrate nitrogen in the effluent is undesirable as it pollutes the ground water. The higher nitrate nitrogen content in the water causes eutrophication.

Chloride: Chloride is a minor constituent of the earth's crust but a major dissolved constituent of most natural waters. Corrosion of metals in the distribution system is accelerated by high chloride concentrations. The chloride concentration of a Vehicle Factory water sample is 75 mg/l. According to WHO, the chloride content is within the allowed range.

Total hardness (TH): Hardness refers to the feature of water that prevents soap from lathering. The total hardness of water is due to presence of cations Ca^{2+}, Mg^{2+}, Fe^{2+}, Mn^{2+} and anions HCO_3^-, SO_4^{2-}, Cl^-, NO_3^-. Human cardiac disease is influenced by water hardness. The value of TH (280 mg/l) was recorded.

Total alkalinity (TA): Hydroxide, carbonate, and bicarbonate are the main sources of alkalinity in natural water. Alkalinity is not detrimental to humans in and of itself. The water sample has a total alkalinity of 710 mg/l. Water sample from Vehicle Factory has shown higher as per the permissible limit as prescribed by WHO.

Sodium (Na): Sodium is an important element when salinity or total dissolved solids (TDS) are considered in the use of water. Many irrigation water quality criteria like SAR, sodium percent are based on the sodium. According to the National Academy of Science, greater sodium levels are linked to cardiovascular disease and pregnancy-related toxaemia in women. Water sample of Vehicle Factory is found within the permissible limit given by WHO.

Residual sodium carbonate (RSC): The RSC of Vehicle Factory is 4.30 meq/l and given in Table 1. The RSC value for Vehicle Factory comes under high category as per IS: 11624 – 1986, but it is fair for irrigation purpose. The RSC content of water depends upon the carbonate and bicarbonate contents of water and the concentrations of calcium and magnesium.

Sodium adsorption ratio (SAR): The SAR of Vehicle Factory is 1.09 millimole/l. The SAR of water depends on the sodium content of water and total hardness of water. The SAR of water sample is low class (less than 10 USSSL). Than SAR point of view water sample are excellent for irrigation purpose.

Other parameters and micro nutrients: Some of the other parameters and micro nutrients like chlorine, bromine, iodine, ammonium nitrogen, phosphate, silica, nitrite, sulfite and zinc are presented in Table 1.

Effect on ground water due to polluting source: Water quality analysis of waste water has been discussed in the previous section. When this water is applied over a field as irrigation or percolate down right from the source itself causes contamination to ground water in long term. The intensity of contamination depends mainly on intensity of impurity of waste water at the source, the length of time for which this problem exists and the strata of soil through which it passes before joining the ground water. In order to assess the effect on ground water quality. Ground water samples from near open well, hand pumps and tube wells were collected and analyzed.

It is suspected that the ground water might have got polluted

due to the polluting sources; therefore the physico-chemical properties of ground water were determined. The possible effect on ground water due to source was calculated in terms of percentage reduction change as:

$$Percentage\ Change = \frac{(Ps-Pg)}{Ps} * 100 \quad (1)$$

where, Ps = Value of parameter in sources, Pg = Value of parameter in ground water.

Physical properties of ground water: Physical properties of waste water obtained from industrial waste (Nala near Vehicle factory) are presented in Table 1.

pH: The pH value of ground water 7.47 (Vehicle Factory) was increased against at the sources with 7.42. All these values come under the permissible limits as per WHO standard.

Electrical conductivity: The EC value registered same in ground water and surface water (1.11 dS/m).

Chemical properties of ground water: Chemical properties of ground water obtained from Industrial waste (Nala near Vehicle factory) are presented in Table 1.

Copper: The value of copper was 0.18 mg/l in ground water sample, which is 55% lesser than in the waste water source. The safe limit of copper 0.05-1.5 mg/l suggest that ground water of these sites falls under safe category for copper point of view.

Chromium: The value of chromium was 0.03 mg/l in ground water sample, which is 62.5% lesser than in the waste water sources. The safe limit of chromium is 0.05 mg/l and suggests that ground water of these sites comes under the safe category.

Sulphate: The value of sulphate was recorded 31.57 mg/l which is 32.89% lesser than the waste water source (Table 1). All samples come under the permissible limit as per Standard of WHO and suggest that ground water of these sites is under the safe category for sulphate point of view.

Iron: Iron in the ground water sample was 0.18 mg/l. These ground water samples showed 65.38% lesser values than the waste water at source (Table 1). The safe limit of iron is 0.3-1.0 mg/l and suggest that ground water of the locality under the safe category in iron point of view.

Nitrate: The NO_3 concentration was maximum 0.27 mg/l in ground water. The percentage reduction change in the NO_3 was 40% . All samples of ground water falls under the permissible limits. The safe limits of NO_3 is 45-100 mg/l.

Chloride: The value of chloride in ground water sample was 44.71 mg/l. The percentage reduction change in ground water from source is 40.38. The safe limit of chloride is 250-1000 mg/l.

Total hardness: The value of total hardness in the ground water was 232.85 mg/l. The percentage reduction change from 16.83% was obtained. All ground water samples come under the permissible limit (300-600 mg/l) as per WHO standard.

Total alkalinity: The concentration of total alkalinity of ground water sample was 530.85 mg/l. The ground water sample was 25.23% lesser than the waste water source. The safe limit of TA is 200-600 mg/l.

Sodium: The concentration of sodium in ground water sample was 109 mg/l. This value is 16.15% lesser than the waste water at source (Table 1). The permissible limit of Na is 200 mg/l.

Residual sodium carbonate: The RSC value of ground water sample was 2.98 me/l. The percentage change is 30.6% (Table 1). As per CGWB and CPCB (2000) the value of RSC is low, which comes under the good class of water for irrigation point of view.

Sodium adsortion ratio: The SAR value of ground water sample was 1.01 millimole/l (Table 1). The percentage change is 7.3%. According to CGWB and CPCB (2000) ground water samples are excellent quality for irrigation point of view.

Other parameters and micro nutrients: Element of halogen group i.e. Cl, Br and iodine decreased when percolate down to the ground water (Table 1). There was considerably decrease in NH_4-N and NO_2-N was leached down to the ground water, the soil prevailing was capable of filtering about 18-90% of this material. The NH_4-N decreasd from 37.62% (Table 1). The NO_2-N was reduced 90% in the ground water samples collected from Vehicle Factory. The PO_4 concentration was 1.42 mg/l in ground water. The percentage change in the concentration of PO_4 was 55.06%. The Si concentration was 3.04 mg/l in ground water. The percentage change in the concentration of Si was 28.63%. The value of Zn was same as ground water as well as water source. The Zinc concentration decreased in the ground water sample in comparison to the waste water source.

Water quality refers to the physical, chemical and biological qualities of a water supply that impact its acceptability for a certain use. Specific purposes require different levels of quality, and a water supply is seen more acceptable if it gives better outcomes or creates fewer difficulties than an alternative water supply[23] . The kind and quantity of dissolved salts in irrigation water can have a significant impact on its quality. Ayers and Westcot [24] provide guidelines for evaluating water quality for irrigation in Table 2. These recommendations are practical and have been used successfully in irrigated agriculture for analysing surface water, groundwater, drainage water, and wastewater constituents [25].

Soil impairment due to waste water irrigation: Soil samples were collected from areas where irrigation from different polluting sources is in practice. The physico-chemical properties of these samples were determined. The results obtained from different test

Table 2. FAO recommendations for maximum concentration in irrigation water[24].

Parameter	Max. value	Parameter	Max. concentration (mg/l)
pH	6.5-8.5	Cadmium	0.01
EC (dS/m)	3.0	Chromium	0.10
Total dissolved solids (mg/l)	2000	Cobalt	0.05
HCO_3 (mg/l)	600	Copper	0.10
SO_4 (mg/l)	1000	Iron	5.0
Cl (mg/l)	1100	Manganese	0.2
Mg (mg/l)	60	Nickel	5.0
Na (mg/l)	90	Lead	2.0
SAR (mmol/l)	<10 excellent, 10-18 good 18-26 fair, >26 poor		

Table 3. Physico-chemical properties of soil.

Parameters	Units	Soil Depth	
		0 cm	30 cm
pH	-	8.0	7.5
EC	(dS/m)	0.9	0.4
OC	(g/kg)	9.7	15.0
Av.N	(ppm)	310.0	405.0
Av.P	(ppm)	28.6	31.3
Av.K	(ppm)	578.5	490.6
Av.S	(ppm)	4.2	4.2
Zn	(ppm)	20.9	20.1
Fe	(ppm)	10.3	14.3
Mn	(ppm)	15.0	3.1
Cu	(ppm)	971.0	856.0
TA	(ppm)	125.0	110.0
Na	(ppm)	87.0	65.0
NH_4-N	(ppm)	59.0	63.0
NO_3-N	(ppm)	27.8	29.3

Table 4. Soil parameters limits.

Class	OC (g/kg)	N (kg/ha)	P (kg/ha)	K (kg/ha)	S (mg/kg)
Low	<5	<250	<10	<200	<10
Medium	5-7.5	250-500	10-20	200-400	10-20
High	>7.5	>500	>20	>400	>20

Critical limits: Zn = 0.5 mg/kg, Cu =<0.5 mg/kg, Fe = 2.5 - 4.5 mg/kg, Mn = 3.5 mg/kg

samples were compared with standard norms presented in Table 4. Salient results are presented in Table 3.

pH: The pH value of soil is an important parameter, which need to be controlled for the maintenance of the soil fertility as it is directly influenced by availability of nutrient. Brady [26] has specified that slightly acidic and slightly alkaline condition is supposed to be best from fertility point of view. The pH value was 8.0 for surface soil and at 30 cm depth 7.5.

Electrical conductivity: Electrical conductivity of soil is related to the total dissolved salt content and is therefore a reliable index of salization. The EC value was found 0.85 dS/m at the surface of soils. At 30 cm depth the value of EC was slightly lower.

Organic carbon: Soils of near Vehicle Nala have high organic carbon both on the surface and at the depth below 30 cm.

Available nitrogen, potassium and phosphorus: Soils irrigated by waste were moderate in nitrogen at surface and 30 cm depth. The value of nitrogen was 310 ppm (at surface) and 405 ppm (30 cm depth). Similarly, soils near Vehicle Factory Nala is sufficiently high in potassium and phosphorus at surface and 30 cm depth. Soils irrigated by waste water of Vehicle Factory Nala were low in sulphur as it ranges below 10 ppm.

Micro nutrient sand other parameters: The waste water irrigated soils showed sufficient values of zinc, iron and manganese. Higher values of Zn, Mn, Cu, Na, TA were at surface than at the 30 cm depth, while Fe, NH_4-N, NO_3-N had higher values at 30 cm depth than surface soil.

Conclusions

The physical and chemical properties of soils are affected by long-term wastewater irrigation. The results demonstrated a considerable decrease in pH, EC and micronutrients when compared to surface waste water and ground water. In order to conserve non-renewable resources, soil deterioration in semi-arid areas must be addressed. As a possible source of nutrients, wastewater irrigation can be utilized as an organic fertilizer to improve the physical and chemical qualities of soils. The buildup of immobile heavy metals in soils is a key drawback of wastewater irrigation. Heavy metal contamination should be researched further to establish the lingering effects of wastewater before it is used for land restoration or as a fertilizer. In order to achieve sustainable agriculture, consistent assessments of both irrigation water and irrigated soils are required to avoid the detrimental impacts of applied wastewater. Furthermore, in order to attain improved soil qualities in the research region, remediation procedures and management plans are required.

Declarations

Ethics Approval and Consent to Participate: Not applicable.
Consent for Publication: Not applicable.
Competing Interests: The authors declare that they have no competing interests.

References

[1]Friedel, J.K., Langer, T., Siebe, C. and Stahr, K. 2000. Effects of long-term wastewater irrigation on soil organic matter, soil microbial biomass and its activities in central Mexico. Biol. Fertil. Soils **31**:414-421.

[2]Couillard, D. 1995. Dynamics of municipal wastewater sludges on forest land. J. Environ. Systems **24**(1):25-46.

[3]Ganjegunte, G., Ulery, A., Niu, G. and Wu, Y. 2018. Organic carbon, nutrient, and salt dynamics in saline soil and switchgrass (*Panicum virgatum* L.) irrigated with treated municipal wastewater. Land Degrad. Dev. **29**(1):80–90.

[4]Ofori, S., Puškácová, A., Ru•icková, I. and Wanner, J. 2021. Treated wastewater reuse for irrigation: Pros and cons. Sci. Total Environ. **760**: 144026.

[5]Magesan, G.N., Williamson, J.C., Sparling, G.P., Schipper, L.A. and Lioyd-Jones, A.R. 1999. Hydraulic conductivity in soils irrigated with wastewaters of deferring strengths: Field and laboratory studies. Aust. J. Soil Res. **37**:391–402.

[6]Pomares, F., Roca, J., Tarazona, F. and Estale, M. 1984. Aerobically digested sewage sludge as N and P fertilizer. In Processing and use of sewage sludge. Dordecth: Reidel. (Commission of the European Communities). pp. 313-315.

[7]Sommers, L.E. 1977. Chemical composition of sewage sludges and analysis of their potential use as fertilizers. Environ. Qual. **6**:225-229.

[8]Seaker, E.M. 1991. Zinc, copper, cadmium and lead in minespoil, water and plants from reclaimed mine land amended with sewage sludge. Water Air Soil Poll. **57-58**:849-859.

[9]Pescod, M.B. 1992. Wastewater treatment and use in agriculture. FAO Irrig. Drain. Pap. 47, Rome, Italy.

[10]Mukherjee, S. and Nelliyat, P. 2007. Ground Water Pollution and Emerging Environmental Challenges of Industrial Effluent Irrigation: A Case Study of Mettupalayam Taluk, Tamilnadu; Madras School of Economics Working Paper 52 p. Available online: https://ssrn.com/abstract=1021153 (accessed on 9 August 2021).

[11]Hajjami, K., Ennaji, M.M., Fouad, S., Oubrim, N., Khallayoune, K. and Cohen, N. 2012. Assessment of helminths health risk associated with reuse of raw and treated wastewater of the Settat city (Morocco). Resour. Environ. **2**:193–201.

[12]Yadav, R.K., Goyal, B., Sharma, R.K., Dubey, S.K. and Minhas, P.S. 2002. Post irrigation impact of domestic sewage effluent on composition of soils, crops and groundwater: a case study. Environ. Int. **28**:481–486.

[13]Tarchouna, L.G., Merdy, P., Raynaud, M., Pfeifer, H.R. and Lucas, Y. 2010. Effects of long-term irrigation with treated wastewater. Part I: Evolution of soil chemical properties. Appl. Geochem. **25**:1703–1710.
[14]Saliba, R., Callieris, R., D'Agostino, D., Roma, R. and Scardigno, A. 2018. Stakeholders' attitude towards the reuse of treated wastewater for irrigation in Mediterranean agriculture. Agric. Water Manag. **204**: 60–68.
[15]Barber, L.B., Rapp, J.L., Kandel, C., Keefe, S.H., Rice, J., Westerhoff, P., Bertolatus, D.W. and Vajda, A.M. 2019. Integrated assessment of wastewater reuse, exposure risk, and fish endocrine disruption in the Shenandoah River watershed. Environ. Sci. Tech. **53**:3429–3440.
[16]Abd-Elwahed, M.S. 2018. Influence of long-term wastewater irrigation on soil quality and its spatial distribution Ann. Agric. Sci. **63**(2):191-199.
[17]APHA-AWWA-WPCF 1998. Standard Methods for the Examination of Water and Wastewater. 20th ed. American Public Health Association, Washington DC. USA.
[18]Peech, N. 1965. Hydrogen ion activity. In Black, C. A., Evans, D. D., White, J.L., Ensminger, L.E. and Clark, F.E. (eds). Methods of Soil Analysis.American Society of Agronomy, Madison, Wisconsin, pp.914-926.
[19]Rhoades, J.D. 1996. Salinity: Electrical conductivity and total dissolved solids. In Sparks, R.L.(ed.). Methods for Soil Analysis, Part 3: Chemical Methods. Soil Science Society of America, Madison, pp. 417-435.
[20]Nelson, D.W. and Sommers, L.E .1996. Total carbon, organic carbon, and organic matter. In Page, A. L. *et al.*(ed.). Methods of Soil Analysis, Part 2. 2nd edn. Agronomy **9**:961–1010. Am. Soc. of Agron., Inc. Madison, WI.
[21]Olsen, R.L. and Dean, L. 1965. Phosphorus. In Black, C. A., Evans, D. D., White, J. L., Ensminger, L. E.and Clark, F. E. (eds). Methods of Soil Analysis. American Society of Agronomy, Madison, Wisconsin, pp. 1035-1049.
[22]MAPA 1994. Ministerio de Agricultura, Pesca y Alimentacio´n, Me´todos oficiales de ana´lisis. Tomo III. Ed. MAPA, Madrid.
[23]Lockett, A.M. 2008. Impact of reuse water on golf course oil and turfgrass parameters monitored over a 4.5 year period. HortScience **43**:1942–2274.
[24]Ayers, R.S. and Westcot, D.W. 1985. Water quality for agriculture. Irrigation and Drainage Paper 29 (Rev. 1) Food and Agriculture Organization (FAO) of the United Nations. Rome, Italy.
[25]Quian. Y.L. and Mecham, B. 2005. Long-term effects of recycled wastewater irrigation on soil chemical properties on golf course fairways. Agronomy Journal **97**:717–721.
[26]Brady, N.C. 1984. The Nature and Properties of Soils. 9th edn. Macmillan Publishing Company, New York, 750 p.

Water Supply

IWA PUBLISHING

Water Supply Vol 22 No 6, 6002 doi: 10.2166/ws.2022.174

Development and evaluation of a water quality index for groundwater quality assessment in parts of Jabalpur District, Madhya Pradesh, India

Sudesh Bhaskar Ghoderao[a], Sarita Gajbhiye Meshram[b,*] and Chandrashekhar Meshram[c]

[a] Department of Chemistry, RNC Arts, JDB Commerce and NSC Science College, Nasik Road, Nasik, Maharashtra 422101, India
[b] Water Resources and Applied Mathematics Research Lab, Nagpur, Maharashtra 440027, India
[c] Department of Mathematics, Jaywanti Haksar Government PG College, College of Chhindwara University, Betul, MP, India
*Corresponding author. E-mail: gajbhiyesarita@gmail.com

SGM, 0000-0001-5453-3791

ABSTRACT

Groundwater is an important source for drinking water supply in Jabalpur District, Madhya Pradesh, India. An attempt has been made in this work to understand the suitability of groundwater for human consumption. The parameters of pH, Electrical Conductivity (EC), Copper (Cu), Chromium (Cr), Sulphate (SO_4), Iron (Fe), Nitrate (NO_3), Chloride (Cl), Total Hardness (TH), Total Alkalinity (TA), and Sodium (Na) were analyzed to estimate the groundwater quality. The water quality index (WQI) has been applied to categorize the water quality, which is quite useful to infer the quality of water for the people and policy makers in the concerned area. The WQI in the study area ranges from 17.90 to 176.88. According to the WQI rating, sites 1, 3, and 4 are not appropriate for drinking water or have low water quality and site 2 has moderate drinking condition, whereas site 5 has excellent drinking condition. The current study suggests that the groundwater of the area with deteriorated water quality needs treatment before consumption.

Key words: groundwater, principal component analysis (PCA), water quality, WQI

HIGHLIGHTS

- WQI values in sites 1, 3 and 4 are 106.99, 176.88, 161.25, showing that the groundwater is not suitable for drinking purposes.
- WQI value in site 5 is 17.90, showing that water is fit for drinking purposes.
- Principal component analysis reveals that four parameters are responsible for the high values of WQI.
- The outcome of the study will be helpful in formulating effective drinking water management measures for residents in the Jabalpur region, India.

GRAPHICAL ABSTRACT

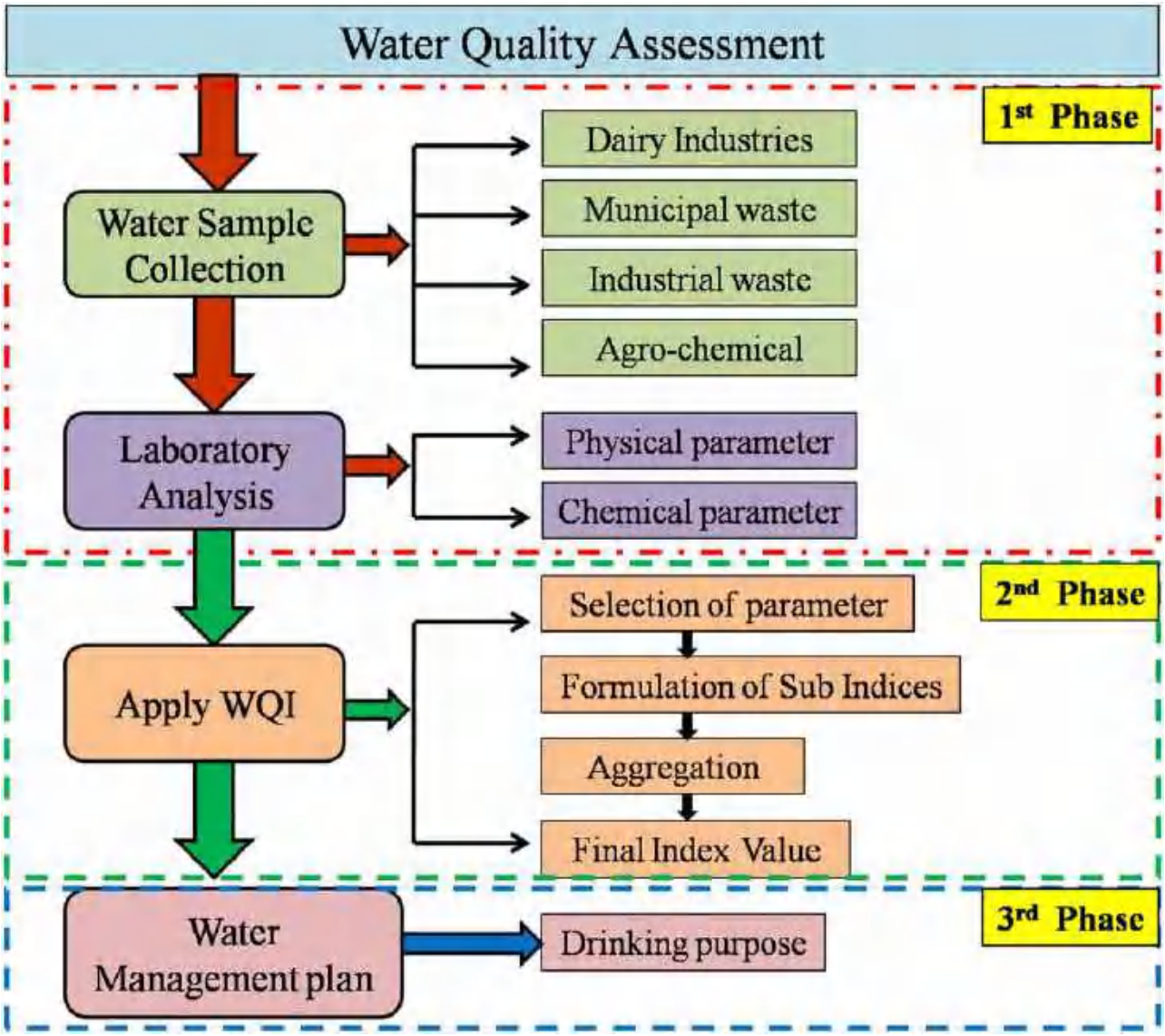

1. INTRODUCTION

The purity of water is essential to all living beings. For example, precipitation, weathering and soil erosion, as well as human-induced variables such as human exploitation of water resources, can all affect the quality of a region's surface water (Meshram *et al.* 2020a, 2020b, 2021a, 2021b). This includes both natural and anthropogenic factors. It is a big problem because of the rapid growth of human population, rapid industrialization, unplanned cities, pollution moving down from the hills to the lowlands, and the excessive use of fertilizers and pesticides in farming (Ouyang *et al.* 2006).

Groundwater is an important natural water resource that has long been used for drinking and irrigation, particularly in dry and semi-arid climates (Ramakrishnaiah *et al.* 2009; Li *et al.* 2018; Adimalla & Qian 2019; Ram *et al.* 2021). Groundwater is important as it can be directly used for potable water (via desalination) and industrial applications (Panagopoulos 2021a, 2021b, 2021c). Despite the fact that groundwater is frequently thought to be the cleanest of all inland water supplies, studies reveal that it is not fully free of contamination, albeit it is expected to be free of suspended solids. The underlying problem with groundwater is that once it has been contaminated, it is impossible to regain its purity. As a result, there is a need for, and apprehension about, groundwater quality conservation and management (Said *et al.* 2004). Because water quality

is dependent on a number of factors, it is widely acknowledged that there are no straightforward explanations for its degradation. Many metrics have significant correlations, and the cumulative effect of their interconnection shows water quality. To assess groundwater quality, the concentrations of many physicochemical parameters in industrial areas are measured and compared with drinking water standards (de França Doria 2010). Groundwater contamination, drinking and irrigation water quality, and geochemical occurrence and distribution have all been investigated all over the world (Narsimha & Sudarshan 2013; Khan & Jhariya 2017; Adimalla & Venkatayogi 2018; He & Wu 2018; Li *et al.* 2018; Zhang *et al.* 2018).

In order to better understand the water quality and ecological status of the studied systems and identify potential factors/sources that influence water systems, a variety of applied mathematics techniques, such as Cluster Analysis (CA), Principal Component Analysis (PCA), Factor Analysis (FA), and Discriminant Analysis (DA), help interpret advanced information matrices and provide a useful tool for reliable water resource management (Simeonov *et al.* 2004). Multivariate statistical methods have been used to define and evaluate surface and freshwater quality, which is important because they can be used to show how natural and anthropogenic sources can change over time and space (Helena *et al.* 2000).

Various researchers have investigated the contamination sources of river water using PCA and FA approaches. Simeonov *et al.* (2003), for example, used PCA to examine the association between a variety of parameters in order to assess water quality in northern Greece. PCA has been found to be a useful tool for analyzing huge datasets and developing analytical methodologies. To investigate the causes of parameter change, Shrestha & Kazama (2007) divided participants into groups based on regional and seasonal features. Although all approaches allow for dimensional reduction, Factor Analysis (FA), Cluster Analysis (CA), and Discriminant Analysis (DA) are commonly employed when the goal is to examine and understand the relationship between the variables, whereas PCA is commonly used when the goal is to focus on data reduction while losing some perception. At a dumpsite, Amadi (2011) used FA to discern between natural and anthropogenic causes of groundwater pollution. CA was used by Azhar *et al.* (2015) and Fathi *et al.* (2018) to group similar sample stations together based on system characteristics. FA reduces data by locating hidden variables (factors) that explain covariance, allowing the original parameters to be stated as a linear combination. Zeinalzadeh & Rezaei (2017) created a two-parameter index that beat the National Sanitation Foundation Water Quality Index (NSFWQI) in detecting changes in river conditions by using PCA to extract the most important indicators from water samples taken from the Shahr Chai River in Iran. Many researchers have considered the use of PCA approaches in a variety of domains (for example: Vega *et al.* 1998; Yu *et al.* 1998; Morales *et al.* 1999; Perkins & Underwood 2000; Bordalo *et al.* 2001; Gangopadhyay *et al.* 2001; Voutsa *et al.* 2001; Bengraïne & Marhaba 2003; Ouyang 2005).

Jabalpur is a region in Madhya Pradesh State (MP), where groundwater is a major water resource for drinking, domestic and agricultural purposes. No efforts have been made to understand the comprehensive evaluation of groundwater quality using the PCA approach in this region. Therefore, groundwater quality in this area is vital in determining the suitability of water for drinking purposes. Thus, the objective of the study is to calculate the WQI of groundwater in order to assess its suitability for human consumption using the PCA approach in the study area. It is expected that the outcome of the study will be helpful in formulating an effective drinking water management measure for residents in the Jabalpur region.

2. MATERIALS AND METHODS

2.1. Study area and data source

The location of Jabalpur (MP) was selected for the present analysis. The research was conducted on four point sources and one non-point wastewater source. The point sources are site 1 (dairy industries), sites 2–3 (municipal waste) and site 4 (industrial waste), and site 5 is a non-point source of agro-chemicals. Jabalpur is located on the Kymore plateau and Satpura hills in the agro-climatic area of 23 °9′ N latitude and 79 °58′ E longitude, at an altitude of 411.78 metres above mean sea level, and has a sub-tropical, sub-humid climate. Summers are hot and dry, and winters are cold and rainy. The temperature at this site can drop below freezing in the winter and exceed 46 °C in the summer, making the environment quite severe (Figure 1).

2.2. Water sampling

The groundwater samples were carried out during the premonsoon (February) period in 2018. A total of 280 groundwater samples were collected from existing hand pumps, bore wells, or open wells and stored in thoroughly prewashed high-quality polyethylene bottles at 4 °C until analysis. The samples were collected at 8:00 AM and 1:00 PM daily from the five sites.

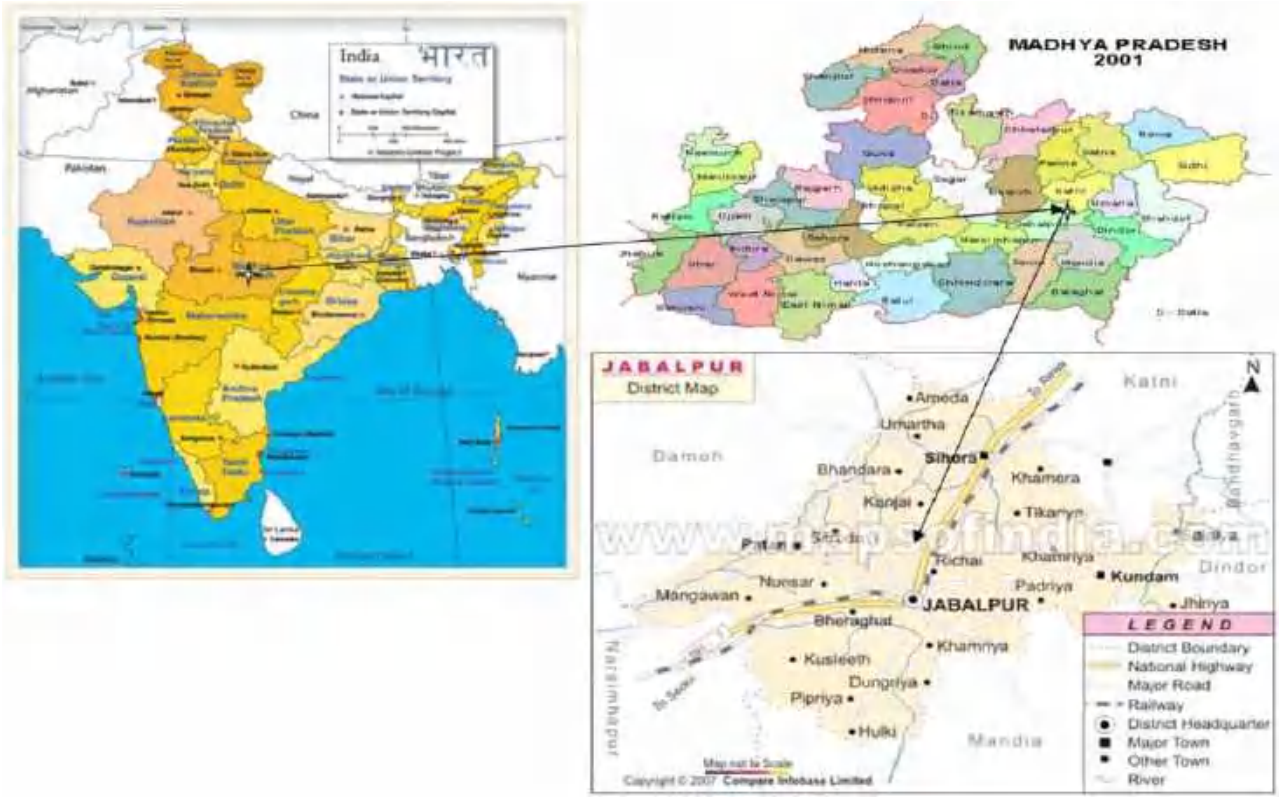

Figure 1 | Location map of the study area.

2.3. Determination of properties of water

The 11 variables examined for the water sample were pH, EC, Cu, Cr, SO_4, Fe, NO_3, Cl, TH, TA, and Na. Table 1 lists the water quality metrics and their abbreviations. All water samples were analyzed using standard procedures recommended by the American Public Health Association (APHA 1992).

2.4. Principal component analysis

To perform the statistical analysis, SPSS 14.0 was used. With a large dataset of interrelated variables, PCA is an excellent method for attempting to explain variation by using a small number of unbiased variables (Simeonov *et al.* 2003). The eigenvalues and eigenvectors of the original variables are extracted from the covariance matrix using the PCA method. By

Table 1 | Water quality parameters and their abbreviation

Parameters	Abbreviation	Unit
pH		–
EC	Electric conductivity	(dS/m)
Cu	Copper	(mg/l)
Cr	Chromium	(mg/l)
SO_4	Sulphate	(mg/l)
Fe	Iron	(mg/l)
NO_3	Nitrate	(mg/l)
Cl	Chloride	(mg/l)
TH	Total hardness	(mg/l)
TA	Total alkalinity	(mg/l)
Na	Sodium	(mg/l)

multiplying the unique correlated variables with an eigenvector, which is a set of coefficients, we get uncorrelated (orthogonal) variables (PC). As a result, the PCs are linear weighted combinations of the distinct variables. The PC keeps track of the most important aspects of the data collection, as well as enabling data reduction with little data loss (Vega *et al.* 1998). It is a powerful pattern-recognition technique that tries to explain the variation of a large number of connected variables by breaking them down into a smaller number of unrelated variables (principal components). PCA is a method for extracting a collection of independent linear combinations of study parameters in order to capture as much variability as possible in a dataset (Panigrahi *et al.* 2007). PCA can be calculated using Equation (1):

$$f_{ij} + f_{i1}z_{i1} + f_{i2}z_{i2} + \cdots \ldots \ldots \ldots f_{im}z_m + e_{ij} \tag{1}$$

where j = measured variable, f = factor loading, z = factor score, e = residual term accounting for errors, i = sample number, and m = total number of factors.

2.5. Water quality index

The Water Quality Index (WQI) is a mathematical method for obtaining a single number to reflect water quality from several water quality measures, created by Horton (1965). Water quality can be assessed by employing a number of commonly used water parameters, such as BOD (Biological Oxygen Demand), temperature, turbidity and conductivity (Kankal *et al.* 2012). Water quality parameters are measured using the WQI, which provides a way to construct a numerical expression that may be used to describe water quality (Miller *et al.* 1986). Using a chosen method or model, the water quality index reduces water quality data to a common scale and aggregates it into one value. All water quality criteria are taken into account in the WQI calculation, which is based on the appropriateness of surface and groundwater for their intended use. The following three processes are the most frequently linked with developing any index:

i. Parameter selection.
ii. Assignment of weightage to all parameters.
iii. Aggregation of sub-indices (or parameter) to produce a final index.

Parameter selection: Parameter selection necessitates three steps. The first step is Principal Component Analysis, which identifies the most meaningful parameters that best represent the entire data collection, allowing for data reduction with minimal loss of original information (Helena *et al.* 2000). After varimaxally rotating the initial factor loading matrix, an attempt is made to arrange the parameters into factors and to exclude those with no substantial linkages to rotated factors or components. In step 3, the covariance explained by each component and its percentage contribution to the overall covariance of the components are determined for rotating loading matrices of factors.

Assignment of weightage to all parameters: A higher weight value indicates that the parameter is more significant. The most difficult aspect of determining the weight of each parameter is that various people may have varying viewpoints. Different parameters are assigned weights based on the designed proportional factors.

Aggregation of sub-indices (parameter) to produce a final index: The process of merging and simplifying a group of water quality parameters is known as aggregation. The following equation describes the WQI aggregation function:

$$WQI = \sum (P1 * w_{P1}) + (P2 * w_{P2}) + (P3 * w_{P3}) + (P4 * w_{P4}) \tag{2}$$

where $P1$, $P2$,….. Pn = water quality parameters; w_{P1}, w_{P2}……..w_{Pn} = weightage of the corresponding parameter.

The above-mentioned water quality metrics are described in depth below, with findings displayed in Table 2.

3. RESULTS AND DISCUSSIONS

3.1. Water quality parameter

The findings of the groundwater sample analysis are shown in Table 2. According to this data, the pH of the water samples ranges from 7.42 to 7.61. These statistics are within the WHO's (World Health Organization) safe limits. Site 2 has the highest average EC value (1.66 dS/m), which is considered high by the USSL (United States Salinity Laboratory). Site 1 comes in second (1.27 dS/m). The lowest EC value (1.03 dS/m) was obtained at site 5. As a result, all of the samples were classified as high. Copper levels in sites 1 through 5 are 0.26 mg/l, 0.13 mg/l, 0.90 mg/l, 0.40 mg/l, and 0.12 mg/l, respectively. The

Table 2 | Physico-chemical properties of water samples

	Location				
Parameter	**Site 1**	**Site 2**	**Site 3**	**Site 4**	**Site 5**
pH	7.50	7.58	7.61	7.42	7.50
EC (dS/m)	1.27	1.66	1.16	1.11	1.03
Cu (mg/l)	0.26	0.13	0.90	0.40	0.12
Cr (mg/l)	0.08	0.07	0.23	0.08	0.04
SO_4 (mg/l)	43	12	60	47	18
Fe (mg/l)	0.92	0.39	0.48	0.52	0.29
NO_3 (mg/l)	1.86	4.8	0.71	0.45	0.62
Cl (mg/l)	42	36	50	75	45
TH (mg/l)	300	240	235	280	260
TA (mg/l)	717	790	900	710	520
Na (mg/l)	488	380	520	130	128

copper concentration in all water tests, according to WHO, is within the permitted range. The highest concentration of Cr is found at site 3 (0.23 mg/l). Sites 1 and 4 (0.08 mg/l), site 2 (0.07 mg/l), and site 5 (0.04 mg/l) have the lowest Cr values.

Drinking water containing more than 400 mg/l of sulphate has a harsh, medicinal taste and can cause gastrointestinal discomfort and catharsis. SO_4 concentrations in water samples from sites 1 to 5 were 43 mg/l, 12 mg/l, 60 mg/l, 47 mg/l, and 18 mg/l, respectively. These SO_4 levels are all within the WHO's acceptable limit. The highest Fe content was found at site 1 (0.92 mg/l), followed by site 4 (0.52 mg/l). The lowest Fe measurement was for site 5 (0.29 mg/l). According to the WHO, the iron concentration in all water samples is below the permitted threshold. As a result of sewage percolation beneath the surface, nitrate is a pollutant present in groundwater. Natural water contains organic nitrate sources, as well as industrial and agricultural contaminants. The highest NO_3 concentration was found at site 2 (4.8 mg/l). Site 1 came next (1.86 mg/l), and site 4 had the lowest NO_3 value (0.45 mg/l). The nitrate amounts in all water tests, according to WHO, are within permissible levels.

Chloride levels in water samples from sites 1 to 5 are 42 mg/l, 36 mg/l, 50 mg/l, 75 mg/l, and 45 mg/l, respectively. According to the WHO, the chloride concentration in all water tests is within the permissible range. A high concentration of chlorine in groundwater makes it hazardous to human health (Pius *et al.* 2012; Sadat-Noori *et al.* 2014). The greatest TH value (300 mg/l) was found at site 1. Site 4 was next (280 mg/l), and site 3 had a TH value of 235 mg/l. All of the water samples have overall hardness levels that are below the WHO's tolerable limit. The main sources of alkalinity in natural water are hydrogen sulphide, carbonate, and bicarbonate. In and of itself, alkalinity is not harmful to people. Total alkalinity values at sites 1 through 5 were 717 mg/l, 790 mg/l, 900 mg/l, 710 mg/l, and 520 mg/l, respectively. The TA levels in water samples from sites 1 to 4 were higher, whereas readings from site 5 were below the WHO's authorized range.

Greater salt levels have been associated with cardiovascular disease and pregnancy-related toxaemia in women, according to the National Academy of Science. The maximum concentration of Na (520 mg/l) is found at site 3. The following two locations are site 1 (488 mg/l) and site 2 (380 mg/l). Site 5 has the lowest Na concentration (128 mg/l). Water samples from sites 4 to 5 were confirmed to be within the WHO's permitted range. According to WHO guidelines, water samples from sites 1 to 3 had higher salt levels. The high concentration of Na indicates weathering of rock-forming minerals and dissolution of soil salts present therein due to evaporation (Stallard & Edmond 1983). The high Na concentration in groundwater may be related to the mechanism of cation exchange (Kim & Yun 2005). Table 3 shows the mean, standard deviation, and coefficient of variation for the water samples that were chosen.

3.2. Principal component analysis (PCA)

In a preliminary assessment prior to doing the precept evaluation, a Pearson correlation matrix was used to ensure the relationship between physicochemical metrics. Table 4 shows the Pearson correlation matrix. The correlations between

Table 3 | Statistics of water quality parameters of groundwater samples

Parameters	Mean	SD	CV (%)
pH	7.52	0.07	0.89
EC	1.25	0.22	17.75
Cu	0.36	0.29	79.46
Cr	0.10	0.07	66.63
SO_4	36.00	18.15	50.40
Fe	0.52	0.22	41.37
NO_3	1.69	1.64	96.78
Cl	49.60	13.49	27.19
TH	263.00	24.42	9.28
TA	727.40	124.21	17.08
Na	329.20	169.93	51.62

Table 4 | Pearson correlation coefficients of physicochemical parameters under study

	pH	EC	Cu	Cr	SO_4	Fe	NO_3	Cl	TH	TA	Na
pH	1.0										
EC	0.40	1.0									
Cu	0.09	0.04	1.0								
Cr	−0.11	0.33	0.08	1.0							
SO_4	0.05	−0.07	−0.35	−0.80	1.0						
Fe	−0.75	−0.29	−0.44	0.22	−0.28	1.0					
NO_3	0.59	**0.61**	0.50	0.58	−0.48	−0.61	1.0				
Cl	0.27	−0.29	0.67	−0.48	−0.06	−0.33	0.02	1.0			
TH	−0.27	0.26	−0.03	−0.57	**0.68**	0.01	−0.40	0.01	1.0		
TA	0.11	**0.87**	0.07	0.23	0.17	−0.32	0.46	−0.42	0.50	1.0	
Na	**0.68**	0.21	−0.45	0.11	−0.19	−0.05	0.21	−0.06	−0.50	−0.21	1.0

Note: bold values show strong correlations of more than 0.60.

the physicochemical parameters under investigation revealed that EC has a strong (0.87) association with total alkalinity, while pH has a moderate (0.6) correlation with Na, EC with NO_3, Cu with chloride, and TH with SO_4. Grouping the traits into components and giving any physical significance is difficult at this time. As a result, in the next stage, the main component analysis is used. The correlation matrix is subjected to principal component analysis.

Table 5 summarizes the loadings, eigenvalues, and variance of each factor, as well as the overall cumulative variance of the variables. A factor with an eigenvalue greater than 1 was taken into account for this study. Using the Kaiser criterion, four distinct varimax factors (VF) were discovered, accounting for 94.62 percent of the entire variation in water quality.

The first VF, best represented by chromium, accounted for 31.39 percent of the total variance (Cr). VF2 was responsible for 24.38 percent of the total variance and had a significant impact on EC and TA. VF3 had a positive loading on pH and Na, and it accounted for 21.60 percent of the variance. VF4 had a significant loading on Cu and Cl, and explained 17.25 percent of the overall variance.

3.3. Derivation of the water quality index

As a starting point, we only include the first four principal components because they explain 94.62 percent of the total variance. Cr, TA, pH and Cu are selected from PC1 through PC4. Afterwards, the eigenvalues associated with each PC axis are ranked according to their importance in terms of the amount of variation they explain (i.e. PC1*31.39; PC2*24.38;

Table 5 | Varimax-rotated component matrix

	Component			
Parameter	**VF1**	**VF2**	**VF3**	**VF4**
pH	−0.04	0.22	**0.93**	0.27
EC	0.08	0.91	0.22	−0.05
Cu	0.23	0.10	−0.19	**0.94**
Cr	**0.91**	0.32	−0.09	−0.19
SO_4	−0.90	0.07	0.03	−0.12
Fe	0.23	−0.38	−0.53	−0.61
NO_3	0.54	0.59	0.40	0.42
Cl	−0.16	−0.41	0.13	0.81
TH	−0.77	0.37	−0.43	0.00
TA	−0.11	**0.98**	−0.10	−0.02
Na	0.20	−0.11	0.86	−0.35
Eigenvalues	3.45	2.68	2.37	1.89
Percentage of variance by component	31.39	24.38	21.60	17.25
Cumulative percentage of variance	31.39	55.77	77.37	94.62

Note: bold values show strong correlations of more than 0.90.

PC3*21.60; PC4*17.25), as shown in Table 5. Cr receives the most weight, whereas Cu receives the least weight (order of importance) (fourth order of importance) (Table 6).

$$WQI = \sum (Cr * w_{Cr}) + (TA * w_{TA}) + (pH * w_{pH}) + (Cu * w_{Cu}) \quad (3)$$

where Cr, TA, pH, Cu = water quality parameters. W_{Cr}, W_{TA}, W_{pH}, W_{Cu} = weightage of the corresponding parameter.

3.4. Water quality index

Water samples from each of the five sites were tested. The Water Quality Index (WQI) was developed for each site based on a large number of linked water quality factors. A WQI was developed based on the four water quality criteria (parameters). The classification of groundwater quality in relation to WQI is shown in Table 7. According to the findings, sites 1, 3, and 4 are plagued by water quality issues and are not appropriate for consumption. Site 2 is in poor drinking condition, while site 5 is in great drinking condition (Table 8). WQI values range from 17.90 to 176.887. It was discovered that groundwater in the majority of the research area is unfit for drinking due to excessive electrical conductivity, Na, and total alkalinity values exceeding the WHO permitted limit (2012).

Most respondents at the sample sites used shallow tube wells to obtain drinking water due to lower installation costs. Water from shallow tube wells has been shown to contain high quantities of iron and arsenic in some regions. As reported by Prusty & Farooq (2020) in coastal districts, water from both shallow and deep tube wells was salty. According to Yisa & Jimoh (2010), greater levels of iron and manganese are related to poor water quality. These characteristics are typical of unplanned

Table 6 | Order of importance of water quality parameters

Parameter	**Rotated factor**	**Square rotated**	**% covariance**	**Importance (%)**	**Order**	**Weightage**
Cr	0.91	0.83	31.39	26.05	1	1.20
TA	0.98	0.96	24.38	23.40	2	1.06
pH	0.93	0.86	21.60	18.58	3	0.94
Cu	0.94	0.88	17.25	15.18	4	0.80

Table 7 | Classification of groundwater quality according to WQI range

Akter *et al.* (2016)		Chaurasia *et al.* (2018)	
WQI Range	Type of water	WQI Range	Type of water
<35	Excellent	<50	Excellent
35–45	Good	50–100	Good water
45–55	Moderate	101–200	Poor water
55–65	Poor	201–300	Very poor
65–75	Very poor	>300	Not suitable for drinking water
>75	Not suitable for drinking water		

Table 8 | Computed water quality index values for sample sites

Location	WQI	Akter *et al.* (2016)	Chaurasia *et al.* (2018)
Site 1	106.9914	Not suitable for drinking water	Poor water
Site 2	52.12459	Moderate	Good water
Site 3	176.887	Not suitable for drinking water	Poor water
Site 4	161.2565	Not suitable for drinking water	Poor water
Site 5	17.9065	Excellent	Excellent

garbage dumping, agricultural run-off containing pesticides or fertilisers, and other environmentally detrimental activities that pollute surface water (Chapman 1996).

There were some limitations to the study. The data for this study was obtained during the premonsoon season (February). It would have been preferable to collect samples throughout the year, taking into account seasonality and well depth. We were unable to collect information on other WHO-recommended chemical parameters since they were outside of our area of work. Other WHO-recommended chemical parameters may be measured in the future.

4. CONCLUSIONS

This paper has highlighted an evaluation of groundwater quality for drinking purposes using water quality index studies in the study region. In this study, a statistical technique (PCA) was used to evaluate variations in groundwater quality. PCA analysis grouped 11 water quality parameters into four factors (Cr, TA, pH, and Cu) of similar water quality characteristics. Based on the obtained information, it is possible to design a future, optimal WQI, which could reduce the number of parameter estimations and associated costs. Principal component analysis helped us figure out what caused the water quality to change.

The WQI values range from 17.90 to 176.887. The high value of WQI at these sites has been found to be mainly from the higher values of EC, Na and total alkalinity (TA) in the groundwater. Water samples from sites 1, 2 and 3 are highly polluted in terms of Na, EC and TA while other elements are within permissible levels.

The water quality evaluation reveals that the groundwater in sites 1, 3, and 4 is unfit for drinking or has poor water quality, and the pollution load is rather significant in comparison with site 2. The groundwater quality in site 5 is suitable for drinking. According to the research, water quality monitoring and management should be prioritised in order to safeguard the groundwater resource from contamination and provide technologies to make groundwater suitable for residential and drinking uses.

FUNDING

Not applicable.

CONFLICT OF INTEREST

All authors declare that they have no conflict of interest.

ETHICAL APPROVAL

This article does not contain any studies with human participants or animals performed by any of the authors.

DATA AVAILABILITY STATEMENT

Data cannot be made publicly available; readers should contact the corresponding author for details.

REFERENCES

Adimalla, N. & Qian, H. 2019 Groundwater quality evaluation using water quality index (WQI) for drinking purposes and human health risk (HHR) assessment in an agricultural region of Nanganur, south India. *Ecotoxicol. Environ. Saf.* **176**, 153–161. doi:10.1016/j.ecoenv.2019.03.066.

Adimalla, N. & Venkatayogi, S. 2018 Geochemical characterization and evaluation of groundwater suitability for domestic and agricultural utility in semi-arid region of Basara, Telangana State, South India. *Appl. Water Sci.* **8** (1), 44. https://doi.org/10.1007/s13201-018-0682-1.

Akter, T., Jhohura, F. T., Akter, F., Chowdhury, T. R., Mistry, S. K., Dey, D., Barua, M. K., Islam, M. A. & Rahman, M. 2016 Water Quality Index for measuring drinking water quality in rural Bangladesh: a cross-sectional study. *J. Health Popul. Nutr.* **35**, 4. http://dx.doi.org/10.1186/s41043-016-0041-5.

Amadi, A. N. 2011 Assessing the effects of Aladimma dumpsite on soil and groundwater using water quality index and factor analysis. *Aust. J. Basic Appl. Sci.* **5** (11), 763–770.

APHA 1992 *Standard Methods for the Examination of Water and Wastewater*, 18th edn. Water Pollution Control Federation, New York, USA.

Azhar, S. C., Aris, A. Z., Yusoff, M. K., Ramli, M. F. & Juahir, H. 2015 Classification of river water quality using multivariate analysis. *Procedia Environ. Sci.* **30**, 79–84. doi:10.1016/j.proenv.2015.10.014.

Bengraïne, K. & Marhaba, T. F. 2003 Using principal component analysis to monitor spatial and temporal changes in water quality. *J. Hazard. Mater. B* **100**, 179–195.

Bordalo, A. A., Nilsumranchit, W. & Chalermwat, K. 2001 Water quality and uses of the Bangpakong River (Eastern Thailand). *Water Res.* **35** (15), 3635–3642.

Chapman, D. 1996 *Water Quality Assessment – A Guide to Use of Biota, Sediments and Water in Environmental Monitoring*. E. & F.N. Spon, Chapman & Hall, London, UK.

Chaurasia, A. K., Pandey, H. K., Tiwari, S. K., Prakash, R., Pandey, P. & Ram, A. 2018 Groundwater quality assessment using Water Quality Index (WQI) in parts of Varanasi District, Uttar Pradesh, India. *J. Geol. Soc. India* **92**, 76–82. http://dx.doi.org/10.1007/s12594-018-0955-1.

De França Doria, M. 2010 Factors influencing public perception of drinking water quality. *Water Policy* **12** (1), 1–19. doi:10.2166/wp.2009.051.

Fathi, E., Zamani-Ahmadmahmoodi, R. & Zare-Bidaki, R. 2018 Water quality evaluation using water quality index and multivariate methods, Beheshtabad River, Iran. *Appl. Water Sci.* **8** (7), 210.

Gangopadhyay, S., Gupta, A. D. & Nachabe, M. H. 2001 Evaluation of ground water monitoring network by principal component analysis. *Ground Water* **39**, 181–191.

He, S. & Wu, J. 2018 Hydrogeochemical characteristics, groundwater quality and health risks from hexavalent chromium and nitrate in groundwater of Huanhe Formation in Wuqi County, northwest China. *Expo. Health* **11**, 125–137. https://doi.org/10.1007/s12403-018-0289-7.

Helena, B., Pardo, R., Vega, M., Barrado, E., Fernandez, J. M. & Fernandez, L. 2000 Temporal evolution of groundwater composition in an alluvial aquifer (Pisuerga River, Spain) by principal component analysis. *Water Res.* **34** (3), 807–816.

Horton, R. K. 1965 An index number for rating water quality. *J. Water Pollut. Control Fed.* **37** (3), 300–306.

Kankal, N. C., Indurkar, M. M., Gudadhe, S. K. & Wate, S. R. 2012 Water quality index of surface water bodies of Gujarat, India. *Asian J. Exp. Sci.* **26** (1), 39–48.

Khan, R. & Jhariya, D. C. 2017 Groundwater quality assessment for drinking purpose in Raipur city, Chhattisgarh using water quality index and geographic information system. *J. Geol. Soc. India* **90**, 69–76. https://doi.org/10.1007/s12594-017-0665-0.

Kim, K. & Yun, S. T. 2005 Buffering of sodium concentration by cation exchange in the groundwater system of a sandy aquifer. *Geochem. J.* **39**, 273–284. https://dx.doi.org/10.2343/geochemj.39.273.

Li, P., He, X., Li, Y. & Xiang, G. 2018 Occurrence and health implication of fluoride in groundwater of loess aquifer in the Chinese Loess Plateau: a case study of Tongchuan, northwest China. *Expo. Health* **11**, 95–107. https://doi.org/10.1007/s12403-018-0278-x.

Meshram, S. G., Alvandi, E., Meshram, C., Kahya, E. & Al-Quraishi, A. M. F. 2020a Application of SAW and TOPSIS in prioritizing watersheds. *Water Resour. Manage.* **34**, 715–732. doi:10.1007/s11269-019-02470-x.

Meshram, S. G., Singh, V. P., Kahya, E., Alvandi, E., Meshram, C. & Sharma, S. K. 2020b The feasibility of multi-criteria decision making approach for prioritization of sensitive area at risk of water erosion. *Water Resour. Manage.* **34**, 4665–4685. doi:10.1007/s11269-020-02681-7.

Meshram, S. G., Adhami, M., Kisi, O., Meshram, C., Duc, P. A. & Khedher, K. M. 2021a Identification of critical watershed for soil conservation using game theory-based approaches. *Water Resour. Manage.* **35**, 3105–3120. https://doi.org/10.1007/s11269-021-02856-w.

Meshram, S. G., Singh, V. P., Kahya, E., Sepehri, M., Meshram, C., Hasan, M. A., Islam, S. & Duc, P. A. 2021b Assessing erosion prone areas in a watershed using interval rough-analytical hierarchy process (IR-AHP) and fuzzy logic (FL). *Stochastic Environ. Res. Risk Assess.* **36**, 297–312. doi:10.1007/s00477-021-02134-6.

Miller, W. W., Joung, H. M., Mahannah, C. N. & Garrett, J. R. 1986 Identification of water quality differences in Nevada through index application. *J. Environ. Qual.* **15**, 265–272.

Morales, M. M., Martí, P., Llopis, A., Campos, L. & Sagrado, J. 1999 An environmental study by factor analysis of surface seawaters in the Gulf of Valencia (western Mediterranean). *Analyt. Chim. Acta* **394**, 109–117.

Narsimha, A. & Sudarshan, V. 2013 Hydrogeochemistry of groundwater in Basara area, Adilabad district, Andhra Pradesh, India. *J. Appl. Geochem.* **15** (2), 224–237.

Ouyang, Y. 2005 Evaluation of river water quality monitoring stations by principal component analysis. *Water Res.* **39** (12), 2621–2635.

Ouyang, Y., Nkedi-Kizza, P., Wu, Q. T., Shinde, D. & Huang, C. H. 2006 Assessment of seasonal variations in surface water quality. *Water Res.* **40** (20), 3800–3810.

Panagopoulos, A. 2021a Beneficiation of saline effluents from seawater desalination plants: fostering the zero liquid discharge (ZLD) approach – a techno-economic evaluation. *J. Environ. Chem. Eng.* **9** (4), 105338. doi:10.1016/j.jece.2021.105338.

Panagopoulos, A. 2021b Energetic, economic and environmental assessment of zero liquid discharge (ZLD) brackish water and seawater desalination systems. *Energy Convers. Manage.* **235**, 113957. doi:10.1016/j.enconman.2021.11395.

Panagopoulos, A. 2021c Study and evaluation of the characteristics of saline wastewater (brine) produced by desalination and industrial plants. *Environ. Sci. Pollut. Res.* **29**, 23736–23749. https://doi.org/10.1007/s11356-021-17694-x.

Panigrahi, S., Acharya, B. C., Panigrahy, R. C., Nayak, B. K., Banarjee, K. & Sarkar, S. K. 2007 Anthropogenic impact on water quality of Chilika lagoon RAMSAR site: a statistical approach. *Wetlands Ecol. Manage.* **15** (2), 113–126.

Perkins, R. G. & Underwood, G. J. C. 2000 Gradients of chlorophyll *a* and water chemistry along an eutrophic reservoir with determination of the limiting nutrient by *in situ* nutrient addition. *Water Res.* **34** (3), 713–724.

Pius, A., Jerome, C. & Sharma, N. 2012 Evaluation of groundwater quality in and around Peenya industrial area of Bangalore, South India using GIS techniques. *Environ. Monit. Assess.* **184** (7), 4067–4077. http://dx.doi.org/10.1007/s10661-011-2244-y.

Prusty, P. & Farooq, S. H. 2020 Seawater intrusion in the coastal aquifers of India – a review. *HydroResearch* **3**, 61–74. doi:10.1016/j.hydres.2020.06.001.

Ram, A., Tiwari, S. K., Pandey, H. K., Chaurasia, A. K., Singh, S. & Singh, Y. V. 2021 Groundwater quality assessment using water quality index (WQI) under GIS framework. *Appl. Water Sci.* **11** (2), 46. doi:10.1007/s13201-021-01376-7.

Ramakrishnaiah, C. R., Sadashivaiah, C. & Ranganna, G. 2009 Assessment of water quality index for the groundwater in Tumkur Taluk, Karnataka State, India. *J. Chem.* **6**, 757424.

Sadat-Noori, S. M., Ebrahimi, K. & Liaghat, A. M. 2014 Groundwater quality assessment using the Water Quality Index and GIS in Saveh-Nobaran aquifer, Iran. *Environ. Earth Sci.* **71**, 3827–3843. http://dx.doi.org/10.1007/s12665-013-2770-8.

Said, A., Stevens, D. K. & Sehlke, G. 2004 An innovative index for evaluating water quality in streams. *Environ. Manage.* **34** (3), 406–414. doi:10.1007/s00267-004-0210-y.

Shrestha, S. & Kazama, F. 2007 Assessment of surface water quality using multivariate statistical techniques: a case study of the Fuji river basin, Japan. *Environ. Modell. Software* **22**, 464–475.

Simeonov, V., Stratis, J. A., Samara, C., Zachariadis, G., Voutsa, D., Anthemidis, A., Sofoniou, M. & Kouimtzis, Th. 2003 Assessment of the surface water quality in Northern Greece. *Water Res.* **37** (17), 4119–4124. doi:10.1016/s0043-1354(03)00398-1.

Simeonov, V., Simeonova, P. & Tzimou-Tsitouridou, R. 2004 Chemometric quality assessment of surface waters: two case studies. *Chem. Eng. Ecol.* **11** (6), 449–469.

Stallard, R. F. & Edmond, J. M. 1983 Geochemistry of the Amazon: 2. *The influence of geology and weathering environment on the dissolved load. J. Geophys. Res.: Oceans* **88**, 9671–9688. http://dx.doi.org/10.1029/JC088iC14p09671

Vega, M., Pardo, R., Barrado, E. & Debán, L. 1998 Assessment of seasonal and polluting effects on the quality of river water by exploratory data analysis. *Water Res.* **32** (12), 3581–3592.

Voutsa, D., Manoli, E., Samara, C., Sofoniou, M. & Stratis, I. 2001 A study of surface water quality in Macedonia, Greece: speciation of nitrogen and phosphorus. *Water Air Soil Pollut.* **129**, 13–32.

Yisa, J. & Jimoh, T. 2010 Analytical studies on water quality index of river Landzu. *Am. J. Appl. Sci.* **7**, 453–458.

Yu, C.-C., Quinn, J. T., Dufournaud, C. M., Harrington, J. J., Rogers, P. P. & Lohani, B. N. 1998 Effective dimensionality of environmental indicators: a principal component analysis with bootstrap confidence intervals. *J. Environ. Manage.* **53**, 101–119.

Zeinalzadeh, K. & Rezaei, E. 2017 Determining spatial and temporal changes of surface water quality using principal component analysis. *J. Hydrol. Reg. Stud.* **13**, 1–10.

Zhang, Y., Wu, J. & Xu, B. 2018 Human health risk assessment of groundwater nitrogen pollution in Jinghui canal irrigation area of the loess region, northwest China. *Environ. Earth Sci.* **77** (7), 273.

First received 26 November 2021; accepted in revised form 5 April 2022. Available online 19 April 2022

Received: 4 October 2021 | Revised: 12 January 2022 | Accepted: 17 January 2022

DOI: 10.1002/bio.4200

RESEARCH ARTICLE

LUMINESCENCE The Journal of Biological and Chemical Luminescence WILEY

Study on luminescence properties of Ce^{3+} and Eu^{3+} ions in a nanocrystalline hexagonal $Zn_4Al_{22}O_{37}$ novel system

Dinesh S. Bobade[1,3] | Yatish R. Parauha[2] | Sanjay J. Dhoble[2] | Prabhakar B. Undre[3]

[1]Department of Physics, RNC Arts, JDB Commerce and NSC Science College, Nashik, Maharashtra, India

[2]Department of Physics, Rashtrasant Tukdoji Maharaj Nagpur University, Nagpur, Maharashtra, India

[3]Department of Physics, Dr. Babasaheb Ambedkar Marathwada University, Aurangabad, Maharashtra, India

Correspondence
Dinesh S. Bobade and Prabhakar B. Undre, Department of Physics, Dr. Babasaheb Ambedkar Marathwada University, Aurangabad, Maharashtra, India.
Email: dsbobade1104@gmail.com; prabhakarundre@yahoo.co.in.

Abstract

The present communication is strongly focused on the investigation of synthesis, structural and luminescence properties of cerium (Ce^{3+})- and europium (Eu^{3+})-activated $Zn_4Al_{22}O_{37}$ phosphors. Ce^{3+}- and Eu^{3+}-doped $Zn_4Al_{22}O_{37}$ novel phosphors were prepared using a solution combustion synthesis route. Structural properties were studied using powder X-ray diffraction and high-resolution transverse electron microscopy. The optical properties were studied using ultraviolet–visible light spectroscopy and Fourier transform infrared spectroscopy; luminescence properties were studied using a photoluminescence (PL) technique. The crystal structure of the prepared $Zn_4Al_{22}O_{37}$ host and Ce^{3+}- and Eu^{3+}-activated $Zn_4Al_{22}O_{37}$ phosphors was investigated and was found to have a hexagonal structure. The measured PL emission spectrum of the Ce^{3+}-doped $Zn_4Al_{22}O_{37}$ phosphor showed an intense and broad emission band centred at 421 nm under a 298 nm excitation wavelength. By contrast, the Eu^{3+}-doped $Zn_4Al_{22}O_{37}$ phosphor exhibited two strong and intense emission bands at approximately 594 nm (orange) and 614 nm (red), which were monitored under 395 nm excitation. The Commission Internationale de l'Eclairage (CIE) colour coordinates of the Ce^{3+}-doped $Zn_4Al_{22}O_{37}$ were investigated and found to be $x = 0.1567$, $y = 0.0637$ (blue) at 421 nm and for Eu^{3+}-doped $Zn_4Al_{22}O_{37}$ were $x = 0.6018$, $y = 0.3976$ (orange) at 594 nm and $x = 0.6779$, $y = 0.3219$ (red) at 614 nm emission. The luminescence behaviour of the synthesized phosphors suggested that these phosphors may be used in lighting applications.

KEYWORDS
FT-IR, HR-TEM, nanophosphor, PL, UV, XRD

1 | INTRODUCTION

Rare earth element-activated phosphors have been used on a large scale in different fields in light emission industries due to their specific characteristics of emission in the visible and near-visible light regions. These rare earths have been widely used as activators in different systems due to their high fluorescence efficiency in which the size of their particles is reduced to the nanoscale level. The different applications of rare earth activated materials are for example fluorescence lamps, cathode-ray tubes, light-emitting diodes (LEDs) for the lighting industry, field-emission displays, and X-ray imaging.[1–6] Ce^{3+}- and Eu^{3+}-activated luminescence materials have attracted the attention of the researchers due to their high lumen output and characteristic emission properties in the visible and near-visible light regions. These Ce^{3+}- and Eu^{3+}-activated luminescence materials have attracted much interest due to their expected luminescence properties. Different types of activator-based luminescence materials such as aluminates, chlorides, nitrides, silicates, borates, phosphates, oxy-nitrides,

etc. have been prepared and applied in the field of luminescence[7,8] Among these, aluminates have demonstrated more advantages such as high luminous efficiency, excellent durability, and low cost, and good physical and chemical stability.[9–11]

Ce^{3+}-doped materials have attracted more interest because their spin and parity allow optical 4f→5d transitions, which have fast radiative lifetimes of ∼10–50 nsec,[6] which is desirable for application in scintillators, LEDs, and field-emission displays. Recently, significant efforts have been made by several research groups on the synthesis and study of various Ce^{3+}-doped fluoride and oxide materials.[12–14] The first white LED was commercialized by the Nichia Company,[15] in which a blue LED was coated with the yellowish phosphor YAG:Ce. The Ce^{3+}-doped $CaAl_{12}O_{19}$, $CaAl_4O_7$, $SrAl_4O_7$, and $SrAl_{12}O_{19}$ samples demonstrated a promising broad emission band that was centred at 355, 320, 330, and 317 nm, respectively. These host crystal structures had great influence on the prominent emission peaks of aluminate-based phosphors.[15] The photoluminescence (PL) emission spectra of the $LiAl_5O_8$ and $NaAl_{11}O_{17}$ phosphors were studied by Nikhare *et al.*[16] and strong Ce^{3+} emission was observed at ∼310 nm for the excitation at a wavelength of 254 nm due to the 5d→4f transition.

The emission of Eu^{3+}-doped phosphors revealed maximum intensities at 580 nm (j = 0), 592 nm (j = 1), 618 nm (j = 2), 650 nm (j = 3), and 690 nm (j = 4) because of the transition from minimum excited state of $^5D_0$ to different ^7F_j (j = 0 to 4). Ideally, weak emissions corresponding to the transition of j = 1, 4, and 5 are observed, whereas red emission at 613 nm and orange emission at 592 nm are seen as dominant. These transitions were strongly influenced by the symmetry acquired by the Eu^{3+} ion and the nature of its surrounding area.[17–19] The red emission at ∼614 nm was attributed to the $^5D_0 \rightarrow {}^7F_2$ transition corresponding to the electric dipole transition and orange emission at ∼591 nm that belonged to the $^5D_0 \rightarrow {}^7F_1$ transition corresponding to a magnetic dipole transition.[20] Kim[21] noted that the transition for $^5D_0 \rightarrow {}^7F_1$ levels at 590 nm was attributed to the Eu^{3+} ion acquired at the symmetrical sites in the crystal, there was also another low intensity peak observed at 610 nm due to Eu^{3+} ions that acquired low symmetry sites in the crystal. Other emission peaks located at 654 nm and 701 nm were attributed to the transitions from $^5D_0 \rightarrow {}^7F_3$ and $^7F_4$ levels, respectively.

As far as rare earth ion-doped zinc aluminates are concerned, a lack of study was observed in systems other than the $ZnAl_2O_4$ system. $ZnAl_2O_4$ has been widely studied and its structural, optical, and electronic properties have been investigated by several researchers.[9–11,22,23] Several investigations have been devoted to incorporating rare earth elements and transition metal ions into the $ZnAl_2O_4$ system.[24–27] Different trivalent rare earth ions such as Dy^{3+}, Tb^{3+}, and Eu^{3+} have been incorporated into $ZnAl_2O_4$ for display applications.[25,28,29] As a result, ultraviolet (UV) photoelectronic devices can be made with $ZnAl_2O_4$.[30,31] Kumar *et al.*[32] investigated a Sm^{3+}-activated $ZnAl_2O_4$ phosphor preparation for characterization and photoluminescence. The luminous and X-ray photoelectron characteristics of $ZnAl_2O_4$:Ce^{3+},Tb^{3+} phosphor were investigated by Tshabalala *et al.*[33]

No attempt, so far, seems to have been made to study other systems in zinc aluminates. The aim of this investigation was to prepare and study the structural and luminescence properties of Ce^{3+}- and Eu^{3+}-activated $Zn_4Al_{22}O_{37}$ phosphors. The samples were prepared using solution combustion synthesis and urea was used as a fuel agent to enhance the combustion. These samples were characterized using X-ray diffraction (XRD), high-resolution transverse electron (HR-TEM) microscopy, UV–visible (UV–vis) light spectroscopy, Fourier transform infrared (FT-IR) spectroscopy and photoluminescence (PL) techniques.

2 | EXPERIMENTAL

2.1 | Sample preparation

Combustion synthesis is one of the easiest, simplest, and large-scale applicable methods for the synthesis of the crystalline and nanostructured materials. Ce^{3+}- and Eu^{3+}-doped $Zn_4Al_{22}O_{37}$ phosphors were prepared by solution combustion using high purity analytical reagent (AR) grade compounds $(ZnNO_3)_2.6H_2O$, $Al(NO_3)_3.9H_2O$, $(NH_4)_2NO_3$, $Ce(NO_3)_3.9H_2O$, Eu_2O_3 and nitric acid as initial raw materials and urea was used as the fuel agent to enhance combustion. All precursors were weighed precisely at a stoichiometric ratio and dissolved in 20 ml distilled water. The solution was stirred for 30 min using a magnetic stirrer to acquire a homogeneous solution. Next, it was placed in a muffle furnace that was maintained at 500°C temperature. The solution was boiled to evolve the gases and created combustion within 5–8 min. By the end of combustion foamy powder samples were formed. The temperature of the solution reached almost 1400°C during combustion and, due to this, nanocrystalline samples were obtained. The prepared powder samples were characterized to investigate the different properties.

2.2 | Characterization

A phase and structural study of $ZnAl_{12}O_{19}$ was carried out using XRD (Bruker D8 Advance) with Cu $K_{\alpha 1}$ irradiation (λ = 1.5406 Å) and operating at 40 kV, 30 mA over the 2θ range 10–80°. A topography and morphology study of $Zn_4Al_{22}O_{37}$ was carried out using HR-TEM (FEI Titan 80–300 TEM). The optical properties (band gaps) were measured using UV–vis spectrophotometry (Shimadzu, Japan) and the luminescence properties are studied using a PL spectrophotometer (Perkin Elmer).

3 | RESULTS AND DISCUSSION

3.1 | X-ray diffraction analysis

The structural properties of the prepared samples were estimated using an XRD technique. Figure 1 shows the powder XRD patterns of

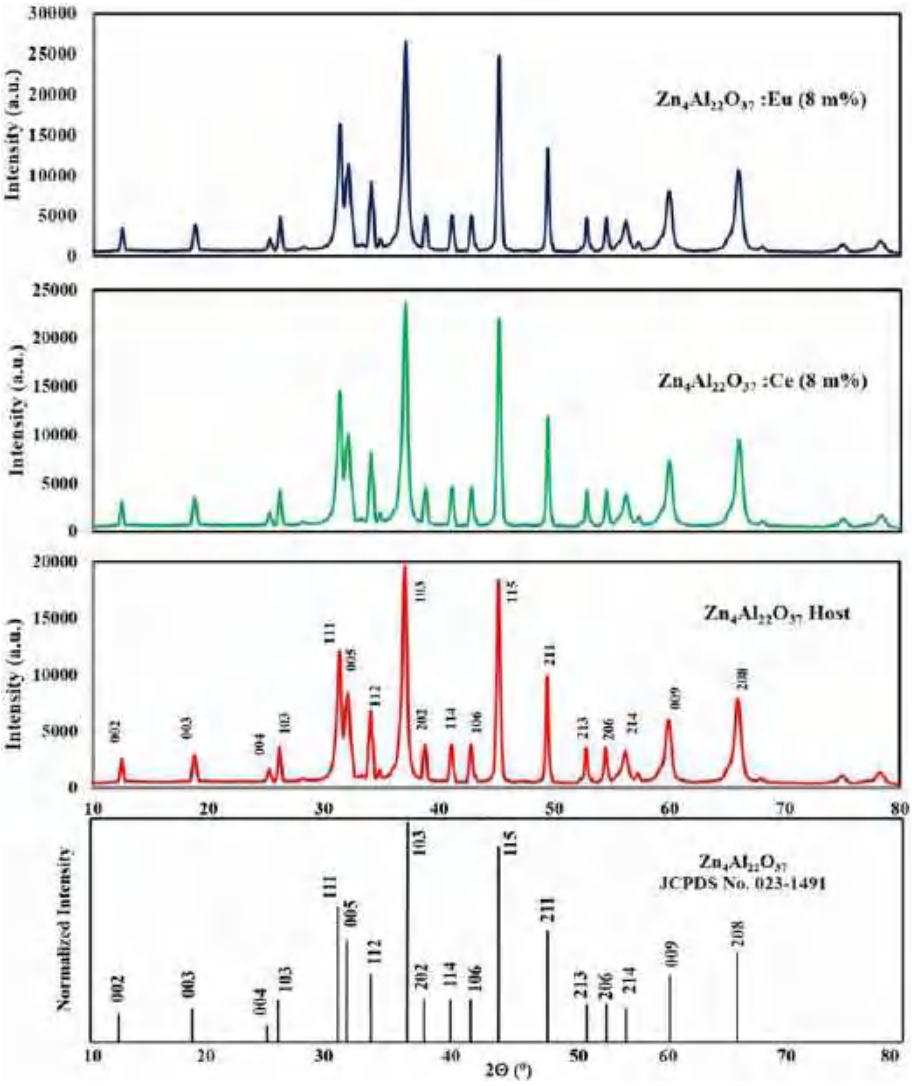

FIGURE 1 X-ray powder diffraction patterns of pure $Zn_4Al_{22}O_{37}$, Ce^{3+}-activated $Zn_4Al_{22}O_{37}$ and Eu^{3+}-activated $Zn_4Al_{22}O_{37}$ phosphors and standard JCPDS file for $Zn_4Al_{22}O_{37}$

(a) host $Zn_4Al_{22}O_{37}$, (b) 0.8 m% Ce^{3+}-activated $Zn_4Al_{22}O_{37}$, and (c) 0.8 m% Eu^{3+}-activated $Zn_4Al_{22}O_{37}$ phosphor taken at a 0.05°/s scanning rate in the range 20–80°.

The determination of lattice parameters is a very time-consuming task and sometimes it is easy to match hkl values with the $\sin^2\theta$. While indexing the 2θ values, some peaks of less intensity might be omitted, then the actual indexing may affect the *hkl* values (Miller indices). Therefore, for hexagonal structures, the analytical method is used to calculate the lattice parameters. Using Bragg's diffraction condition and the interplanar distance, we could obtain the equation for $\sin^2\theta$ as:

$$\sin^2\theta = \frac{\lambda^2}{4a^2}\left[\frac{4}{3}\left(h^2+hk+l^2\right)+\frac{l^2}{(c/a)^2}\right] \quad (1)$$

where $\sin^2\theta$ values can be calculated using the lattice parameters *a*, *c*, and the *hkl* values. For given structure the lattice parameters *a* and *c* are constants, then the $\sin^2\theta$ values depend upon *h*, *k*, and *l*. The above Equation (1) was converted into simplified form as:

$$\sin^2\theta = A\left(h^2+hk+k^2\right)+Cl^2 \quad (2)$$

where $A=\frac{\lambda^2}{3a^2}$, $C=\frac{\lambda^2}{4c^2}$ and *hkl* are integers. The values of h^2+hk+k^2 were obtained by choosing $l=0$ and then A was calculated. The value C was calculated from the equation $h^2+hk+k^2=0$ and choosing the values of $l=0$, 1, 2, 3, 4, etc. The constant C was calculated using the following equation:

$$Cl^2 = \sin^2\theta - A\left(h^2+hk+k^2\right) \quad (3)$$

The values of the lattice parameters *a* and *c* were estimated using A and C (constants) and other Miller indices were estimated using Equation (1). The Miller indices corresponding to high intensity peaks are listed in Table 1. The lattice parameters were calculated and these were $a = 5.6790$, $c = 13.7100$, $\alpha = 90°$, $\beta = 90°$ and $\gamma = 120°$. Also structure calculations were carried out using Endeavour software and estimated atomic positions of the prepared $Zn_4Al_{22}O_{37}$ are given in Table 2.

TABLE 1 Crystallite size calculation of $Zn_4Al_{22}O_{37}$

Sr. no.	2 θ(°)	d (Å)	FWHM	Crystallite size (nm)	Miller indices (*hkl*)
1	12.5	7.0754	0.3028	26.08	002
2	18.8	4.7162	0.3873	20.23	010
3	25.3	3.5173	0.4054	19.12	400
4	26.2	3.3985	0.342	22.62	013
5	28.2	3.1618	0.6622	11.63	110
6	31.4	2.8465	0.5123	14.92	014
7	32.1	2.7860	0.6206	12.30	111
8	32.6	2.7420	0.3472	21.96	005
9	34.19	2.6201	0.3943	19.47	112
10	37.1	2.4212	0.5199	14.48	113
11	38.8	2.3189	0.294	25.48	022
12	41.1	2.1943	0.3419	21.75	114
13	42.8	2.1110	0.3517	21.03	106
14	45.2	2.0043	0.3905	18.78	115
15	49.4	1.8433	0.3704	19.48	121
16	52.8	1.7323	0.4323	16.46	008
17	54.5	1.6822	0.3661	19.29	213
18	56.2	1.6353	0.5607	12.49	124
19	57.3	1.6065	0.5187	13.44	117
20	59.9	1.5428	0.6124	11.24	009
21	65.9	1.4161	0.6746	9.88	208
22	68	1.3774	0.2667	24.69	222
23	75	1.2653	0.6074	10.37	314
24	78.3	1.2200	0.9348	6.59	400

The prominent diffracted intensity peaks with *hkl* values are shown in Figure 1. High intensity peaks were observed for the prepared samples, which denoted the highly crystalline nature of the samples. The XRD pattern peaks of the synthesized samples were well matched with the standard Joint Committee on Powder Diffraction Standards (JCPDS) file no. 23-1491 of $Zn_4Al_{22}O_{37}$, as shown in Figure 1. In the diffraction patterns, no impurity peak was observed, which indicated that the dopants Ce^{3+} and Eu^{3+} were well incorporated in the host $Zn_4Al_{22}O_{37}$.

The crystallite size (D) was calculated using Debye–Scherer formula given below:

$$D = \frac{0.9\lambda}{\beta\cos\theta} \quad (4)$$

where, D is the crystallite size, 0.9 is the particle shape factor, λ is the wavelength of incident X-rays, β is the full width at half maximum (FWHM) of the *hkl* reflection and θ is the Bragg diffraction angle of the *hkl* reflection. The crystallite size for each *hkl* reflection was calculated and was observed in the 6.6–26 nm range, as shown in Table 2. The average crystallite size of pure $Zn_4Al_{22}O_{37}$ was determined to be 17 nm.

Atomic visualization is done by using Vesta software and it is shown in Figure 3. The hexagonal structure (space group P-6) was characterized as having close-packed arrays of oxygen atoms with polyhedral sites occupied by heterovalent cations. The different atomic structures of $Zn_4Al_{22}O_{37}$ unit cell are shown in Figure 3. The structure is of type $A_4B_{22}C_{37}$ and its atomic positions are presented in Table 2.

The coordination diagram with the ball-and-stick model is shown in Figure 2(a), which denotes that the Zn and Al atoms were coordinated by the oxygen atoms. These Zn and Al atoms occupied the central positions of the different polyhedral geometries, as shown in Figure 2(b). In this unit cell, the Zn atom had an ionic radius of 0.60 Å and its maximum coordinated number was observed to be 6. The Al atom hadan ionic radius of 0.54 Å and its coordinated eight oxygen atoms had ionic radii of 1.02 Å. The different lattice planes are shown in Figure 2(c–f) and this animation was created using Vesta software.

3.2 | High-resolution transmission electron spectroscopy analysis

HR-TEM technique is a very powerful tool to study of morphology, surface topography, crystal structure, and chemical composition of materials. The high energetic electron beam is diffracted through the sample and carries the structural and morphological information

TABLE 2 Atomic parameters of $Zn_4Al_{22}O_{37}$

Sr.no.	Atom	Oxidation state	Wyckoff positions	Atomic positions		
				x	y	z
1	Zn1	2	2*i*	0.6666	0.3333	0.42179
2	Zn2	2	1*d*	0.3333	0.6666	0.5000
3	Al1	3	3*j*	0.0796	0.6166	0
4	Al2	3	6 *L*	0.6632	0.0041	0.3249
5	Al3	3	6 *L*	0.4106	0.0369	0.1391
6	Al4	3	2 *g*	0	0	0.26991
7	Al5	3	2 *h*	0.3333	0.6666	0.2248
8	O1	−2	2*i*	0.6666	0.3333	0.1409
9	O2	−2	6 *L*	0.0155	0.5195	0.2362
10	O3	−2	6 *L*	0.1280	0.2786	0.3917
11	O4	−2	6 *L*	0.2375	0.0891	0.2076
12	O5	−2	3*j*	0.3986	0.0854	0
13	O6	−2	6 *L*	0.244	0.4001	0.0947
14	O7	−2	3 *k*	0.4011	0.00982	0.5
15	O8	−2	2*i*	0.6666	0.3333	0.3160
16	Zn3	2	1*b*	0	0	0.5
17	Al6	3	2 *g*	0	0	0.1039
18	Al7	3	1*e*	0.6666	0.3333	0
19	O9	−2	2 *h*	0.3333	0.6666	0.3261
20	O10	−2	1*a*	0	0	0

of the sample. The transmitted and diffracted beams are captured and diffraction pattern images for the prepared $Zn_4Al_{22}O_{37}$ are shown in Figure 3(a). The bright spots of atoms in concentric circles are clearly seen in the pattern. The interplanar distances for each ring were calculated in real space and these were observed to be consistent with the interplanar distance obtained using the XRD technique. The particle size was calculated using the HR-TEM image, as shown in Figure 3(b). The particle size was calculated using ImageJ software and was found to be a 20 nm average in size. Figure 3(c) shows the graph of the particle size calculation histogram. The surface topography images were captured at different areas, as shown in Figure 4. The d spacings between the crystallographic planes were estimated at different regions of the image in Figure 4(a) and corresponding *hkl* planes are shown in Figure 4(b–f). The lattice fringe width or d-spacing was calculated using ImageJ software. The scale of the image was calibrated using the straight line tool. The different regions were selected using the rectangle tool and the image was cropped. Then, the fast Fourier transform (FFT) process was carried out to find the position of the brightest point in the inverse lattice. The inverse FFT value was taken and then, by adjusting the threshold, the lattice fringes appeared in the image. These fringes from the different regions are shown in Figure 4(b–f). The lattice spacing was calculated using the plot profile. In the plot profile, by counting the number of peaks in a certain length, the lattice spacing is calculated.

3.3 | Ultraviolet–visible spectroscopy analysis

In most optical characterization techniques, the samples are bombarded with different types of radiation to study the different characteristics of the samples. UV–vis spectroscopy characterization is one of these techniques. In UV–vis spectroscopy the material is irradiated with UV–vis photons and emerging radiation is collected and data are constructed. Figure 5 demonstrates the UV–vis absorbance spectra of the Ce^{3+}- and Eu^{3+}-activated $Zn_4Al_{22}O_{37}$ and host $Zn_4Al_{22}O_{37}$. The band gap was modified by doping with Ce^{3+} and Eu^{3+} into $Zn_4Al_{22}O_{37}$. A blue shift occurred in the absorbance edge due to doping with Ce^{3+} and Eu^{3+} into the $Zn_4Al_{22}O_{37}$ system. From the UV–vis absorbance spectra, it is seen that the band gap energy of the host $Zn_4Al_{22}O_{37}$ decreased following Ce^{3+} doping in it. Incorporation of Ce^{3+} and Eu^{3+} ions into the $Zn_4Al_{22}O_{37}$ host created the discrete energy levels of Ce^{3+} and Eu^{3+} in the energy band gap of the host $Zn_4Al_{22}O_{37}$. When the Ce^{3+}- and Eu^{3+} ion-doped $Zn_4Al_{22}O_{37}$ phosphor was excited by UV–vis irradiation, then less energy was required for the excitation of the valence band electrons because of the decrease in the separation between the highest occupied and lowest unoccupied levels. The absorbance spectra consisted of an absorption band near 200 nm observed in both doped and undoped phosphor and related to the host material due to the characteristic transitions from metal–oxygen (Zn–O or Al–O) bands. A broad band was observed at 298 nm due to the

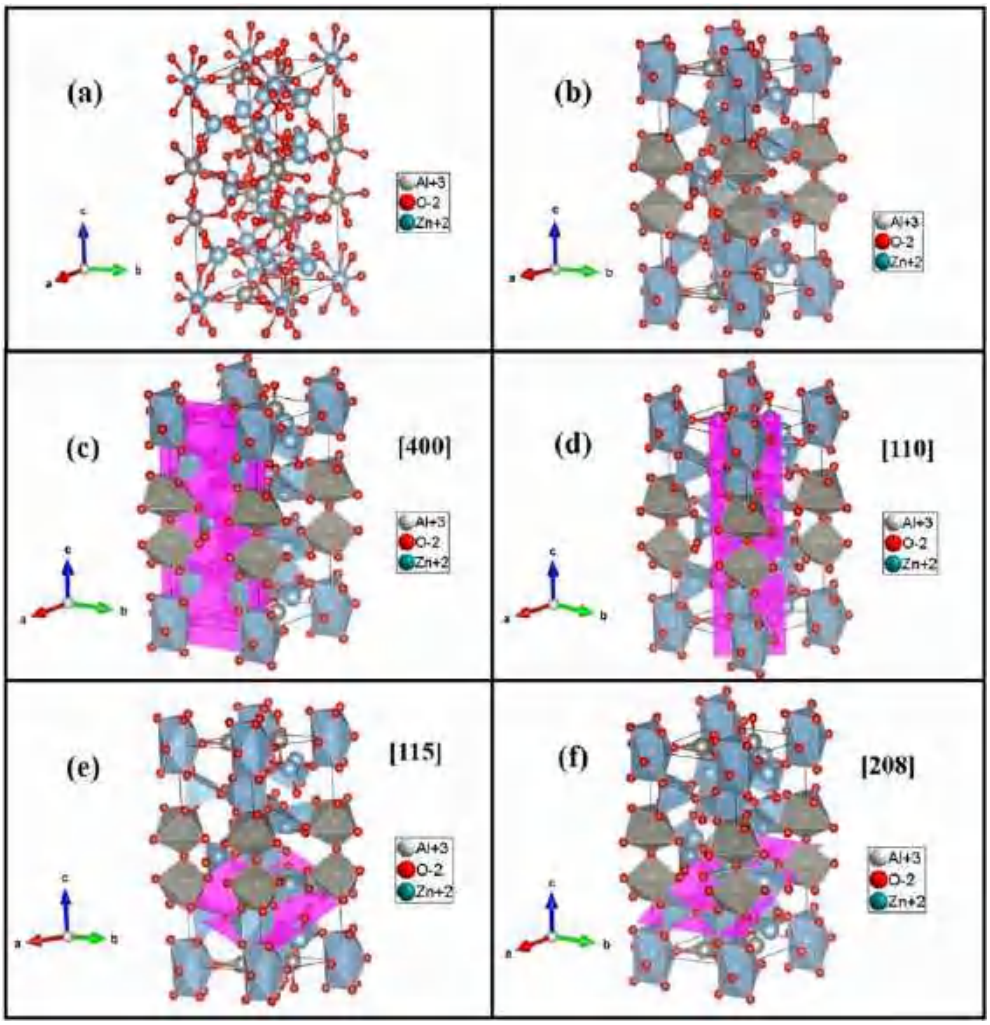

FIGURE 2 (a) Coordination ball-and-stick model of the $Zn_4Al_{22}O_{37}$ unit cell. (b) Polyhedral model of the $Zn_4Al_{22}O_{37}$ unit cell. (c–f) Different lattice planes (*hkl*) of the $Zn_4Al_{22}O_{37}$ unit cell

Ce–O band and a small shoulder peak was observed at 374 nm due to the Eu–O band.

Using the absorbance spectra, band gaps were calculated for pure and Ce^{3+}- and Eu^{3+}-activated $Zn_4Al_{22}O_{37}$ based on Kubelka–Munk theory.[34] To determine an optical energy gap, the Tauc plot approach was used. The Tauc equation was used to determine the optical band gap as given below:

$$\alpha = \frac{C(h\nu - E_g)^n}{h\nu} \quad (5)$$

where, α is the absorption coefficient, h is Plank's constant, ν is photon frequency, C is a constant, and Eg is the optical energy gap.[35] In the Tauc equation, the power n is a constant related to different types of electronic transitions (n = 1/2, 2, 3/2, or 3 for directly allowed, indirectly allowed, directly forbidden, and indirectly forbidden transitions, respectively). The curves in Figure 6 exhibited nonlinear and linear parts that denoted the characteristics of the directly allowed transitions. Therefore, in the Tauc equation the value of n was chosen as ½, then Equation (5) becomes:

$$(\alpha h\nu)^2 = A(h\nu - E_g) \quad (6)$$

The optical band gaps were calculated by plotting an $(\alpha h\nu)^2$ versus hν graph, the values of Eg were obtained by extrapolating the linearly fitted curves to $(\alpha h\nu)^2 = 0$. The optical band gap energies of pure $Zn_4Al_{22}O_{37}$, Ce^{3+}-activated $Zn_4Al_{22}O_{37}$, and Eu^{3+}-activated $Zn_4Al_{22}O_{37}$ were calculated and these were 4.13 eV, 3.33 eV, and 3.82 eV, respectively.

3.4 | Fourier transform infrared analysis

FT-IR spectroscopy was used to study molecular bonding and the strength of organic materials as well as inorganic materials. This technique measures the absorption/transmission of infrared radiation from a material by varying the wavenumber. FT-IR absorption bands identify molecular compositions and the structures of the samples. The molecules in the material absorb the incident infrared radiation and vibrate with a characteristic energy. This energy corresponds to

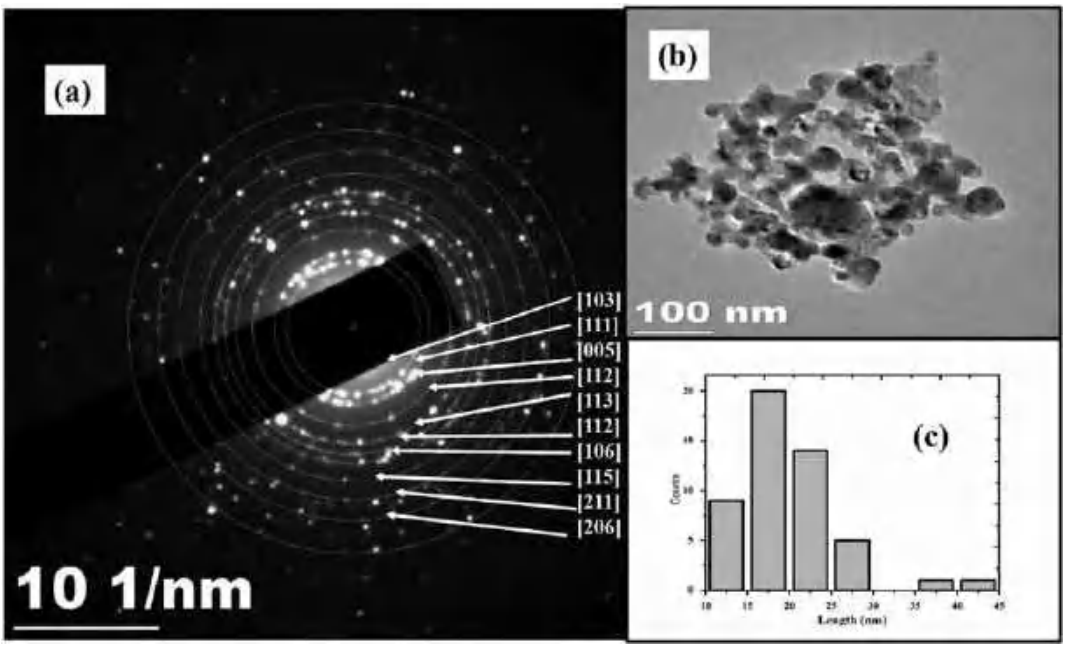

FIGURE 3 (a) Electron diffraction pattern for $Zn_4Al_{22}O_{37}$ using high-resolution transmission electron microscopy (HR-TEM). (b) HR-TEM image of $Zn_4Al_{22}O_{37}$. (c) Particle size calculation histogram

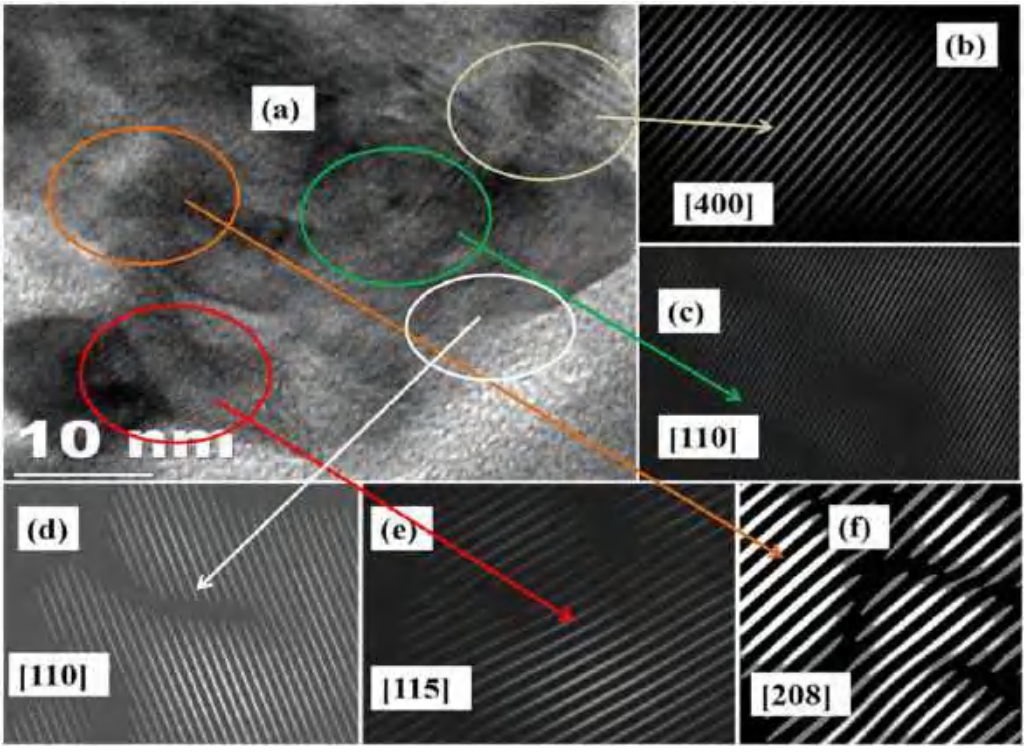

FIGURE 4 (a–f) Lattice planes of $Zn_4Al_{22}O_{37}$

the molecular structure of the material. In this technique, data are represented in terms of the intensity versus the wavenumber (cm^{-1}). The intensity is expressed in terms of the percentage of light absorbance or transmittance of each wavenumber.

Figure 7 shows the FT-IR spectra of (a) $Zn_4Al_{22}O_{37}$, (b) Ce^{3+}-activated $Zn_4Al_{22}O_{37}$, and (c) Eu^{3+}-activated $Zn_4Al_{22}O_{37}$. The absorption bands in the range 500–850 cm^{-1} correspond to the bending and stretching vibrations of the O—M—O and M—O bonds (where M = Zn,

Al, Ce, and Eu).[36] The absorption bands between 500 and 1000 cm^{-1} are related to the stretching and bending vibrations of the Al—O bonds.[37–39] The Al^{3+} ions located at octahedral sites of AlO_6 and tetrahedral AlO_4 denote the bending modes in the range 750–850 cm^{-1}. Zn^{2+} ions located at the centre of the ZnO_4 tetrahedral sites created the vibrations in between 500–750 cm^{-1}.[40] The absorption bands in between 500–750 cm^{-1} denoted the stretching and bending modes of the Al—O bonds in the octahedral coordination state.[38] The modes of stretching at 590 cm^{-1} were observed mainly due to the vibrations of three valence bonds with oxygen with octahedral locations.[41,42] The modes of stretching vibrations at 644 cm^{-1} were denoted the divalent ion bonded with oxygen atoms in the tetrahedral locations.[41,42] Stretching modes that corresponded to 590 cm^{-1} and 644 cm^{-1} were attributed to the T_{2g} modes and the vibrations at 420 nm were attributed to the E_g modes.[31] The modes of vibrations at the shoulder peak at 806 cm^{-1} occurred due to the Al—O bonds in the tetrahedral locations.[42,43]

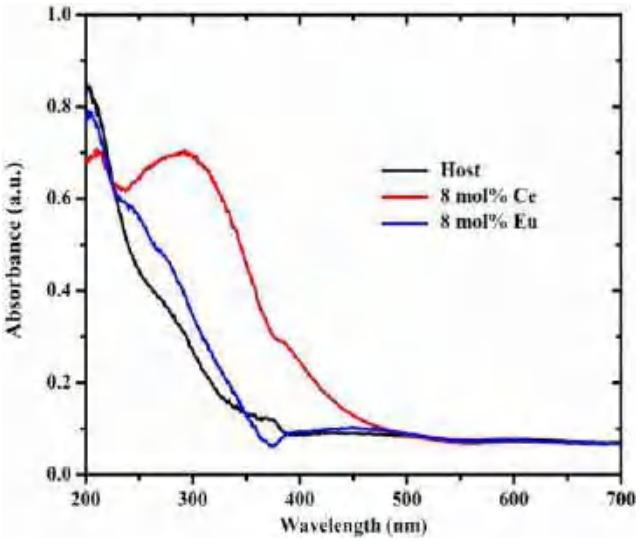

FIGURE 5 Ultraviolet–visible light absorbance spectra of the $Zn_4Al_{22}O_{37}$ host, Ce^{3+}-activated $Zn_4Al_{22}O_{37}$, and Eu^{3+}-activated $Zn_4Al_{22}O_{37}$

3.5 | Photoluminescence properties

3.5.1 | Luminescence of Ce^{3+}-activated $Zn_4Al_{22}O_{37}$

Ce^{3+} activators in the solid matrix exhibit the concentration-dependent luminescence properties of the host material. After particular concentration of the Ce^{3+} activators, quenching in the emission properties was carried out in the form of lattice vibrations. The quenching in the lumen output predicts that the Ce^{3+} ions pair comes closer to each other and dissipates the energy in terms of the phonons in the lattice. Therefore, the doping concentration of Ce^{3+} in the materials is one of the key factors to obtain the high light yield. To study the concentration-dependent luminescence properties, we varied the concentration of Ce^{3+} at 1 mol%, 2 mol%, 5 mol%, 8 mol%, and 10 mol% in the $Zn_4Al_{22}O_{37}$ matrix.

Figure 8 demonstrates the excitation spectrum of the Ce^{3+} (8 mol%)-activated $Zn_4Al_{22}O_{37}$ phosphor monitored under the 421 nm wavelength. The excitation spectrum denoted the broad band excitation peak at the 298 nm wavelength that ranged from 225 nm to 350 nm. The peak at 298 nm denoted the transition of 4f→5d in the Ce^{3+} ion. The PL emission characteristics of the Ce^{3+}-activated $Zn_4Al_{22}O_{37}$ phosphor were studied by monitoring the excitation wavelength at 298 nm (Figure 9). Ce^{3+} ions in the $Zn_4Al_{22}O_{37}$ matrix showed broad band luminescence at 421 nm. The lowest sublevels of 5d could be further split into different components due to the spin-orbit coupling. The Ce^{3+} broad band luminescence in the $Zn_4Al_{22}O_{37}$

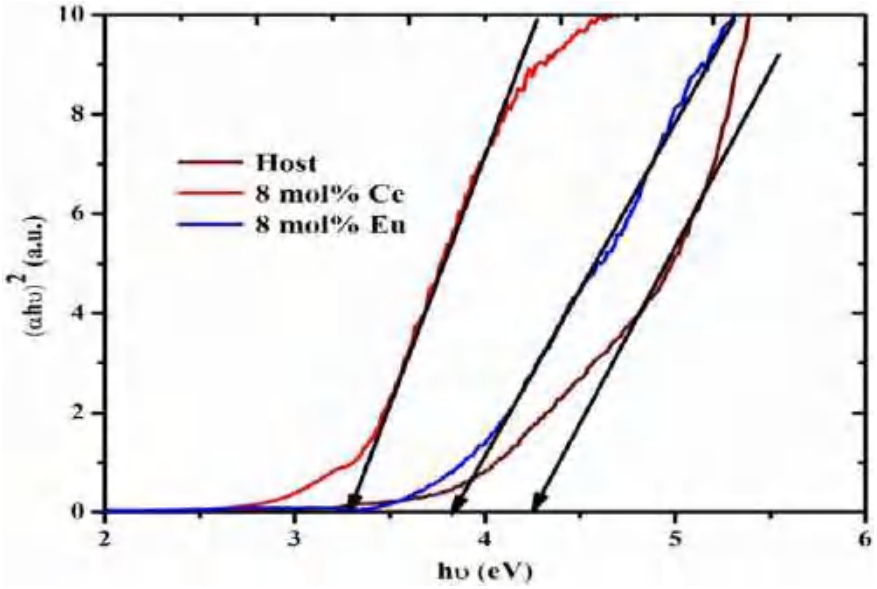

FIGURE 6 Optical band gap energies of the $Zn_4Al_{22}O_{37}$ host, Ce^{3+}-activated $Zn_4Al_{22}O_{37}$ and Eu^{3+}-activated $Zn_4Al_{22}O_{37}$ using a Tauc plot

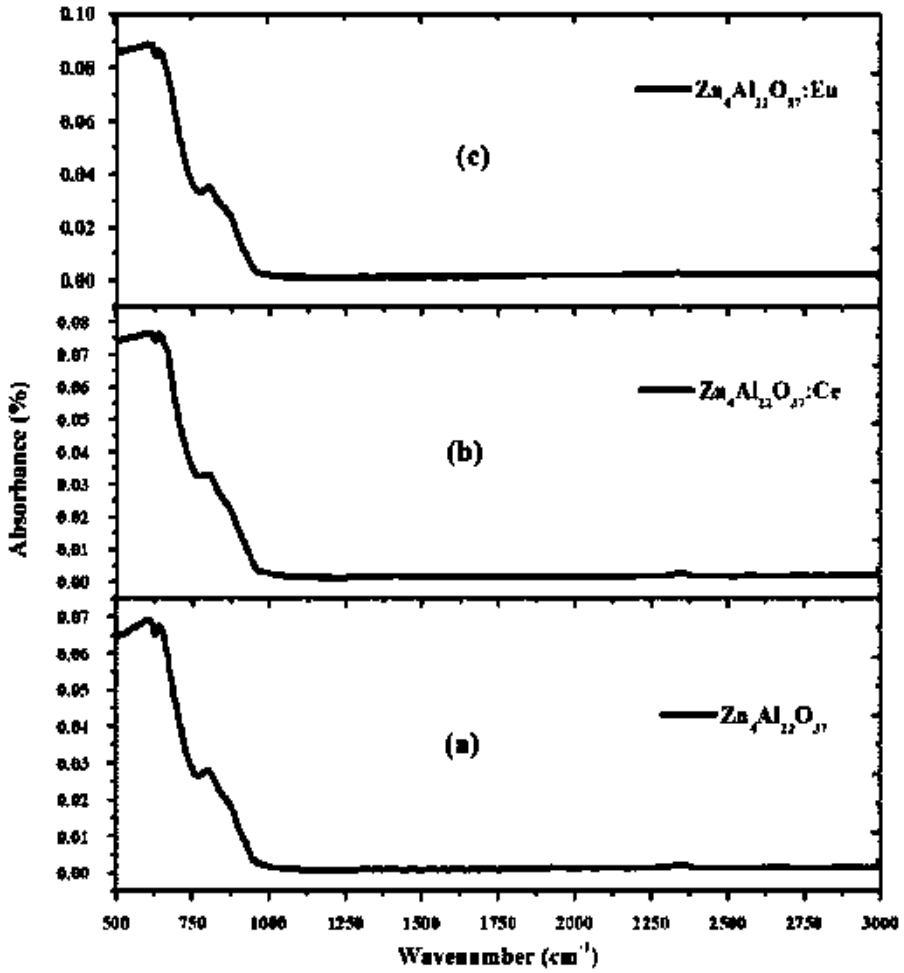

FIGURE 7 Fourier transform infrared spectra of (a) $Zn_4Al_{22}O_{37}$ host, (b) 8 mol% Ce^{3+}-activated $Zn_4Al_{22}O_{37}$ and (c) 8 mol% Eu^{3+}-activated $Zn_4Al_{22}O_{37}$

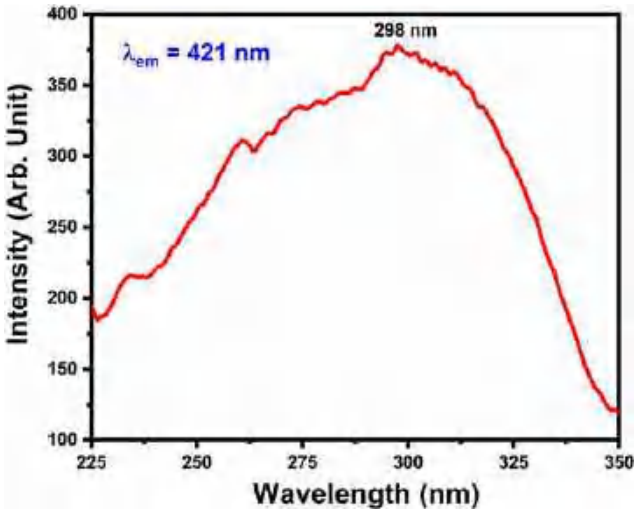

FIGURE 8 Photoluminescence excitation spectra of Ce^{3+}-activated $Zn_4Al_{22}O_{37}$ monitored under 421 nm emission

phosphor was due to the transitions from the lowest level 5d to the spin-orbit split of the 4f sublevels $^2F_{5/2}$ and $^2F_{7/2}$.[44–46] The emission from the Ce^{3+} centres was strongly influenced by the crystal field strength and the surrounding nature of the chemical bonding. The two doublet bands of the Ce^{3+} ions appeared for the lower (1 and 2 mol%) doping concentration of the Ce^{3+} ions in $Zn_4Al_{22}O_{37}$. The doublet bands merged into one broad band emission at 421 nm. Following the increase in doping concentration, the first peak at 405 nm shifted to 421 nm and for 8 mol% both peaks merged and resulted in one broad peak at 421 nm. Photoluminescence emission represented the increase in doping concentration of the Ce^{3+} ions in $Zn_4Al_{22}O_{37}$, increasing the intensity of emission up to 8 mol% doping concentration. Furthermore, it was observed that the emission intensity decreased when the concentration of Ce^{3+} ions was increased to more than 8 mol% (Figure 10), which might be possibly due to the concentration quenching (CQ) effect of luminescence. The CQ effect was caused by an excess of rare earth ions (Ce^{3+}). When the rare earth ions came closer to each other the absorbed energy was not utilized in terms of emission, but was transferred from one rare earth ion to the next. Therefore the emission became increasingly weaker. As the concentration of Ce^{3+} ions was increased, the distance between the Ce^{3+} ions decreased, therefore the intensity of the emission decreased.

Figure 11 denotes the Gaussian fitting curve of the Ce^{3+}-activated $Zn_4Al_{22}O_{37}$. The Gaussian fitting curve estimated two

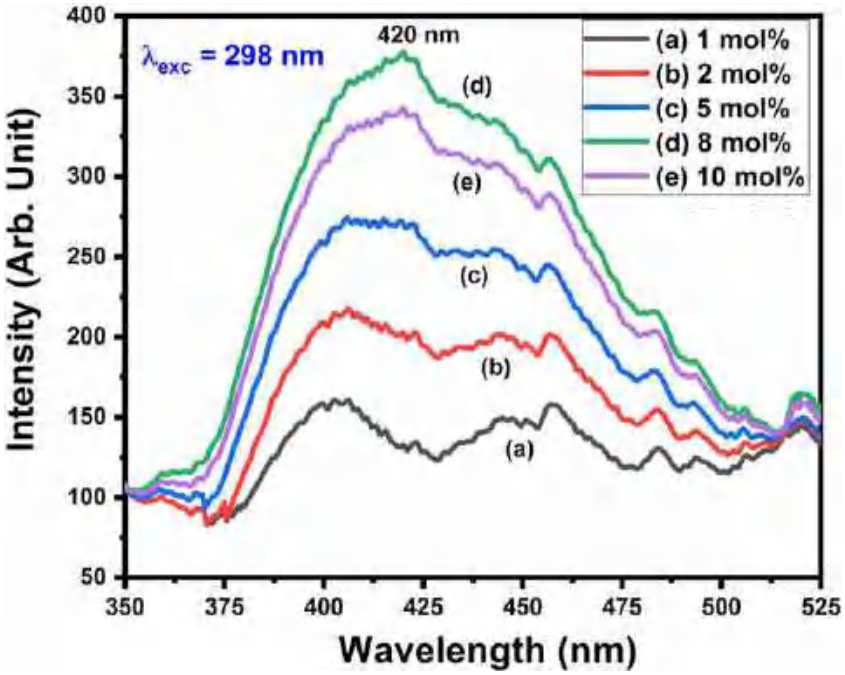

FIGURE 9 Photoluminescence emission spectra of Ce^{3+}-activated $Zn_4Al_{22}O_{37}$ monitored under 298 nm excitation

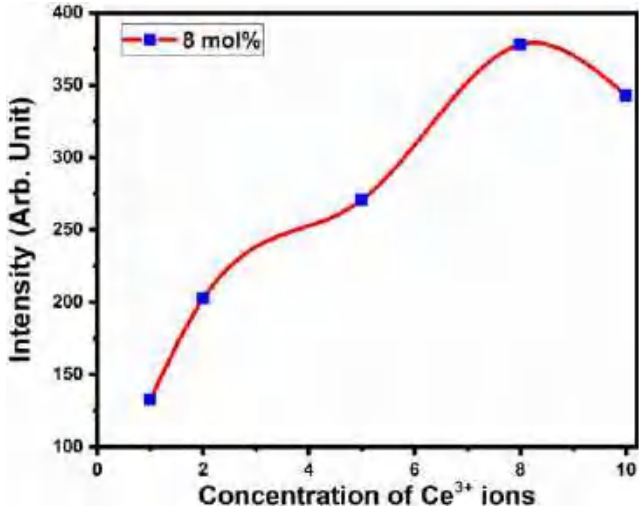

FIGURE 10 Variation in emission intensity with variation in the Ce^{3+} ions

emission peaks at 405 nm (24 691 cm^{-1}) and 466 nm (22 471 cm^{-1}) that corresponded to the 5d states of the $^2F_{5/2}$ and $^2F_{7/2}$ transitions of the Ce^{3+} ions, respectively. The energy level difference between two fitted peaks was observed at 2219 cm^{-1}, which was consistent with the 2000 cm^{-1} theoretical value.[47] A Stokes shift (ΔS) was observed at ~2580 cm^{-1} that was observed larger than that of the other Ce^{3+}-doped aluminates.[47] The Stokes shift increase was due to the Ce^{3+} ions that had been strongly attached to the surrounding ions in the host.[48]

The energy levels of the Ce^{3+} ions are illustrated in the schematic diagram in Figure 12(a). When the Ce^{3+}-activated $Zn_4Al_{22}O_{37}$ was excited by the 298 nm, the Ce^{3+} ions were excited to the 5d levels. These ions relaxed nonradiatively in the crystal and captured the lowest 5d state. The excited ions returned to the $^2F_{5/2}$ and $^2F_{7/2}$ sublevels of the 4f state by emitting the broad band emission. The ions relaxed to the 5d lower level from 5d higher levels using a multiphonon relaxation process.

3.5.2 | Eu^{3+} luminescence in $Zn_4Al_{22}O_{37}$

Eu^{3+}-activated phosphors exhibited different narrow peaks with different wavelengths and were 590–596 nm, 614–620 nm, 656–669 nm, and 689–701 nm, which corresponded to the $^5D_0 \rightarrow {}^7F_1$, $^5D_0 \rightarrow {}^7F_2$, $^5D_0 \rightarrow {}^7F_3$ and $^5D_0 \rightarrow {}^7F_4$ transitions, respectively. Eu^{3+} luminescence is very sensitive to the crystal field and surrounding molecules in the host. Figure 13 shows the PL excitation spectra of Eu^{3+}-activated $Zn_4Al_{22}O_{37}$ that was monitored under 594 nm emission. The maximum intensity peak was observed at 395 nm in the excitation spectrum due to $^7F_0 \rightarrow {}^5L_6$ transition. To study the concentration dependence of the luminescence, the concentrations of Eu^{3+} doping were varied and were 1 mol%, 2 mol%, 5 mol%, 8 mol% and 10 mol% in the $Zn_4Al_{22}O_{37}$ matrix.

The emission spectra of the Eu^{3+}-activated $Zn_4Al_{22}O_{37}$ phosphor were monitored under the wavelength 395 nm, as shown in Figure 14. The emission spectra of Eu^{3+}-activated $Zn_{4-x}Al_{22}O_{37}$ had two high intensity peaks at 594 nm and 614 nm. The peak at 594 nm was attributed to the $^5D_0 \rightarrow {}^7F_1$ transition. The transition $^5D_0 \rightarrow {}^7F_1$ denotes the Eu^{3+} ions acquired by the low symmetry sites in the crystal and corresponded to the magnetic dipole interactions.[49–53] The peak at 614 nm was assigned to the electronic transitions carried from $^5D_0 \rightarrow {}^7F_2$ in the Eu^{3+} ion. The transition $^5D_0 \rightarrow {}^7F_2$ was strongly correlated with the surrounding crystal field effect on the Eu^{3+} ions.[18,50]

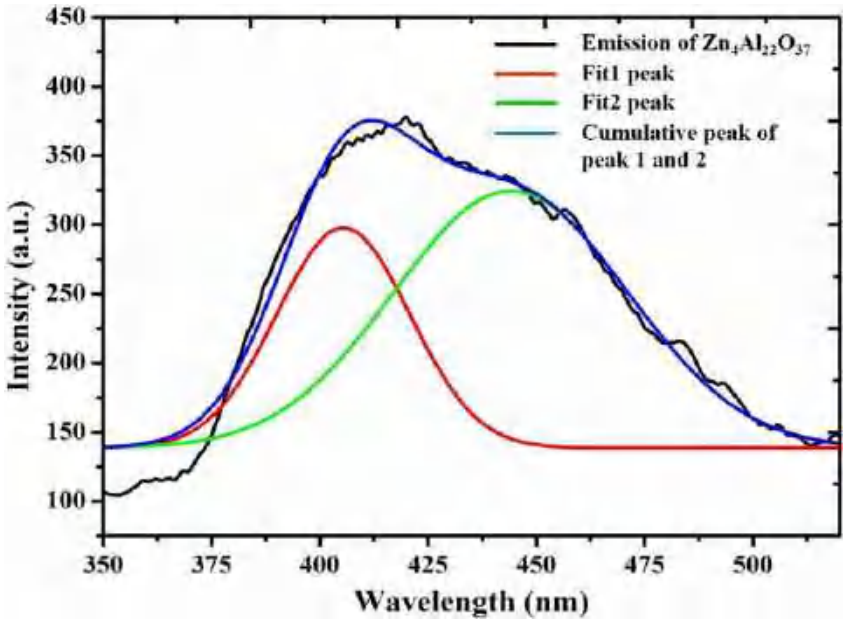

FIGURE 11 Gaussian fitting curve of emission spectra of Ce^{3+}-activated $Zn_4Al_{22}O_{37}$

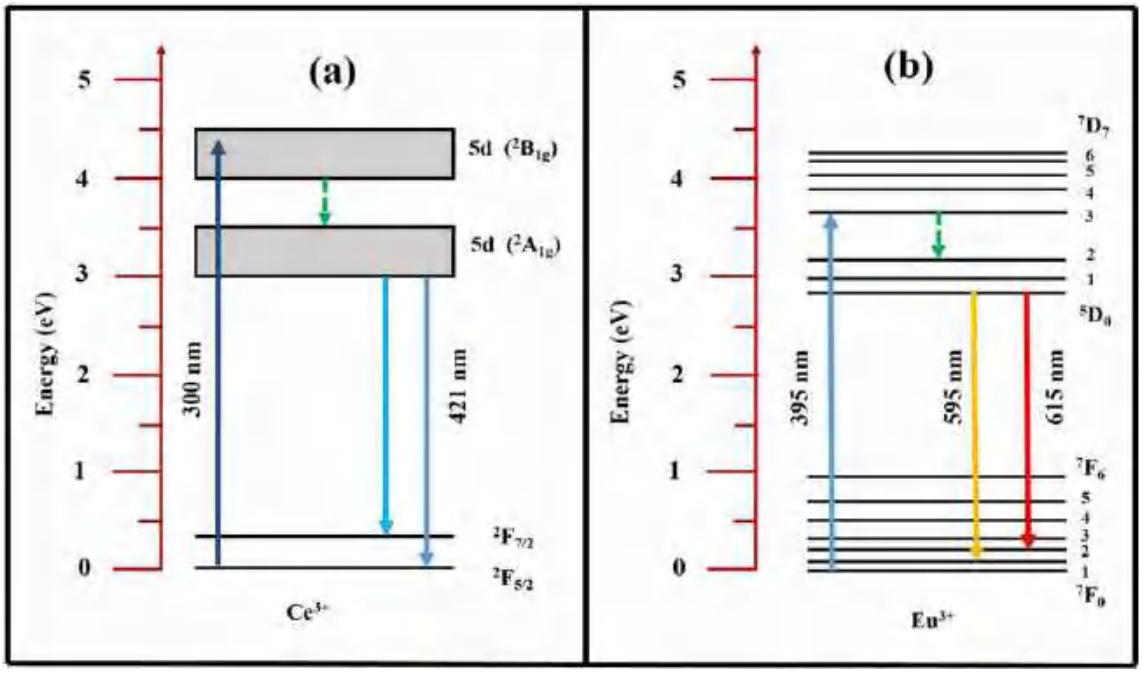

FIGURE 12 Energy level diagrams of (a) Ce^{3+} ions and (b) Eu^{3+} ions

Figure 15 shows the variation in emission intensity corresponding to different concentrations of Eu^{3+} ions. The emission intensity increased up to the 8 mol% concentration, at more than this concentration the emission intensity decreased due to the CQ effect. There was no shift of wavelength due to change in doping concentration, but intensity variation only was observed. Therefore these phosphors may be applicable for the orange/red emissions.

The energy levels of the Eu^{3+} ions are illustrated in Figure 12(b). The Eu^{3+} ions absorbed radiation when excited by 395 nm wavelength radiation and is shown by the blue arrow in the energy level diagram. After relaxation in 5d levels, there were two transitions at wavelengths 594 nm and 614 nm. The transition at 594 nm was attributed to the $^5D_0 \rightarrow {}^7F_1$ change and the transition at 614 nm was due to the $^5D_0 \rightarrow {}^7F_2$ change

3.6 | Colour coordinates

The colour coordinates (x, y) were determined using a radiant imaging colour calculator program that refers to the 1931 Commission

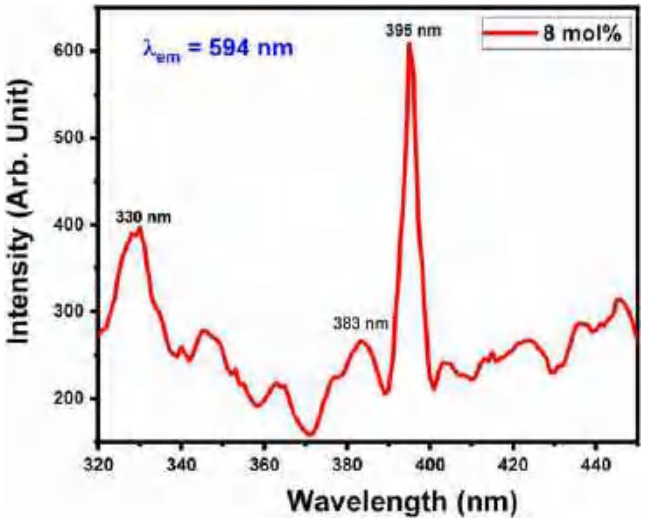

FIGURE 13 Photoluminescence excitation spectra of Eu^{3+}-activated $Zn_4Al_{22}O_{37}$ monitored under 594 nm emission

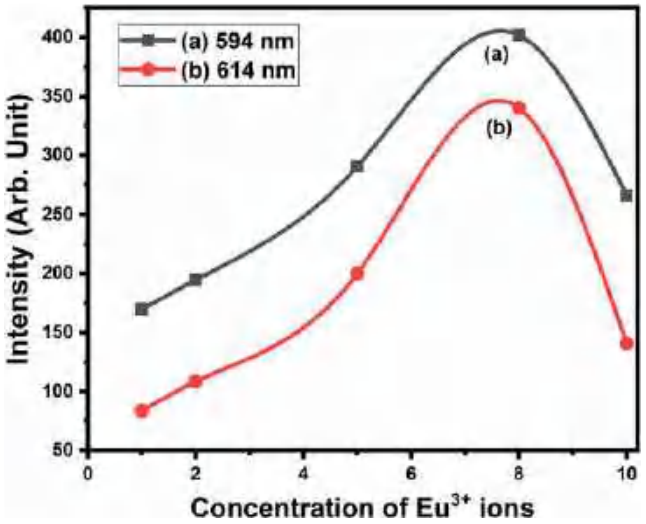

FIGURE 15 Variation in emission intensity with variation in the Eu^{3+} ions

FIGURE 14 Photoluminescence emission spectra of Eu^{3+}-activated $Zn_4Al_{22}O_{37}$ monitored under 395 nm excitation

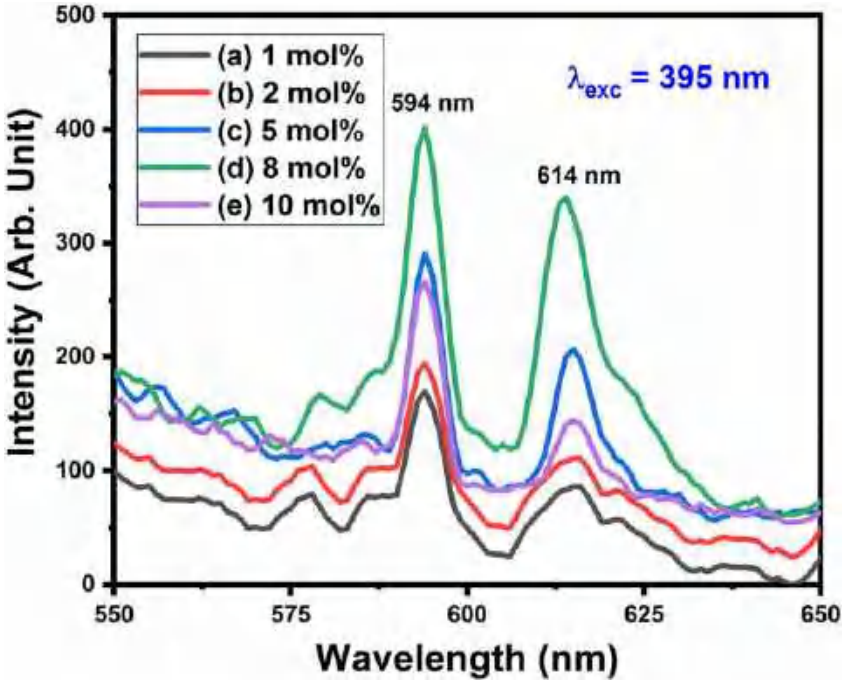

Internationale de l'Eclairage (CIE) standard source [illuminants Cs (0.3101, 0.3162)].[54,55] The colour coordinates were estimated using the following relationships:[56]

$$x = \frac{X}{X+Y+Z}, y = \frac{Y}{X+Y+Z} \text{ and } z = \frac{Z}{X+Y+Z} \quad (7)$$

Equation 7 denotes the three tristimulus values X, Y, and Z for a colour with spectral power distribution P(λ) and these values could be calculated using Equation 8:

$$X = \int_{\lambda_1}^{\lambda_2} P(\lambda)\,\bar{x}(\lambda)\,d\lambda, X = \int_{\lambda_1}^{\lambda_2} P(\lambda)\,\bar{x}(\lambda)\,d\lambda \text{ and } Y = \int_{\lambda_1}^{\lambda_2} P(\lambda)\,\bar{y}(\lambda)\,d\lambda \quad (8)$$

where λ_1 to λ_2 is the wavelength range of the PL emission spectrum, $\bar{x}(\lambda)$, $\bar{y}(\lambda)$, and $\bar{z}(\lambda)$ are three colour matching functions; and the wavelength of equivalent monochromatic light is λ. The estimated colour coordinates of Ce^{3+}-activated $Zn_4Al_{22}O_{37}$ for the 8 mol% concentration were x = 0.1567, y = 0.0637 (blue) at 420 nm emission, as shown in Figure 16 by point A. The corresponding tristimulus coordinates of Ce^{3+}-activated $Zn_4Al_{22}O_{37}$ were estimated also and these were

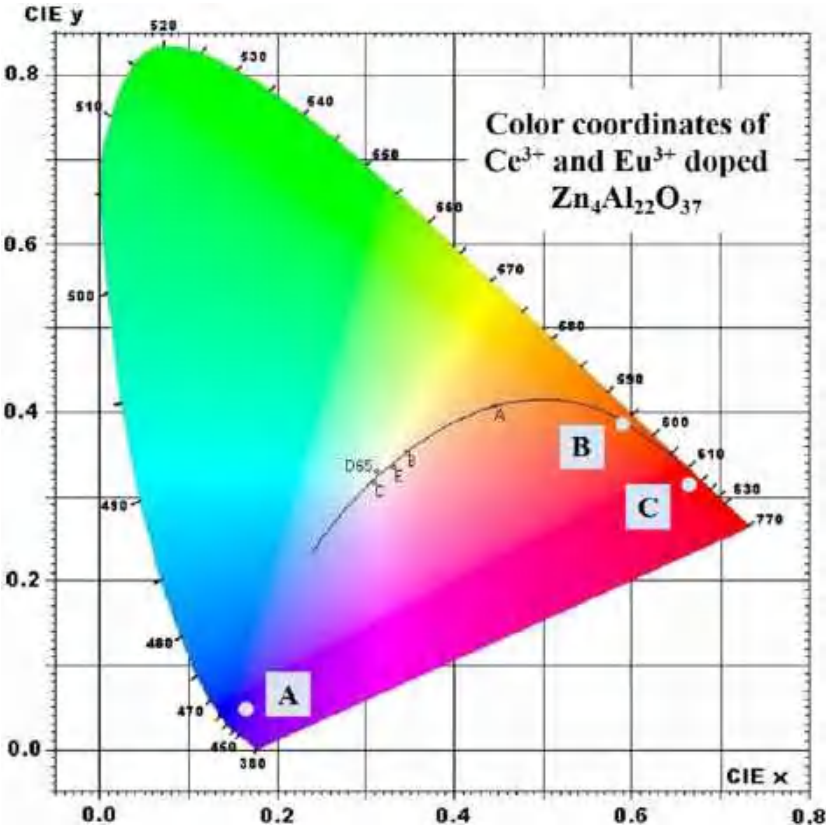

FIGURE 16 Colour coordinates of Ce^{3+}-activated $Zn_4Al_{22}O_{37}$ and Eu^{3+}-activated $Zn_4Al_{22}O_{37}$

X = 6.66, Y = 4.07 and Z = 0.01. The estimated colour coordinates of Eu^{3+}-activated $Zn_4Al_{22}O_{37}$ for the 8 mol% concentration were x = 0.6018, y = 0.3976 (orange) at 594 nm and x = 0.6779, y = 0.3219 (red) at 614 nm as shown in Figure 16 by points B and C respectively. The corresponding tristimulus coordinates for Eu^{3+}-activated $Zn_4Al_{22}O_{37}$ were X = 7.38, Y = 4.88, Z = 0.01 (orange) and X = 8.71, Y = 4.14, Z = 0.00 (red).

4 | CONCLUSION

Ce^{3+}- and Eu^{3+}-activated $Zn_4Al_{22}O_{37}$ phosphors were successfully prepared using solution combustion synthesis and their structural, morphological, and luminescence properties were investigated. XRD showed the hexagonal structure of the prepared $Zn_4Al_{22}O_{37}$ host, Ce^{3+}-activated $Zn_4Al_{22}O_{37}$ and Eu^{3+} activated $Zn_4Al_{22}O_{37}$. HR-TEM measurements showed the nanocrystalline nature of the particles. Ce^{3+}-activated $Zn_4Al_{22}O_{37}$ phosphor produced blue emission at 421 nm (5d→4f) under the 298 nm excitation. Under 395 nm excitation, the Eu^{3+}-activated $Zn_4Al_{22}O_{37}$ phosphor produced showed emission at 594 nm ($^5D_0 \rightarrow {}^7F_1$) and 614 nm ($^5D_0 \rightarrow {}^7F_2$). Luminescence intensity increased with variation in doping concentration and the 0.8 mol% concentration was observed as the optimum concentration. The colour coordinates of Ce^{3+}- and Eu^{3+}-activated $Zn_4Al_{22}O_{37}$ confirmed that these phosphors may be useful for UV absorption and visible light emission lighting applications.

ORCID

Dinesh S. Bobade https://orcid.org/0000-0003-4960-4772
Yatish R. Parauha https://orcid.org/0000-0002-7968-3160

REFERENCES

[1] C. M. Mehare, Y. R. Parauha, N. S. Dhoble, C. Ghanty, S. J. Dhoble, *J. Mol. Struct.* **2020**, *1212*, 127957.
[2] Q. He, C. Hu, *Opt. Mater.* **2014**, *38*, 286.
[3] Y. R. Parauha, V. Chopra, S. J. Dhoble, *Mater. Res. Bull.* **2020**, *131*, 110971.
[4] P. Wang, X. Xu, J. Qiu, X. Yu, Q. Wang, *Opt. Mater.* **1826**, *2014*(11), 36.
[5] C. R. García, L. A. Diaz-Torres, J. Oliva, G. A. Hirata, *Opt. Mater.* **2014**, *37*, 520.
[6] S. Li, X. Peng, X. Liu, Z. Huang, *Opt. Mater.* **2014**, *38*, 242.
[7] C. Ronda, *WILEY-VCH Verlag GmbH & Co*, KGaA, Weinheim **2008**.
[8] S. J. Dhoble, Vijay B. Pawade, Hendrik C. Swart & V. Chopra Elsevier Ltd., 2020
[9] C. Peng, G. Li, D. Geng, M. Shang, Z. Hou, J. Lin, *Mater. Res. Bullet.* **2012**, *47*(11), 3592.
[10] S. Menon, B. Dhabekar, E. A. Raja, S. P. More, T. K. G. Rao, R. K. Kher, *J. Lumin.* **2018**, *128*, 673.
[11] D. Zhang, C. Wang, Y. Liu, Q. Shi, W. Wang, Y. Zhai, *J. Lumin.* **2012**, *132*, 1529.
[12] G. E. Malashkevich, M. Melnichenko, E. Poddenezhny, A. A. Boiko, *J. Non-Cryst. Solids.* **1999**, *260*, 141.
[13] H. Bi, W. Cai, L. Zhang, *Mater. Res. Bull.* **2000**, *35*, 1495.
[14] R. Reisfeld, H. Minti, A. Patra, D. Ganguli, *M. Gaft* **1998**, *54*, 2143.
[15] K. A. Gedekar, S. P. Wankhede, S. V. Moharil, R. M. Belekar, *J. Mater. Sci.: Mater. Elect.* **2018**, 294466.
[16] G. N. Nikhare, S. C. Gedam, S. J. Dhoble, *J. Lumin.* **2013**, *137*, 290.

[17] V. Singh, J. Zhu, V. Natarajan, **2006**, *203*, 2058.
[18] W. B. Dai, M. Zhou, Z. Y. Xian, L. K. Zeng, *RSC Adv.* **2014**, *4*, 25470.
[19] G. Li, T. Long, Y. Song, G. Gao, J. Xu, B. An, S. Gan, G. Hong, *J. Rare Earth* **2010**, *28*, 22.
[20] Y. R. Parauha, S. J. Dhoble, *Luminescence* **2010**, 2.
[21] J. H. Kim, *Phys. B: Phys. Cond. Matter.* **2016**, *505*, 52.
[22] M. T. Tsai, Y. X. Chen, P. J. Tsai, Y. K. Wang, *Thin Solid Films* **2010**, *518*, 9.
[23] X. Y. Chen, C. Ma, Z. J. Zhang, B. N. Wang, *Mater. Sci. Eng.* **2008**, *B151*, 224.
[24] G. Rani, *Powder Technol.* **2017**, *312*, 354.
[25] P. Kumari, Y. Dwivedi, *J. Lumin.* **2016**, *178*, 407.
[26] M. Kumar, S. K. Gupta, *J. Lumin.* **2015**, *168*, 151.
[27] V. Singh, R. P. S. Chakradhar, J. L. Rao, D.-K. Kim, *J. Lumin.* **2008**, *128*, 394.
[28] M. Zawadzki, J. Wrzyszcz, W. Strek, D. Hreniak, *J. Alloys Compd.* **2001**, *323*, 279.
[29] W. Strek, P. Dereń, A. Bednarkiewicz, M. Zawadzki, J. Wrzyszcz, *J. Alloys Compd.* **2008**, *300-301*, 456.
[30] D. P. Dutta, R. Ghildiyal, A. K. Tyagi, *J. Phys. Chem. C* **2009**, *113*, 16954.
[31] R. Khenata, M. Sahnoun, H. Baltache, M. Rérat, A. H. Reshak, Y. Al-Douri, B. Bouhafs, *Phys. Lett. A* **2005**, *344*, 271.
[32] S. Mathur, M. Veith, M. Haas, H. Shen, N. Lecerf, V. Huch, S. Hüfner, R. Haberkorn, H. P. Beck, M. Jilavi, *J. Am. Ceram. Soc.* **2001**, *84*, 1921.
[33] M. Kumar, V. Natarajan, S. V. Godbole, *Bull. Mater. Sci.* **2014**, *37*, 1205.
[34] J. Tauc, A. Menth, *J. Non-Crys. Solids.* **1972**, *8*, 569.
[35] D. L. Wood, J. Tauc, *Phys. Rev. B* **1972**, *5*, 3144.
[36] M. A. Subhan, T. Ahmed, P. Sarker, T. T. Pakkanen, M. Suvanto, M. Horimoto, H. Nakata, *J. Lumin.* **2014**, *148*, 98.
[37] S. F. Wang, G. Z. Sun, S. F. Wang, L. M. Fang, L. Lei, X. Xiang, X. T. Zu, *Sci. Repor.* **2015**, *5*, 12849.
[38] D. L. Ge, Y. J. Fan, C. L. Qi, Z. X. Sun, *J. Mater. Chem.* **2013**, *A1*, 1651.
[39] I. B. Huang, Y. S. Chang, H. L. Chen, C. C. Hwang, C. J. Jian, Y. S. Chen, M. T. Tsai, *Thin Solid Films* **2014**, *570*(301), 451.
[40] S. Janakov, L. Salavcova, G. Renaudin, Y. Filinchuk, D. Boyer, P. Boutinau, *J. Phys. Chem. Solids* **2007**, *68*(5–6), 1147.
[41] H. A. Mohammed, R. A. Rasool, *Raf. J. Sci.* **2019**, *28*(3), 33.
[42] V. M. Grošev, M. Vrankić, A. Maksimović, V. Mandić, *J. Alloys Compd.* **2017**, *697*, 90.
[43] T. Tangcharoen, J. T. Thienprasert, C. Kongmark, *Mater. Sci.* **2020**.
[44] X. He, X. Liu, R. Li, B. Yang, K. Yu, M. Zeng, R. Yu, *Sci. Report.* **2016**, *6*, 22238.
[45] Z. Pan, W. Li, Y. Xu, Q. Hu, Y. Zheng, *RSC Advan.* **2016**, *6*, 20458.
[46] A. Selot, M. Aynyas, M. Tiwari, K. Dev, *AIP Conf. Procee.* **2016**, *1728*, 02026.
[47] X. Zhang, B. Park, N. Choi, J. Kim, G. C. Kim, J. H. Yoo, *Mater. Lett.* **2009**, *63*, 700.
[48] V. B. Pawade, N. S. Dhoble, S. J. Dhoble, *Solid State Sci.* **2012**, *14*, 607.
[49] D. S. Bobade, Y. R. Parauha, S. J. Dhoble, P. B. Undre, *Optik* **2021**, *227*, 166119.
[50] V. B. Pawade, S. J. Dhoble, *Solid State Sci.* **2012**, *14*(5), 607.
[51] H. Liu, Y. Hao, H. Wang, J. Zhao, P. Huang, B. Xu, *J. Lumin.* **2011**, *131*(11), 2422.
[52] J. Kaur, Y. Parganiha, V. Dubey, *Phys. Res. Intern.* **2013**, 494807, 1.
[53] D. S. Bobade, P. B. Undre, *Integr. Ferroelectr.* **2020**, *205*, 72.
[54] K.N. Shinde, S.J. Dhoble, H.C. Swart, K. Park, *Springer*, **2012**.
[55] Color calculator version 2, A Software from Radiant Imaging, Inc., **2007**.
[56] J. Yang, B. Chen, E. Y. Bun Pun, B. Zhai, H. Lin, *J. Lumin.* **2013**, *134*, 622.

FWHM, full width half maximum.

How to cite this article: D. S. Bobade, Y. R. Parauha, S. J. Dhoble, P. B. Undre, *Luminescence* **2022**, *37*(3), 500. https://doi.org/10.1002/bio.4200

Advances and Applications in Mathematical Sciences
Volume 22, Issue 2, December 2022, Pages 407-433

CRANK-NICOLSON METHOD FOR TIME FRACTIONAL DRUG CONCENTRATION EQUATION IN CENTRAL NERVOUS SYSTEM

UTTAM KHARDE, KALYANRAO TAKALE and SHRIKRISHNA GAIKWAD

Department of Mathematics
S.N. Arts, D.J.M. Commerce
and B.N.S. Science College (Autonomous)
Sangamner-422605(M.S.), India

Department of Mathematics
R.N.C. Arts, J.D.B. Commerce
and N.S.C. Science College
Nashik Road, Nashik-422101, (M.S.), India
E-mail: kalyanraotakale1@gmail.com

Department of Mathematics
New Arts, Commerce and Science College
Ahmednagar-414001, (M.S.), India
E-mail: sbgmathsnagar@gmail.com

Abstract

Recently, the treatment of central nervous system (CNS) diseases is a major problem in modern clinical world. Now, there are many drugs available that treat symptoms rather than the disease, therefore, new drugs and new techniques of treatment are needed. In human, cerebrospinal fluid (CSF) is easily accessible fluid that can be used to predict the drug concentration in CNS target site. This process can be represented by mathematical model of drug concentration equation with the help of integer order partial derivatives, but fractional order modeled scribes the drug concentration at CNS target site more precisely. Therefore, the purpose of this paper is to develop the fractional order Crank-Nicolson finite difference scheme to solve the time fractional drug concentration equation, formulated with Caputo fractional derivative. Also, we prove that the scheme is unconditionally stable and convergent. As an application of

2020 Mathematics Subject Classification: 26A33, 34A08, 97N40.
Keywords: Fractional Differential Equation, Caputo Derivative, Crank-Nicolson Finite Difference Scheme, CNS, Python.
*Corresponding author; E-mail: uttamkharde@gmail.com
Received June 2, 2021; Accepted December 14, 2021

this scheme, numerical solutions of fractional order drug concentration equation in the central nervous system is examined to verify the stability and these solutions are simulated graphically using Python.

1. Introduction

Fractional calculus is a newly developed branch of mathematics which deals with the study of derivatives and integrations of arbitrary order. In recent years, many areas of applied science and technology have used fractional order approach to describe certain phenomena and processes. Fractional order mathematical models describing the physical phenomena are appears in many applications of sciences, such as the fractional diffusion equation [24], fractional subdiffusion equation [31], fractional wave equation [6, 24], fractional Boussinesq's equation [28], fractional heat equation, fractional viscoelastic theory [2], etc. The arbitrary order mathematical model provides better physical analysis rather than integer order model, because it provides results at any inter-mediate stage by considering all the inputs starting from initial stage rather than only previous stage [12]. Many dynamical models of physics, engineering, biomedical, fluid dynamics, hydrology, etc. [4, 3, 7, 12, 15, 18, 19, 21] are modeled by fractional order partial differential equations. Now a days, due to its tremendous applications in various fields, a remarkable attention has been given to find its exact and approximate solution. Due to non-local nature of fractional derivative, many fractional differential equations do not have exact solutions. Therefore, to solve the fractional differential equations, numerical techniques are more demanding. To develop numerical methods for solving fractional differential equations, which are accurate and timely efficient is the primary challenge to researchers. We observed that the fractional derivatives in Caputo sense is more feasible to analyze the physical problem and it allowed to deal with integer-order initial and boundary conditions [7]. Finite difference method is one of the more effective and commonly used method to solve fractional differential equations. In the literature [9, 10, 11, 14, 17, 20, 23, 25, 26, 28], finite difference method is successfully used to obtain the numerical solutions of fractional differential equations.

Now a days, Pharmacokinetics is the branch of Pharmacology which study the drug absorption, distribution, metabolism and excretion in human body [13]. In Pharmacology, one of the significant challenge is the

development of drugs targeting disease of the central nervous system (CNS). Due to medical ethics, direct measurement of brain concentration is restricted and due to presence of bloodbra in barrier (BBB), the prediction of target site concentration of CNS drug is more complicated [32]. Many researchers [9, 29, 30, 32] in pharmacology has developed a physiologically based pharmacokinetics modeling describing a drug concentration in CNS. The Advection-Diffusion equation describes the evolution of a concentration profile due to diffusion and advection simultaneously [1]. A mathematical modeling describing the drug concentration in CNS based on Advection-Diffusion equation is studied in [5]. In this context, we study the fractional order drug concentration equation in the central nervous system. Furthermore, we develop the Crank-Nicolson fractional order finite difference scheme for fractional order drug concentration equation and obtain its approximate solution. There are many numerical techniques developed for solving fractional differential equations using mathematical softwares [6, 10, 16]. We observed that, Python is a high level multi-purpose programming language having large number of mathematical tools. Recently, Python is used for teaching as well as research in various branches of applied mathematics. Therefore, in this connection we develop Python programme to obtain the numerical solution of the drug concentration equation by the proposed scheme.

We organized the paper as follows: In section 2, we develop the fractional order Crank-Nicolson finite difference scheme for time fractional drug concentration equation. Section 3 is devoted for stability of the solution obtained by the scheme. In section 4, convergence of the scheme is discussed up to the length. In section 5, the approximate solution of the time fractional drug concentration equation is computed and it is simulated graphically by Python. We consider the time fractional drug concentration equation with initial and boundary conditions as follows

$$\frac{\partial^{\alpha} c(x,t)}{\partial t^{\alpha}} = -v\frac{\partial c(x,t)}{\partial x} + D\frac{\partial^2 c(x,t)}{\partial x^2},\ 0 < \alpha \le 1,\ 0 \le x \le L,\ 0 \le t \le T \quad (1.1)$$

$$\text{initial condition: } c(x,0) = 0,\ 0 < x < L \quad (1.2)$$

$$\text{boundary conditions: } c(0,t) = g(t),\ \frac{\partial c(L,t)}{\partial x} = 0,\ t \ge 0 \quad (1.3)$$

where $c(x, t)$ is the drug concentration in CSF space at time t and place x, v is the flow velocity and D is the diffusion coefficient. We discretized time fractional order derivative in the Caputo sense.

The Caputo derivative of order α is defined as follows [22, 23]

$$\frac{\partial^{\alpha} c(x, t)}{\partial t^{\alpha}} = \frac{1}{\Gamma(1-\alpha)} \int_0^t (x-\tau)^{-\alpha} \frac{\partial c(x, \tau)}{\partial \tau} d\tau, \; 0 < \alpha \leq 1 \tag{1.4}$$

where $\Gamma(\cdot)$ is the gamma function defined as

$$\Gamma(\alpha) = \int_0^{\infty} e^{-x} x^{\alpha-1} dx. \tag{1.5}$$

2. Finite Difference Scheme

In this section, we develop the fractional order Crank-Nicolson finite difference scheme for time fractional drug concentration equation (1.1)-(1.3). For this, we define $x_i = i\Delta x$, $i = 0, 1, 2, 3, \ldots, M$ and $t_k = k\Delta t$, $k = 0, 1, 2, 3, \ldots, N$, where $\Delta x = \frac{L}{M}$ and $\Delta t = \frac{T}{N}$. Let $c(x_i, t_k)$, $i = 0, 1, 2, 3, \ldots, M$ and $k = 0, 1, 2, 3, \ldots, N$, be the exact solution of time fractional drug concentration equation (1.2)-(1.3) at mesh point (x_i, t_k) and let c_i^k be the numerical approximation at point (x_i, t_k). The time fractional drug concentration equation with initial and boundary conditions (1.1)-(1.3) is discretized by using the second order accurate central difference formula for space derivative and finite difference formula for the time fractional derivative for each interior grid point $(i\Delta x, k\Delta t)$. At time level $t = t_{k+1}$, the Caputo time fractional derivative of order α is discretized as follows

$$\left(\frac{\partial^{\alpha} c}{\partial t^{\alpha}}\right)_{(x_i, t_{k+1})} = \frac{1}{\Gamma(1-\alpha)} \int_0^{t_{k+1}} (t_{k+1} - s)^{-\alpha} \frac{\partial c(x_i, s)}{\partial s}$$

$$= \frac{1}{\Gamma(1-\alpha)} \sum_{j=0}^{k} \int_{t_j}^{t_{j+1}} (t_{k+1} - s)^{-\alpha} \left[\frac{c_i^{j+1} - c_i^j}{\Delta t} + O(\Delta t)\right] ds$$

$$= \frac{1}{\Gamma(1-\alpha)} \sum_{j=0}^{k} \left[\frac{c_i^{j+1} - c_i^j}{\Delta t} + O(\Delta t) \right] \int_{t_j}^{t_{j+1}} (t_{k+1} - s)^{-\alpha} ds$$

$$= \frac{1}{\Gamma(1-\alpha)} \sum_{j=0}^{k} \left[\frac{c_i^{j+1} - c_i^j}{\Delta t} + O(\Delta t) \right] \left[\frac{(k-j+1)^{1-\alpha} - (k-j)^{1-\alpha}}{(1-\alpha)(\Delta t)^{\alpha-1}} \right]$$

$$= \frac{(\Delta t)^{-\alpha}}{\Gamma(2-\alpha)} \sum_{j=0}^{k} [c_i^{k-j+1} - c_i^{k-j} + O(\Delta t)][(j+1)^{1-\alpha} - j^{1-\alpha}]$$

$$= \frac{(\Delta t)^{-\alpha}}{\Gamma(2-\alpha)} \sum_{j=0}^{k} [c_i^{j+1} - c_i^{k-j} + O(\Delta t)] b_j$$

$$= \frac{(\Delta t)^{-\alpha}}{\Gamma(2-\alpha)} \sum_{j=0}^{k} b_j [c_i^{j+1} - c_i^{k-j}] + \frac{(\Delta t)^{-\alpha}}{\Gamma(2-\alpha)} \sum_{j=0}^{k} b_j O(\Delta t)$$

where $b_j = (j+1)^{1-\alpha} - j^{1-\alpha}$, $j = 0, 1, 2, 3, \ldots, k$.

Since, $k\Delta t \le T$ is finite, the above equation can be written as,

$$\left(\frac{\partial^\alpha c}{\partial t^\alpha} \right)_{(x_i, t_{k+1})} = \frac{(\Delta t)^{-\alpha}}{\Gamma(2-\alpha)} [c_i^{k+1} - c_i^k] + \frac{(\Delta t)^{-\alpha}}{\Gamma(2-\alpha)} \sum_{j=1}^{k} b_j [c_i^{k-j+1} - c_i^{k-j}] + O(\Delta t). \tag{2.1}$$

Furthermore, the space derivatives $\frac{\partial c}{\partial x}$ is disretized as follows

$$\left(\frac{\partial c}{\partial x} \right)_{(x_i, t_{k+1})} = \frac{c_{i+1}^k - c_{i-1}^k}{2\Delta x} + O(\Delta x) \tag{2.2}$$

The space derivative $\frac{\partial^2 c}{\partial x^2}$ is discretized by using second order central difference scheme as follows

$$\left(\frac{\partial^2 c}{\partial x^2} \right)_{(x_i, t_{k+1})} = \frac{\delta_x^2 c_i^{k+1} + \delta_x^2 c_i^k}{2}$$

$$\therefore \left(\frac{\partial^2 c}{\partial x^2}\right)_{(x_i, t_{k+1})} = \frac{1}{2\Delta x^2}[c_{i-1}^{k+1} - 2c_i^{k+1} + c_{i+1}^{k+1} + c_{i-1}^{k} - 2c_i^{k} + c_{i+1}^{k}] + O(\Delta x^2) \quad (2.3)$$

where δ_x is the central difference operator.

Now, using equations (2.1), (2.2) and (2.3) in equation (1.1), we obtain

$$\frac{(\Delta t)^{-\alpha}}{\Gamma(2-\alpha)}[c_i^{k+1} - c_i^k] + \frac{(\Delta t)^{-\alpha}}{\Gamma(2-\alpha)}\sum_{j=1}^{k} b_j[c_i^{k-j+1} - c_i^{k-j}]$$

$$= \frac{-v}{2\Delta x}[c_{i+1}^{k} - c_{i-1}^{k}] + \frac{D}{2\Delta x^2}[c_{i-1}^{k+1} - 2c_i^{k+1} + c_{i+1}^{k+1} + c_{i-1}^{k} - 2c_i^{k} + c_{i+1}^{k}]$$

This gives, $[c_i^{k+1} - c_i^k] + \sum_{j=1}^{k} b_j[c_i^{k-j+1} - c_i^{k-j}]$

$$= -v\frac{(\Delta t)^{\alpha}\Gamma(2-\alpha)}{2\Delta x}[c_{i+1}^{k} - c_{i-1}^{k}]$$

$$+ D\frac{(\Delta t)^{\alpha}\Gamma(2-\alpha)}{2\Delta x^2}[c_{i-1}^{k+1} - 2c_i^{k+1} + c_{i+1}^{k+1} + c_{i-1}^{k} - 2c_i^{k} + c_{i+1}^{k}]$$

By taking $\mu = v\frac{(\Delta t)^{\alpha}\Gamma(2-\alpha)}{2\Delta x}$ and $r = D\frac{(\Delta t)^{\alpha}\Gamma(2-\alpha)}{2\Delta x^2}$, we get

$$[c_i^{k+1} - c_i^k] + \sum_{j=1}^{k} b_j[c_i^{k-j+1} - c_i^{k-j}] = -\mu[c_{i+1}^{k} - c_{i-1}^{k}]$$

$$+ r[c_{i-1}^{k+1} - 2c_i^{k+1} + c_{i+1}^{k+1} + c_{i-1}^{k} - 2c_i^{k} + c_{i+1}^{k}]$$

$$-rc_{i-1}^{k+1} + (1+2r)c_i^{k+1} - rc_{i+1}^{k+1} = (r+\mu)c_{i-1}^{k} + (1-2r)c_i^{k} + (r-\mu)c_{i+1}^{k}$$

$$- \sum_{j=1}^{k} b_j(c_i^{k-j+1} - c_i^{k-j}) \quad (2.4)$$

After simplification, for $k = 0, 1, 2, 3, \ldots, N,$ we obtain

$$-rc_{i-1}^{k+1} + (1+2r)c_i^{k+1} - rc_{i+1}^{k+1} = (r+\mu)c_{i-1}^{k} + (1-2r-b_1)c_i^{k} + (r-\mu)c_{i+1}^{k}$$

$$- \sum_{j=1}^{k} (b_j - b_{j+1}) c_i^{k-j} + b_k c_i^0. \tag{2.5}$$

Now, put $k = 0$ in equation (2.4), we get

$$- r c_{i-1}^{k+1} + (1 + 2r) c_i^1 - r c_{i+1}^1 = (r + \mu) c_{i-1}^0 + (1 - 2r) c_i^0 + (r - \mu) c_{i+1}^0. \tag{2.6}$$

Finally, the initial condition $c(x, 0) = 0 (0 < x < L)$ is approximated as follows:

$$c_i^0 = 0, \; i = 1, 2, 3, \ldots, M. \tag{2.7}$$

Also, the boundary conditions $c(0, t) = g(t)$ and $\frac{\partial c(L, t)}{\partial x} = 0 (t \geq 0)$ are approximated as follows

$$c(0, t_k) = g(t_k) \text{ implies } c_0^k = g(t_k), \; k = 0, 1, 2, 3, \ldots, N \tag{2.8}$$

and

$$\frac{\partial c(L, t_k)}{\partial x} = 0 \text{ implies } \frac{c_{M+1}^k - c_{M-1}^k}{2\Delta x} = 0$$

This gives,

$$c_{M+1}^k = c_{M-1}^k, \; k = 0, 1, 2, 3, \ldots, N. \tag{2.9}$$

Thus, the complete discretized time fractional drug concentration equation with initial and boundary condition is as follows

$$- r c_{i-1}^1 + (1 + 2r) c_i^1 - r c_{i+1}^1 = (r + \mu) c_{i-1}^0 + (1 - 2r) c_i^0 + (r - \mu) c_{i+1}^0, \text{ for } k = 0 \tag{2.10}$$

$$- r c_{i-1}^{k+1} + (1 + 2r) c_i^{k+1} - r c_{i+1}^{k+1} = (r + \mu) c_{i-1}^k + (1 - 2r - b_1) c_i^k + (r - \mu) c_{i+1}^k + \sum_{j=1}^{k} (b_j - b_{j+1}) c_i^{k-j} + b_k c_i^0, \text{ for } k \geq 1 \tag{2.11}$$

$$\text{initial condition: } c_i^0 = 0, \; i = 1, 2, 3, \ldots, M \tag{2.12}$$

$$\text{boundary conditions: } c_0^k = g(t_k), \; c_{M+1}^k = c_{M-1}^k, \; k = 0, 1, 2, 3, \ldots, N \tag{2.13}$$

where $\mu = v\frac{(\Delta t)^{\alpha}\Gamma(2-\alpha)}{2\Delta x}$, $r = D\frac{(\Delta t)^{\alpha}\Gamma(2-\alpha)}{2\Delta x^2}$, $b_j = (j+1)^{1-\alpha} - j^{1-\alpha}$, $j = 1, 2, 3, \ldots$ and $k = 0, 1, 2, 3, \ldots, N$, $i = 1, 2, 3, \ldots, M$.

Therefore, the discretized fractional order Crank-Nicolson finite difference scheme (2.10)-(2.13) can be expressed in matrix form as follows

$$AC^1 = BC^0 + S^0, \text{ for } k = 0 \tag{2.14}$$

$$AC^{k+1} = FC^k + \sum_{j=1}^{k-1}(b_j - b_{j+1})C^{k-j} + b_k C^0 + S^k, \text{ for } k \geq 1 \tag{2.15}$$

$$\text{initial condition: } c_i^0 = 0,\ i = 1, 2, 3, \ldots, M \tag{2.16}$$

$$\text{boundary conditions: } c_0^k = g(t_k),\ c_{M+1}^k = c_{M-1}^k,\ k = 0, 1, 2, 3, \ldots, N \tag{2.17}$$

where $C^k = (c_1^k, c_2^k, c_3^k, \ldots, c_M^k)^T$, $S^k = ((r+\mu)g(t_k) + rg(t_{k+1}), 0, 0, \ldots, 0)^T$ is a constant matrix,

$$A = \begin{pmatrix} 1+2r & -r & & & & & & \\ -r & 1+2r & -r & & & & & \\ & \ddots & \ddots & \ddots & & & & \\ & & -r & 1+2r & -r & & & \\ & & & \ddots & \ddots & \ddots & & \\ & & & & -r & 1+2r & -r & \\ & & & & & -2r & 1+2r & \end{pmatrix}$$

$$B = \begin{pmatrix} 1-2r & r-\mu & & & & & & \\ r+\mu & 1-2r & r-\mu & & & & & \\ & \ddots & \ddots & \ddots & & & & \\ & & r+\mu & 1-2r & r-\mu & & & \\ & & & \ddots & \ddots & \ddots & & \\ & & & & r+\mu & 1-2r & r-\mu & \\ & & & & & 2r & 1-2r & \end{pmatrix}$$

and

$$F=\begin{pmatrix} 1-2r-b_1 & r-\mu & & & & & & \\ r+\mu & 1-2r-b_1 & r-\mu & & & & & \\ & \ddots & \ddots & \ddots & & & & \\ & & r+\mu & 1-2r-b_1 & r-\mu & & & \\ & & & \ddots & \ddots & \ddots & & \\ & & & & r+\mu & 1-2r-b_1 & r-\mu & \\ & & & & & 2r & 1-2r-b_1 & \end{pmatrix}$$

3. Stability

In this section, we discuss the stability of solution of the fractional order Crank-Nicolson finite difference scheme (2.10)-(2.13) developed for the time fractional drug concentration equation (1.1)-(1.3) with initial and boundary conditions.

Lemma 3.1. *The eigenvalues of* $M\times M$ *tri-diagonal matrix*

$$\begin{pmatrix} a & b & & & & & \\ c & a & b & & & & \\ & \ddots & \ddots & \ddots & & & \\ & & c & a & b & & \\ & & & \ddots & \ddots & \ddots & \\ & & & & c & a & b \\ & & & & & c & a \end{pmatrix}$$

are given as

$$\lambda_s = a + 2\sqrt{bc}\cos\left(\frac{s\pi}{M+1}\right),\ s = 1, 2, 3, \ldots, M$$

where a, b *and* c *are either real or complex numbers* [25].

Lemma 3.2. *If* $\lambda_j(A)$, $j = 1, 2, 3, 4, \ldots, M-1$ *represent eigenvalues of a matrix* A, *then following conditions are hold*

(i) $\lambda_j(A) \geq 1$

(i) $\| A^{-1} \|_2 \leq 1$, *where* $\| \cdot \|_2$ *is the second norm of matrix*.

Proof. By the Gerschgorin's circle theorem [25], if λ is a eigenvalue of a square matrix $[a_{ij}]$ then λ is in at least one of the following disc

$$| \lambda - a_{ij} | \leq \sum_{l=1,\ l \neq j}^{M} a_{lj},\ l = 1, 2, 3, \ldots, M. \tag{3.1}$$

Thus, each eigenvalue λ of a square matrix $[a_{ij}]$ satisfy at least one of the following inequality

$$| \lambda | \leq \sum_{i=1}^{M} | a_{ij} | \tag{3.2}$$

$$| \lambda | \geq | a_{ij} | - \sum_{i=1,\ i \neq j}^{M} | a_{ij} | \tag{3.3}$$

Now, we use inequality (3.3) to prove the condition (i) for the matrix A as

$$| \lambda_1(A) | \geq | (1 + 2r) + (-r) | = 1 + r \geq 1$$

$$| \lambda_2(A) | \geq | (1 + 2r) + (-r) + (-r) | = 1$$

$$| \lambda_3(A) | \geq | (1 + 2r) + (-r) + (-r) | = 1$$

$$\vdots$$

$$| \lambda_M(A) | \geq | (1 + 2r) + (-r) + (-r) | = 1$$

Thus, $| \lambda_j | \geq 1,\ j = 1, 2, 3, \ldots, M.$

To prove condition (ii), we have

$$\| A \|_2 = \max_{1 \leq j \leq M} | \lambda_j(A) |.$$

Therefore, from condition (i), we get

$$\| A \|_2 \geq 1.$$

Hence,

$$\| A^{-1} \|_2 \leq 1$$

This complete the proof. □

Lemma 3.3. *The discretized fractional order Crank-Nicolson finite difference scheme with initial and boundary conditions* (2.10)-(2.13) *is*

solvable for each time step unconditionally.

Proof. To prove the solvability of equations (2.10) and (2.12), it is enough to prove that matrix A is invertible [8, 27]. We observed that, the first and last row of matrix A is diagonally dominant. For other rows, the diagonal element is $1+2r$ and the sum of the absolute values of the non-diagonal element in the same row is,

$$|(-r)| + |(-r)| = 2r.$$

Hence, for each row, we have $1+2r > 2r$. Thus, matrix A is strictly diagonally dominant. Hence, matrix A is invertible. This shows that the solvability of the finite difference scheme. □

Lemma 3.4. *If* $\lambda_s(B)$ *and* $\lambda_s(F)$ *represents the eigenvalues of B and F respectively*, *then following conditions are hold*

(i) $|\lambda_s(B)| \le 1, |\lambda_s(F)| \le 1, s = 1, 2, 3, \ldots, M$

(ii) $\| B \|_2 \le 1, \| F \|_2 \le 1, s = 1, 2, 3, \ldots, M.$

Theorem 3.5. *The solution of the fractional order Crank-Nicolson finite difference scheme* (2.10)-(2.13) *for time fractional drug concentration equation* (1.1)-(1.3) *is unconditionally stable*.

Proof. To prove the developed finite difference scheme is unconditionally stable, we will prove that

$$\| C^n \|_2 \le K \| C^0 \|_2, n = 1, 2, 3, \ldots$$

where K is positive integer independent of x and t.

For $n = 1,$ from equation (2.14), we obtain

$$C^1 = A^{-1}BC^0 + A^{-1}S^0$$

$$\therefore \| C^1 \|_2 \le \| A^{-1} \|_2 \| B \|_2 \| C^0 \|_2 + \| A^{-1} \|_2 \| S^0 \|_2$$

$$\le \| C^0 \|_2 + \| S^0 \|_2$$

$$\le \| C^0 \|_2 + K_1 \| C^0 \|_2, \text{ where } \| S^0 \|_2 = K_1, \text{ a constant.}$$

Thus, result is true for $n = 1.$

For $n \leq k$, let us assume that

$$\| C^k \|_2 \leq K \| C^0 \|_2.$$

Now, for $n = k + 1$, from equation (2.15), we obtain

$$C^{k+1} = A^{-1}FC^k + A^{-1}\sum_{j=1}^{k-1}(b_j - b_{j+1})C^{k-j}b_kC^0 + A^{-1}S^K.$$

$$\therefore \| C^{k+1} \|_2 \leq \| C^k \|_2 + \sum_{j=1}^{k-1}(b_j - b_{j+1}) \| C^{k-j} \|_2 + b_k \| C^0 \|_2 + \| S^K \|_2$$

$$= \| C^k \|_2 + [(b_1 - b_2) \| C^{k-1} \|_2 + (b_2 - b_3) \| C^{k-2} \|_2 + \ldots + (b_{k-1} - b_k) \| C^1 \|_2]$$

$$+ b_k \| C^0 \|_2 + \| S^k \|_2$$

$$\leq K_1 \| C^0 \|_2 + [(b_1 - b_2) + (b_2 - b_3) + \ldots + (b_{k-1} - b_k)]K_2 \| C^0 \|_2 + b_k \| C^0 \|_2 + K_3$$

$$\leq [K_1 + b_1 + (1 - K_2)b_k] \| C^0 \|_2 + K_3 \| C^0 \|_2$$

$$= K \| C^0 \|_2.$$

Hence, by induction, for all n, we have

$$\| C^n \|_2 \leq K \| C^0 \|_2$$

where K is a positive number independent of x and t.

Therefore, this shows that the scheme is unconditionally stable.

This complete the proof. □

4. Convergence

In this section, we discuss the convergence of the scheme. Let Ω be the region $[0, L] \times [0, T]$. We introduce the vector, $\overline{C}^k = (\bar{c}(x_0, t_k), \bar{c}(x_1, t_k), \bar{c}(x_2, t_k), \ldots, \bar{c}(x_M, t_k))^T$ of size $M + 1$, which represent the exact solution of the time fractional drug concentration equation (1.1)-(1.3) at time level t_k.

Let $\tau^k = (\tau_1^k, \tau_2^k, \tau_3^k, \ldots, \tau_M^k)^T$ be the vector of truncation error at time level t_k. Since $\overline{C}^k$ is the exact solution of the equation (1.1)-(1.3), we have

$$A\overline{C}^1 = B\overline{C}^0 + S^0 + \tau^1, \text{ for } k = 0. \tag{4.1}$$

$$A\overline{C}^{k+1} = F\overline{C}^k + \sum_{j=1}^{k-1}(b_j - b_{j+1})\overline{C}^{k-j} + b_k\overline{C}^0 + S^k + \tau^{k+1}, \text{ for } k \geq 1. \tag{4.2}$$

Lemma 4.1. *The coefficient* b_j, $j = 0, 1, 2, 3, \ldots$ *satisfy the following conditions*

(i) $b_j > 0$

(ii) $b_j > b_j + 1$.

Theorem 4.2. *The fractional order Crank-Nicolson finite difference scheme* (2.10)-(2.13) *for time fractional drug concentration equation* (1.1)-(1.3) *is unconditionally convergent*.

Proof. We set, $E^k = \overline{C}^k - C^k = (e_1^k, e_2^k, e_3^k, \ldots, e_M^k)^T$ be the error vector in the solution at time level t_k. Furthermore, we assume that $| e_l^k | = \max\limits_{1\leq i\leq M} | e_i^k | = \| E^k \|_\infty$ and $\tau_l^k = \max\limits_{1\leq i\leq M} | \tau_i^k |$, for $l = 1, 2, 3, \ldots$

Then, using equation (2.10), we obtain

$$\begin{aligned} | e_l^1 | &= | -re_{i-1}^1 + (1+2r)e_i^1 - re_{i+1}^1 | \\ &\leq (r+\mu)| e_{i-1}^0 | + (1-2r)| e_i^0 | + (r-\mu)| e_{i+1}^0 | + | \tau_l^1 | \\ &\leq (r+\mu+1-2r+r-\mu) \max_{1\leq i\leq M} | e_i^0 | + \max_{1\leq i\leq M} | \tau_i^1 | \\ &= \| E^0 \|_\infty + \max_{1\leq i\leq M} | \tau_i^1 | \end{aligned}$$

$$\therefore \| E^1 \|_\infty \leq \| E^0 \|_\infty + \max_{1\leq i\leq M} | \tau_i^1 |$$

Now, from equation (2.11), we obtain

$$| e_l^{k+1} | = | -re_{i-1}^{k+1} + (1+2r)e_i^{k+1} - re_{i+1}^{k+1} |$$

$$\leq (r+\mu)|\, e_{i-1}^{k} \,| + (1-2r-b_1)|\, e_i^{k} \,| + (r-\mu)|\, e_{i+1}^{k} \,| + \sum_{j=1}^{k-1}(b_j - b_{j+1})|\, e_i^{k-j} \,|$$

$$+ b_k|\, e_i^{0} \,| + |\, \tau_l^{k+1} \,|$$

$$= (r+\mu)|\, e_{i-1}^{k} \,| + (1-2r-b_1)|\, e_i^{k} \,| + (r-\mu)|\, e_{i+1}^{k} \,| + (b_1 - b_2)|\, e_i^{k-1} \,|$$

$$+ (b_2 - b_3)|\, e_i^{k-2} \,| + \ldots + (b_{k-1} - b_k)|\, e_i^{1} \,| + b_k|\, e_i^{0} \,| + |\, \tau_i^{k+1} \,|$$

$$= [(r+\mu) + (1-2r-b_1) + (r-\mu)]|\, e_l^{k} \,| + [(b_1 - b_2) + (b_2 - b_3) + \ldots + (b_{k-1} - b_k)]$$

$$|\, e_l^{k} \,| + b_k|\, e_l^{k} \,| + \max_{1\leq i\leq M}|\, \tau_i^{k+1} \,|$$

$$= \|\, E^{k} \,\|_{\infty} + \max_{1\leq i\leq M}|\, \tau_i^{k+1} \,|.$$

This is true for every k, therefore we have

$$\|\, E^{k+1} \,\|_{\infty} \leq \|\, E^{k} \,\|_{\infty} + \max_{1\leq i\leq M}|\, \tau_i^{k+1} \,|$$

Hence, by induction, we get

$$\|\, E^{n+1} \,\|_{\infty} \leq \|\, E^{n} \,\|_{\infty} + \max_{1\leq i\leq M}|\, \tau_i^{n+1} \,|$$

As $\|\, E^{0} \,\|_{\infty} = 0$, implies $\|\, E^{n} \,\|_{\infty} = 0$.

Therefore, $\|\, E^{n+1} \,\|_{\infty} \leq \max_{1\leq i\leq M}|\, \tau_i^{n+1} \,|$.

Since $\max_{1\leq i\leq M}|\, \tau_i^{n+1} \,| \to 0$ as $(\Delta x, \Delta t) \to (0, 0)$, implies that $\|\, E^{n+1} \,\|_{\infty} \to 0$ uniformly on Ω as $(\Delta x, \Delta t) \to (0, 0)$.

Therefore, this shows that for any x and t, as $(\Delta x, \Delta t) \to (0, 0)$, the vector C^n converges to $\overline{C}^n$.

Hence, this complete the proof. □

5. Python Programme

In this section, we develop the algorithm for solving the discretized

scheme (2.10)-(2.13) using Python programme. Here we compute c_i^k at each mesh point (x_i, t_k) using the proposed scheme by Python. The algorithm for the scheme (2.14)-(2.17) is as follows

(i) Define $g(t_k)$ for each $k = 0, 1, 2, 3, \ldots, N$.

(ii) Compute the matrix A, B and F.

(iii) Compute C^0 and S^0, then compute C^1.

(iv) Compute S^1. Then using C^1, compute C^2.

(v) Compute S^k. Then compute C^{k+1} for each $k = 2, 3, 4, \ldots, N$.

Now, we develop the python programme DCE for complete discretized scheme (2.14)-(2.17) as follows:

Inputs:

g - boundary condition at x=0.

C - drug concentration

L - spatial length

T - end time

D - diffusion coefficient of drugs

mu - μ

a - fractional order α of time derivative

t1 - time at which solution to be estimated.

Output of Python programme DCE is the approximate value of vector $C(x_i, t_k)$.

```
import scipy
from scipy import *
import math
from math import *
```

```
def g(k):
    return(c(0,t))
import numpy as np
def DCE(g,v,L,T,dx,dt,D,a,t1):
    r=dt**a*D*math.gamma(2-a)/(2*dx**2)
    mu=v*dt**a*math.gamma(2-a)/(2*dx)
    N=int(round(T/dt))
    M=int(round(L/dx))
    t=np.linspace(0,N*dt,N+1)
    x=np.linspace(0,M*dx,M+1)
    A = np.zeros((M+1, M+1))
    A[0, 0] = 1+2*r
    A[0, 1]=-r
    A[M,M-1]=-2*r
    A[M, M] = 1+2*r
    for i in range(1, M):
        A[i, i-1] = -r
        A[i, i] = 1+2*r
        A[i, i+1] = -r
B=np.zeros((M+1,M+1))
B[0,0]=1-2*r
B[0,1]=r-mu
B[M,M-1]=2*r
B[M,M]=1-2*r
for i in range(1,M):
   B[i, i-1] = r+mu
```

```
    B[i, i] = 1-2*r
    B[i, i+1] = r-mu
F=np.zeros((M+1,M+1))
F[0,0]=1-2*r-((1+1)**(1-a)-1**(1-a))
F[0,1]=r-mu
F[M,M-1]=2*r
F[M,M]=1-2*r-((1+1)**(1-a)-1**(1-a))
for i in range(1,M):
    F[i, i-1] = r+mu
    F[i, i] = 1-2*r-((1+1)**(1-a)-1**(1-a))
    F[i, i+1] = r-mu
C=np.zeros((N+1,M+1))
S0=np.zeros(M+1)
S0[0]=(r+mu)*g(t[0])+r*g(t[1])
b0=B@C[0]+S0
C[1]=scipy.linalg.solve(A,b0)
S1=np.zeros(M+1)
S1[0]=(r+mu)*g(t[1])+r*g(t[2])
b1=F@C[1]+S1
C[2]=scipy.linalg.solve(A,b1)
for k in range(2,N):
    ek=(k+1)**(1-a)-k**(1-a)
    Sk=np.zeros(M+1)
    Sk[0]=(r+mu)*g(t[k])+r*g(t[k+1])
    sum=np.zeros(M+1)
    for j in range(1,k):
```

```
        sum=sum+((j+1)**(1-a)-j**(1-a)-(j+2)**(1-a)+(j+1)**(1-a))*C[k-j]
    bk=F@C[k]+sum+ek*C[0]+Sk
    C[k+1][:]=scipy.linalg.solve(A,bk)
t1=int(t1/dt)
return(x,C[t1])
```

6. Numerical Solutions

In this section, we obtain the approximate solution of time fractional drug concentration equation (1.1)-(1.3) by a developed fractional order Crank-Nicolson finite difference scheme (2.10)-(2.13).

6.1 Test Problem 1. Steady State Concentration

In pharmacology, the steady state of drug is an important fundamental concept. Steady-state is a situation during which the concentration of drug in the body is stable. In the treatment of CNSdisease, understanding of steady-state is important for choosing the right dose and determining the dosing interval to achieve a desire steady-state concentration. This is the situation corresponds to where maintenance dose is given in order to keep the drug concentration constant in the brain ECF [5]. If the concentration in brain ECF remains constant, then we will obtain the drug concentration in the CSF changes along the CSF space by the following drug concentration equation

$$\frac{\partial^{\alpha} c(x,\, t)}{\partial t^{a}} = -v\,\frac{\partial c(x,\, t)}{\partial x} + D\,\frac{\partial^{2} c(x,\, t)}{\partial x^{2}},\ 0 < \alpha \le 1,\ 0 \le x \le 8,\ t \ge 0$$

$$\text{initial condition: } c(x,\, 0) = 0,\ 0 \le x < 8$$

$$\text{boundary conditions: } c(0,\, t) = 3,\ \frac{\partial c(8,\, t)}{\partial x} = 0\,(t \ge 0).$$

The exact solution of the problem for $\alpha = 1$ is given as [5]

$$c(x,\, t) = \frac{3}{2}\left(erfc\left(\frac{x - vt}{2\sqrt{Dt}}\right) + e^{\frac{vx}{D}} erfc\left(\frac{x + vt}{2\sqrt{Dt}}\right)\right).$$

With the help of Python programme DCE, we calculate the drug concentration $c(x,\, t)$ for anytime t_k. The numerical solutions of the time

fractional drug concentration equation obtained by developed scheme for $\alpha = 1.0, 0.9, 0.8$ with the parameters $v = 0.5$, $D = 0.7$, $\Delta x = 0.01$ and $\Delta t = 0.001$ is represented graphically in Figure 1. Furthermore, we simulate the numerical solution of the time fractional drug concentration equation for different values of x in Figure 2. The exact solution and numerical solution for $\alpha = 1$ with the parameters $v = 0.5$, $D = 0.7$, $\Delta x = 0.01$ and $\Delta t = 0.001$ at time $t = 2$ are shown in Table 1. We observed that the magnitude of the error of exact solution and numerical solution is of $O(\Delta t + (\Delta x)^2)$.

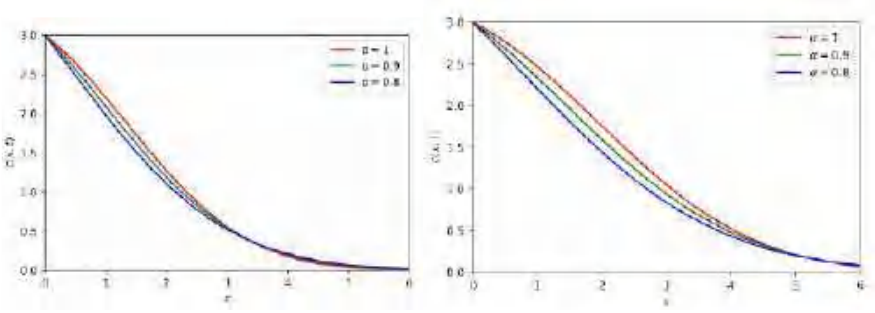

(a) $t = 2$ (b) $t = 3$

Figure 1. Drug concentration profile with the parameters $v = 0.5$, $D = 0.7$, $\Delta x = 0.01$, $\Delta t = 0.001$ and $\alpha = 1.0, 0.9, 0.8$.

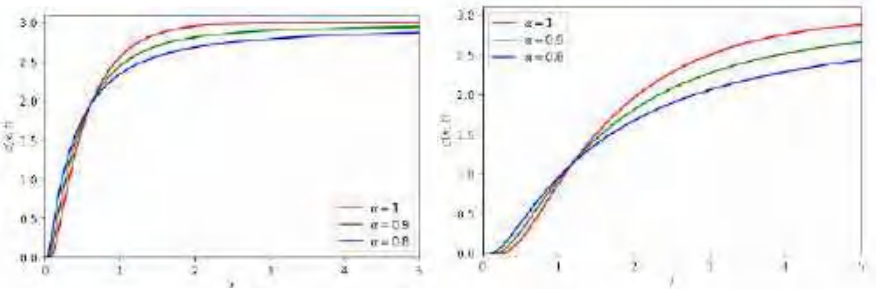

(a) $x = 1$ (b) $x = 2$

Figure 2. Numerical solution of steady state concentration for $x = 1$ and $x = 2$ with the parameters $v = 0.5$, $D = 0.7$, $T = 5$, $\Delta x = 0.01$ and $\Delta t = 0.001$.

Table 1. Comparision of exact solution and numerical solution for $\alpha = 1$, $t = 2$, $v = 0.5$, $D = 0.7$, $\Delta x = 0.01$ and $\Delta t = 0.001$.

x	Exact Solution	Numerical Solution	Error $e_i^k = \| \bar{c}_i^k - c_i^k \|$
0.0	3.0	2.993907278649013	0.006092721350987151
0.5	2.6456568378800114	2.637640626024081	0.0080162118559306
1.0	2.210862045444807	2.2016244916677286	0.009237553777078578
1.5	1.7395672793993147	1.7300687648213946	0.009498514577920059
2.0	1.2820481022496093	1.2732489286656066	0.008799173584002729
2.5	0.8812918247063797	0.8739078798391523	0.007383944867227377
3.0	0.5631456958949884	0.5575140861890188	0.0056316097059696535
3.5	0.33360708628476354	0.3296952147891131	0.003911871495650421
4.0	0.1828205165043782	0.1803422974511022	0.0024782190532759985
4.5	0.09251994640668684	0.0910867844617443	0.0014331619449425431
5.0	0.04317739107570287	0.042420349641816124	0.0007570414338867459
5.5	0.018560555515715397	0.01819513741539206	0.00036541810032333574
6.0	0.007342283849504758	0.007181092835093199	0.00016119101441155938

6.2 Test Problem 2. Elimination Phase

The elimination phase of drug is the case corresponds to the drug being present in the CSF in the lateral ventricles at some concentration c_0 [5]. At $t = 0$, the injection is stopped and the elimination begins. This case is relevant for concentration-time profile on coarse time scale. Since the drug aggregation happens quite fast in the case of intravenous injection, it will not visible on such a time-scale and we will see only elimination phase in the plot. This phenomenon is study by the following time-fractional drug concentration equation

$$\frac{\partial^\alpha c(x, t)}{\partial t^\alpha} = -v \frac{\partial c(x, t)}{\partial x} + D \frac{\partial^2 c(x, t)}{\partial x^2}, \; 0 < \alpha \leq 1, \; x \leq 6, \; t \geq 0$$

$$\text{initial condition: } c(x, 0) = 0, \; 0 < x < 6$$

boundary conditions: $c(0, t) = 3e^{-t}$, $\frac{\partial c(6, t)}{\partial x} = 0 (t \geq 0)$.

The exact solution of the problem for $\alpha = 1$ is given as [5]

$$c(x, t) = \frac{3}{2} e^{-t} \left(e^{\frac{(v-y)x}{2D}} erfc\left(\frac{x - yt}{2\sqrt{Dt}} \right) + e^{\frac{(v+y)x}{2D}} erfc\left(\frac{x + yt}{2\sqrt{Dt}} \right) \right)$$

where $y = \sqrt{v^2 - 4D}$. The numerical solutions of the time fractional drug concentration equation obtained by developed scheme for $\alpha = 1.0, 0.9, 0.8$ with the parameters $v = 1$, $D = 0.2$, $\Delta x = 0.01$ and $\Delta t = 0.001$ are represented graphically in Figure 3 by Python programme DCE. Furthermore, we simulate the numerical solutions of the time fractional drug concentration equation for different values of x in Figure 4. In Table 2, we compare the exact solution and numerical solution of the time fractional drug concentration equation for $\alpha = 1$ with the parameters $v = 1$, $D = 0.2$, $\Delta x = 0.01$ and $\Delta t = 0.001$ at time $t = 2$. Moreover, we observe that the error in the calculation is of $O(\Delta t + (\Delta x)^2)$.

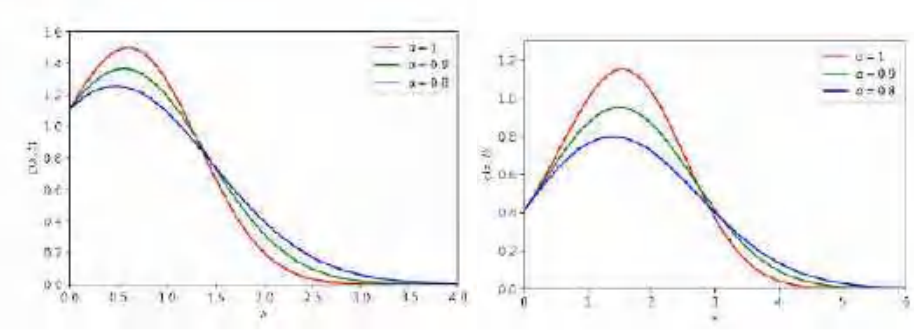

(a) $t = 1$ (b) $t = 2$

Figure 3. Drug concentration profile with the parameters $v = 1$, $D = 0.2$, $\Delta x = 0.01$, $\Delta t = 0.001$ and $\alpha = 1.0, 0.9, 0.8$.

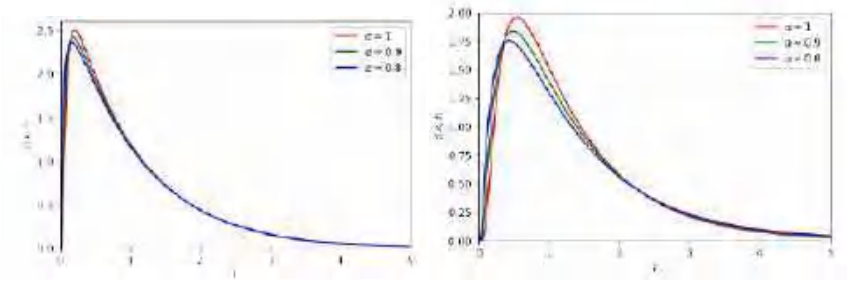

(a) $x = 0.2$ (b) $x = 0.5$

Figure 4. Numerical solution for drug elimination for $x = 0.2$ and $x = 0.5$ with the parameters $v = 1$, $D = 0.2$, $t = 5$, $\Delta x = 0.01$ and $\Delta t = 0.001$.

Table 2. Comparision of exact solution and numerical solution for $\alpha = 1$, $t = 2$, $v = 1$, $D = 0.2$, $\Delta x = 0.01$ and $\Delta t = 0.001$.

x	Exact Solution	Numerical Solution	Error $e_i^k = \| \bar{c}_i^k - c_i^k \|$
0.0	0.40600584970983805	0.4108789821823356	0.004873132472497543
0.5	0.690643252642077	0.6969777675627705	0.006334514920693479
1.0	0.9910421336946248	0.9965539539700895	0.005511820275464707
1.5	1.147116277674832	1.1484516174662687	0.0013353397914366294
2.0	1.0385500472139912	1.0343063307369158	0.004243716477075443
2.5	0.72077795551975	0.7133503723003761	0.007427583219373868
3.0	0.37847592991323475	0.3718015170776765	0.006674412835558252
3.5	0.14906463756342395	0.14515526386486594	0.003909373698558011
4.0	0.04377805649358062	0.04219236700542997	0.0015856894881506461
4.5	0.009547713552140515	0.009091836821831855	0.0004558767303086599
5.0	0.0015417744244616016	0.001447866329388511	9.390809507309065e-05
0.0	0.40600584970983805	0.4108789821823356	0.004873132472497543
0.5	0.690643252642077	0.6969777675627705	0.006334514920693479

6.3 Test Problem 3. Drug Aggregation

The drug aggregation corresponds to the case in which drug is given continuously over a longer period of time [5]. The drug reaches the CSF at time $t = 0$ and no drug was present in the brainECF and CSF before that. The injection is continued long enough in order to reach the steady state

concentration and is not stopped within the period of time considered. This phenomenon is study by the following time-fractional drug concentration equation

$$\frac{\partial^{\alpha} c(x, t)}{\partial t^{\alpha}} = -v \frac{\partial c(x, t)}{\partial x} + D \frac{\partial^2 c(x, t)}{\partial x^2}, \; 0 < \alpha \leq 1, \; x \leq 5, \; t \geq 0$$

$$\text{initial condition: } c(x, 0) = 0, \; 0 < x < .$$

$$\text{boundary conditions: } c(0, t) = 3e^{-t}, \; \frac{\partial c(5, t)}{\partial x} = 0 (t \geq 0).$$

The exact solution of the problem for $\alpha = 1$ is given as [5]

$$c(x, t) = \frac{3}{2}\left(erfc\left(\frac{x - vt}{2\sqrt{Dt}}\right) + e^{\left(\frac{vx}{D}\right)} erfc\left(\frac{x + vt}{2\sqrt{Dt}}\right) \right.$$

$$\left. - e^{-t}\left(e^{\frac{(v-y)x}{2D}} erfc\left(\frac{x - yt}{2\sqrt{Dt}}\right) + e^{\frac{(v+y)x}{2D}} erfc\left(\frac{x + yt}{2\sqrt{Dt}}\right)\right)\right)$$

where $y = \sqrt{v^2 - 4D}$. With the help of developed python programme DCE, the numerical solutions of the time fractional drug concentration equation for $\alpha = 1.0, 0.9, 0.8$ with the parameters $v = 1$, $D = 0.2$, $\Delta x = 0.01$ and $\Delta t = 0.001$ is represented graphically in Figure 5. Furthermore, we simulate the numerical solutions of the time fractional drug concentration equation for different values of x in Figure 6. In the Table 3, we compare the exact solution and numerical solution at time $t = 3$ for $\alpha = 1$ with the parameters $v = 1$, $D = 0.2$, $\Delta x = 0.01$ and $\Delta t = 0.001$. We observe that the magnitude of the error between the exact solution and numerical solution is of $O(\Delta t + (\Delta x)^2)$.

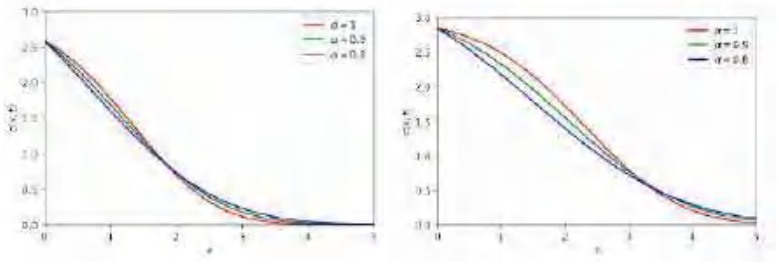

(a) $t = 2$ (b) $t = 3$

Figure 5. Drug concentration profile with the parameters $v = 1$, $D = 0.2$, $\Delta x = 0.01$, $\Delta t = 0.001$ and $\alpha = 1.0, 0.9, 0.8$.

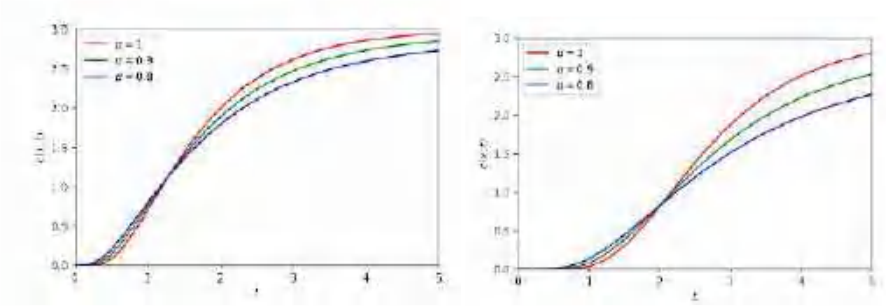

(a) $x = 1$ (b) $x = 2$

Figure 6. Numerical solution for drug aggregation for $x = 1$ and $x = 2$ with the parameters $v = 1$, $D = 0.2$, $\Delta x = 0.01$ and $\Delta t = 0.001$.

Table 3. Comparision of exact solution and numerical solution for $\alpha = 1$, $t = 3$, $v = 1$, $D = 0.2$, $\Delta x = 0.\ 01$ and $\Delta t = 0.001$.

x	Exact Solution	Numerical Solution	Error $e_i^k = \| \bar{c}_i^k - c_i^k \|$
0.0	2.8506387948964083	2.8486584009974187	0.0019803938989895187
0.5	2.717400152250943	2.7140190061622556	0.003381146088687448
1.0	2.495369092986084	2.490061111986018	0.005307981000065798
1.5	2.1654336714236244	2.157966519981535	0.007467151442089204
2.0	1.7376742713960167	1.7284649530934093	0.009209318302607405
2.5	1.2617161036485738	1.251930562993927	0.009785540654646763

3.0	0.8126564196023055	0.8038171392485197	0.008839280353785783
3.5	0.4565234712200368	0.44980441741804056	0.006719053801996222
4.0	0.22062447196653884	0.21636491470986893	0.004259557256669905
4.5	0.09072778152906447	0.08873837701972355	0.001989404509340917
5.0	0.03147838582653009	0.040396872611049295	0.008918486784519203

7. Conclusion

(i) We successfully develop the fractional order Crank-Nicolson finite difference scheme for the time fractional drug concentration equation in the central nervous system.

(ii) The stability and convergence of the developed scheme are both investigated.

(iii) Furthermore, we successfully develop the Python programme for the time fractional drug concentration equation in the central nervous system.

(iv) The performance and efficiency of the developed scheme is numerically tested using some numerical experiments. We observe that the error in the calculation is $O((\Delta t)^{2-\alpha} + (\Delta x)^2)$.

(v) Finally, we conclude that Python is a very powerful tool for obtaining the numerical solutions of the time fractional drug concentration equation.

References

[1] José Francisco Gómez Aguilar and Margarita Miranda Hernández, Space-Time Fractional Diffusion-Advection Equation with Caputo Derivative, Abstract and Applied Analysis (2014), 1-8.

[2] Teodor M. Atanackovic, Fractional Calculus with Applications in Mechanics, ISTE Ltd/JohnWiley and Sons Inc, Hoboken, NJ, 2013.

[3] Teodor M. Atanacković, Stevan Pilipović, Bogoljub Stanković and Dusan Zorica, Fractional Calculus with Applications in Mechanics: Vibrations and Diffusion Processes, John Wiley and Sons, Inc., Hoboken, USA, January 2014.

[4] Isa Abdullahi Baba, A fractional-order bladder cancer model with BCG treatment effect, Computational and Applied Mathematics 38(2) 37 March 2019.

[5] Laila Kristin Gabriel, A Mathematical Model for Estimating Drug Concentrations in Human Brain Fluid, Mathematisch Instituut, Universiteit Leiden, page 78, September 2016.

[6] Krishna Ghode, Kalyanrao Takale and Shrikisan Gaikwad, New technique for solving time fractional wave equation: Python, Journal of Mathematical and Computational Science 11(5) (2021), 5327-5343.

[7] R. Hilfer, Applications of Fractional Calculus in Physics, World Scientific, March 2000.

[8] Mark Hayden Holmes, Introduction to Numerical Methods in Differential Equations, Texts in Applied Mathematics, Springer-Verlag, New York, 2007.

[9] Sunil S. Jambhekar and Philip J. Breen, Basic Pharmacokinetics, Pharmaceutical Press, May 2009.

[10] Suryakant Jogdand, Kalyanrao Takale and V. C. Borkar, Fractional Order Finite Difference Scheme for Soil Moisture Diffusion Equation and its Applications, IOSR Journal of Mathematics 5(4) (2013), 12-18.

[11] Suryakant Jogdand, Kalyanrao Takale and A. Jagtap, Finite difference approximation for space fractional soil moisture diffusion equation and its application, IOSR Journal of Mathematics 8(4) (2013), 1-8.

[12] Hardik Joshi and Brajesh Kumar Jha, Fractional-order mathematical model for calcium distribution in nerve cells, Computational and Applied Mathematics 39(56), 2020.

[13] Bertram G. Katzung, Basic and Clinical Pharmacology, McGraw-Hill Medical, New York, 2012.

[14] M. Yu Kokurin, S. I. Piskarev and M. Spreafico, Finite-Difference Methods for Fractional Differential Equations of Order 1/ 2, Journal of Mathematical Sciences 230(6) (2018), 950-960.

[15] T. A. M. Langlands, B. I. Henry and S. L. Wearne, Fractional cable equation models for anomalous electro diffusion in nerve cells: Infinite domain solutions, Journal of Mathematical Biology 59(6) (2009), 761-808.

[16] Hans Petter Langtangen and Svein Linge, Finite Difference Computing with PDEs: A Modern Software Approach, Volume 16 of Texts in Computational Science and Engineering, Springer International Publishing, Cham, 2017.

[17] Changpin Li and Fanhai Zeng, Finite difference methods for fractional differential equations, International Journal of Bifurcation and Chaos 22(04) (2012), 1230014 pp 28.

[18] Richard L. Magin, Fractional calculus models of complex dynamics in biological tissues, Computers and Mathematics with Applications 59(5) (2010), 1586-1593.

[19] Kolade Matthew Owolabi and Abdon Atangana, Numerical Methods for Fractional Differentiation, Springer Series in Computational Mathematics, Springer Singapore, 2019.

[20] M. Ozisik, Helcio Orlande, Marcelo Colaco and R. M. Cotta, Finite Difference Methods in Heat Transfer: Second Edition, CRC Press, January 2017.

[21] Carla M. A. Pinto and J. A. Tenreiro Machado, Fractional model for malaria transmission under control strategies, Computers and Mathematics with Applications 66(5) (2013), 908-916.

[22] Igor Podlubny, Fractional Differential Equations: An Introduction to Fractional Derivatives, Fractional Differential Equations, to Methods of Their Solution and Some of Their Applications, Elsevier, October 1998.

[23] S. G. Samko, A. A. Kilbas and O. I. Marichev, Fractional Integrals and Derivatives: Theory and Applications, Gordon and Breach Science Publishers, Switzerland; Philadelphia, Pa., USA, 1993.

[24] W. R. Schneider and W. Wyss, Fractional diffusion and wave equations, Journal of Mathematical Physics 30(1) (1989), 134-144.

[25] G. D. Smith, Numerical Solution of Partial Differential Equations: Finite Difference Methods, Oxford Applied Mathematics and Computing Science Series, Oxford University Press, Oxford, New York, third edition, December 1985.

[26] Bhausaheb R. Sontakke and Abhijeet S. Shelke, Approximate scheme for time fractional diffusion equation and its applications, Global Journal of Pure and Applied Mathematics 13(8) (2017), 14.

[27] K. C. Takale, D. B. Dhaigude and V. R. Nikam, Douglas Higher Order Finite Difference Scheme for One Dimensional Pennes Bioheat Equation, International Journal of Advanced Engineering and Application (2011), 5.

[28] Kalyanrao Takale, Fractional Order Finite Difference Scheme for Space Fractional Boussinesq's Equations and its Applications, Int. Jr. of Mathematical Sciences and Applications 3(1) (2013), 343-353.

[29] Joost Westerhout, Bart Ploeger, Jean Smeets, Meindert Danhof and Elizabeth C. M. de Lange, Physiologically Based Pharmacokinetic Modeling to Investigate Regional Brain Distribution Kinetics in Rats, The AAPS Journal 14(3) (2012), 543-553.

[30] Joost Westerhout, Dirk-Jan van den Berg, Robin Hartman, Meindert Danhof and Elizabeth C. M. de Lange, Prediction of methotrexate CNS distribution in different species – influence of disease conditions, European Journal of Pharmaceutical Sciences 57 (2014), 11-24.

[31] Lifei Wu, Xiaozhong Yang and Yanhua Cao, An alternating segment Crank Nicolson parallel difference scheme for the time fractional sub-diffusion equation, Advances in Difference Equations (1) (2018), 287.

[32] Yamamoto Yumi et al., Predicting Drug Concentration-Time Profiles in Multiple CNS Compartments Using a Comprehensive Physiologically-Based Pharmacokinetic Model: PBPK Model for Brain Target-Site Concentrations, CPT: Pharmacometrics and Systems Pharmacology 6(11) (2017), 765-777.

Advances and Applications in Mathematical Sciences
Volume 22, Issue 2, December 2022, Pages 503-526

PYTHON: POWERFUL TOOL FOR SOLVING SPACE-TIME FRACTIONAL TRAVELING WAVE EQUATION

KRISHNA GHODE, KALYANRAO TAKALE, SHRIKISAN GAIKWAD and KIRANKUMAR BONDAR

Department of Mathematics
B. K. Birla College of Arts
Science and Commerce, Kalyan
Thane-421301, (M.S.), India

Department of Mathematics
RNC Arts, JDB Commerce and
NSC Science College, Nashik Road
Nashik-422101, (M. S.), India
E-mail: kalyanraotakale1@gmail.com

Department of Mathematics
New Atrs, Commerce and Science College
Ahmadnagar-414001, (M. S.), India
E-mail: sbgmathsnagar@gmail.com

Department of Mathematics
Government Vidarbha Institute
of Science and Humanities
Amravati 444604, (M.S.), India
E-mail: klbondar75@rediffmail.com

Abstract

The aim of this paper is to investigate the solution of space-time fractional traveling wave equation by Crank-Nicolson finite difference method using Python Programme. Also, we prove the scheme is unconditionally stable and convergent. Furthermore, we develop the Python programme for the proposed scheme and estimate the error. Finally, we obtain the numerical solutions of some test problems and simulated graphically by a Python programme.

2020 Mathematics Subject Classification: 35L05, 26A33, 65M06.

Keywords: Fractional traveling wave equation, Caputo derivative, Grunwald-Letnikov derivative, stability, Python etc.

*Corresponding author; E-mail: ghodekrishna@gmail.com

Received September 17, 2021; Accepted January 1, 2022

1. Introduction

In recent years, fractional differential equations are becoming a significant implement in the analysis and modeling of scientific problems in a broad array of fields such as physics, engineering, biology, finance, economics and earthquakes study etc. [2, 6, 9, 11, 10, 17]. There has been increasing attention in the description of physical and chemical processes using equations involving fractional derivatives and integrals. The study of fractional differential equations has been a highly focused in recent years. But most of the fractional differential equations do not have exact solutions. Traveling wave analysis is the most significant approach to study linear and non-linear partial differential equations. This study leads to various types of solutions such as soliton solutions, periodic solutions, kink solutions, cuspons solutions, compacton solutions, peakon solutions etc. [18]. The traveling wave solutions of fractional order partial differential equations are useful to analyses the mechanisms of phenomena as well as further application in various fields. Though, finding traveling wave solutions is not a straightforward task at all, therefore researchers are preferring finite difference schemes.

The finite difference approximations for derivatives are one of the simplest and the efficient method to solve fractional order partial differential equations [1, 3, 14, 13, 16]. Therefore, in this connection we develop the Crank-Nicolson finite difference scheme for space time fractional traveling wave equation and obtain its solution using Python programme. Recently, many researchers have shifted from compiled languages to interpreted problem solving environments, such as MATLAB, Maple, Octave, *R* etc. [5, 12, 15]. The Python is now rising as a potentially competitive replacement to MATLAB, Octave, and other similar environments [4, 7]. The popularity of Python is because of simple and clean syntax of the commands, incorporation of simulation and visualization, interactive execution of commands with instantaneous feedback and lots of built-in functions available and work efficiently on arrays in compiled code. Now a days, researchers are using Python due to its simplicity, wealth of available support and the NumPy package, which provides contiguous multi-dimensional array structures with a large library of array operations.

The plan of the paper is as follows: In section 2, the Crank-Nicolson finite difference scheme is developed for space-time fractional traveling wave equation. The section 3 is devoted for stability of the scheme and the question of convergence is proved in section 4. The last section is devoted for Python programme and numerical solution of the space-time fractional traveling wave equations.

We consider the following space-time fractional traveling wave equation

$$\frac{\partial^{\alpha} V}{\partial t^{\alpha}} = C^2 \frac{\partial^{\beta} V}{\partial x^{\beta}},\ t \in [0,\ T],\ x \in [0,\ L],\ 1 < \alpha \le 2,\ 1 < \beta \le 2 \tag{1.1}$$

subject to the initial conditions:

$$V(x,\ 0) = f(x),\ \frac{\partial}{\partial t} V(x,\ 0) = g(x),\ x \in [0,\ L] \tag{1.2}$$

and boundary conditions:

$$V(0,\ t) = 0,\ V(L,\ t) = 0,\ t > 0 \tag{1.3}$$

where $V(x,\ t)$ is the displacement of wave at position x and time t, and C is the velocity of wave. The Caputo time fractional derivative of order α is defined as follows [8],

$$\frac{\partial^{\alpha} V}{\partial t^{\alpha}} = \frac{1}{\Gamma(m - \alpha)} \int_0^t (t - \zeta)^{m-\alpha-1} \frac{\partial^m V(x,\ \zeta)}{\partial \zeta^m} d\zeta$$

where m is a integer such that $m - 1 < \alpha \le m$. The right shifted Grunwald-Letnikov space fractional derivative of order β is defined as follows [8],

$$\frac{\partial^{\alpha} V}{\partial t^{\alpha}} = \lim_{M \to \infty} \frac{1}{h^{\beta}} \sum_{l=0}^{M} \frac{\Gamma(l - \beta)}{\Gamma(-\beta)\Gamma(l + 1)} V(x - (l - 1)h,\ t).$$

2. Finite Difference Scheme

In this section, we discretized the space-time fractional traveling wave equation (1.1)-(1.3) using Crank-Nicolson finite difference scheme. Let $x_i = ih,\ i = 0, 1, 2, \ldots, M$ and $t_n = nk,\ n = 0, 1, 2, \ldots, N$, where $h = \frac{L}{M}$

and $k = \frac{T}{M}$. Let V_i^n be the numerical approximation of $V(x, t)$ at point (ih, nk), where h and k are spatial and temporal sizes respectively. We discretized the Caputo time fractional derivative as follows:

$$\left(\frac{\partial^\alpha V}{\partial t^\alpha}\right)_{(x_i,\, t_{n+1})} = \frac{1}{\Gamma(2-\alpha)} \int_0^{t_{n+1}} (t_{n+1} - \zeta)^{1-\alpha} \frac{\partial^2 V(x_i, \zeta)}{\partial \zeta^2} d\zeta$$

$$= \frac{1}{\Gamma(2-\alpha)} \sum_{j=0}^{n} \int_{j^k}^{(j+1)k} \eta^{1-\alpha} \frac{\partial^2 V(x_i, t_{n+1} - \eta)}{\partial \eta^2} d\eta$$

$$= \frac{1}{\Gamma(2-\alpha)} \sum_{j=0}^{n} \left(\frac{V_i^{n-j+1} - 2V_i^{n-j} + V_i^{n-j-1}}{k^2} + O(k) \right)$$

$$\times \int_{j^k}^{(j+1)k} \eta^{1-\alpha} d\eta$$

$$= \frac{k^{2-\alpha}}{\Gamma(3-\alpha)} \sum_{j=0}^{n} \left(\frac{V_i^{n-j+1} - 2V_i^{n-j} + V_i^{n-j-1}}{k^2} + O(k) \right)$$

$$\times ((j+1)^{2-\alpha} - j^{2-\alpha})$$

$$= \frac{k^{-\alpha}}{\Gamma(3-\alpha)} \sum_{j=0}^{n} (V_i^{n-j+1} - 2V_i^{n-j} + V_i^{n-j-1})((j+1)^{2-\alpha} - j^{2-\alpha})$$

$$+ \frac{k^{2-\alpha}}{\Gamma(3-\alpha)} O(k) \sum_{j=0}^{n} ((j+1)^{2-\alpha} - j^{2-\alpha})$$

$$= \frac{k^{-\alpha}}{\Gamma(3-\alpha)} \sum_{j=0}^{n} (V_i^{n-j+1} - 2V_i^{n-j} + V_i^{n-j-1})((j+1)^{2-\alpha} - j^{2-\alpha})$$

$$+ \frac{k^{2-\alpha}}{\Gamma(3-\alpha)} (n+1)^{2-\alpha} O(k)$$

As $(n+1)k$ is finite, then above formula can be rewritten as

$$\left(\frac{\partial^{\alpha} V}{\partial t^{\alpha}}\right)_{(x_i,\, t_{n+1})} =$$

$$\frac{k^{-\alpha}}{\Gamma(3-\alpha)} \sum_{j=0}^{n} (V_i^{n-j+1} - 2V_i^{n-j} + V_i^{n-j-1})((j+1)^{2-\alpha} - j^{2-\alpha}) + O(k) \qquad (2.1)$$

where

$$b_j = (j+1)^{2-\alpha} - j^{2-\alpha},\ j = 0, 1, 2, \ldots, n$$

We use the right shifted Grunwald formula to discretized the space fractional derivative as follows [8]:

$$\frac{\partial^{\beta} V}{\partial t^{\beta}} = \frac{1}{h^{\beta}} \sum_{l=0}^{i+1} w_l V_{i-l+1}^{n} + O(h) \qquad (2.2)$$

where

$$w_l = \frac{\Gamma}{\Gamma(-\beta)\Gamma(l+1)},\ l = 0, 1, 2, \ldots, M.$$

which called the normalized Grunwald weights. They can be found by the recursive formula:

$$w_0 = 1,\ w_l = w_{l-1}\left(1 - \frac{\beta+1}{l}\right)$$

Now, putting (2.1) and (2.2) in equation (1.1), we obtain the Crank-Nicloson type numerical approximation of space-time fractional traveling wave equation (1.1) as follows:

$$\frac{k^{-\alpha}}{\Gamma(3-\alpha)} \sum_{j=0}^{n} b_j (V_i^{n-j+1} - 2V_i^{n-j} + V_i^{n-j-1}) = C^2 \frac{1}{2h^{\beta}}$$

$$\left[\sum_{l=0}^{i+1} w_l V_{i-l+1}^{n+1} + \sum_{l=0}^{i+1} w_l V_{i-l+1}^{n}\right]$$

$$\sum_{j=0}^{n} b_j(V_i^{n-j+1} - 2V_i^{n-j} + V_i^{n-j-1}) = \frac{C^2\Gamma(3-\alpha)k^\alpha}{2h^\beta}\left[\sum_{l=0}^{i+1} w_l V_{i-l+1}^{n+1} + \sum_{l=0}^{i+1} w_l V_{i-l+1}^{n}\right]$$

We simplify the above equation and obtain

$$V_i^{n+1} - 2V_i^n + V_i^{n-1} + \sum_{j=1}^{n} b_j(V_i^{n-j+1} - 2V_i^{n-j} + V_i^{n-j-1})$$

$$= r\left[\sum_{l=0}^{i+1} w_l V_{i-l+1}^{n+1} + \sum_{l=0}^{i+1} w_l V_{i-l+1}^{n}\right]$$

where $r = \dfrac{C^2\Gamma(3-\alpha)k^\alpha}{2h^\beta}$.

$$V_i^{n+1} - r\sum_{j=1}^{i+1} w_l V_{i-l+1}^{n+1} = 2V_i^n + V_i^{n-1} - \sum_{j=1}^{n} b_j(V_i^{n-j+1} - 2V_i^{n-j} + V_i^{n-j-1})$$

$$+ r\sum_{l=0}^{i+1} w_l V_{i-l+1}^{n} \tag{2.3}$$

The initial conditions are approximated as follows:

$$V(x_i, 0) = f(x_i) \text{ implies } V_i^0 = f(x_i),\ i = 1, 2, \ldots, M-1 \tag{2.4}$$

and

$$\frac{\partial}{\partial t} V(x_i, t_0) = g(x_i) \text{ implies } \frac{V_i^1 - V_i^{-1}}{2k} = g(x_i)$$

$$V_i^{-1} = V_i^1 - 2kg(x_i),\ i = 1, 2, \ldots, M-1. \tag{2.5}$$

Also, the boundary conditions are approximated as follows:

$$V(0, t_n) = 0 \text{ implies } V_0^n = 0,\ n = 1, 2, \ldots, N-1$$

and

$$V(L, t_n) = 0 \text{ implies } V_M^n = 0,\ n = 1, 2, \ldots, N-1$$

We put $n = 0$ in equation (2.3) and using equation (2.5), we obtain

$$V_i^1 - \frac{r}{2}\sum_{l=0}^{i+1} w_l V_{i-l+1}^1 = V_i^0 + kg(x_i) + \frac{r}{2}\sum_{l=0}^{i+1} w_l V_{i-l+1}^0$$

and for $n = 1, 2, \ldots, N-1$, we get

$$V_i^{n+1} - r\sum_{l=0}^{i+1} w_l V_{i-l+1}^{n+1} = 2V_i^n - V_i^{n-1} - \sum_{j=1}^{n-1} b_j (V_i^{n-j+1} - 2V_i^{n-j} + V_i^{n-j-1})$$

$$- 2b_n (V_i^1 - V_i^0 + kg(x_i)) + r\sum_{l=0}^{i+1} w_l V_{i-l+1}^n$$

The complete discretized space-time fractional traveling wave equation with initial and boundary conditions is written as follows:

$$V_i^1 - \frac{r}{2}\sum_{l=0}^{i+1} w_l V_{i-l+1}^1 = V_i^0 + kg(x_i) + \frac{r}{2}\sum_{l=0}^{i+1} w_l V_{i-l+1}^0 \tag{2.6}$$

for $n = 0$,

$$V_i^{n+1} - r\sum_{l=0}^{i+1} w_l V_{i-l+1}^{n+1} = 2V_i^n - V_i^{n-1} - \sum_{j=1}^{n-1} b_j (V_i^{n-j+1} - 2V_i^{n-j} + V_i^{n-j-1})$$

$$- 2b_n (V_i^1 - V_i^0 + kg(x_i)) + r\sum_{l=0}^{i+1} w_l V_{i-l+1}^n, \tag{2.7}$$

initial condition:

$$V_i^0 = f(x_i),\ i = 1, 2, \ldots, M-1 \tag{2.8}$$

boundary conditions:

$$V_i^n = 0,\ V_M^n = 0,\ n = 1, 2, \ldots, N-1 \tag{2.9}$$

The discretized finite difference scheme (2.6)-(2.9) can be written in matrix form as follows:

for $n = 0$,

$$AV^1 = (2I - A)V^0 + F_1 \tag{2.10}$$

for $n \geq 1$,

$$(2A - I)V^{n+1} = ((4 - b_1)I - 2A)V^n + \sum_{j=1}^{n-1}(2b_j - b_{j-1} - b_{j+1})V_i^{n-j}$$

$$- b_n V^1 + (2b_n - b_{n-1})V^0 + 2b_n kg(x_i)I, \tag{2.11}$$

initial condition:

$$V_i^0 = f(x_i),\ i = 1, 2, \ldots, M - 1 \tag{2.12}$$

boundary conditions:

$$V_i^n = 0,\ V_M^n = 0,\ n = 1, 2, \ldots, N - 1 \tag{2.13}$$

where $V^n = [V_1^n, V_2^n, \ldots, V_{M-1}^n]^T$, $F = [kg(x_1), kg(x_2), \ldots, kg(x_{M-1})]^T$, I is an identity matrix of order $(n-1)\times(n-1)$ and matrix A is defined as follows

$$A = (a_{ij})_{(M-1)\times(M-1)} = \begin{cases} 1 - \frac{r}{2}w_1, & j = i \\ -\frac{r}{2}w_0, & j = i+1 \\ -\frac{r}{2}w_{i-j+1}, & j \leq i-1 \\ 0, & j \geq i+2 \end{cases}$$

Lemma 2.1. *The coefficient* b_j, $j = 1, 2, \ldots$ *satisfy*

(i) $b_j > 0$

(ii) $b_j > b_{j+1}$

Lemma 2.2. *Grunwald-Letnikov coefficients* w_l *satisfy*:

(i) $w_0 = 1,\ w_1 = -\beta,\ w_2 = \frac{\beta(\beta-1)}{2}$

(ii) $1 \geq w_2 \geq w_3 \geq \ldots \geq 0$

(iii) $\sum_{l=0}^{n} w_l < 0$, $n \geq 1$.

3. Stability

Let $\bar{V}_i^n$ and V_i^n are exact and approximate solutions of the equation (1.1)-(1.3) respectively and ε_i^n be the error at each mesh point (x_i, t_n), then

$$\varepsilon_i^n = \bar{V}_i^n - V_i^n$$

From equations (2.6)-(2.7), we obtain for $n = 0$,

$$\varepsilon_i^1 - \frac{r}{2}\sum_{l=0}^{i+1} w_l \varepsilon_{i-l+1}^1 = \varepsilon_i^0 + \frac{r}{2}\sum_{l=0}^{i+1} w_l \varepsilon_{i-l+1}^0 \tag{3.1}$$

for $n \geq 1$,

$$\varepsilon_i^{n+1} - r\sum_{l=0}^{i+1} w_l \varepsilon_{i-l+1}^{n+1} = 2\varepsilon_i^n - \varepsilon_i^{n-1} - \sum_{j=1}^{n-1} b_j(\varepsilon_i^{n-j+1} - 2\varepsilon_i^{n-j} + \varepsilon_i^{n-j-1})$$

$$- 2b_n(\varepsilon_i^1 - \varepsilon_i^0) + r\sum_{l=0}^{i+1} w_l \varepsilon_{i-l+1}^n. \tag{3.2}$$

Theorem 3.1. *The solution of Crank-Nicolson finite difference scheme given by* (2.6)-(2.9) *developed for equation* (1.1)-(1.3) *is unconditionally stable.*

Proof. We denote the error vector by $E^n = (\varepsilon_1^n, \varepsilon_2^n, \ldots, \varepsilon_{M-1}^n)^T$ for $0 \leq n \leq N$. Also, we assume that

$$| \varepsilon^n | = \max_{1 \leq i \leq M-1} | \varepsilon_i^n | = \| E^n \|_\infty, \text{ for } n = 0, 1, 2, \ldots, N.$$

Using mathematical induction, we will prove that $\| E^n \|_\infty \leq K_1 \| E^0 \|_\infty$, for $n = 0, 1, 2, \ldots, N$, where K_1 is a positive number independent of h and k. Now, using Lemma (2.2) and equation (3.1), we obtain

$$| \varepsilon_i^1 | \leq | \varepsilon_i^1 | - \frac{r}{2}\sum_{l=0}^{i+1} w_l | \varepsilon_{i-l+1}^1 |$$

$$\leq \mid \varepsilon_i^1 - \frac{r}{2}\sum_{l=0}^{i+1} w_l \varepsilon_{i-l+1}^1 \mid$$

$$\leq \mid \varepsilon_i^0 - \frac{r}{2}\sum_{l=0}^{i+1} w_l \varepsilon_{i-l+1}^0 \mid$$

$$\mid \varepsilon_i^0 \mid + \frac{r}{2}\sum_{l=0}^{i+1} w_l \mid \varepsilon_{i-l+1}^1 \mid \leq \left(1 + \frac{r}{2}\sum_{l=0}^{i+1} w_l\right) \mid \varepsilon^0 \mid \leq K_1 \mid \varepsilon^0 \mid$$

$$\| E^1 \|_\infty \leq K_1 \| E^0 \|_\infty$$

Suppose that

$$\| E^q \|_\infty \leq K_1 \| E^0 \|_\infty,$$

for $q \leq n$ and K_1 is independent of h and k.

Using Lemma (2.2), we have $2 - b_1 > 0$, $b_{j-1} - 2b_j > 0$, $2b_n - b_{n-1} > 0$. Consider,

$$\mid \varepsilon_i^{n+1} \mid \leq \mid \varepsilon_i^{n+1} \mid - r\sum_{l=0}^{i+1} w_l \mid \varepsilon_{i-l+1}^{n+1} \mid$$

$$\leq \mid \varepsilon_i^{n+1} - r\sum_{l=0}^{i+1} w_l \varepsilon_{i-l+1}^{n+1} \mid$$

$$\leq \mid 2\varepsilon_i^n - \varepsilon_i^{n-1} - \sum_{l=0}^{n-1} b_j(\varepsilon_i^{n-j+1} - 2\varepsilon_i^{n-j} + \varepsilon_i^{n-j-1}) - 2b_n(\varepsilon_i^1 - \varepsilon_i^0) + r\sum_{l=0}^{i+1} w_l \varepsilon_{i-l+1}^n \mid$$

$$\leq \mid (2 - b_1)\varepsilon_i^n + \sum_{l=0}^{n-1}(2b_j - b_{j-1} - b_{j+1})\varepsilon_i^{n-j} - b_n\varepsilon_i^1 + (2b_n - b_{n-1})\varepsilon_i^0$$

$$+ r\sum_{l=0}^{i+1} w_l \varepsilon_{i-l+1}^n \mid$$

$$\leq (2-b_1)|\ \varepsilon_i^n\ | + \sum_{j=1}^{n-1}(b_{j-1}+b_{j+1}-2b_j)|\ \varepsilon_i^{n-j}\ | + b_n|\ \varepsilon_i^1\ | + (2b_n-b_{n-1})|\ \varepsilon_i^0\ |$$

$$+ r\sum_{l=0}^{i+1} w_l|\ \varepsilon_{i-l+1}^n\ |$$

$$\leq \left(2-b_1+\sum_{j=1}^{n-1}(b_{j-1}+b_{j+1}-2b_j)+b_n+2b_n-b_{n-1}+r\sum_{l=0}^{i+1}w_l\right)|\ \varepsilon^0\ |$$

$$\leq \left(2(1-b_1)+2(2b_n-b_{n-1})+r\sum_{l=0}^{i+1}w_l\right)|\ \varepsilon^0\ | \leq K_1|\ \varepsilon^0\ |$$

Therefore, $\| E^{n+1} \|_\infty \leq K_1 \| E^0 \|_\infty$, where K_1 is a positive constant independent of h and k. Hence, by mathematical induction, for all $n = 1, 2, \ldots, N$, we have

$$\| E^n \|_\infty \leq K_1 \| E^0 \|_\infty$$

This completes the proof. □

4. Convergence

In this section, we discuss the question of convergence. Let $\overline{V}_i^n$ be the exact solution of space-time fractional traveling wave equation (1.1)-(1.3) and τ_i^n be the local truncation error for $1 \leq i \leq M$. Then, from (2.6)-(2.9), we have

$$\tau_i^1 = \overline{V}_i^1 - \frac{r}{2}\sum_{l=0}^{i+1} w_l \overline{V}_{i-l+1}^1 - \overline{V}_i^0 - kg(x_i) - \frac{r}{2}\sum_{l=0}^{i+1} w_l \overline{V}_{i-l+1}^0 = O(h+k) \tag{4.1}$$

and for $1 \leq n \leq N-1$,

$$\tau_i^{n+1} = \overline{V}_i^{n+1} - r\sum_{l=0}^{i+1} w_l \overline{V}_{i-l+1}^{n+1} - 2\overline{V}_i^n + \overline{V}_i^{n-1} + \sum_{j=1}^{n-1} b_j(\overline{V}_i^{n-j+1} - 2\overline{V}_i^{n-j} + \overline{V}_i^{n-j-1})$$

$$+ 2b_n(\overline{V}_i^1 - \overline{V}_i^0 - kg(x_i)) - r\sum_{l=0}^{i+1} w_l \overline{V}_{i-l+1}^n = O(h+k) \tag{4.2}$$

Theorem 4.1. *Let* $\overline{V}_i^n$ *be the exact solution of* (1.1)-(1.3) *and* $\overline{V}_i^n$ *be the numerical solution of finite difference scheme* (2.6)-(2.9) *at each mesh point* (x_i, t_n). *Then there exist a positive constant* K_2 *independent of h and k such that*

$$\| \overline{V}_i^n - V_i^n \| \leq K_2(h+k), 1 \leq n \leq N.$$

Proof. Let e_i^n be the error at each mesh point (x_i, t_n), then

$$\| e_i^n \| = \| \overline{V}_i^n - V_i^n \|$$

Now, we denote the error vector by $e^n = (e_1^n, e_2^n, \ldots, e_{M-1}^n)^T$ for $1 \leq n \leq N$ and local truncation error vector by $\tau^n = (\tau_1^n, \tau_2^n, \ldots, \tau_{M-1}^n)^T$ for time level n. From equations (4.1)-(4.2), we get

$$e_i^1 - \frac{r}{2}\sum_{l=0}^{i+1} w_l e_{i-l+1}^1 = e_i^0 + \frac{r}{2}\sum_{l=0}^{i+1} w_l e_{i-l+1}^0 + \tau_i^1 \tag{4.3}$$

for $n \geq 1$,

$$e_i^{n+1} - r\sum_{l=0}^{i+1} w_l e_{i-l+1}^{n+1} = 2e_i^n - e_i^{n-1} - \sum_{j=1}^{n-1} b_j(e_i^{n-j+1} - 2e_i^{n-j} + e_i^{n-j-1})$$

$$+ 2b_n(e_i^1 - e_i^0) + r\sum_{l=0}^{i+1} w_l e_{i-l+1}^n + \tau_i^{n+1}. \tag{4.4}$$

Using mathematical induction, we will prove that $\| e^n \|_\infty \leq K_2(h+k)$. For $n = 1$, we have

$$| e_i^1 | \leq | e_i^1 | - \frac{r}{2}\sum_{l=0}^{i+1} w_l | e_{i-l+1}^1 |$$

$$\leq \mid e_i^1 - \frac{r}{2}\sum_{l=0}^{i+1} w_l e_{i-l+1}^1 \mid$$

$$\leq \mid e_i^0 - \frac{r}{2}\sum_{l=0}^{i+1} w_l e_{i-l+1}^0 + \tau_i^1 \mid \leq \left[1 + \frac{r}{2}\sum_{l=0}^{i+1} w_l\right] \mid e_i^0 \mid + \mid \tau_i^1 \mid \leq \mid \tau_i^1 \mid \leq K_2(h+k)$$

Therefore, $\| e^1 \|_\infty \leq K_2(h+k)$, where K_2 is independent of h and k. Suppose that

$$\| e^q \|_\infty \leq K_2(h+k),$$

for $q \leq n$ and K_2 is independent of h and k. Consider,

$$\mid e_i^{n+1} \mid \leq \mid e_i^{n+1} \mid - r\sum_{l=0}^{i+1} w_l \mid e_{i-l+1}^{n+1} \mid$$

$$\leq \mid e_i^{n+1} - r\sum_{l=0}^{i+1} w_l e_{i-l+1}^{n+1} \mid$$

$$\leq \mid 2e_i^n - e_i^{n-1} - \sum_{l=0}^{n-1} b_j(e_i^{n-j+1} - 2e_i^{n-j} + e_i^{n-j-1}) - 2b_n(e_i^1 - e_i^0)$$

$$+ r\sum_{l=0}^{i+1} w_l e_{i-l+1}^n + \tau_i^{n+1} \mid$$

$$\leq \mid (2-b_1)e_i^n + \sum_{l=0}^{n-1}(2b_j - b_{j-1} - b_{j+1})e_i^{n-j} - b_n e_i^1 + (2b_n - b_{n-1})e_i^0$$

$$+ r\sum_{l=0}^{i+1} w_l e_{i-l+1}^n + \tau_i^{n+1} \mid$$

$$\leq (2-b_1) \mid e_i^n \mid + \sum_{j=1}^{n-1}(b_{j-1} + b_{j+1} - 2b_j) \mid e_i^{n-j} \mid + b_n \mid e_i^1 \mid + r\sum_{l=0}^{i+1} w_l \mid e_{i-l+1}^n \mid + \mid \tau_i^{n+1} \mid$$

$$\leq \left(2 - b_1 + \sum_{j=1}^{n-1} (b_{j-1} + b_{j+1} - 2b_j) + b_n + r \sum_{l=0}^{i+1} w_l \right) K_2'(h+k) + | \tau_i^{n+1} |$$

$$\leq \left(2(1 - b_1) + 2(2b_n - b_{n-1}) + r \sum_{l=0}^{i+1} w_l \right) K_2'(h+k) + | \tau_i^{n+1} | \leq K_2(h+k)$$

Therefore, $\| e^{n+1} \|_\infty \leq K_2(h+k)$.

Hence, by mathematical induction, for all $n = 1, 2, \ldots, N,$ we have

$$\| e^n \|_\infty \leq K_2(h+k)$$

This completes the proof. □

5. Python Programme

In this section, we develop the Python programme-CN for Crank-Nicolson finite difference scheme (2.6)-(2.9) to solve space-time fractional traveling wave equation (1.1)-(1.3) numerically. We compute $\overline{V}_i^n$ at each grid point (x_i, t_n) using the scheme (2.6)-(2.9). The algorithm is given below:

1. Compute $V_i^0 = f(x_i)$, $i = 0, 1, 2, \ldots, M$.

2. Compute V_i^1, $i = 0, 1, 2, \ldots, M$.

3. Compute V_i^{n+1}, for each $n = 1, 2, \ldots, N-1$, $i = 0, 1, 2, \ldots, M$.

Now, we develop the Python programme-CN for complete discretized scheme (2.6)-(2.9) as follows:

Inputs:

f - initial displacement

g - initial velocity

C - velocity of wave

L - spatial length

T - end time

h - space step size

k - temporal step size

a - fractional order α of time derivative

b - fractional order β of space derivative

t1 - time level, at which solution has to be estimate

Output of Python programme CN is the approximate value of vector $V(x_i, t1)$.

```
import math
import numpy as np
import scipy.linalg
def CN(f,g,C,T,L,a,b,h,k,t1):
r=(C**2*math.gamma(3-a)*k**a)/(2*h**b)
N=int(round(T/k))
M=int(round(L/h))
t=np.linspace(0,N*k,N+1)
x=np.linspace(0,M*h,M+1)
V=np.zeros((N+1,M+1))
for i in range(0,M+1):
V[0][i]=f(x[i])
A1 = np.zeros((M-1, M-1))
A2 = np.zeros((M-1, M-1))
b1 = np.zeros(M-1)
b2 = np.zeros(M-1)
w = np.zeros(M+1)
w[0]=1
for l in range(1,M+1):
```

```
w[l]=w[l-1]*(1-((1+b)/l))
for i in range(0,M-1):
A1[i][i]=1-(r/2)*w[1]
for i in range(0,M-2):
A1[i][i+1]=-(r/2)*w[0]
for i in range(1,M-1):
for j in range(0,i):
A1[i][j]=-(r/2)*w[i-j+1]
for i in range(1,M):
s=0
for l in range(0,i+2):
s=s+w[l]*V[0][i-l+1]
b1[i-1]=V[0][i]+k*g(x[i])+(r/2)*s
V[1][1:M]=scipy.linalg.solve(A1, b1)
V[1][0]=0;V[1][M]=0
for i in range(0,M-1):
A2[i][i]=1-r*w[1]
for i in range(0,M-2):
A2[i][i+1]=-r*w[0]
for i in range(1,M-1):
for j in range(0,i):
A2[i][j]=-r*w[i-j+1]
for n in range(1,N):
for i in range(1,M):
s1,s2=0,0
for j in range(1,n):
```

```
s1=s1+((j+1)**(2-a)-j**(2-a))*(V[n-j+1][i]-2*V[n-j][i]+V[n-j-1][i])
s1=s1+2*((n+1)**(2-a)-(n)**(2-a))*(V[1][i]-V[0][i]-k*g(x[i]))
for l in range(0,i+2):
s2=s2+w[l]*V[n][i-l+1]
b2[i-1]=2*V[n][i]-V[n-1][i]-s1+r*s2
V[n+1][1:M]=scipy.linalg.solve(A2, b2)
V[n+1][0]=0;V[n+1][M]=0
t1=int(t1/k)
return(x,V[t1])
```

Numerical experiment 1. We consider the following space-time fractional traveling wave equation:

$$\frac{\partial^{\alpha} V}{\partial t^{\alpha}} = C^2 \frac{\partial^{\beta} V}{\partial x^{\beta}}, \ (x, t) \in \Omega = [0, 1] \times [0, 1] \tag{5.1}$$

with initial conditions:

$$V(x, 0) = \sin(2\pi x), \ \frac{\partial}{\partial t} V(x, 0) = 0, \ x \in [0, 1] \tag{5.2}$$

and boundary conditions,

$$V(0, t) = 0, \ V(1, t) = 0, \ t \in (0, 1] \tag{5.3}$$

The exact solution to this problem for $\alpha = 2$, $\beta = 2$ and $C = 1$ as follows:

$$V(x, t) = \sin(2\pi x)\cos(2\pi t)$$

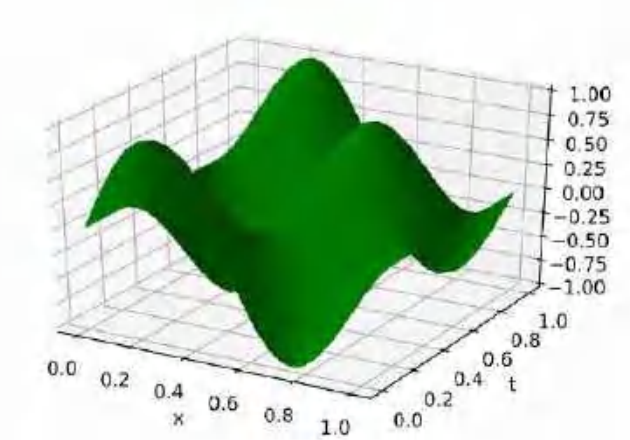

Figure 1. Periodic solution of traveling wave equation.

Using the python programme-CN, we estimate the value of $V(x, t)$ for any time level t_n. Let $\varepsilon(h, k)$ be the maximum error between exact and numerical solutions with temporal and spatial grid sizes k and h respectively. The temporal and spatial order of convergence are computed using

$$\text{temporal order} = \log_2\left(\frac{\varepsilon(h, 2k)}{\varepsilon(h, k)}\right), \quad \text{spatial order} = \log_2\left(\frac{\varepsilon(2h, k)}{\varepsilon(h, k)}\right).$$

In Table 1, we obtain the maximum error and order of convergence in temporal direction at time $t = 1$ with $h = 2^{-10}$.

Table 1. Maximum errors and temporal orders of convergence at $t = 1$, $h = 2^{-10}$.

k	Maximum error	Order
2^{-5}	0.264489	–
2^{-6}	0.142758	0.89
2^{-7}	0.074186	0.94
2^{-8}	0.037816	0.97
2^{-9}	0.019091	0.98
2^{-10}	0.009592	0.99

In Table 2, we obtain the maximum error and order of convergence in spatial direction at

Table 2. Maximum errors and spatial orders of convergence at $x = 0.9999$, $k = 2^{-10}$.

h	Maximum error	Order
2^{-2}	0.999371	–
2^{-3}	0.706478	0.50
2^{-4}	0.382055	0.88
2^{-5}	0.194462	0.97
2^{-6}	0.097388	0.99
2^{-7}	0.048439	1.00

$x = 0.9999$ with $k = 2^{-10}$.

From Table 1 and 2, we observe that the proposed finite difference scheme is first-order accurate in temporal as well as spatial direction. The order of convergence obtained in the numerical results agreed to the theoretical analysis. In Figure 2, we compare the exact and numerical solutions obtained by the Crank-Nicolson scheme and observe that the numerical solution is enormously agreed with the exact solution.

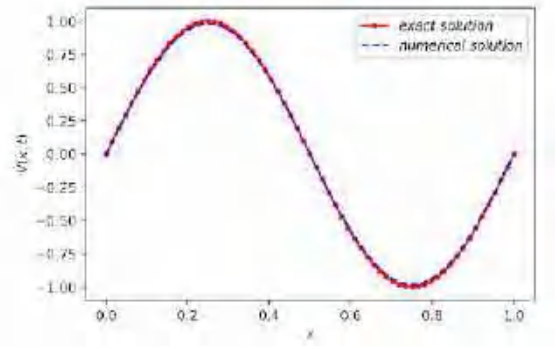

Figure 2. Comparison between exact and the numerical solutions with the parameters $h = 2^{-6}$, $k = 2^{-9}$, $t = 1$, $C = 1$.

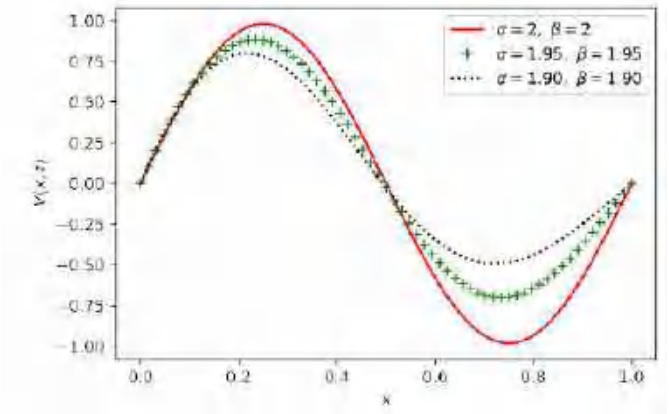

Figure 3. Comparison of the numerical solutions with the parameters $h = 2^{-6}$, $k = 2^{-9}$, $t = 1$, $C = 1$.

From Figure 3, we observed that the obtained solutions are stable and sufficiently approximate to the exact solutions and therefore, we conclude that the proposed scheme gives accurate results and stable solutions. Hence, Python is a powerful tool to obtain the numerical solutions of space-time fractional traveling wave equation.

Numerical experiment 2. We consider the following space-time fractional traveling wave equation:

$$\frac{\partial^{\alpha} V}{\partial t^{\alpha}} = C^2 \frac{\partial^{\beta} V}{\partial t^{\beta}}, (x, t) \in \Omega = [0, 1] \times [0, 1]$$

subject to initial conditions:

$$V(x, 0) = 0, \frac{\partial}{\partial t} V(x, 0) = 2\pi C \sin(2\pi x), x \in (0, 1]$$

and boundary conditions,

$$V(0, t) = 0, V(1, t) = 0, t \in (0, 1]$$

The exact solution to this problem for $\alpha = 2, \beta = 2$ is $V(x, t) = \sin(2\pi x)\sin(2C\pi t)$. In Table 3 and 4, we obtain the order of convergence in temporal and spatial directions respectively.

Table 3. Maximum errors and temporal orders of convergence at $t = 0.75$, $h = 2^{-8}$.

k	Maximum error	Order
2^{-6}	0.106548	–
2^{-7}	0.055491	0.94
2^{-8}	0.028306	0.97
2^{-9}	0.014285	0.98
2^{-10}	0.007166	0.99
2^{-11}	0.003580	1.00

Table 4. Maximum errors and spatial orders of convergence at $x = 0.9999$, $k = 2^{-10}$.

h	Maximum error	Order
2^{-2}	1.107705	–
2^{-3}	0.723289	0.61
2^{-4}	0.383607	0.91
2^{-5}	0.194308	0.98
2^{-6}	0.097193	0.99
2^{-7}	0.048326	1.00

From these tables, it can be seen that the proposed finite difference scheme is first-order accurate in temporal as well as spatial direction.

In Figure 4, we obtain the numerical solutions using proposed finite difference scheme for different values of t for $\alpha = 1.9$, $\beta = 1.8$.

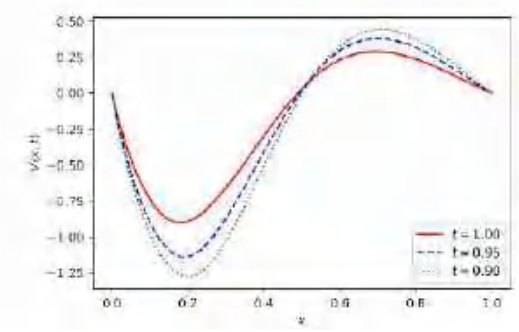

Figure 4. Behavior of the numerical solutions with the parameters $\alpha = 1.9$, $\beta = 1.8$, $h = 2^{-6}$, $k = 2^{-9}$, $C = 1$.

From Figure 4, we observe that solutions obtained by proposed scheme are stable and converges appropriately to the solution obtained at $t = 1$. In Figure 5, we obtain the numerical solutions for different values of α and β at $t = 0.7$.

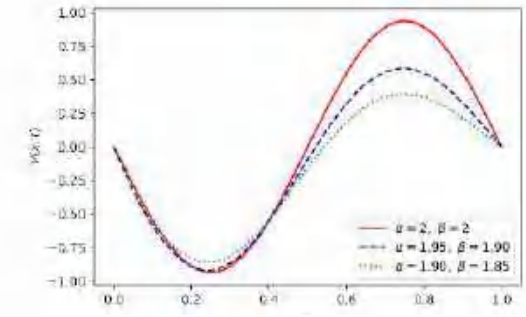

Figure 5. Behavior of the numerical solutions with the parameters $h = 2^{-6}$, $k = 2^{-9}$, $C = 1$, $t = 0.7$.

We observe that solutions obtained by proposed scheme are converges to the solution obtained for $\alpha = 2$, $\beta = 2$.

6. Conclusions

(i) We develop the Crank-Nicolson finite difference scheme for space-time fractional traveling wave equation.

(ii) Furthermore, we proved that the developed scheme is unconditionally stable and convergent.

(iii) We successfully develop a python programme for space-time fractional traveling wave equation and obtain the numerical solutions of the test problems and estimate the error.

(iv) Also, we found that the finite difference scheme is numerically stable and the results are compatible with our theoretical analysis.

(v) Finally, we conclude that Python is a powerful tool for obtaining the numerical solutions of space-time fractional traveling wave equation because the numerical results are very close to the exact solutions.

References

[1] Elham Afshari, Behnam Sepehrian and Ali Mohamad Nazari, Finite difference method for solving the space-time fractional wave equation in the Caputo form, Fractional Differential Calculus 1 (2015), 55-63.

[2] R. Hilfer, Applications of Fractional Calculus in Physics, World Scientific, March 2000.

[3] Suryakant Jogdand, Sharvari Kulkarni and Kalyanrao Takale, On fractional order crank-nicolson finite difference scheme for space-time fractional convection diffusion equation, International Journal of Research and Analytical Reviews 6(1) (2019), 50-55.

[4] Hans Petter Langtangen and Svein Linge, Finite Difference Computing with PDEs: A Modern Software Approach, volume 16 of Texts in Computational Science and Engineering, Springer International Publishing, Cham, 2017.

[5] Jichun Li and Yi-Tung Chen, Computational partial differential equations using MATLAB. 2020. OCLC: 1127853350.

[6] Yuri Luchko, Fractional wave equation and damped waves, Journal of Mathematical Physics 54(3) (2013), 031505.

[7] Sam Morley, Applying math with python: practical recipes for solving computational math problems using Python programming and its libraries, Packt Publishing, Birmingham Mumbai, 2020.

[8] Igor Podlubny, Fractional differential equations: an introduction to fractional derivatives, fractional differential equations, to methods of their solution and some of their applications, Number V. 198 in Mathematics in science and engineering, Academic Press, San Diego, 1999.

[9] Arsen Pskhu and Sergo Rekhviashvili, Fractional Diffusion {Wave Equation with Application in Electrodynamics, Mathematics 8(11) (2020) 20-86.

[10] Fathalla A. Rihan, Numerical Modeling of Fractional-Order Biological Systems, Abstract and Applied Analysis 1 (2013), 1-11.

[11] Enrico Scalas, Rudolf Goreno and Francesco Mainardi, Fractional calculus and continuous-time finance, Physica A: Statistical Mechanics and its Applications 284(1-4) (2000), 376-384.

[12] Karl A. Seeler, Finite Difference Methods and MATLAB, In System Dynamics, Springer New York, New York, NY (2014), 467-517.

[13] G. W. Shrimangale, T. L. Holambe and K. C. Takale, Fractional order crank-nicolson finite difference scheme for time-space fractional radon diffusion equation in charcoal medium, International Journal of Research and Analytical Reviews 6(1) (2019), 831-836.

[14] G. D. Smith, Numerical solution of partial differential equations: finite difference methods, Oxford applied mathematics and computing science series, Clarendon Press; Oxford University Press, Oxford [Oxfordshire] : New York, 3rd ed. edition, 1985.

[15] Roelof J. Stroeker and Johan F. Kaashoek, Discovering Mathematics with Maple, Birkhauser Basel, Basel, 1999.

[16] K. C. Takale, V. R. Nikam and S. R. Kulkarni, Fractional order finite difference scheme for space fractional diffusion equation, Engineering and Automation Problems 3 (2014), 120-124.

[17] Yanfei Wang, Yaxin Ning and Yibo Wang, Fractional Time Derivative Seismic Wave Equation Modeling for Natural Gas Hydrate, Energies 13(22) (2020), 5901.

[18] Abdul-Majid Wazwaz, Partial differential equations and solitary waves theory, Nonlinear physical science, Higher Education Press Springer, Beijing Berlin, 2009.

Available online at http://scik.org
J. Math. Comput. Sci. 11 (2021), No. 6, 7805-7820
https://doi.org/10.28919/jmcs/6610
ISSN: 1927-5307

NUMERICAL SOLUTION OF STOCHASTIC TIME FRACTIONAL HEAT TRANSFER EQUATION WITH ADDITIVE NOISE

ARCHANA MOURYA[1,*], KALYANRAO TAKALE[2], SHRIKISAN GAIKWAD[3]

[1]Department of Applied Science and Maths, K. K. Wagh Institute of Engg. Edu. and Research Nashik, India
[2]Department of Mathematics, RNC Arts, JDB Commerce and NSC Science College, Nashik-Road, Nashik, India
[3]Department of Mathematics, New Arts, Commerce and Science College, Ahmednagar, India

Abstract. In the present paper, we developed an explicit finite difference scheme for stochastic time fractional heat transfer equation. Furthermore, we proved the conditional stability of the solution of the scheme and analyze the effect of the multiplier of the random noise in mean square stability. Also, we discuss the convergence of the explicit scheme in the mean square sense. The approximate solution of the practical problem is obtain by developed scheme and it is represented graphically by Mathematica software.

Keywords: fractional derivative; time fractional; stochastic heat equation; explicit scheme; stability; mean square.
2010 AMS Subject Classification: 34K37, 65M30, 35R60.

1. INTRODUCTION

Stochastic partial differential equations are very useful in describing random effects occuruing in the fields of science, engineering and mathematical finance. Several numerical methods have been developed to solve stochasstic partial differential equations (SPDEs), Allen [2] has constructed finite element and difference approximation of some linear SPDEs. Kamrani and

*Corresponding author
E-mail address: archana1704@gmail.com
Received August 07, 2021

Hosseini [9] discussed explicite and implicit finite difference methods and their stability convergence for general SPDEs. Furthermore, Soheili et al. [29] presented higher order finite difference scheme and Saul'yev scheme for solving linear parabolic SPDEs.

Now a days, fractional calculus is a developing branch of mathematics which deals with the derivative and integrals of non-integer order and attracted lots of attention in several fields such as physics, chemistry, engineering, hydrology and finance. Recently, fractional diffusion equations are becoming more popular in many areas of applications [11, 14, 23, 27, 37] and stochastic fractional partial differential equations[1, 36] etc. Stochastic partial differential equations with fractional time derivative can be used to describe random effects on transport of particles in medium with thermal memory or particles subjected to sticking and trapping [4]. The theoretical analysis of fractional stochastic partial differential equations have been intensively investigated in the literature [4, 15, 16], also, Sweilam et al. [31] presented compact finite difference method to solve stochastic fractional advection diffusion equation. Amaneh et al [3] introduced stochastic generalized fractional diffusion equation and used finite difference method for finding numerical solution. Chen et al [4] introduced a class of SPDEs with time fractional derivatives and proved existence and uniqueness of their solutions.

The classical heat equation deals with heat propagation in homogeneous medium and the time fractional diffusion equation has been widely used to model the anomalous diffusion exhibiting sub diffusive behavior due to particle sticking and trapping phenomena [13]. When noise is introduced in partial differential equations, turns it to SPDEs. According to the nature of the noise term there are two main classes of SPDEs like SPDEs with additive noise and SPDEs with multiplicative noise. In additive SPDEs, noise term does not depends on the state of the system, while the noise term depends on the state of the system in multiplicative SPDEs. Additive noise occurs due to temporal fluctuations of internal degrees of freedom, while multiplicative noise arrives due to random variations of some external control parameters [8]. Fractional stochastic partial differential equation considers both memory and environmental noise effect. Now a days, Liu et al [36] studied some properties of a class of fractional stochastic heat equations. Babaei et al [1] applied a spectral collection method to solve a class of time fractional heat equation driven by Brownian motion. Guang-an Zou [6] presented a Galerkin finite element

method for time fractional stochastic heat equation driven by multiplicative noise. Stochastic fractional heat equations driven by additive noise are yet to be investigated. At the same time, it is very difficult to find exact solution of stochastic fractional heat equations by analytical methods but finite difference methods that gives large algebraic system to solve in place of differential equation. In this connection, the theme of this paper is to develop a fractional order explicit finite difference scheme for stochastic time fractional heat transfer equation (STFHTE) driven by additive noise with initial and boundary conditions, given as follows,

$$\frac{\partial^{\alpha} S(x,t)}{\partial t^{\alpha}} = D\frac{\partial^2 S(x,t)}{\partial x^2} + \sigma \dot{W}(t);\ (x,t) \in \Omega : [0,L] \times [0,T]$$

$$Initial\ condition:\ S(x,0) = S_0(x),\ 0 \leq x \leq L$$

$$Boundary\ conditions:\ S(0,t) = S(L,t) = 0,\ x \to \infty,\ t \geq 0$$

where, $D > 0$ is the diffusivity constant, $\sigma > 0$ is the constant noise intensity, i.e.additive noise. Now, $W(t)$ is one dimensional standard Winner process, where $\dot{W}(t) = \frac{\partial W(t)}{\partial t}$, such that white noise $\Delta W(t)$ is a random variable generated from Gaussian distribution with zero mean and standard deviation Δt and S(x,t) is temperature at the position x and at time t. Here, $\frac{\partial^{\alpha} S(x,t)}{\partial t^{\alpha}}$ is Caputo time fractional derivative of order α. We consider the following definitions for further developments.

Definition 1.1. *The Caputo time fractional derivative of order* α, $(0 < \alpha \leq 1)$ *is defined as follows* [22]

$$\frac{\partial^{\alpha} S(x,t)}{\partial t^{\alpha}} = \begin{cases} \frac{1}{\Gamma 1-\alpha} \int_0^t \frac{\partial S(x,t)}{\partial \xi} \frac{d\xi}{(t-\xi)^{\alpha}}, & 0 < \alpha < 1 \\ \frac{\partial S(x,t)}{\partial t}, & \alpha = 1 \end{cases}$$

where $\Gamma(.)$ is a Gamma function.

Definition 1.2. ***Euler-Maruyama Scheme:***

For the d-dimensional Stochastic differential equation of Itó type [25]

$$\begin{cases} dS(t) = f(t,S(t))dt + g(t,S(t))dW(t), t \geq 0 \\ S(0) = S_0 \in R^d, \end{cases}$$

where $f, g : R^d \to R^d$, the Euler-Maruyama Scheme for computing approximations S_i^k takes the form

$$S_i^{k+1} = S_i^k + f(S_i^k)\Delta t + g(S_i^k)\Delta W_k,$$

where

$$\Delta W^k = W(t_{k+1} - W(t_k) = W((k+1)\Delta t) - W(k\Delta t)$$

and $\Delta W^k \sim \mathcal{N}(0, \Delta t)$.

Definition 1.3. *A sequence of random variables $\{X_{n_k}\}$, $(n, k > 0)$ converges in mean square to random variable X if $\lim_{n_k \to \infty} ||X_{n_k} - X|| = 0$* [30].

Definition 1.4. *A Stochastic difference scheme is stable in mean square if there are positive constants ε, δ and constants k, b such that* [30]

$$E|S_i^{k+1}|^2 \leq ke^{bt}|S^0|^2$$

for all $0 \leq t = (k+1)\Delta t$, $0 \leq \Delta x \leq \varepsilon$ and $0 \leq \Delta t \leq \delta$.

Definition 1.5. *A Stochastic difference scheme $L_i^k S_i^k = G_i^k$ approximating Stochastic partial differential equation $L_v = G$ is convergent in mean square at time $t = (k+1)\Delta t$ if*

$$E|S_i^k - S|^2 \to 0,$$

as $i \to \infty$, $n \to \infty$, $(\Delta x, \Delta t) \to (0,0)$ and $(i\Delta x, k\Delta t) \to (x,t)$ [30].

Definition 1.6. *The symmetric second order difference quotient in space at time level $t = t_k$ is given as follows* [28]

$$\frac{\partial^2 S(x,t)}{\partial x^2} = \frac{S(x_{i-1}, t_k) - 2S(x_i, t_k) + S(x_{i+1}, t_k)}{h^2}$$

We organize the paper as follows: In section 2 , we develop the explicit fractional order finite difference scheme for Stochastic time fractional heat transfer equation. The stability of the solution is proved in section 3 and section 4 deals with convergence of the scheme. Finally, in the last section, the numerical solutions of Stochastic time fractional heat transfer equation is obtained and simulated graphically by Mathematica.

2. FINITE DIFFERENCE SCHEME

We consider the following Stochastic time fractional heat transfer equation driven by additive noise (STFHTE) with initial and boundary conditions

$$\frac{\partial^\alpha S(x,t)}{\partial t^\alpha} = D\frac{\partial^2 S(x,t)}{\partial x^2} + \sigma\dot{W}(t);\ (x,t) \in \Omega : [0,L]\times[0,T] \tag{1}$$

$$\textit{Initial condition}:\ S(x,0) = S_0(x),\ 0 \le x \le L \tag{2}$$

$$\textit{Boundary conditions}:\ S(0,t) = S(L,t) = 0,\ t \ge 0 \tag{3}$$

where, $D > 0$ is the diffusivity constant, $\sigma > 0$ is the constant noise intensity, i.e.additive noise. Now, $W(t)$ is one dimensional standard Winner process, where $\dot{W}(t) = \frac{\partial W(t)}{\partial t}$, such that white noise $\Delta W(t)$ is a random variable generated from Gaussian distribution with zero mean and standard deviation Δt. Note that for $\alpha = 1$, we recover in the limit the well known Stochastic heat transfer equation of Markovian process

$$\frac{\partial S(x,t)}{\partial t} = D\frac{\partial^2 S(x,t)}{\partial x^2} + \sigma\dot{W}(t),\ x \in R;\ t \ge 0.$$

For the numerical approximation of the explicit scheme, we define $h = \frac{L}{N}$ and $\tau = \frac{T}{N}$ the space and time steps respectively, such that $t_k = k\tau$; $k = 0,1,\cdots,N$ be the integration time $0 \le t_k \le T$ and $x_i = ih$ for $i = 0,1,\cdots,N$. Define $S_i^k = S(x_i,t_k)$ and let S_i^k denote the numerical approximation at the mesh point (x_i,t_k) to the exact solution $S(x_i,t_k)$.

The time fractional derivative $\frac{\partial^\alpha S(x,t)}{\partial t^\alpha}$ at the mesh point (x_i,t_{k+1}), $i = 1,2,\cdots N-1$, $k = 0,1,2,\cdots$. is approximated as follows

$$\begin{aligned}\frac{\partial^\alpha S(x_i,t_{k+1})}{\partial t^\alpha} &\approx \frac{1}{\Gamma(1-\alpha)}\int_0^{t_{k+1}} \frac{1}{(t_{k+1}-\xi)^\alpha}\frac{\partial S(x_i,\xi)}{\partial \xi}d\xi \\ &= \frac{1}{\Gamma(1-\alpha)}\sum_{j=0}^{k}\frac{S(x_i,t_{j+1}) - S(x_i,t_j)}{\tau}\int_{j\tau}^{(j+1)\tau}\frac{d\xi}{(t_{k+1}-\xi)^\alpha} \\ &= \frac{1}{\Gamma(1-\alpha)}\sum_{j=0}^{k}\frac{S(x_i,t_{j+1}) - S(x_i,t_j)}{\tau}\int_{(k-j)\tau}^{(k+1-j)\tau}\frac{d\eta}{\eta^\alpha}\end{aligned}$$

$$= \frac{1}{\Gamma(1-\alpha)} \sum_{j=0}^{k} \frac{S(x_i, t_{k+1-j}) - S(x_i, t_{k-j})}{\tau} \int_{(j)\tau}^{(j+1)\tau} \frac{d\eta}{\eta^{\alpha}}$$

$$= \frac{\tau^{1-\alpha}}{\Gamma(2-\alpha)} \sum_{j=0}^{k} \frac{S(x_i, t_{k+1-j}) - S(x_i, t_{k-j})}{\tau} \times [(j+1)^{1-\alpha} - j^{1-\alpha}]$$

(4)
$$\frac{\partial^{\alpha} S(x_i, t_{k+1})}{\partial t^{\alpha}} = \frac{\tau^{-\alpha}}{\Gamma(2-\alpha)} [S(x_i, t_{k+1}) - S(x_i, t_k)] + \frac{\tau^{-\alpha}}{\Gamma(2-\alpha)} \sum_{j=1}^{k} b_j [S(x_i, t_{k+1-j}) - S(x_i, t_{k-j})]$$

where $b_j = (j+1)^{1-\alpha} - j^{1-\alpha},\ j = 0, 1, 2, \cdots, k.$

We adopt a symmetric second order difference quotient in space at time level $t = t_k$ for approximating the second order space derivative,

$$\frac{\partial^2 S(x,t)}{\partial x^2} = \frac{S(x_{i-1}, t_k) - 2S(x_i, t_k) + S(x_{i+1}, t_k)}{h^2}. \tag{5}$$

Therefore, from equations , (4) and (5), we approximated the Stochastic fractional heat transfer equation (1) as follows

$$\frac{\tau^{-\alpha}}{\Gamma(2-\alpha)} [S_i^{k+1} - S_i^k] + \frac{\tau^{-\alpha}}{\Gamma(2-\alpha)} \sum_{j=1}^{k} b_j [S_i^{k-j+1} - S_i^{k-j})]$$

$$= D \frac{[S(x_{i-1}, t_k) - 2S(x_i, t_k) + S(x_{i+1}, t_k)]}{h^2} + \sigma \frac{W((k+1)\tau) - W(k\tau)}{\tau} \tag{6}$$

After simplification, we get

$$S_i^{k+1} = rS_{i-1}^k + (1 - 2r - b_1) S_i^k + rS_{i+1}^k + \sum_{j=1}^{k-1} (b_j - b_{j+1}) S_i^{k-j}$$

$$+ b_k S_i^0 + a \left[\frac{W((k+1)\tau) - W(k\tau)}{\tau} \right] \tag{7}$$

where $i = 1, 2, \cdots, N-1,\ k = 0, 1, 2, \cdots.,\ r = \frac{D\,\tau^{\alpha}\Gamma(2-\alpha)}{h^2},\ a = \sigma\tau^{\alpha}\Gamma(2-\alpha)$ and $b_j = (j+1)^{1-\alpha} - j^{1-\alpha},\ j = 1, 2, \cdots k.$

The initial condition is approximated as $S_i^0 = S_0,\ i = 1, 2, \cdots, N-1.$

The boundary conditions are approximated as $S_0^k = 0,\ S_N^k = 0,\ k = 0, 1, 2, \cdots, N-1.$

$$S_i^{k+1} = rS_{i-1}^k + (1 - 2r - b_1) S_i^k + rS_{i+1}^k + \sum_{j=1}^{k-1} (b_j - b_{j+1}) S_i^{k-j} + b_k S_i^0 + aW^k \tag{8}$$

where, $W^k \sim \sqrt{k\tau}\,\mathcal{N}(0,1)$, $k = 0,1,2,\cdots N-1$.

Therefore, the complete discretization of STFHTE with initial and boundary conditions is

$$S_i^1 = rS_{i-1}^0 + (1-2r)S_i^0 + rS_{i+1}^0 \; for\, k = 0 \tag{9}$$

$$S_i^{k+1} = rS_{i-1}^k + (1-2r-b_1)S_i^k + rS_{i+1}^k + \sum_{j=1}^{k-1}(b_j - b_{j+1})S_i^{k-j} + b_k S_i^0 + aW^k,\; for\, k \geq 1 \tag{10}$$

$$\text{Initial condition: } S_i^0 = S_0, i = 1,2,\cdots,N-1. \tag{11}$$

$$\text{Boundary conditions: } S_0^k = 0 \; and \; S_N^k = 0. \tag{12}$$

where $r = \frac{D\,\tau^\alpha \Gamma(2-\alpha)}{h^2}$, $a = \sigma\tau^\alpha\Gamma(2-\alpha)$ and $b_j = (j+1)^{1-\alpha} - j^{1-\alpha}$, $j = 0,1,2,\cdots,k$.

Therefore, the fractional approximated IBVP $(9)-(12)$ can be written in the following matrix equation form

$$S^1 = BS^0,\; for\, k = 0 \tag{13}$$

$$S^{k+1} = AS^k + \sum_{j=1}^{k-1}(b_j - b_{j+1})S^{k-j} + b_k S^0 + + aW^k,\; for\, k \geq 1 \tag{14}$$

where $S^k = (S_1^k, S_2^k, ..., S_{N-1}^k)^T$, $k = 0,1,2...,N-1$, A and B are tri-diagonal matrices of order $N-1$ given by

$$A = \begin{pmatrix} (1-2r-b_1) & r & 0 & 0\cdots & 0 & 0 & 0 \\ r & (1-2r-b_1) & r & 0\cdots & 0 & 0 & 0 \\ 0 & r & (1-2r-b_1) & r\cdots & 0 & 0 & 0 \\ \vdots & \vdots & \vdots & \vdots\ddots & \vdots & \vdots & \vdots \\ \vdots & \vdots & \vdots & \vdots\ddots & \vdots & \vdots & \vdots \\ 0 & 0 & \cdots & 0\cdots & r & (1-2r-b_1) & r \\ 0 & 0 & \cdots & 0\cdots & 0 & r & (1-2r-b_1) \end{pmatrix}$$

$$B = \begin{pmatrix} (1-2r) & r & 0 & 0\cdots & 0 & 0 & 0 \\ r & (1-2r) & r & 0\cdots & 0 & 0 & 0 \\ 0 & r & (1-2r) & r\cdots & 0 & 0 & 0 \\ \vdots & \vdots & \vdots & \vdots\ddots & \vdots & \vdots & \vdots \\ \vdots & \vdots & \vdots & \vdots\ddots & \vdots & \vdots & \vdots \\ 0 & 0 & \cdots & 0\cdots & r & (1-2r) & r \\ 0 & 0 & \cdots & 0\cdots & 0 & r & (1-2r) \end{pmatrix}.$$

3. STABILITY

In the present section, we discuss the stability of the solution of fractional order explicit finite difference scheme $(9)-(12)$ for the Stochastic time fractional heat transfer equation $(1)-(3)$.

Theorem 3.1. *The solution of stochastic time fractional heat transfer equation* $(1)-(3)$ *obtained by developed fractional order explicit finite difference scheme* $(9)-(12)$ *is conditionally stable in mean square sense, when* $r \leq \min\left\{ \frac{1}{2}, \frac{1-b_1}{2} \right\}, 0 \leq b_1 \leq 1$.

Proof: Proof: We define $E|S^k|^2 = \sup_{1\leq i\leq N-1} E|S_i^k|^2$, where $S^k = (S_1^k,\ S_2^k,\ S_3^k \cdots,\ S_{N-1}^k)^T$.
Then equation (9) leads to

$$\begin{aligned} E|S_i^k| &= E|rS_{i-1}^0 + (1-2r)S_i^0 + rS_{i+1}^0|^2 \\ &\leq |r+(1-2r)+r|^2 \sup_{1\leq i\leq N-1} E|S_i^0|^2, (\text{when}\, 1-2r \geq 0 \Rightarrow r \leq \frac{1}{2}) \\ \therefore E|S_i^1|^2 &\leq KE|S^0|^2, \text{ when } r \leq \frac{1}{2}. \end{aligned}$$

We assume that

$$E|S_i^k|^2 \leq KE|S^0|^2,\ \forall n \leq k.$$

Then we prove

$$E|S_i^{k+1}|^2 \leq KE|S^0|^2 \,\text{for}\, n = k+1.$$

From equation (10), we obtain

$$E\left|S_i^{k+1}\right|^2 = E\left|rS_{i-1}^k + (1-2r-b_1)S_i^k + rS_{i+1}^k + \sum_{j=1}^{k-1}(b_j - b_{j+1})S_i^{k-j} + b_k S_i^0 + aW^k\right|^2$$

$$E\left|S_i^{k+1}\right|^2 \leq E\left|rS_{i-1}^k + (1-2r-b_1)S_i^k + rS_{i+1}^k + \sum_{j=1}^{k-1}(b_j - b_{j+1})S_i^{k-j} + b_k S_i^0 + a\sqrt{\Delta t}V_n\right|^2$$

when $(1-2r-b_1) \geq 0 \Rightarrow r \leq \frac{1-b_1}{2}$, where $V_n \sim \mathcal{N}(0,1)$ and V_n is Normally distributed with mean 0 and variance 1 i.e. $\mathcal{N}(0,1)$ random variable.

We know that $E[V_n] = 0$ and $E[V_n^2] = 1$, therefore,

$$\begin{aligned}
E|S_i^{k+1}|^2 &\leq |r + (1-2r-b_1) + r + (b_1 - b_2 + b_2 - b_3 + \cdots + (b_{k-1} - b_k) + b_k|^2 \sup_{1\leq i\leq N-1} E|S_i^k|^2 \\
&\quad + (a^2\Delta t) \sup_{1\leq i\leq N-1} E|S_i^0|^2 \\
&\leq \sup_{1\leq i\leq N-1} E|S_i^k|^2 + a^2\Delta t \sup_{1\leq i\leq N-1} E|S_i^0|^2 \\
&\leq (1+a^2\Delta t) \sup_{1\leq i\leq N-1} E|S_i^0|^2 \\
&\leq K \sup_{1\leq i\leq N-1} E|S_i^0|^2, \text{ where } K = (1+a^2\Delta t). \\
&\leq KE|S^0|^2, \text{ where } K = (1+a^2\Delta t).
\end{aligned}$$

Hence, by induction, we prove

$$E|S_i^k|^2 \leq KE|S^0|^2, \ \forall n, K = (1+a^2\Delta t), \text{ when } r \leq \min\left\{\ \tfrac{1}{2}, \tfrac{1-b_1}{2}\ \right\}, 0 \leq b_1 \leq 1.$$

Therefore, we prove that the solution of the scheme is conditionally stable in mean square sense.

4. CONVERGENCE

In the present section, we discuss convergence of the fractional order explicit finite difference scheme $(9)-(12)$ developed for the STFHTE $(1)-(3)$.

Theorem 4.1. *The fractional order explicit finite difference scheme* $(9)-(12)$ *for stochastic time fractional heat transfer equation* $(1)-(3)$ *is convergent in mean square sense with* $r \leq \min\left\{\frac{1}{2}, \frac{1-b_1}{2}\right\}$.

Proof: Let $\bar{S}^k = \left(\bar{S}_1^k, \bar{S}_2^k, \bar{S}_3^k, \cdots, \bar{S}_{N-1}^k\right)^T$ and $S^k = \left(S_1^k, S_2^k, S_3^k, \cdots, S_{N-1}^k\right)^T$ be the vectors of exact solution and approximate solution of the STFHET $(1)-(3)$ respectively. Then the fractional order explicit finite difference scheme $(9)-(12)$ becomes

$$\bar{S}_i^{k+1} = r\bar{S}_{i-1}^k + (1-2r-b_1)\bar{S}_i^k + r\bar{S}_{i+1}^k + \sum_{j=1}^{k-1}(b_j - b_{j+1})\bar{S}_i^{k-j} + b_k\bar{S}_i^0 + aW^k + T^k \tag{15}$$

where T^k is vector of truncation error at time level t_k. Suppose, $|e_i^k| = |\bar{S}_i^k - S_i^k|$ is the error vector. Let us assume that

$$E|e_l^k|^2 = \max_{1\le i\le N-1} E|e_i^k|^2 = ||E^{*^k}||_\infty^2 \text{ and } T_l^k = \max_{1\le i\le N-1}|T_i^k| = h^2O\big(\tau+h^2\big) \text{for } l = 1,2,3,\cdots$$

For k=0, from equation (9), we obtain

$$\begin{aligned}
E|e_l^1|^2 &= E|re_{i-1}^0 + (1-2r)e_i^0 + re_{i+1}^0|^2 + r|\tau_i^1| \\
&\le |r+(1-2r)+r|^2E|e_l^0|^2 + r|\tau_l^1| \ \ (\text{when } 1-2r\ge 0 \Rightarrow r\le \frac{1}{2}) \\
&\le E|e_l^0|^2 + r|\tau_l^1| \\
&\le E|e_l^0|^2 + r|\tau_l^1| \\
&\le E|e_l^0|^2 + rh^2O(\tau+h^2) \\
\therefore E\|E^{*^1}\|_\infty^2 &\le E\|E^{*^0}\|_\infty^2 + \tau^\alpha\Gamma(2-\alpha)O(\tau+h^2)
\end{aligned}$$

For $n=k$, we assume that

$$E\|E^{*^k}\|_\infty^2 \le E\|E^{*^0}\|_\infty^2 + k\tau^\alpha\Gamma(2-\alpha)O(\tau+h^2).$$

For $n=k+1$, we prove that

$$E\|E^{*^{k+1}}\|_\infty^2 \le E\|E^{*^0}\|_\infty^2 + (k+1)\tau^\alpha\Gamma(2-\alpha)O(\tau+h^2).$$

Now, from (10), we have

$$
\begin{aligned}
E\|e_l^{k+1}\|^2 &= E|re_{i-1}^k + (1-2r-b_1)e_i^k + re_{i+1}^k + \sum_{j=1}^{k-1}(b_j - b_{j+1})e_i^{k-j} + b_k e_i^0|^2 + r|\tau_l^k| \\
&\leq |r + (1-2r-b_1) + r + (b_1 - b_2 + b_2 - b_3 + \cdots + b_{k-1} + b_k) \\
&\qquad + b_k|^2 E|e_l^k|^2 + r|\tau_l^k| \qquad (when\ 1-2r-b_1 \geq 0 \Rightarrow r \leq \frac{1-b_1}{2}) \\
&\leq E|e_l^k|^2 + r|\tau_l^k| \\
&\leq E\|E^{*^k}\|_\infty^2 + r|\tau_l^k| \\
&\leq \left(E\|E^{*^0}\|_\infty^2 + k\tau^2\Gamma(2-\alpha)O(\tau+h^1)\right) + \tau^\alpha\Gamma(2-\alpha)O(\tau+h^2) \\
&\leq E\|E^{*^0}\|_\infty^2 + (k+1)\tau^\alpha\Gamma(2-\alpha)O(\tau+h^2) \\
\therefore E\|E^{*^{k+1}}\|_\infty^2 &\leq E\|E^{*^0}\|_\infty^2 + (k+1)\tau^\alpha\Gamma(2-\alpha)O(\tau+h^2).
\end{aligned}
$$

Therefore, we conclude that $E|\bar{S}_i^k - S_i^k|^2 \to 0$ as $(h,\tau) \to (0,0)$ when $r \leq \min\left\{\frac{1}{2}, \frac{1-b_1}{2}\right\}$. Hence, we prove that the scheme is conditionally convergent in mean square sense. This completes the proof.

5. NUMERICAL SOLUTIONS

We consider the following stochastic time fractional heat transfer equation with initial and boundary conditions

$$\frac{\partial^\alpha S}{\partial t^\alpha} = \frac{\partial^2 S}{\partial x^2} + \sigma\dot{W}(t), 0 < x < 1, 0 < t < 1 \tag{16}$$

$$\text{initial condition: } S(x,0) = \sin\pi x,\ 0 \leq x \leq 1 \tag{17}$$

$$\text{boundary conditions: } S(0,t) = S(1,t) = 0, t \geq 0. \tag{18}$$

where $0 < \alpha \leq 1$, $\sigma > 0$ is the constant noise intensity. Now, $W(t)$ is one dimensional standard Winner process, where $\dot{W}(t) = \frac{\partial W(t)}{\partial t}$, such that white noise $\Delta W(t)$ is a random variable generated from Gaussian distribution with zero mean and standard deviation Δt. In Figure 1, we plot the exact solution of stochastic heat transfer equation in absence of noise term.

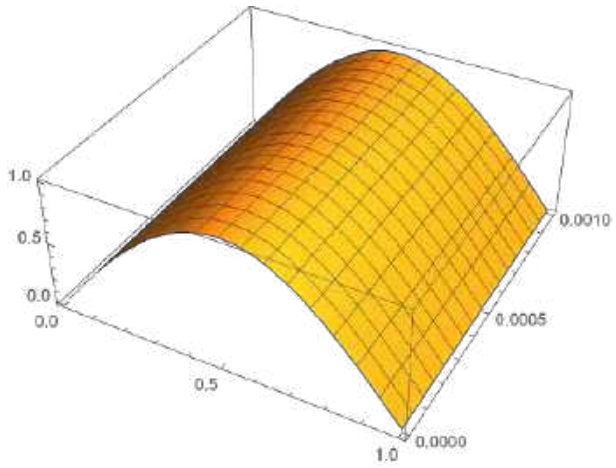

FIGURE 1. The exact solution of Stochastic heat transfer equation $(5.1)-(5.3)$ without noise.

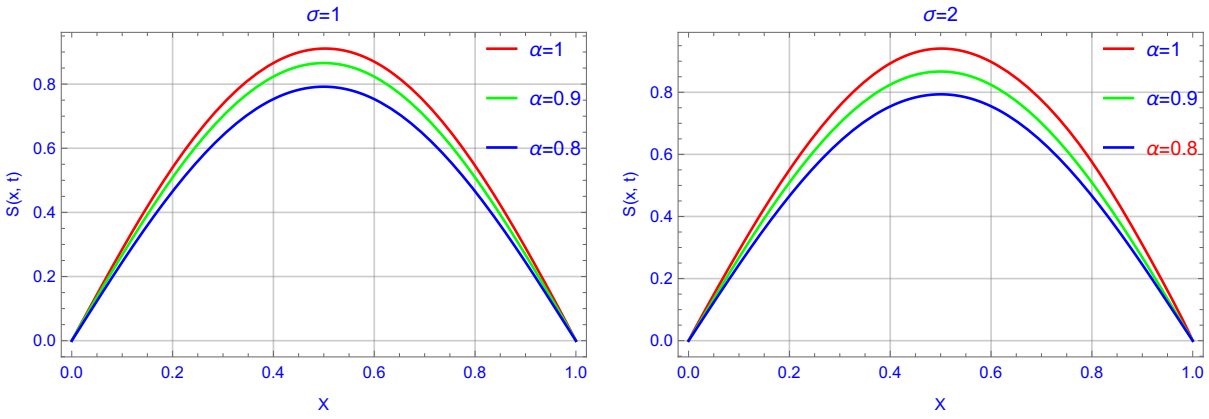

(A) σ=1 (B) σ=2

FIGURE 2. Approximation solution of the STFHTE with constant noise intensity $\sigma = 1,2$ and the parameters $\alpha = 1,0.9,0.8$ respectively.

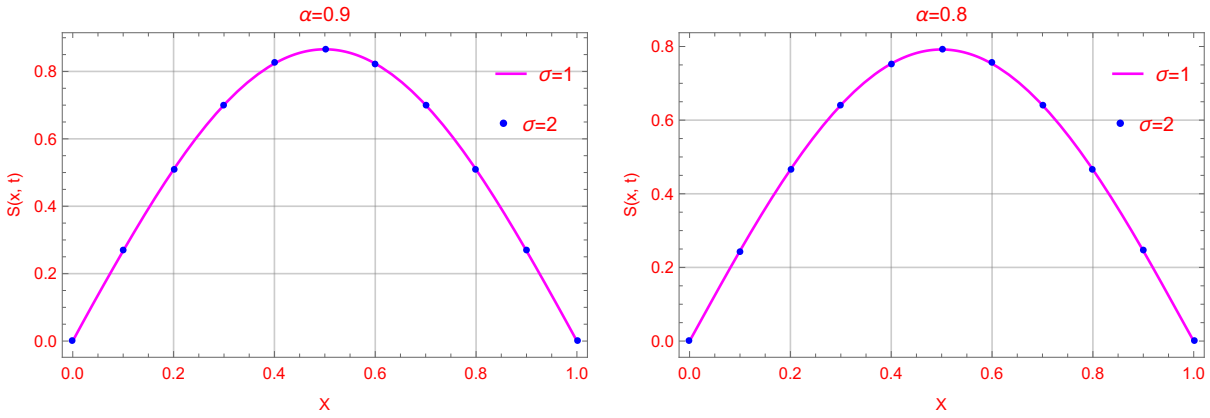

(A) α=0.9 (B) α=0.8

FIGURE 3. Comparison of approximation solution of the STFHTE with constant noise intensity $\sigma = 1,2$ and the parameters $\alpha = 0.9, 0.8$ respectively.

In Figure 2, we obtain the numerical solution of the STFHTE (5.1)-(5.3) for $\alpha = 1, 0.9, 0.8$ with additive noise $\sigma = 1,2$ respectively and observed that these solutions are good approximation to the exact solutions. Therefore the developed fractional order explicit finite difference scheme provides a effective approximate solution. We observed that as α increased the amplitude of the solution behavior is increased. From Figure 3, we observed that the approximate solutions of STFHTE (5.1)-(5.3) for $\alpha = 0.8$ and $\alpha = 0.9$ with $\sigma = 1,2$ are approximately same. Therefore we conclude that if the additive noise intensity changes the numerical solutions are approximately same.

6. CONCLUSIONS

(1) In present paper, we successfully developed the fractional order explicit finite difference scheme for Stochastic time fractional heat transfer equation.

(2) The stability and consistency of the scheme are investigated for Stochastic time fractional heat transfer equation in mean square sense and the bound of stability is $r \leq \min\left\{\frac{1}{2}, \frac{1-b_1}{2}\right\}$, where $0 \leq b_1 \leq 1$.

(3) The numerical examples with plots of the results are given to demonstrate the efficiency of the scheme. It has been observed that the numerical scheme is very powerful and provide approximate solution which is very near to the exact solution.

CONFLICT OF INTERESTS

The author(s) declare that there is no conflict of interests.

REFERENCES

[1] A. Babaei, H. Jafari, S. Banihashemi, A Collocation Approach for Solving Time-Fractional Stochastic Heat Equation Driven by an Additive Noise, Symmetry. 12 (2020), 904.

[2] E.J. Allen, S.J. Novosel, Z. Zhang, Finite element and difference approximation of some linear stochastic partial differential equations, Stoch. Stoch. Rep. 64 (1998), 117–142.

[3] A. Sepahvandzadeh, B. Ghazanfari, N. Asadian, Numerical Solution of Stochastic Generalized Fractional Diffusion Equation by Finite Difference Method, Math. Comput. Appl. 23 (2018), 53.

[4] Z.-Q. Chen, K.-H. Kim, P. Kim, Fractional time stochastic partial differential equations, Stoch. Proc. Appl. 125 (2015), 1470–1499.

[5] D. Dhaigude, K. Takale, A weighted average finite difference schemefor one dimensional pennes bioheat equation, Proc. Neural Parallel Sci. Comput. 4 (2010), 124-128.

[6] G. Zou, A Galerkin finite element method for time-fractional stochastic heat equation, Computers Math. Appl. 75 (2018), 4135–4150.

[7] M.G. Hahn, K. Kobayashi, S. Umarov, Fokker-Planck-Kolmogorov equations associated with time-changed fractional Brownian motion, Proc. Amer. Math. Soc. 139 (2011), 691–691.

[8] T. Kamppeter, F.G. Mertens, E. Moro, A. Sánchez, A.R. Bishop, Stochastic vortex dynamics in two-dimensional easy-plane ferromagnets: Multiplicative versus additive noise, Phys. Rev. B. 59 (1999), 11349–11357.

[9] M. Kamrani, S. Mohammad Hosseini, The role of coefficients of a general SPDE on the stability and convergence of a finite difference method, J. Comput. Appl. Math. 234 (2010), 1426–1434.

[10] A. A. Kilbas, H. M. Srivastava and J. J. Trijillo, Theory and Applications of Fractional Differential Equations, North-Holland Mathematical Studies, Vol 24, (2006).

[11] J. Klafter, I.M. Sokolov, Anomalous diffusion spreads its wings, Phys. World. 18 (2005), 29–32.

[12] Y. Lin, C. Xu, Finite difference/spectral approximations for the time-fractional diffusion equation, J. Comput. Phys. 225 (2007), 1533–1552.

[13] M.M. Meerschaert, A. Sikorskii, Stochastic models for fractional calculus, De Gruyter Studies in Mathematics, 43, (2012).

[14] R. Metzler, J. Klafter, The random walk's guide to anomalous diffusion: a fractional dynamics approach, Phys. Rep. 339 (2000), 1–77.

[15] J.B. Mijena, E. Nane, Intermittence and space-time fractional stochastic partial differential equations, Potential Anal. 44 (2016), 295-312.

[16] J. B. Mijena, E. Nane, Space - time fractional stochastic fractional differential equations, Stoch. Process. Appl. 125 (2015), 3301-3326.

[17] K. S. Miller, B. Ross, An introduction to the Fractional Calculus and Fractional Differential Equations, John Wiley and Sons, New York, (1993).

[18] W. W. Mohammed et al. Mean square convergent finite difference scheme for stochastic parabolic PDEs, Amer. J. Comput. Math. 4 (2014), 280-288.

[19] S. Momani, Z. Odibat, Numerical comparison of methods for solving linear differential equations of fractional order, Chaos Solitons Fractals. 31 (2007), 1248–1255.

[20] M. Namjoo, A. Mohebbian, Approximation of stochastic advection-diffusion equations with finite difference scheme, J. Math. Model. 4 (2016), 1-18.

[21] M. Namjoo, A. Mohebbian, Analysis of stability and convergence of a finite difference approximation for stochastic partial differential equations, Comput. Meth. Differ. Equ. 7 (2019), 334-358.

[22] I. Podlubny, Fractional Differential equations, Academic Press, San Diago (1999).

[23] J. Pruss, Evolutionary integral equations and applications, Monogr. Math. 87, (1983).

[24] M. Rehman, R. A. Khan, A numerical method for solving boundary value problems for fractional differential equations, Appl. Math. Model. 36(3) (2012), 894-907.

[25] C. Roth, Difference methods for stochastic partial differential equations, Z. Angew. Math. 82 (2002), 821-830.

[26] S.G. Samko, A.A. Kilbas and O.I. Marichev, Fractional Integrals and Derivatives: Theory and Applications, Gordan and Breach, Newark, N. J., (1993).

[27] R. Schumer, D.A. Benson, M.M. Meerschaert, S.W. Wheatcraft, Eulerian derivation of the fractional advection-dispersion equation, J. Contaminant Hydrol. 48 (2001), 69-88.

[28] G.D. Smith, Numerical Solution of Partial Differential Equations, 2nd edition, Clarendon Press, Oxford, (1978).

[29] A.R. Soheili, M.B. Niasar, M. Arezoomanadan, Approximation of stochastic parabolic differential equations with two different finite difference scheme, Bull. Iran. Math. Soc. 61-83, (2011).

[30] T.T. Soong, Random Differential equations in science and engineering, Academic Press, New York, (1973).

[31] N.H.Sweilam, D.M. El-Sakout and M.M.Muttardi, Compact finite difference method to numerically solving a stochastic fractional advection diffusion equation, Adv. Differ. Equ, 2020 (2020), 189.

[32] K. Takale, Fractional order finite difference scheme for space fractional diffusion equation, Eng. Autom. Probl. 120-124, (2014).

[33] K.C. Takale, V.R. Nikam, S. Kulkarni, Fractional order finite difference scheme for space fractional diffusion equation, Eng. Autom. Probl. 120-124, (2014).

[34] K. Takale, M. Datar, S. Kulkarni, Approximate solution of space fractional partial differential equations and applications, Int. J. Eng. Computer Sci. Eng. 5 (2018), 216-220.

[35] J.B. Walsh, An introduction to stochastic partial differential equations, lecture notes in mathematics, Springer-Verlag, 1180 (1986), 265-439.

[36] W. Liu, K. Tian, M. Foodun, On some properties of a class of fractional stochastic heat equations, J. Theor. Probab. 30 (2017), 1310-1333.

[37] L. von Wolfersdorf, An identification of memory kernels in linear theory of heat equation, Math. Methods Appl. Sci. 17 (1994), 919-932.

Malaya Journal of Matematik, Vol. 8, No. 3, 1078-1084, 2020

https://doi.org/10.26637/MJM0803/0060

Numerical solution of time fractional Kuramoto-Sivashinsky equation by Adomian decomposition method and applications

Sharvari Kulkarni[1]*, Kalyanrao Takale[2], Shrikisan Gaikwad[3]

Abstract

In the paper, we develop the Adomian Decomposition Method for fractional order nonlinear Kuramoto-Sivashinsky (KS) equation. Caputo fractional derivatives are used to define fractional derivatives. We know that KS equation has many applications in physical phenomenon such as reaction diffusion system, long waves on the boundary of two viscous fluids and hydrodynamics. In this paper, we will solve time fractional KS equation which may help to researchers for their work. We solve some examples numerically, which will show the efficiency and convenience of Adomian Decomposition Method.

Keywords

Kurmoto-Sivashinsky equation, Fractional derivative, Adomian Decomposition Method, Convergence, Mathematica.

AMS Subject Classification

26A33, 30E25, 34A12, 34A34, 34A37, 37C25, 45J05.

[1] *Department of Mathematics, Model College , Dombivali, Thane-421201, Maharashtra, India.*
[2] *Department of Mathematics, RNC Arts, JDB Commerce and NSC Science College, Nashik-422101, Maharashtra, India.*
[3] *Department of Mathematics, New Atrs, Commerce and Science College, Ahmadnagar-414001, Maharashtra, India.*
***Corresponding author**: [1] sharvari12july@gmail.com; [2]kalyanraotakale@rediffmail.com; [3]sbgmathsnagar@gmail.com
Article History: Received **11** February **2020**; Accepted **22** June **2020**

Contents

1. Introduction

In the present scenario fractional calculus is useful in the various fields of science. In past few years, the increase of interest in the subject is witnessed by series of conferences, research papers and several monographs. The dynamic models of a large number of phenomena can be modeled by fractional order partial differential equations which are characterized by fractional space and/or time derivatives [2]. Fractional calculus is pragmatic to archetypal occurrences dependent damping behavior of many viscoelastic materials, continuum mechanics, statistical mechanics, economics etc [1]. But, many times it is difficult to obtain exact solutions, hence numerical methods must be used. Now a days, Adomian Decomposition Method (ADM) is used to obtain the solution of fractional differential equations . This method gives rapidly convergent series solutions by using a few iterations for both linear and nonlinear equations. This method is very useful to avoid linearization, perturbation, massive computation and transformations [3, 4]. Various instabilities and spatio - temporal chaotic behavior are exhibited in many thermodynamical systems. Pattern formation, travelling wave problems, reaction-diffusion systems, long waves on thin films, unstable drift waves in plasmas etc. are some of the physical phenomenon which arise from chaotic instabilities. In this context Kuramoto-Sivashinsky (KS) equation has a wide range of applicability in science. It is used to model fluctuations of the position of a flame front, the motion of a fluid going down a vertical wall, spatially uniform oscillating chemical reaction in a homogeneous medium, solitary pulses in a falling thin film [5] etc. It is also useful to physical problems such as viscous flow problems, hydrodynamics in thin films,

Belousov-Zhabotinsky reactions and instabilities of solidification fronts of dilute binary alloys [6]. Kuramoto Sivashinsky equation was developed by Kuramoto and Sivashinsky is written as follow

$$w_t + \lambda_1 w w_x + \lambda_2 w_{xx} + \lambda_3 w_{xxxx} = 0 \tag{1.1}$$

where λ_1, λ_2, λ_3 are unknown parameters. The second order and fourth order spatial derivatives are making this equation's behaviour complicated and interesting. The nonlinear term transforms energy from low to high wave numbers. Also, Maziar Raissi and George have developed methodology applied to the problem of learning, system identification or data-driven discovery of partial differential equation and provides new direction to design learning machines without requiring large quantities of data. They gave following observations for values of parameters λ_1, λ_2, λ_3 with clean and noisy data [7]:
(i) The correct KS partial differential equation is

$$w_t + w w_x + w_{xx} + w_{xxxx} = 0 \tag{1.2}$$

(ii) The identified KS partial differential equation **(clean data)** is

$$w_t + 0.952 w w_x + 1.005 w_{xx} + 0.980 w_{xxxx} = 0 \tag{1.3}$$

(iii) The identified KS partial differential equation **One percent noisy data** is

$$w_t + 0.908 w w_x + 0.951 w_{xx} + 0.927 w_{xxxx} = 0 \tag{1.4}$$

Recently, some researchers have used Homotopy Perturbation Method [8], He's Variational Iteration Method [9] and Lattice Boltzmann mehod [10] to solve KS equation. Saad A. Manna, Fadhil H. Easif [11] have used ADM to solve KS equation. Weishi Yin, Fei Xu et.al. found the asymptotic expansion of solutions to time-space fractional KS equation by residual power series method [12].
Therefore, models which represent wave phenomenon needs to study travelling wave solutions. As per Abdul Wazwaz, in the study of solitary wave theory, we can obtain travelling wave solutions. These solutions are used by scientists to study various physical applications in plasma physics. In [13], the researchers used Bogning-Dijeumen Tchalo-Kofane method (BDK Method) to solve very strong nonlinear KS equation. By applying BDK method they make up modulated soliton solution of KS equation. In paper [14] KS equation was solved by truncated expansion method and compared with Ansatz method. Also researchers analyzed new solitary wave solutions of KS equation with comparison of solutions given by Chen and Zhand, Wazwaz and Wazaan. In this connection in our paper, we used ADM to solve time fractional KS equation because ADM is a powerful method to obtain the solution of linear and nonlinear fractional partial differential equations of higher order.
We organize the paper as follows: We have given some formulae and theorem in Section 2, which are useful for further developments. Section 3, is devoted for ADM to solve time fractional KS equation and prove convergence. In section 4, numerical problems are solved and presented their solutions graphically by using mathematica software.

2. Preliminaries

Some basic concepts, which we will be using are as follows:-

Definition 2.1. *The Caputo fractional derivative [?] of the function $f(x)$ is defined as*

$$\begin{aligned} D_*^{\beta} f(x) &= J^{(m-\beta)} D^m f(x) \\ &= \frac{1}{\Gamma(m-\beta)} \int_0^x \frac{1}{(x-t)^{(1-m+\beta)}} f^{(m)}(t) dt, \\ &\text{for } m-1 < \beta \le m,\ m \in N, x > 0,\ f \in C_{-1}^m. \end{aligned}$$

Properties:
For $f(x) \in C_\mu$, $\mu \ge -1$, $\alpha, \beta \ge 0$ and $\gamma > -1$ [15], we have

(i) $J^\alpha J^\beta f(x) = J^{\alpha+\beta} f(x)$,

(ii) $J^\alpha J^\beta f(x) = J^\beta J^\alpha f(x)$,

(iii) $J^\alpha x^\gamma = \frac{\Gamma(\gamma+1)}{\Gamma(\alpha+\gamma+1)} x^{(\alpha+\gamma)}$.

Lemma 2.2. *If $m-1 < \alpha \le m$, $m \in N$ and $f \in C_\mu^m$, $\mu \ge -1$, then*

$$\begin{aligned} &D_*^\alpha \, J^\alpha f(x) = f(x) \\ &J^\alpha D_*^\alpha f(x) = f(x) - \sum_{k=0}^{m-1} f^{(k)}(0^+) \frac{x^k}{k!}, x > 0. \end{aligned}$$

3. Fractional Adomian Decomposition Method

We consider following time fractional KS equation to develop the time Fractional ADM [15] for solving KS equation,

$$w_t^\alpha + \lambda_1 w w_x + \lambda_2 w_{xx} + \lambda_3 w_{xxxx} = 0,\ \ 0 < \alpha \le 1, t > 0 \tag{3.1}$$

$$\text{initial condition} : w(x,0) = f(x) \tag{3.2}$$

We will operate J^α on R.H.S. and L.H.S. of equation,

$$J^\alpha \left[w_t^\alpha + \lambda_1 w w_x + \lambda_2 w_{xx} + \lambda_3 w_{xxxx} = 0 \right] = 0,\ 0 < \alpha \le 1, t > 0$$

Now, consider following decomposition series:-

$$w(x,t) = \sum_{n=0}^{\infty} w_n(x,t) \tag{3.3}$$

The decomposed series of nonlinear terms $Nw(x,t)$ are:

$$Nw(x,t) = \sum_{n=0}^{\infty} A_n \tag{3.4}$$

where the formula for Adomian polynomial is as follows:

$$A_n = \frac{1}{n!}\left[\frac{d^n N}{d\lambda^n}\left(\sum_{k=0}^{n}\lambda^k u_k\right)\right]_{\lambda=0} \tag{3.5}$$

From (3.3) and using lemma (2.1), we get

$$\sum_{n=0}^{\infty} w_n(x,t) = \sum_{k=0}^{m-1}\frac{\partial^k w(x,0)}{\partial t^k}\frac{t^k}{k!} - J^\alpha\left[\lambda_2\sum_{n=0}^{\infty}D_x^2 w_n(x,t)\right.$$

$$\left.+\lambda_3\sum_{n=0}^{\infty}D_x^4 w_n(x,t)+\lambda_1\sum_{n=0}^{\infty}A_n\right],\ x>0$$

The value of $w_n(x,t)$, $n\geq 0$ can be obtained as follows:

$$w_0(x,t) = w(x,0) = f(x) \tag{3.6}$$

$$w_{n+1}(x,t) = -J^\alpha\left[\lambda_2 D_x^2 w_n(x,t)+\lambda_3 D_x^4 w_n(x,t)+\lambda_1 A_n\right] \tag{3.7}$$

For , $x>0$, now we can obtain solution by calculating value of each component.

$$\phi_N(x,t) = \sum_{n=0}^{N-1} w_n(x,t) \tag{3.8}$$

$$\lim_{N\to\infty}\phi_N = w(x,t) \tag{3.9}$$

Theorem 3.1. ***Uniqueness Theorem*** *[16]*
Consider time fractional KS equation for $\lambda_1=1$, $\lambda_2=1$, *and* $\lambda_3=1$, *as follows*

$$w_t^\alpha + ww_x + w_{xx} + w_{xxxx} = 0,\ \ 0<\alpha\leq 1, t>0 \tag{3.10}$$

$$\textit{initial condition}: w(x,0) = f(x) \tag{3.11}$$

The equation has a unique solution whenever $0<\gamma<1$ *where* $\gamma = \frac{(C_1+C_2+C_3)t^\alpha}{\Gamma\alpha+1}$.

Proof:- Let $X=(C(I),\|.\|)$ be the Banach space of all continuous functions on $I=[0,T]$ with norm

$$\|w(t)\| = \max_{t\in I}\mid w(t)\mid.$$

We define a mapping $M: X\to X$, such that

$$M(w(t)) = f(x) - J^\alpha N(w(t)) - J^\alpha S(w(t)) - J^\alpha F(w(t)).$$

Now, $N(w(t))$ denotes nonlinear term and $S(w(t))$ denotes second order spatial term and $F(w(t))$ denotes fourth order spatial term. Also nonlinear term $N(w(t))$ is Lipschitzian that is

$$\mid N(w)-N(p)\mid\leq C_1\mid w-p\mid$$

where C_1 is Lipschitz constant. Let $w,w'\in X$, we have

$$||M(w)-M(w')|| = \max_{t\in I}|-J^\alpha N(w(t))-J^\alpha S(w(t)-J^\alpha F(w(t)$$

$$+J^\alpha N(w'(t))+J^\alpha S(w'(t)+J^\alpha F(w'(t)|$$

$$=\max_{t\in I}\mid -J^\alpha(Nw-Nw')-J^\alpha(Sw-Sw')-J^\alpha(Fw-Fw')\mid$$

$$=\max_{t\in I}\mid J^\alpha(Nw-Nw')+J^\alpha(Sw-Sw')+J^\alpha(Fw-Fw')\mid$$

$$\leq\max_{t\in I}\mid J^\alpha(Nw-Nw')\mid+\mid J^\alpha(Sw-Sw')\mid+\mid J^\alpha(Fw-Fw')\mid$$

Now suppose $S(w(t))$ and $F(w(t))$ are also Lipschitzian that is

$$\mid S(w)-S(p)\mid\leq C_2\mid w-p\mid$$

and

$$\mid F(w)-F(p)\mid\leq C_3\mid w-p\mid,$$

where C_2 and $C_3$are Lipschitz constants.
Therefore

$$\| M(w)-M(w')\|\leq\max_{t\in I}(C_1J^\alpha\mid w-w'\mid+C_2J^\alpha\mid w-w'\mid$$

$$+C_3J^\alpha\mid w-w'\mid)\leq(C_1+C_2+C_3)\| w-w'\|\frac{t^\alpha}{\Gamma\alpha+1}$$

$$\| M(w)-M(w')\|\leq\gamma\| w-w'\|, where\ \gamma=\frac{(C_1+C_2+C_3)t^\alpha}{\Gamma\alpha+1}$$

Therefore, whenever $0<\gamma<1$, the mapping is contraction. Hence with the reference of Banach fixed point theorem for contraction, we proved that equation has unique solution.

Theorem 3.2. ***Convergence Theorem****[16]*
Let Q_n *be the* n^{th} *partial sum, that is*

$$Q_n = \sum_{i=0}^{n} w_i(x,t) \tag{3.12}$$

Then we shall prove that $\{Q_n\}$ *is a Cauchy sequence in Banach space* X.

Proof: For proving this theorem, we consider

$$\| Q_{n+p}-Q_n\| = \max_{t\in I}\mid Q_{n+p}-Q_n\mid$$

$$=\max_{t\in I}|\sum_{i=n+1}^{n+p}w_i(x,t)|$$

$$=\max_{t\in I}|-J^\alpha\sum_{i=n+1}^{n+p}Sw_{i-1}(x,t)-J^\alpha\sum_{i=n+1}^{n+p}Fw_{i-1}(x,t)$$

$$-J^\alpha\sum_{i=n+1}^{n+p}Nw_{i-1}(x,t)|$$

$$=\max_{t\in I}|J^\alpha SQ_{n+p-1}-SQ_{n-1}+J^\alpha FQ_{n+p-1}-FQ_{n-1}$$

$$+J^\alpha NQ_{n+p-1}-NQ_{n-1}|$$

$$\leq\max_{t\in I}J^\alpha(|(SQ_{n+p-1}-SQ_{n-1}|)+\max_{t\in I}J^\alpha(|(FQ_{n+p-1}-FQ_{n-1}|)$$

$$+\max_{t\in I}J^\alpha|NQ_{n+p-1}-NQ_{n-1}|$$

$$\leq C_2\max_{t\in I}J^\alpha(|(Q_{n+p-1}-Q_{n-1}|)+C_3\max_{t\in I}J^\alpha(|(Q_{n+p-1}-Q_{n-1}|)$$

$$+C_1 \max_{t\in I} J^{\alpha}|Q_{n+p-1}-Q_{n-1}|$$
$$\leq (C_1+C_2+C_3)\frac{t^{\alpha}}{\Gamma\alpha+1} \parallel Q_{n+p-1}-Q_{n-1} \parallel$$
$$\parallel Q_{n+p}-Q_n \parallel \leq \gamma \parallel Q_{n+p-1}-Q_{n-1} \parallel,$$

where $\gamma=(C_1+C_2+C_3)\frac{t^{\alpha}}{\Gamma\alpha+1}$

$$\parallel Q_{n+p}-Q_n \parallel \leq \gamma \parallel Q_{n+p-1}-Q_{n-1} \parallel$$

Similarly, we have

$$\begin{aligned}\parallel Q_{n+p}-Q_n \parallel &\leq \gamma^2 \parallel Q_{n+p-2}-Q_{n-2} \parallel\\ &\vdots\\ &\leq \gamma^n \parallel Q_p-Q_0 \parallel\\ &\leq \gamma^n \parallel Q_1-Q_0 \parallel,\ for p=1\\ &\leq \gamma^n \parallel w_1 \parallel\end{aligned}$$

Now, for $n>m$, where $n,m\in N$,

$$\begin{aligned}\parallel Q_n-Q_m \parallel &\leq \parallel Q_{m+1}-Q_m \parallel + \parallel Q_{m+2}-Q_{m+1} \parallel\\ &\quad +\cdots+ \parallel Q_n-Q_{n-1} \parallel\\ &\leq (\gamma^m+\gamma^{m+1}+\cdots+\gamma^{n-1}) \parallel w_1 \parallel\\ &\leq \gamma^m\left[\frac{1-\gamma^{n-m}}{1-\gamma}\right] \parallel w_1 \parallel\end{aligned}$$

Since, $0<\gamma<1$, then $1-\gamma^{n-m}<1$, so we have,

$$\parallel Q_n-Q_m \parallel \leq \frac{\gamma^m}{1-\gamma} \parallel w_1 \parallel$$

Since, $w(t)$ is bounded, therefore $\parallel w_1 \parallel<\infty$

$$\lim_{n\to\infty} \parallel Q_n-Q_m \parallel \to 0$$

Hence, we proved that solution is convergent because $\{Q_n\}$ is a Cauchy sequence in X.

4. Numerical Examples

Example 4.1: We will consider the following time fractional KS equation

$$w_t^{\alpha}+ww_x+w_{xx}+w_{xxxx}=0,\ 0<\alpha\leq 1, t>0 \quad (4.1)$$

$$\text{initial condition}: w(x,0)=\sec h^2\left(\frac{x}{2}\right) \quad (4.2)$$

Now, using equations (3.6) and (3.7), we have

$$w_0(x,t)=w(x,0)=f(x)$$
$$w_{k+1}(x,t)=-J^{\alpha}\left[A_k+D_x^2 w_k(x,t)+D_x^4 w_k(x,t)\right],\ x>0$$
$$w_0(x,t)=w(x,0)=\sec h^2\left(\frac{x}{2}\right)$$
$$w_1(x,t)=-J^{\alpha}\left[A_0+D_x^2 w_0(x,t)+D_x^4 w_0(x,t)\right]$$

$$\begin{aligned}A_0=w_0(w_0)_x&=\left[-\frac{1}{2}\tan h\left(\frac{x}{4}\right)+\tan h^3\left(\frac{x}{4}\right)\right.\\ &\quad\left.-\frac{1}{2}\tan h^5\left(\frac{x}{4}\right)\right]\\ D_x^2 w_0(x,t)&=\left[-\frac{1}{8}\sec h^2\left(\frac{x}{4}\right)+\frac{3}{8}\tan h^2\left(\frac{x}{4}\right)\right.\\ &\quad\left.-\frac{3}{8}\tan h^4\left(\frac{x}{4}\right)\right]\\ D_x^2 w_0(x,t)&=\left[-\frac{1}{8}\left(1-\tan h^2\left(\frac{x}{4}\right)\right)+\frac{3}{8}\tan h^2\left(\frac{x}{4}\right)\right.\\ &\quad\left.-\frac{3}{8}\tan h^4\left(\frac{x}{4}\right)\right]\\ D_x^2 w_0(x,t)&=\left[-\frac{1}{8}+\frac{1}{2}\tan h^2\left(\frac{x}{4}\right)-\frac{3}{8}\tan h^4\left(\frac{x}{4}\right)\right]\\ D_x^4 w_0(x,t)&=\left[\frac{1}{16}\sec h^2\left(\frac{x}{4}\right)-\frac{15}{32}\tan h^2\left(\frac{x}{4}\right)\sec h^2\left(\frac{x}{4}\right)\right.\\ &\quad\left.+\frac{15}{32}\tan h^4\left(\frac{x}{4}\right)\sec h^2\left(\frac{x}{4}\right)\right]\\ D_x^4 w_0(x,t)&=\left[\frac{1}{16}\left(1-\tan h^2\left(\frac{x}{4}\right)\right)-\frac{15}{32}\tan h^2\left(\frac{x}{4}\right)\right.\\ &\quad\left.+\frac{15}{32}\tan h^4\left(\frac{x}{4}\right)\left(1-\tan h^2\left(\frac{x}{4}\right)\right)\right]\\ D_x^4 w_0(x,t)&=\left[\frac{1}{16}-\frac{17}{32}\tan h^2\left(\frac{x}{4}\right)+\frac{15}{16}\tan h^4\left(\frac{x}{4}\right)\right]\end{aligned}$$

$$\begin{aligned}w_1(x,t)&=-J^{\alpha}\left[A_0+D_x^2 w_0(x,t)+D_x^4 w_0(x,t)\right]\\ w_1(x,t)&=-J^{\alpha}\left[-\frac{1}{2}\tan h\left(\frac{x}{4}\right)+\tan h^3\left(\frac{x}{4}\right)-\frac{1}{2}\tan h^5\left(\frac{x}{4}\right)\right.\\ &\quad\left.-\frac{3}{8}\tan h^4\left(\frac{x}{4}\right)+\frac{1}{16}-\frac{17}{32}\tan h^2\left(\frac{x}{4}\right)\right]\\ w_1(x,t)&=-J^{\alpha}\left[-\frac{1}{16}-\frac{1}{2}\tan h\left(\frac{x}{4}\right)-\frac{1}{32}tanh^2\left(\frac{x}{4}\right)\right.\\ &\quad\left.+\frac{9}{16}\tan h^4\left(\frac{x}{4}\right)-\frac{1}{2}\tan h^5\left(\frac{x}{4}\right)-\frac{15}{32}\tan h^6\left(\frac{x}{4}\right)\right]\\ w_1(x,t)&=\left[\frac{1}{16}+\frac{1}{2}\tan h\left(\frac{x}{4}\right)+\frac{1}{32}\tan h^2\left(\frac{x}{4}\right)-\tan h^3\left(\frac{x}{4}\right)\right.\\ &\quad\left.-\frac{9}{16}\tan h^4\left(\frac{x}{4}\right)+\frac{1}{2}\tan h^5\left(\frac{x}{4}\right)\right]\frac{t^{\alpha}}{\Gamma(\alpha+1)}\\ &\vdots\end{aligned}$$

After calculating and substituting values of various components, we have

$$w(x,t)=w_0(x,t)+w_1(x,t)+\cdots$$
$$\begin{aligned}w(x,t)&=\sec h^2\left(\frac{x}{2}\right)+\left[\frac{1}{16}+\frac{1}{2}\tan h\left(\frac{x}{4}\right)+\frac{1}{32}\tan h^2\left(\frac{x}{4}\right)\right.\\ &\quad-\tan h^3\left(\frac{x}{4}\right)-\frac{9}{16}\tan h^4\left(\frac{x}{4}\right)+\frac{1}{2}\tan h^5\left(\frac{x}{4}\right)\\ &\quad\left.+\frac{15}{32}\tan h^6\left(\frac{x}{4}\right)\right]\frac{t^{\alpha}}{\Gamma(\alpha+1)}\cdots\end{aligned}$$

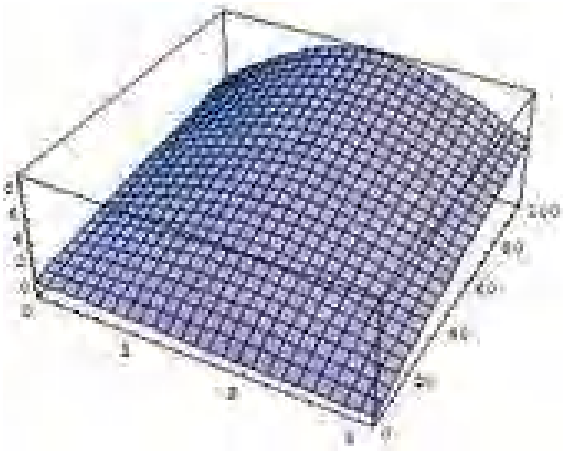

Figure 1. 3DPlot of time fractional KS eqn for $\alpha = 1$

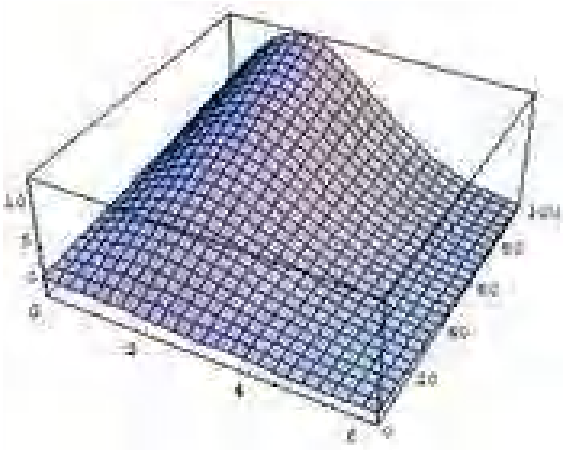

Figure 2. 3DPlot of time fractional KS eqn with $\alpha = 0.9$

Example 4.2: We will solve the following time fractional KS equation

$$w_t^\alpha + ww_x + w_{xx} + w_{xxxx} = 0,\ \ 0 < \alpha \leq 1, t > 0 \quad (4.3)$$

$$\text{initial condition} : w(x,0) = cos\left(\frac{x}{2}\right) \quad (4.4)$$

Now, using equation (3.3) and (3.6), we have

$$w_0(x,t) = w(x,0) = f(x)$$

$$w_{k+1}(x,t) = -J^\alpha\left[A_k + D_x^2 w_k(x,t) + D_x^4 w_k(x,t)\right],\ x > 0$$

$$w_0(x,t) = w(x,0) = cos\left(\frac{x}{2}\right)$$

$$w_1(x,t) = -J^\alpha\left[D_x^2 w_0(x,t) + D_x^4 w_0(x,t) + A_0\right]$$

$$A_0 = w_0(w_0)_x = -\frac{1}{4}\sin(x)$$

$$D_x^2 w_0(x,t) = -\frac{1}{4}cos\left(\frac{x}{2}\right),\ \ D_x^4 w_0(x,t) = \frac{1}{16}\cos\left(\frac{x}{2}\right)$$

$$w_1(x,t) = \left[\frac{1}{4}\sin x + \frac{1}{4}\cos\left(\frac{x}{2}\right) - \frac{1}{16}\cos\left(\frac{x}{2}\right)\right]\frac{t^\alpha}{\Gamma(\alpha+1)}$$

$$w_1(x,t) = \left[\frac{1}{4}\sin x + \frac{3}{16}\cos\left(\frac{x}{2}\right)\right]\frac{t^\alpha}{\Gamma(\alpha+1)}$$

$$w_2(x,t) = -J^\alpha\left[D_x^2 w_1(x,t) + D_x^4 w_1(x,t) + A_1\right]$$

$$A_1 = w_1(w_0)_x + w_0(w_1)_x$$

$$A_1 = \left[-\frac{9}{64}\sin(x) + \frac{1}{4}\cos\left(\frac{3x}{2}\right)\right]\frac{t^\alpha}{\Gamma(\alpha+1)}$$

$$D_x^2 w_1(x,t) = \left[-\frac{1}{4}\sin(x) - \frac{3}{64}\cos\left(\frac{x}{2}\right)\right]\frac{t^\alpha}{\Gamma(\alpha+1)}$$

$$D_x^4 w_1(x,t) = \left[\frac{1}{4}\sin(x) + \frac{3}{256}\cos\left(\frac{x}{2}\right)\right]\frac{t^\alpha}{\Gamma(\alpha+1)}$$

$$w_2(x,t) = \left[\frac{9}{64}\sin(x) + \frac{9}{256}\cos\left(\frac{x}{2}\right)\right]\frac{t^{2\alpha}}{\Gamma(2\alpha+1)}$$

$$\vdots$$

After calculating and substituting values of various components, we have

$$w(x,t) = w_0(x,t) + w_1(x,t) + + \cdots \quad (4.5)$$

$$w(x,t)$$
$$= \cos\left(\frac{x}{2}\right) + \left[\frac{1}{4}\sin x + \frac{3}{16}\cos\left(\frac{x}{2}\right)\right]\frac{t^\alpha}{\Gamma(\alpha+1)}$$
$$+ \left[\frac{9}{64}\sin(x) + \frac{9}{256}\cos\left(\frac{x}{2}\right)\right]\frac{t^{2\alpha}}{\Gamma(2\alpha+1)} + \cdots$$

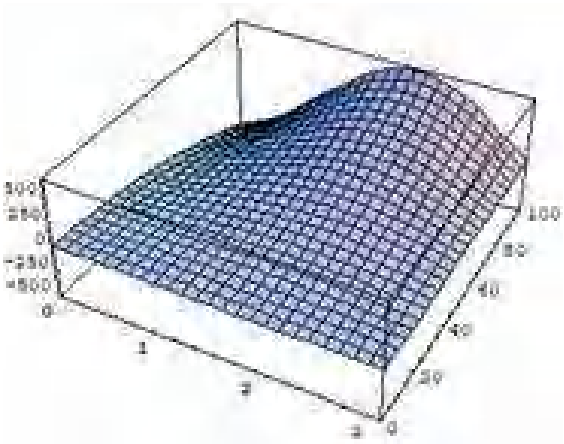

Figure 3. Plots of time fractional KS eqn $\alpha = 1$

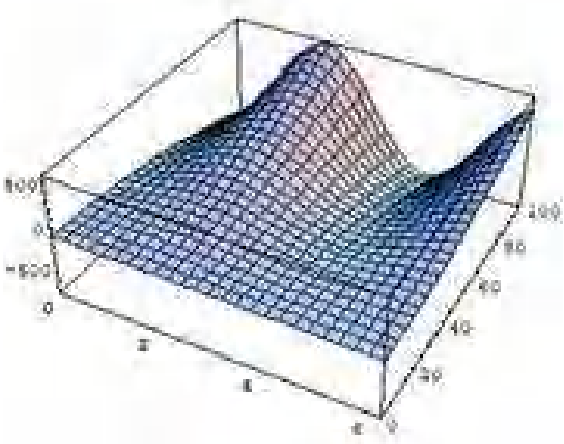

Figure 4. Plots of time fractional KS eqn with $\alpha = 0.9$

5. Conclusion

The time fractional KS equation is solved by using ADM and we can say that the formula of ADM polynomials is powerful to obtain the solution of nonlinear fractional partial differential equation. The graphical presentation of solutions of time fractional KS equation reveals the reliability of the mathematical procedure. We also prove the uniqueness and convergence theorem for time fractional KS equation.

Acknowledgment

The authors are threatful to all referee's for their useful comments and suggestions.

References

[1] I. Podlubny, *Fractional Differential equations* Academic Press, San Diago, (1999).

[2] S. Jogdand, S. Kulkarni and K.C.Takale, Error Analysis of solution of time fractional convection diffusion equation, *JETIR*, 6(3)(2019), 1–12.

[3] J. Biazar and E. Babolian, Solution of the system of ordinary differential equations by Adomian Decomposition Method, *Appl. Math. Comput.,* 147(3)(2004), 713–719.

[4] H. Jafari, Solving a system of nonlinear fractional differential equations using Adomian Decomposition, *Journal of Computational and Applied Mathematics,* 196(2006), 644–651.

[5] M. Lakestani and M. Dehghan, Numerical Solutions of the generalised Kuramoto Sivashinsky equation using B- spline functions, *Applied Mathematical Modelling,* 36(2012), 605–617.

[6] D. Anders, M. Dittmann, A higher-order finite element approach to the Kuramoto Sivashinsky equation, *ZAMM. Z. Angew Math. Mech.*, 92(2012), 599–607.

[7] M. Raissi and G. E. Karniadakis, Hidden Physics Models: Machine Learning of Nonlinear Partial Differential Equations, *Division of Applied Mathematics,* Brown University, Providence, RI, 2912, USA, Journal of Computational Physics, (2017).

[8] M. G. Porshokouhi and B. Rahimi, Application of Homotopy Perturbation Method for solution of Kuramoto Sivashinsky equation, *International Mathematical Forum*, 6(45)(2011), 2225–2230.

[9] M. G. Porshokouhi, Application of He's VIM for solution of the family of Kuramoto Sivashinsky equation, *Journal of King Saud University Science*, 23(2011), 407–411.

[10] H. Lai and C. Ma, Lattice Boltzmann method for the generalized Kuramoto Sivashinsky equation, *Physica A : Statistical Mechanics and its applications*, 388(8)(2009), 1405–1412.

[11] S.A.Manna and F. H.Easif, ADM for solving the Kuramoto Sivashinsky equation, *IOSR Journal of Mathematics*, 10(1)(2014), 08–12.

[12] W. Yin, F. Xu, Asymptotic Expansion of the Solutions to Time-Space Fractional Kuramoto-Sivashinsky equation,

Hindawi Publishing Corporation Advances in Mathematical Physics, (2016), 12–20.

[13] C. T. D. Tchaho, J. R. Bogning, Modulated Soliton Solution of the modified Kuramoto-Sivashinsky equations, *American Journal of Computational and Applied Mathematics*, 2(5)(2012), 218–224.

[14] N. A. Kudryashov and M. B. Soukharev, Popular ansatz methods and solitary waves solutions of Kuramoto-Sivashinsky equations, *Hindawi Publishing Corporation Advances in Mathematical Physics*, (2016), 12 pages.

[15] S. Momani, Z. Odibat, Analytical solutions of a time fractional Navier-Stokes equation by Adomian decomposition method, *Appl. Math. Comput.* , 177(2)(2006), 488–494.

[16] S. Saha Ray, New Approach for General Convergence of the ADM, *World Applied Sciences Journal*, 32 (11)(2014), 2264–2268.

★★★★★★★★★
ISSN(P):2319 – 3786
Malaya Journal of Matematik
ISSN(O):2321 – 5666
★★★★★★★★★

Available online at http://scik.org
J. Math. Comput. Sci. 11 (2021), No. 5, 5327-5343
https://doi.org/10.28919/jmcs/6048
ISSN: 1927-5307

NEW TECHNIQUE FOR SOLVING TIME FRACTIONAL WAVE EQUATION: PYTHON

KRISHNA GHODE[1,*], KALYANRAO TAKALE[2], SHRIKISAN GAIKWAD[3]

[1]Department of Mathematics, B. K. Birla College of Arts, Science and Commerce, Kalyan, India
[2]Department of Mathematics, RNC Arts, JDB Commerce and NSC Science College, Nashik Road, Nashik, India
[3]Department of Mathematics, New Arts, Commerce and Science College, Ahmednagar, India

Abstract. In this paper, we develop the fractional order explicit finite difference scheme for time fractional wave equation. Furthermore, we prove the scheme is conditionally stable and convergent. As an application of the scheme numerical solution of the test problem is obtained by Python Programme and represented graphically.

Keywords: fractional wave equation; Caputo derivative; finite difference scheme; stability and Python.
2010 AMS Subject Classification: 35R11, 65M06, 35L05, 26A33.

1. INTRODUCTION

Fractional order partial differential equations are widely used in many areas like physics, engineering, finance, medical sciences etc.[2, 8], as they can provide an adequate and precise description of the models, which cannot be revealed by integer-order differential equations. Recently, the fractional wave equation is occurs in many studies such as acoustics, electromagnetic, seismic study etc[3, 10, 18]. It also describes the movement of strings, wires and fluid surfaces[12]. Any wave or motion can be express in terms of a sum of sine or sinusoidal waves. The traveling wave solution of the wave equation was first published by d'Alembert in 1747[7].

*Corresponding author
E-mail address: ghodekrishna@gmail.com
Received May 16, 2021

The traveling wave solutions of fractional order partial differential equations are deeply helpful to realise the mechanisms of the phenomena as well as their further application in real-world. Finite difference method is also one of the very effective method for solving fractional order partial differential equations [1, 4, 14, 15, 16, 17].

Recently, several authors have developed different numerical techniques for solving differential equations using mathematical software[5, 6, 11]. Python is a high-level interpreted programming language that has a vast standard library and a lot of modern software engineering tools. It allows fast exploration of various ideas as well as efficient implementation. It has been used for teaching and research in various branches of pure and applied mathematics[19]. Therefore, in this connection we develop the explicit finite difference scheme for time-fractional wave equation and obtain its solution using Python programme.

We organize the paper as follows: In section 2, we develop the explicit finite difference scheme for time fractional wave equation. The section 3 is devoted for stability of solution of the scheme and the convergence is proven in section 4. In section 5, we develop a python programme for the proposed scheme and numerical experiments are performed to confirm stability and convergence of the scheme.

We consider the following time-fractional wave equation with initial and boundary conditions:

$$\frac{\partial^\alpha V}{\partial t^\alpha} = C^2 \frac{\partial^2 V}{\partial x^2}, \quad 1 < \alpha \leq 2, \quad (x,t) \in \Omega = [0,L] \times [0,T] \tag{1}$$

initial conditions:

$$V(x,0) = f(x), \quad \frac{\partial}{\partial t} V(x,0) = g(x), \quad x \in [0,L] \tag{2}$$

boundary conditions:

$$V(0,t) = 0, \quad V(L,t) = 0, \quad t \in (0,T] \tag{3}$$

where $V(x,t)$ is the amplitude of wave at position x and time t, and C is the velocity of wave. Here, $\frac{\partial^\alpha V}{\partial t^\alpha}$ is Caputo time fractional derivative of order α, which is defined as follows[9]:

$$\frac{\partial^\alpha V}{\partial t^\alpha} = \frac{1}{\Gamma(m-\alpha)} \int_0^t (t-\zeta)^{m-\alpha-1} \frac{\partial^m V(x,\zeta)}{\partial \zeta^m} d\zeta$$

where m is a integer such that $m-1 < \alpha \leq m$.

2. FINITE DIFFERENCE SCHEME

Let V_i^n be the numerical approximation of $V(x,t)$ at point (ih,nk), where h and k are spatial and temporal sizes respectively. Let $x_i = ih,\ i = 0,1,2,\ldots,M$ and $t_n = nk,\ n = 0,1,2,\ldots,N$, where $h = \frac{L}{M}$ and $k = \frac{T}{N}$. Now, the fractional order wave equation (1) - (3) is discretized by using the second-order accurate central difference formula for the derivative term in space and the Caputo finite difference formula for the time α-order fractional derivative for each interior grid point (ih,nk). We discretized the second order space derivative by second-order accurate central difference formula as follows:

$$\left(\frac{\partial^2 V}{\partial x^2}\right)_{(x_i,t_n)} = \frac{V_{i+1}^n - 2V_i^n + V_{i-1}^n}{h^2} + O(h^2) \tag{4}$$

and Caputo time fractional derivative as follows:

$$\begin{aligned}
\left(\frac{\partial^\alpha V}{\partial t^\alpha}\right)_{(x_i,t_n)} &= \frac{1}{\Gamma(2-\alpha)}\int_0^{t_n}(t_n-\zeta)^{1-\alpha}\frac{\partial^2 V(x_i,\zeta)}{\partial \zeta^2}d\zeta \\
&= \frac{1}{\Gamma(2-\alpha)}\sum_{j=0}^{n-1}\int_{jk}^{(j+1)k}\eta^{1-\alpha}\frac{\partial^2 V(x_i,t_n-\eta)}{\partial \eta^2}d\eta \\
&= \frac{1}{\Gamma(2-\alpha)}\sum_{j=0}^{n-1}\left[\frac{V_i^{n-j+1}-2V_i^{n-j}+V_i^{n-j-1}}{k^2}+O(k^2)\right]\int_{jk}^{(j+1)k}\eta^{1-\alpha}d\eta \\
&= \frac{k^{2-\alpha}}{\Gamma(3-\alpha)}\sum_{j=0}^{n-1}\left[\frac{V_i^{n-j+1}-2V_i^{n-j}+V_i^{n-j-1}}{k^2}+O(k^2)\right]\left[(j+1)^{2-\alpha}-j^{2-\alpha}\right] \\
&= \frac{k^{2-\alpha}}{\Gamma(3-\alpha)}\sum_{j=0}^{n-1}\left[\frac{V_i^{n-j+1}-2V_i^{n-j}+V_i^{n-j-1}}{k^2}\right]\left[(j+1)^{2-\alpha}-j^{2-\alpha}\right] \\
&\quad + \frac{k^{2-\alpha}}{\Gamma(3-\alpha)}\sum_{j=0}^{n-1}\left[(j+1)^{2-\alpha}-j^{2-\alpha}\right]O(k^2) \\
&= \frac{k^{-\alpha}}{\Gamma(3-\alpha)}\sum_{j=0}^{n-1}\left[V_i^{n-j+1}-2V_i^{n-j}+V_i^{n-j-1}\right]\left[(j+1)^{2-\alpha}-j^{2-\alpha}\right] \\
&\quad + \frac{k^{2-\alpha}}{\Gamma(3-\alpha)}n^{2-\alpha}O(k^2)
\end{aligned}$$

As $nk \le T$ is finite, then above formula can be rewritten as

$$\left(\frac{\partial^\alpha V}{\partial t^\alpha}\right)_{(x_i,t_n)} = \frac{k^{-\alpha}}{\Gamma(3-\alpha)}\sum_{j=0}^{n-1} b_j\left(V_i^{n-j+1}-2V_i^{n-j}+V_i^{n-j-1}\right)+O(k^2) \tag{5}$$

where

$$b_j = (j+1)^{2-\alpha} - j^{2-\alpha}, \quad j = 0,1,2,\ldots,n-1$$

Now, putting (4) and (5) in equation (1), we obtain

$$\frac{k^{-\alpha}}{\Gamma(3-\alpha)} \sum_{j=0}^{n-1} b_j \left(V_i^{n-j+1} - 2V_i^{n-j} + V_i^{n-j-1} \right) = C^2 \left(\frac{V_{i+1}^n - 2V_i^n + V_{i-1}^n}{h^2} \right)$$

$$\sum_{j=0}^{n-1} b_j \left(V_i^{n-j+1} - 2V_i^{n-j} + V_i^{n-j-1} \right) = \frac{\Gamma(3-\alpha)k^{\alpha}C^2}{h^2} \left(V_{i+1}^n - 2V_i^n + V_{i-1}^n \right)$$

$$V_i^{n+1} - 2V_i^n + V_i^{n-1} + \sum_{j=1}^{n-1} b_j \left(V_i^{n-j+1} - 2V_i^{n-j} + V_i^{n-j-1} \right) = \frac{\Gamma(3-\alpha)k^{\alpha}C^2}{h^2} \left(V_{i+1}^n - 2V_i^n + V_{i-1}^n \right)$$

After simplification, we get

$$V_i^{n+1} = 2V_i^n - V_i^{n-1} + \mu \left(V_{i+1}^n - 2V_i^n + V_{i-1}^n \right) - \sum_{j=1}^{n-1} b_j \left(V_i^{n-j+1} - 2V_i^{n-j} + V_i^{n-j-1} \right) \tag{6}$$

where $\mu = \frac{\Gamma(3-\alpha)k^{\alpha}C^2}{h^2}$.

The initial conditions are approximated as follows:

$$V(x_i,0) = f(x_i) \text{ implies } V_i^0 = f(x_i),\ i = 1,2,\ldots,M-1 \tag{7}$$

and

$$\frac{\partial}{\partial t} V(x_i,t_0) = g(x_i) \text{ implies } \frac{V_i^1 - V_i^{-1}}{2k} = g(x_i)$$

$$V_i^{-1} = V_i^1 - 2kg(x_i),\ i = 1,2,\ldots,M-1 \tag{8}$$

Also, the boundary conditions are approximated as follows:

$$V(0,t_n) = 0 \text{ implies } V_0^n = 0,\ n = 1,2,\ldots,N-1$$

and

$$V(L,t_n) = 0 \text{ implies } V_M^n = 0,\ n = 1,2,\ldots,N-1$$

Now, putting $n = 0$ in equation (6) and using equation (8), we obtain

$$V_i^1 = V_i^0 + kg(x_i) + \frac{\mu}{2} \left(V_{i+1}^0 - 2V_i^0 + V_{i-1}^0 \right)$$

For $n = 1$, we have

$$V_i^2 = 2V_i^1 - V_i^0 + \mu \left(V_{i+1}^1 - 2V_i^1 + V_{i-1}^1 \right)$$

and for $n = 2,3,\ldots,N-1$, we have

$$V_i^{n+1} = 2V_i^n - V_i^{n-1} + \mu\left(V_{i+1}^n - 2V_i^n + V_{i-1}^n\right) - \sum_{j=1}^{n-1} b_j\left(V_i^{n-j+1} - 2V_i^{n-j} + V_i^{n-j-1}\right)$$

The complete discretized time-fractional wave equation with initial and boundary conditions is written as follows:

$$V_i^1 = V_i^0 + kg(x_i) + \frac{\mu}{2}\left(V_{i+1}^0 - 2V_i^0 + V_{i-1}^0\right) \tag{9}$$

$$V_i^2 = 2V_i^1 - V_i^0 + \mu\left(V_{i+1}^1 - 2V_i^1 + V_{i-1}^1\right) \tag{10}$$

$$\begin{aligned} V_i^{n+1} &= 2V_i^n - V_i^{n-1} + \mu\left(V_{i+1}^n - 2V_i^n + V_{i-1}^n\right) \\ &\quad - \sum_{j=1}^{n-1} b_j\left(V_i^{n-j+1} - 2V_i^{n-j} + V_i^{n-j-1}\right), \text{ for } n = 2,3,\ldots N-1, \end{aligned} \tag{11}$$

initial condition:

$$V_i^0 = f(x_i),\ i = 1,2,\ldots,M-1 \tag{12}$$

boundary conditions:

$$V_0^n = 0,\ V_M^n = 0,\ n = 1,2,\ldots,N-1 \tag{13}$$

The discretized finite difference scheme (9)-(13) can be written in matrix form as follows:

$$V^1 = A_1 V^0 + F \tag{14}$$

$$V^2 = 2A_1 V^1 - V^0 \tag{15}$$

$$\begin{aligned} V^{n+1} &= A_2 V^n + (-1 + 2b_1 - b_2)V^{n-1} + (-b_1 + 2b_2 - b_3)V^{n-2} + \ldots \\ &\quad + (-b_{n-2} + 2b_{n-1})V^1 + (-b_{n-1})V^0, \text{ for } n = 2,3,\ldots N-1, \end{aligned} \tag{16}$$

initial condition:

$$V_i^0 = f(x_i), \quad i = 1,2,\ldots,M-1 \tag{17}$$

boundary conditions:

$$V_0^n = 0, \quad V_M^n = 0, \quad n = 1,2,\ldots,N-1 \tag{18}$$

where $V^n = \left[V_1^n, V_2^n, \ldots, V_{M-1}^n\right]^t$, $F = [kg(x_1), kg(x_2), \ldots, kg(x_{M-1})]^t$,

$$A_1 = \begin{pmatrix} 1-\mu & \frac{\mu}{2} & & & & & & \\ \frac{\mu}{2} & 1-\mu & \frac{\mu}{2} & & & & & \\ & \ddots & \ddots & \ddots & & & & \\ & & \frac{\mu}{2} & 1-\mu & \frac{\mu}{2} & & & \\ & & & \ddots & \ddots & \ddots & & \\ & & & & \frac{\mu}{2} & 1-\mu & \frac{\mu}{2} & \\ & & & & & \frac{\mu}{2} & 1-\mu \end{pmatrix}$$

and

$$A_2 = \begin{pmatrix} 2-2\mu-b_1 & \mu & & & & & & \\ \mu & 2-2\mu-b_1 & \mu & & & & & \\ & \ddots & \ddots & \ddots & & & & \\ & & \mu & 2-2\mu-b_1 & \mu & & & \\ & & & \ddots & \ddots & \ddots & & \\ & & & & \mu & 2-2\mu-b_1 & \mu & \\ & & & & & \mu & 2-2\mu-b_1 \end{pmatrix}$$

3. STABILITY

In this section, we discuss the stability of solution of the explicit finite difference scheme (9)-(13) develop for time-fractional wave equation (1)-(3).

Lemma 3.1. *The eigenvalues of the $N \times N$ tri-diagonal matrix*

$$\begin{pmatrix} a & b & & & & & \\ c & a & b & & & & \\ & \ddots & \ddots & \ddots & & & \\ & & c & a & b & & \\ & & & \ddots & \ddots & \ddots & \\ & & & & c & a & b \\ & & & & & c & a \end{pmatrix}$$

are given as

$$\lambda_s = a + 2\sqrt{bc}\cos\left(\frac{s\pi}{N+1}\right),\ s = 1,2,\ldots,N$$

where a, b and c may be real or complex[13].

Theorem 3.2. *The solution of fractional order explicit finite difference scheme (9)-(13) for time-fractional wave equation (1)-(3) is conditionally stable.*

Proof. The eigenvalues of tri-diagonal matrix A_1 are given by,

$$\begin{aligned}\lambda_s(A_1) &= 1-\mu+2\sqrt{\frac{\mu^2}{4}}\cos\left(\frac{s\pi}{M}\right),\ \text{for } s = 1,2,\ldots M-1\\ &= 1-\mu+\mu\cos\left(\frac{s\pi}{M}\right)\\ &\leq 1-\mu+\mu = 1\end{aligned}$$

$$\begin{aligned}\lambda_s(A_1) &= 1-\mu+\mu\cos\left(\frac{s\pi}{M}\right),\ \text{for } s = 1,2,\ldots M-1\\ &\geq 1-\mu-\mu\\ &\geq 1-2\mu\\ &\geq -1\ \text{ when }\ 1-2\mu \geq -1 \Rightarrow \mu \leq 1\end{aligned}$$

Therefore, we have

$$|\lambda_s(A_1)| \leq 1 \text{ for } 0 < \mu \leq 1 \tag{19}$$

Similarly, eigenvalues of tri-diagonal matrix $2A_1$ are given by,

$$\begin{aligned}\lambda_s(2A_1) &= 2-2\mu+2\mu\cos\left(\frac{s\pi}{M}\right),\ \text{for } s = 1,2,\ldots M-1\\ &\geq 2-2\mu-2\mu\\ &\geq 2-4\mu\\ &\geq -1\ \text{ when }\ 2-4\mu \geq -1 \Rightarrow \mu \leq \frac{3}{4}\end{aligned}$$

$$\begin{aligned}\lambda_s(2A_1) &= 2-2\mu+2\mu\cos\left(\frac{s\pi}{M}\right),\ \text{for } s = 1,2,\ldots M-1\\ &= 2-4\mu\sin^2\left(\frac{s\pi}{2M}\right)\\ &\leq 1\end{aligned}$$

when $2-4\mu\sin^2\left(\frac{s\pi}{2M}\right)\leq 1 \Rightarrow 1\leq 4\mu\sin^2\left(\frac{s\pi}{2M}\right)\Rightarrow 1\leq 4\mu \Rightarrow \frac{1}{4}\leq\mu$.

Therefore, we have

$$|\lambda_s(2A_1)|\leq 1 \text{ for } \frac{1}{4}\leq\mu\leq\frac{3}{4} \tag{20}$$

Now, the eigenvalues of tri-diagonal matrix A_2 are given by,

$$\begin{aligned}\lambda_s(A_2) &= 2-2\mu-b_1+2\mu\cos\left(\frac{s\pi}{M}\right), \text{ for } s=1,2,\ldots M-1\\ &\geq 2-2\mu-b_1-2\mu\\ &\geq 2-4\mu-b_1\\ &\geq -1 \text{ when } 2-4\mu-b_1\geq -1\Rightarrow\mu\leq\frac{3-b_1}{4}\end{aligned}$$

$$\begin{aligned}\lambda_s(A_2) &= 2-2\mu-b_1+2\mu\cos\left(\frac{s\pi}{M}\right), \text{ for } s=1,2,\ldots M-1\\ &= 2-b_1-4\mu\sin^2\left(\frac{s\pi}{2M}\right)\\ &\leq 1\end{aligned}$$

when $2-b_1-4\mu\sin^2\left(\frac{s\pi}{2M}\right)\leq 1\Rightarrow 1-b_1\leq 4\mu\sin^2\left(\frac{s\pi}{2M}\right)\Rightarrow 1-b_1\leq 4\mu\Rightarrow\frac{1-b_1}{4}\leq\mu$.

Hence, we have

$$|\lambda_s(A_2)|\leq 1 \text{ for } \frac{1-b_1}{4}\leq\mu\leq\frac{3-b_1}{4}. \tag{21}$$

Therefore, from equations (19), (20) and (21), we prove the spectral radius $\rho(A)$ of matrices $A=A_1,2A_1,A_2$, satisfies $\rho(A)\leq 1$ if

$$\max\left\{0,\frac{1}{4},\frac{1-b_1}{4}\right\}\leq\mu\leq\min\left\{1,\frac{3}{4},\frac{3-b_1}{4}\right\}$$

Hence, this proves the theorem. □

4. CONVERGENCE

In this section, we discuss the question of convergence. Let $\overline{V}_i^n$ be the exact solution of time-fractional wave equation (1)-(3) and τ_i^n be the local truncation error for $1\leq i\leq M$. The finite difference scheme (9)-(13) will become

$$\tau_i^1=\overline{V}_i^1-\overline{V}_i^0-kg(x_i)-\frac{\mu}{2}\left(\overline{V}_{i+1}^0-2\overline{V}_i^0+\overline{V}_{i-1}^0\right)=O(h^2+k^2)$$

$$\tau_i^2 = \overline{V}_i^2 - 2\overline{V}_i^1 + \overline{V}_i^0 + \mu\left(\overline{V}_{i+1}^1 - 2\overline{V}_i^1 + \overline{V}_{i-1}^1\right) = O(h^2+k^2)$$

and for $2 \le n \le N-1$,

$$\tau_i^{n+1} = \overline{V}_i^{n+1} - 2\overline{V}_i^n + \overline{V}_i^{n-1} - \mu\left(\overline{V}_{i+1}^n - 2\overline{V}_i^n + \overline{V}_{i-1}^n\right) + \sum_{j=1}^{n-1} b_j\left(\overline{V}_i^{n-j+1} - 2\overline{V}_i^{n-j} + \overline{V}_i^{n-j-1}\right) = O(h^2+k^2)$$

Lemma 4.1. *The coefficient $b_j,\ j = 1,2,\ldots$ satisfy*

(i) $b_j > 0$

(ii) $b_j > b_{j+1}$

Theorem 4.2. *Let $\overline{V}_i^n$ be the exact solution of time-fractional wave equation (1)-(3) and V_i^n be the numerical solution of explicit finite difference scheme (9)-(13) at each mesh point (x_i,t_n). Then there exist a positive constant K independent of h and k such that*

$$\|\overline{V}_i^n - V_i^n 1\| \le K(h^2+k^2),\ \textit{when}\ \frac{1}{4} \le \mu \le \frac{3-b_1}{4}.$$

Proof. Let e_i^n be the error at each mesh point (x_i,t_n), then

$$e_i^n = \overline{V}_i^n - V_i^n$$

Now, we denote the error vector by $e^n = (e_1^n, e_2^n, \ldots, e_{M-1}^n)$ for $1 \le n \le N$ and local truncation error vector by $\tau^n = (\tau_1^n, \tau_2^n, \ldots, \tau_{M-1}^n)$ for time level n. From equations (14)-(16), we obtain

$$e^1 = A_1 e^0 + \tau^1$$

$$e^2 = 2A_1 e^1 - e^0 + \tau^2$$

$$\begin{aligned} e^{n+1} &= A_2 e^n + (-1+2b_1+b_2)e^{n-1} + (-b_1+2b_2-b_3)e^{n-2} + \ldots \\ &\quad + (-b_{n-2}+2b_{n-1})e^1 + (-b_{n-1})e^0 + \tau^{n+1} \qquad \text{for } n = 2,3,\ldots N-1. \end{aligned}$$

Using mathematical induction, we will prove that $\|e^n\|_\infty \le K(h^2+k^2)$.

For $n = 1$, we have

$$\max_{1\le i\le M-1} |e_i^1| \le \|e^1\|_\infty = \|A_1 e^0 + \tau^1\|_\infty \le \|\tau^1\|_\infty \le K(h^2+k^2)$$

where K is independent of h and k. Also for $n = 2$, we have

$$\begin{aligned}\max_{1\le i\le M-1}|e_i^2| \le \|e^2\|_\infty &= \|2A_1e^1 - e^0 + \tau^2\|_\infty \\ &\le \|2A_1e^1\|_\infty + \|\tau^2\|_\infty \\ &\le \|e^1\|_\infty + \|\tau^2\|_\infty \\ &\le K_1(h^2+k^2) + K_2(h^2+k^2) \\ &\le K(h^2+k^2)\end{aligned}$$

where K is independent of h and k.

Suppose that

$$\max_{1\le i\le M-1}|e_i^r| \le \|e^r\|_\infty \le K(h^2+k^2)$$

for $r \le n$ and K is independent of h and k.

Consider,

$$\begin{aligned}\max_{1\le i\le M-1}|e_i^{n+1}| \le \|e^{n+1}\|_\infty &\le \|A_2e^n + (-1+2b_1-b_2)e^{n-1} + (-b_1+2b_2-b_3)e^{n-2} + \dots \\ &\quad + (-b_{n-2}+2b_{n-1})e^1 + (-b_{n-1})e^0 + \tau^{n+1}\|_\infty \\ &\le \|A_2\|.\|e^n\|_\infty + \|(-1+2b_1-b_2)e^{n-1} + (-b_1+2b_2-b_3)e^{n-2} + \dots \\ &\quad + (-b_{n-2}+2b_{n-1})e^1 + (-b_{n-1})e^0 + \tau^{n+1}\|_\infty \\ &\le \|A_2\|.\|e^n\|_\infty + |-1+2b_1-b_2|.\|e^{n-1}\|_\infty + |-b_1+2b_2-b_3|.\|e^{n-2}\|_\infty + \\ &\quad \dots + |-b_{n-2}+2b_{n-1})|.\|e^1\|_\infty + |-b_{n-1}|.\|e^0\|_\infty + \|\tau^{n+1}\|_\infty \\ &\le (1+1-2b_1+b_2+b_1-2b_2+b_3+\dots \\ &\quad + b_{n-2}-2b_{n-1}+b_{n-1}+2(-b_{n-2}+2b_{n-1}))K_2(h^2+k^2) + K_1(h^2+k^2) \\ &\le (2-b_1+2(-b_{n-2}+2b_{n-1})+b_{n-1})K_2(h^2+k^2) + K_1(h^2+k^2) \\ &\le K(h^2+k^2)\end{aligned}$$

where K is a positive constant independent of h and k. Hence, by mathematical induction, for all

$n = 1,2,\dots,N$, we have

$$\max_{1\le i\le M-1}|e_i^n| \le \|e^n\|_\infty \le K(h^2+k^2)$$

Therefore, we conclude that if

$$\frac{1}{4} \leq \mu \leq \frac{3-b_1}{4}$$

then $\|e^n\|_\infty \to 0$ as $(h,k) \to (0,0)$. Therefore, we proves that V_i^n converges to $\overline{V}_i^n$.

This completes the proof. □

5. PYTHON PROGRAMME

We compute V_i^n at each grid point (x_i, t_n) using proposed scheme by Python. Now, the algorithm for scheme (9)-(13) as follows:

(1) Compute $V_i^0 = f(x_i), \quad i = 0,1,2,\ldots,M.$

(2) Compute $V_i^1, V_i^2, \quad i = 0,1,2,\ldots,M.$

(3) Compute V_i^{n+1}, for each $n = 2,3,\ldots,N-1,\ i = 0,1,2,\ldots,M.$

Now, we develop the Python programme TFW for complete discretized scheme (9)-(13) as follows:

Inputs:

f - initial displacement

g - initial velocity

C - velocity of wave

L - spatial length

T - end time

k - temporal size

mu - μ

a - fractional order α of time derivative

t1 - time level, at which solution has to be estimate

Output of Python programme TFW is the approximate value of vector $V(x_i, t1)$.

```
import numpy as np
def TFW(f,g,C,L,T,k,mu,a,t1):
    d=(gamma(3-a)*(k)**a*C**2)/mu
    h=sqrt(d)
    N=int(round(T/k))
    M=int(round(L/h))
    t=np.linspace(0,N*k,N+1)
x=np.linspace(0,M*h,M+1)
V=np.zeros((N+1,M+1))
for i in range(0,M+1):
    V[0][i]=f(x[i])
for i in range(1,M):
    V[1][i]=V[0][i]+k*g(x[i])+0.5*mu*(V[0][i+1]-2*V[0][i]+V[0][i-1])
V[1][0]=0; V[1][M]=0
for i in range(1,M):
    V[2][i]=2*V[1][i]-V[0][i]+mu*(V[1][i+1]-2*V[1][i]+V[1][i-1])
V[2][0]=0; V[2][M]=0
for n in range(2,N):
    for i in range(1,M):
        S=0
        for j in range(1,n):
            S=S+((j+1)**(2-a)-j**(2-a))*(V[n-j+1][i]-2*V[n-j][i]+V[n-j-1][i])
        V[n+1][i]=2*V[n][i]-V[n-1][i]+mu*(V[n][i+1]-2*V[n][i]+V[n][i-1])-S
    V[n+1][0]=0; V[n+1][M]=0
return(x,V[t1])
```

Numerical Solutions:

We consider the following time-fractional wave equation:

$$\frac{\partial^\alpha V}{\partial t^\alpha} = C^2 \frac{\partial^2 V}{\partial x^2}, \quad (x,t) \in \Omega = [0,1] \times [0,1]$$

with initial conditions:

$$V(x,0) = \sin(5\pi x) + 2\sin(7\pi x), \quad \frac{\partial}{\partial t} V(x,0) = 0, \quad x \in [0,1]$$

and boundary conditions,

$$V(0,t) = 0, \quad V(1,t) = 0, \quad t \in (0,1]$$

The exact solution to this problem is

$$V(x,y) = \sin(5\pi x)\cos(5\pi Ct) + 2\sin(7\pi x)\cos(7\pi Ct)$$

Using the python programme TFW, we estimate the value of $V(x,t)$ for any time level t_n. In Table 1, we compare the exact solution and numerical solution for $\alpha = 1.99$ with parameters

$h = \frac{1}{100}$, $k = \frac{1}{150}$, $C = 1$ and $t = 1$.

TABLE 1. Comparison of exact solution and numerical solution for $\alpha = 1.99, h = \frac{1}{100}, k = \frac{1}{150}, C = 1, t = 1$

x	Exact solution	Numerical solution	Difference between the solutions
0.1	-2.6180339887	-2.2165435008	0.40149
0.2	1.9021130326	1.5695507898	0.33256
0.3	0.3819660113	0.3714258869	0.01054
0.4	-1.1755705046	-0.9700357352	0.20553
0.5	1.0	0.7689195118	0.23108
0.6	-1.1755705046	-0.9700357352	0.20553
0.7	0.3819660113	0.3714258869	0.01054
0.8	1.9021130326	1.5695507898	0.33256
0.9	-2.6180339887	-2.2165435008	0.40149
1.0	0.0	0.0	0.0

In Table 2, we compare the exact solution and numerical solution for parameters $\alpha = 2, h = \frac{1}{100}, k = \frac{1}{150}, C = 1$ and $t = 1$.

From these tables, we conclude that the proposed scheme gives accurate results and stable solutions. Using the Python programme TFW, we obtain numerical solutions of time fractional wave equation for $\alpha = 1.97, 1.98, 1.99$ and compare with exact solution with the parameters $\mu = \frac{3}{4}, k = \frac{1}{100}, C = 1$, $t = 1$ and represented graphically in Figure 1.

We obtain the numerical solutions for $\mu = 0.9$ and 1.0 with parameters $\alpha = 1.5, k = \frac{1}{100}, C = 1$, $t = 1$ and represented graphically using Python programme TFW in Figure 2.

We observe that $\mu > 0.75$ then approximate solution obtained by the develop scheme using Python programme TFW is unstable.

TABLE 2. Comparison of exact and numerical solution for $\alpha = 2, h = \frac{1}{100}, k = \frac{1}{150}, C = 1, t = 1$

x	Exact solution	Numerical solution	Relative error $e_i^n = \|\overline{V}_i^n - V_i^n\|$
0.1	−2.6180339887	−2.6175015948	0.000532
0.2	1.9021130326	1.9015345652	0.000578
0.3	0.3819660113	0.3821136465	0.000147
0.4	−1.1755705046	−1.1752129921	0.000357
0.5	1.0	0.9994320835	0.000567
0.6	−1.1755705046	−1.1752129921	0.000357
0.7	0.3819660113	0.3821136465	0.000147
0.8	1.9021130326	1.9015345652	0.000578
0.9	−2.6180339887	−2.6175015948	0.000532
1.0	0.0	0.0	0.0

FIGURE 1. The nature of approximate solutions for the parameters $\mu = \frac{3}{4}, k = \frac{1}{100}, t = 1, C = 1$

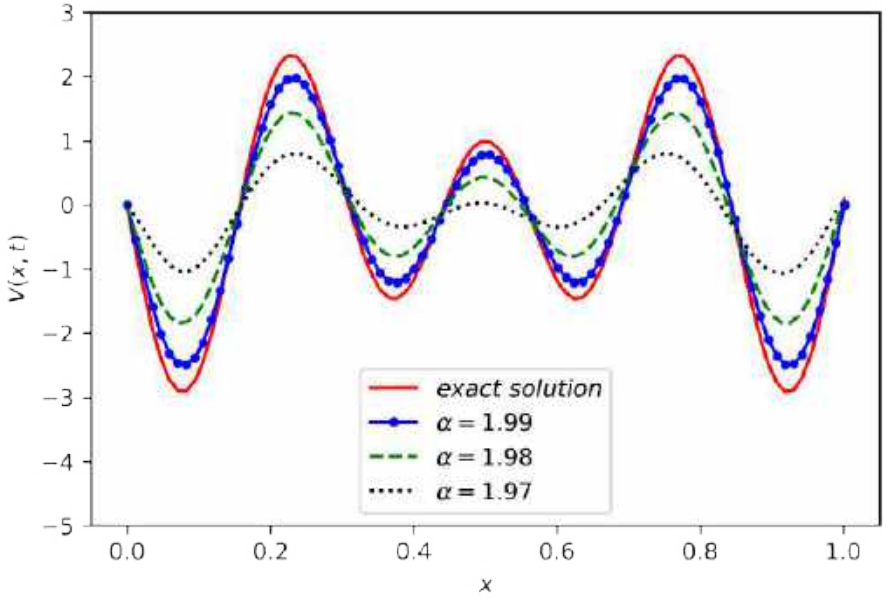

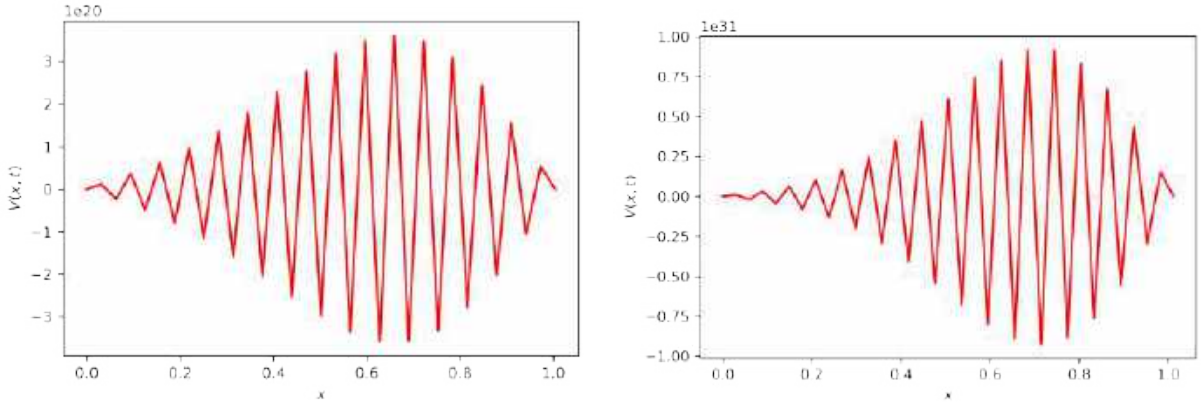

(A) $\mu = 0.9$ (B) $\mu = 1.0$

FIGURE 2. The nature of approximate solutions for the parameters $\alpha = 1.5, t = 1, C = 1, k = \frac{1}{100}$

6. CONCLUSIONS

(i) We successfully develop the fractional order finite difference scheme for time fractional wave equation.

(ii) Theoretically, we proved that the developed scheme is conditionally stable and bound of stability is $\frac{1}{4} \leq \mu \leq \frac{3-b_1}{4}$, where $0 \leq b_1 \leq 1$.

(iii) The convergence of the scheme is theoretically proved by using maximum norm method.

(iv) We successfully develop a python programme for time fractional wave equation.

(v) Analysis shows that the finite difference scheme is numerically stable and the results are compatible with our theoretical analysis.

(vi) We observe that Python is very powerful tool, which allows for the convenient computation of finite difference schemes for solving fractional order differential equations. The numerical solution of test problem is obtained successfully by Python programme and represented graphically.

CONFLICT OF INTERESTS

The author(s) declare that there is no conflict of interests.

REFERENCES

[1] D. Dhaigude, K. Takale, A weighted average finite difference scheme for one dimensional pennes bioheat equation, Proc. Neural Parallel Sci. Comput. 4 (2010), 124-128.

[2] R. Hilfer, Applications of Fractional Calculus in Physics, World Scientific, Singapore, 2000.

[3] S. Holm, S.P. NÃ¤sholm, F. Prieur, R. Sinkus, Deriving fractional acoustic wave equations from mechanical and thermal constitutive equations, Computers Math. Appl. 66 (2013), 621–629.

[4] S. Jogdand, K. Takale, A. Jagtap, Finite difference approximation for space fractional soil moisture diffusion equation and its application, IOSR J. Math. 8 (2013), 01–08.

[5] H.P. Langtangen, S. Linge, Finite Difference Computing with PDEs: A Modern Software Approach, volume 16 of Texts in Computational Science and Engineering. Springer International Publishing, Cham, 2017.

[6] J. Li, Y.-T. Chen, Computational partial differential equations using MATLAB, CRC Press, Boca Raton, 2020.

[7] R.B. Lindsay, Acoustics: historical and philosophical development, Benchmark papers in acoustics, Dowden, Hutchinson and Ross, Stroudsburg, PA, 1973.

[8] Y. Luchko, Fractional wave equation and damped waves, J. Math. Phys. 54 (2013), 031505.

[9] I. Podlubny, Fractional differential equations: an introduction to fractional derivatives, fractional differential equations, to methods of their solution and some of their applications, Number v. 198 in Mathematics in science and engineering, Academic Press, San Diego, 1999.

[10] A. Pskhu, S. Rekhviashvili, Fractional Diffusion–Wave Equation with Application in Electrodynamics, Mathematics, 8 (2020), 2086.

[11] K.A. Seeler, Finite Difference Methods and MATLAB, In System Dynamics, pages 467–517, Springer New York, New York, NY, 2014.

[12] J. Singh, D. Kumar, D. Baleanu, S. Rathore, On the local fractional wave equation in fractal strings, Math. Meth. Appl. Sci. 42 (2019), 1588–1595.

[13] G.D. Smith, Numerical Solution of Partial Differential Equations: Finite Difference Methods, Clarendon Press, Oxford, 1985.

[14] Kalyanrao Takale. Fractional order finite difference scheme for space fractional boussinesq's equation and its application. International Journal of Mathematical Sciences and Applications, 3, 01 2013.

[15] K.C. Takale, V.R. Nikam, S.R. Kulkarni, Fractional order finite difference scheme for space fractional diffusion equation, Eng. Autom. Probl. 3 (2014), 120–124.

[16] K. Takale, M. Datar, S. Kulkarni, Approximate solution of space fractional partial differential equations and its applications, Int. J. Eng. Res. Computer Sci. Eng. 5 (2018), 216–220.

[17] K. Takale, D. Dhaigude, V. Nikam, Douglas higher order finite difference scheme for one dimensional pennes bioheat equation, Int. J. Adv. Eng. Appl. 06 (2011).

[18] Y. Wang, Y. Ning, Y. Wang, Fractional Time Derivative Seismic Wave Equation Modeling for Natural Gas Hydrate, Energies, 13 (2020), 5901.

[19] M. Ziółkowski, L. Stepień, M.R. Stepień, A. Gola, Applications of Python programs in solving of equations based on selected numerical methods, Sci. Issues Jan Dlugosz Univ. Czestochowa, Mathematics, 22 (2017), 31–45.

Available online at http://scik.org
J. Math. Comput. Sci. 2022, 12:47
https://doi.org/10.28919/jmcs/4720
ISSN: 1927-5307

ANALYSIS OF FRACTIONAL SUSCEPTIBLE-EXPOSED-INFECTIOUS (SEI) MODEL OF COVID-19 PANDEMIC FOR INDIA

KALYANRAO TAKALE[1], JAGDISH SONAWANE[2,*], BHAUSAHEB SONTAKKE[3], AMJAD SHAIKH[4]

[1]Department of Mathematics, RNC Arts, JDB Commerce and NSC Science College, Nashik-Road, Nashik, India

[2]Department of Mathematics, R.H. Sapat College of Engineering, Management Studies and Research Center, Nashik, India

[3]Department of Mathematics, Pratishthan Mahavidyalaya, Paithan, Aurangabad, India

[4]Department of Mathematics, AKI's Poona College of Arts, Science and Commerce, Camp, Pune, India

Abstract. The purpose of this article is to develop and analyse COVID-19 pandemic for India in terms of mathematical equations. We consider the basic Susceptible-Exposed-Infectious (SEI) epidemic model and develop the SEI model of COVID-19 for India. We use Adomian decomposition method to find solution of the group of fractional differential equations. We discuss the stability by using Routh-Hurwitz criterion for disease-free equilibria point and endemic equilibrium point. We obtain approximate solution of the group of fractional differential equations and its solution represented graphically by Mathematica software, that will be helpful to mininize the infection.

Keywords: COVID-19; fractional derivatives; differential equation; Caputo fractional derivative; Adomian decomposition method; Mathematica.

2010 AMS Subject Classification: 34A08, 34A34, 65L20, 92D30, 65H10.

*Corresponding author

E-mail address: jagdish.sonawane555@gmail.com

Received October 04, 2021

1. INTRODUCTION

The Pandemic of a new human corona virus, named as COVID-19 by WHO officially is an ongoing Pandemic. The first case was detected in the month of December 2019 in Wuhan, Hubei, Chiana. As of $03:27$ UTC on 30^{th} April 2020, a total of $3,193,886$ cases are confirmed, in more than 185 countries and 200 territories, including 26 cruise ships and $227,638$ deaths. The first Patient of Corona-Virus was found on 30^{th} January 2020 in India. Ministry of Health and Family Welfare (MHFW) have confirmed 33050 cases upto 30^{th} April 2020.

Now a days, many real world problems in the field of biology, physics, engineering, financial and sociological can be represented in terms of group of non-linear ordinary and fractional order differential equations. Most of the time researchers are not able to find analytical solution of non-linear ordinary and fractional differential equations; due to that we use numerical methods to obtain their approximate solutions. Recently, there are several methods have been studied by many researchers to find solution of ordinary and fractional differential equations. Few methods are exponential Galerkin method introduced by Yuzbasi and Karayir[27], collacation method presented by Mastorakis[15], the exponential collaction method proposed by Yuzbasi[26],Galerkin finite element method given by Al-Omari et.al.[1], the adomian decomposition method improves [3],[9], the multistep method proposed by Hojiati et.al[4]. Many reserachers are investigating numerical and analystical methods to solve differential equation containing fractional derivatives given in [31, 32, 33, 34, 35].

Mathematical system of the transmitted diseases play an important role in understanding spread of disese and taking measures to controll disease. After the start of the emanation in Wuhan, many researchers modelled various mathematical structures for the purpose of estimations and predictions for the Corona virus. In the paper, [21] researcher studied Age structured impact of social distancing on the COVID-19 of India. More literature pertaining to this can be refer in ([28, 29, 30]).

Considering this base data and the SEI model published by WHO on 31^{st} January, 2020 for Chiana, we develop the Fractional Susceptible-Exposed-Infectious(SEI) Epidemic Model of COVID-19 for India, which form the group of non-linear fractional differential equations given in the next section.

1.1. Fractional SEI Model. We know that the WHO used SEI models to characterize and prediction the initial stage of the novel-COVID-19 emanation in Wuhan, China. In this connection, we develop SEI model of COVID-19 for India. The model structure is given below. In case

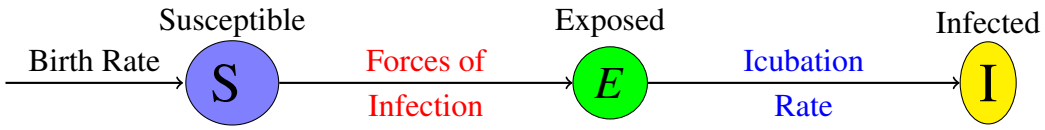

FIGURE 1. SEI Epidemic Model

of India, we considered few modifications like number of people infected by animal source are taken zero, average number of people infected by an infectious person over the average duration of infection is totally considered as rate of transmission, travelers entering Wuhan is replaced by travelers entering in population of India and Population traveling out of Wuhan is replaced by travelers exit from population of India. By observing the model it is clear that the travel data is conclusive, because it directly affects the spread. Note that, COVID 19 enters in India through the persons having foreign travel history. Therefore, our modified SEI model, along with compartment wise explanation and description of defining parameters for COVID 19 for India is presented below

$$\frac{dS}{dt} = -\frac{S}{N} \times [\beta \times I] + \mu_I \times N - \mu_0 \times S$$

Rate of change of number of susceptible person = − The susceptible portion of population × Rate of Transmission × Number of people infected by infectious people + Travelers entering in population × Total population − Travelers exit the population × Number of susceptible population

$$\frac{dE}{dt} = \frac{S}{N} \times [\beta \times I] - \frac{E}{D_E} - \mu_0 \times E$$

Rate of change of number of exposed person	=	The susceptible portion of population	×	Rate of Transmission	×	Number of people infected by infectious people	−	Number of exposed people over the average exposed period	−	Travelers exit the population	×	Number of exposed person

$$\frac{dI}{dt} = \frac{E}{D_E} - \frac{I}{D_I} - \mu_0 \times I$$

Rate of change of number of infected person	=	Number of exposed people over the average exposed period	−	Number of infected people over the average infection period	−	Travelers exit the population	×	Number of exposed person

where S = Number of susceptible persons, N = Total population, E = Number of Exposed persons, I = Number of Infected persons, β = Rate of transmission, μ_I = Number of travelers entering in population, μ_0 = Number of travelers exit the population, D_E = Average exposed period, D_I = Average infected period.

Thus above SEI model can be written as system of ordinary differential equations as follows

$$\left.\begin{aligned} \frac{dS}{dt} &= -\frac{\beta}{N}[SI] + \mu N - \mu S \\ \frac{dE}{dt} &= \frac{\beta}{N}[SI] - (\sigma_E + \mu)E \\ \frac{dI}{dt} &= \sigma_E E - (\sigma_I + \mu)I \end{aligned}\right\} \tag{1}$$

Motivated by the above literature applications of epidemic mathematical models, in this paper we are studying dynamics of novel coronavirus SEI model derived in (1) in the from of system

of the nonlinear differential equations involving Caputo fractional derivative operator of order α such that $\alpha \in (0,1]$ as follows

$$\left.\begin{aligned} D^{\alpha} S &= -\frac{\beta}{N}[SI] + \mu N - \mu S \\ D^{\alpha} E &= \frac{\beta}{N}[SI] - (\sigma_E + \mu)E \\ D^{\alpha} I &= \sigma_E E - (\sigma_I + \mu)I \end{aligned}\right\} \tag{2}$$

with initial conditions

$$S(0) = S_0,\ E(0) = E_0,\ I(0) = I_0. \tag{3}$$

We arrange the paper as per folowing sequence: In section 2, we discuss few basic definitions of fractional calculus. In Section 3, we discuss about Adomian Decomposition Method to solve fractional SEI model. In Section 4, we comment about equilibrium points and stability and calculate basic reproduction number R_0. In section 5, we find the solution of fractional SEI model and represent their solutions graphically by Mathematica software. Section 6 is devoted to conclusions.

2. PRELIMINARIES

In this section, we study some basic definition of fractional integral, fractional derivative and their properties for further development. We use the Caputo's definition due to its convenience for initial conditions of the differential equations.

Definition 2.1. *A real function $f(t), t > 0$, is said to be in the space $C_\delta, \delta \in R$ if there exist a real number $p > \delta$such that $f(t) = t^p f_1(t)$, where $f_1(t) \in C[0,\infty)$ and it is said to be in the space C_δ^m if and only if $f^{(m)}(t) \in C_\delta$, $m \in N$.*

Definition 2.2. ***Riemann-Liouville Fractional integral:***
If $f(t) \in C[a,b]$ and $a < t < b$ then

$${}_aI_t^{\alpha} f(t) = \frac{1}{\Gamma(\alpha)} \int_a^t (t-s)^{\alpha-1} f(s) ds, \tag{4}$$

where $\alpha \in (-\infty,\infty)$ is called the Riemann-Liouville fractional integral of order α.

Definition 2.3. ***M.Caputo Fractional Derivative:***

If $f(t) \in C[a,b]$ and $a < t < b$ then

$$ {}_a^C D_t^\alpha f(t) = {}_a I_t^{n-\alpha} D^n f(t) = \frac{1}{\Gamma(n-\alpha)} \int_a^t (t-s)^{n-\alpha-1} f^n(s) ds, \tag{5} $$

where $\alpha \in (n-1,n)$ is called the Caputo fractional derivative of order α.

- **Properties:**

For $f(t) \in C_\delta,\ \delta \geq -1,\ \alpha, \beta > 0,$ and $\gamma > -1$, we have

(i)$I^\alpha I^\beta = I^{\alpha+\beta}$,

(ii)$I^\alpha I^\beta = I^\beta I^\alpha$,

(iii)$I^\alpha t^\gamma = \frac{\Gamma(\gamma+1)}{\Gamma(\alpha+\gamma+1)} t^{\alpha+\gamma}$.

3. ADM FOR THE SYSTEM OF FRACTIONAL ORDINARY DIFFERENTIAL EQUATIONS

Consider the system of fractional ordinary differential equation

$$ D^\alpha u_i = G_i(t, u_1, u_2, \cdots, u_n),\ \ i = 1,2,\cdots,n. \tag{6} $$

where D^α is the Caputo fractional differential operator.

Applying operator I^α on (6), we have.

$$ u_i = \sum_{i=0}^{[\alpha_i]} \frac{C_i^k u_i}{k!} + I^\alpha G_i(t, u_1, u_2, \cdots, u_n),\ i = 1,2,\cdots,n. \tag{7} $$

We consider the series solution of equation (7) is

$$ u_i = \sum_{j=0}^{\infty} u_{ij} \tag{8} $$

$$ G_i(t, u_1, u_2, \cdots, u_n) = \sum_{j=0}^{\infty} A_{ij}(u_{i0}, u_{i1}, \cdots, u_{in}) \tag{9} $$

where $A_{ij}(u_{i0}, u_{i1}, \cdots, u_{in})$ are called Adomian polynomials.

By substituting (8) and (9) in (7), we get

$$ \sum_{j=0}^{\infty} u_{ij} = \sum_{i=0}^{[\alpha_i]} \frac{C_i^k u_i}{k!} + I^\alpha \left[\sum_{j=0}^{\infty} A_{ij}(u_{i0}, u_{i1}, \cdots, u_{in}) \right] $$

$$ = \sum_{i=0}^{[\alpha_i]} \frac{C_i^k u_i}{k!} + \sum_{j=0}^{\infty} I^\alpha [A_{ij}(u_{i0}, u_{i1}, \cdots, u_{in})] $$

From this we define,

$$u_{i0} = \sum_{i=0}^{[\alpha_i]} \frac{C_i^k u_i}{k!}$$

$$u_{i(n+1)} = I^{\alpha}\left[A_{in}(u_{i0}, u_{i1}, \cdots, u_{in})\right],\ n = 0,1,2,3,\cdots \tag{10}$$

In order to determine the Adomian polynomial, we introduce a parameter λ and (9) becomes,

$$G_i\left(t, \sum_{j=0}^{\infty} u_{1,j}\lambda^j, \cdots, \sum_{j=0}^{\infty} u_{n,j}\lambda^j\right) = \sum_{j=0}^{\infty} A_{ij}\lambda^j \tag{11}$$

Let $G_{i\lambda}(t) = \sum_{j=0}^{\infty} u_{i,j}\lambda^j$, then

$$A_{ij} = \frac{1}{j!}\left[\frac{d^j}{d\lambda^j} G_{i\lambda}(u_1, u_2, \cdots, u_n)\right]_{\lambda=0} \tag{12}$$

where

$$G_{i\lambda}(u_1, u_2, \cdots, u_n) = G_i(t, u_{1\lambda}, u_{2\lambda}, \cdots, u_{n\lambda}) \tag{13}$$

In view of (12) and (13), we get

$$\begin{aligned} A_{ij} &= \frac{1}{j!}\frac{d^j}{d\lambda^j}\left[G_i(t, u_{1\lambda}, u_{2\lambda}, \cdots, u_{n\lambda})\right]_{\lambda=0} \\ &= \frac{1}{j!}\frac{d^j}{d\lambda^j}\left[G_i(t, \sum_{j=0}^{\infty} u_{1,j}\lambda^j, \cdots, \sum_{j=0}^{\infty} u_{n,j}\lambda^j)\right]_{\lambda=0} \\ &= \left[\frac{1}{j!}\frac{d^j}{d\lambda^j} G_i(t, \sum_{j=0}^{\infty} u_{1,j}\lambda^j, \cdots, \sum_{j=0}^{\infty} u_{n,j}\lambda^j)\right]_{\lambda=0} \end{aligned} \tag{14}$$

Hence, the equation (10) and (14) leads to following recurrence relation

$$u_{i0} = \sum_{i=0}^{[\alpha_i]} \frac{C_i^k u_i}{k!}$$

$$u_{i(n+1)} = I^{\alpha}\left[\frac{1}{j!}\frac{d^j}{d\lambda^j} G_i(t, \sum_{j=0}^{\infty} u_{1,j}\lambda^j, \cdots, \sum_{j=0}^{\infty} u_{n,j}\lambda^j)\right]_{\lambda=0},\ n = 0,1,2,3,\cdots \tag{15}$$

We can approximate the solution u_i by the truncated series

$$G_{ik} = \sum_{j=0}^{k-1} u_{i,j},\ \lim_{k\to\infty} G_{ik} = u_i(t).$$

4. Equilibrium Points, Stability and Basic Reproductive Number R_0

Theorem 4.1. *The Diseases free equilibria (DFE) point and the Endemic equilibrium (EE) point for SEI model are* $(s^*, e^*, i^*) = (1, 0, 0)$ *and*

$$(s^*, e^*, i^*) = \left(\frac{(\sigma_E - \mu)(\sigma_I - \mu)}{\beta \sigma_E}, \frac{\mu}{(\sigma_E - \mu)} - \frac{\mu(\sigma_I - \mu)}{\sigma_E \beta}, \frac{\mu \sigma_E}{(\sigma_E - \mu)(\sigma_I - \mu)} - \frac{\mu}{\beta} \right)$$

respectively.

Proof: Now, substituting $s = \frac{S}{N}$, $e = \frac{E}{N}$, $i = \frac{I}{N}$ in to the system of equations (1), we obtain

$$\left.\begin{aligned} \frac{ds}{dt} &= -\beta s i - \mu + \mu s = f(s,e,i) \\ \frac{de}{dt} &= \beta s i - (\sigma_E + \mu) e = g(s,e,i) \\ \frac{di}{dt} &= \sigma_E e - (\sigma_I + \mu) i = h(s,e,i) \end{aligned}\right\} \tag{16}$$

Now, diseases free equilibria (DFE) can be found by substituting $i^* = 0$ in linearization of system (16) that is

$$f(s,e,i) = 0,\ g(s,e,i) = 0,\ h(s,e,i) = 0$$

Thus

$$\left.\begin{aligned} -\beta s i + \mu - \mu s &= 0 \\ \beta s i - (\sigma_E + \mu) e &= 0 \\ \sigma_E e - (\sigma_I + \mu) i &= 0 \end{aligned}\right\} \tag{17}$$

Putting $i^* = 0$ in third equation of system (17) we get $e^* = 0$.

By adding first two equations of the system (17), we get $\mu(1-s) - (\sigma_E + \mu) e = 0$, therefore $s^* = 1$.

Thus, DFE point is $(s^*, e^*, i^*) = (1, 0, 0)$.

We obtain the endemic equilibrium point, from third equation of system (17) as follows

$$e^* = \frac{(\sigma_I + \mu)}{\sigma_E} i^*.$$

From the second equation of (17), we get

$$\beta s^* i^* = (\sigma_E + \mu) e^*$$

Thus,

$$s^* = \frac{(\sigma_E + \mu)(\sigma_I + \mu)}{\beta\, \sigma_E}$$

From the first equation of (17), we get

$$\beta\, s^* i^* = \mu\,(1 - s^*)$$

Thus, we obtain

$$i^* = \frac{\mu\, \sigma_E}{(\sigma_E + \mu)(\sigma_I + \mu)} - \frac{\mu}{\beta}$$

Hence,

$$e^* = \frac{\mu}{(\sigma_E + \mu)} - \frac{\mu\,(\sigma_I + \mu)}{\sigma_E\, \beta}$$

Thus, the endemic equilibrium point for SEI model is

$$(s^*, e^*, i^*) = \left(\frac{(\sigma_E + \mu)(\sigma_I + \mu)}{\beta\, \sigma_E}, \frac{\mu}{(\sigma_E + \mu)} - \frac{\mu\,(\sigma_I + \mu)}{\sigma_E\, \beta}, \frac{\mu\, \sigma_E}{(\sigma_E + \mu)(\sigma_I + \mu)} - \frac{\mu}{\beta} \right).$$

Lemma 4.1. ***Rourth-Hurwitz Criteria***[20]

For the cubic equation $\lambda^3 + a_1\lambda^2 + a_2\lambda + a_3 = 0$ *conditions for* $Re(\lambda) < 0$ *is*

$$a_1 > 0, a_2 > 0, a_3 > 0, a_1\, a_2 - a_3 > 0.$$

Theorem 4.2. ***Stability*** [18]

If J is the Jacobian matrix of order $(k \times k)$ *for a nonlinear system of k first order equations, then trajectory of the system that is equilibrium point will have stable behavior when real part of all eigenvalues is negative.*

Proof: The Jacobian matrix of SEI model is evaluated as follows

$$J(s^*, e^*, i^*) = \begin{bmatrix} f_s & f_e & f_i \\ g_s & g_e & g_i \\ h_s & h_e & h_i \end{bmatrix} = \begin{bmatrix} -\beta\, i - \mu & 0 & -\beta\, s \\ \beta\, i & -\sigma_E - \mu & \beta\, s \\ 0 & \sigma_E & -\sigma_I - \mu \end{bmatrix} \tag{18}$$

The Jacobian Matrix of SEI model at DFE is as below

$$J(1,0,0) = \begin{bmatrix} -\mu & 0 & -\beta \\ 0 & -\sigma_E - \mu & \beta \\ 0 & \sigma_E & -\sigma_I - \mu \end{bmatrix} \tag{19}$$

To find its eigenvalue, we must have to solve $det[J(1,0,0)-\lambda I_3]=0$.

Therefore

$$det[J(1,0,0)-\lambda I_3]=(-\mu-\lambda)\,[\lambda^2+(\sigma_E+2\,\mu+\sigma_I)\,\lambda+(\sigma_E\,\sigma_I+\mu\,\sigma_E+\mu\,\sigma_I+\mu^2-\beta\,\sigma_E)]=0.$$

Therefore, eigenvalues are

$$\lambda_1=-\mu,\ \lambda_{2,3}=\frac{-(\sigma_E+2\,\mu+\sigma_I)\pm\sqrt{(\sigma_E-\sigma_I)^2-4\,\beta\,\sigma_E}}{2}$$

According to (4.2), DEF is stable if

$$\sqrt{(\sigma_E-\sigma_I)^2-4\,\beta\,\sigma_E}<(\sigma_E+2\,\mu+\sigma_I)$$

In addition to stability of DFE, we have to discuss stability of EE.

Let us find eigenvalues of EE of SEI model. Consider $det[J(s^*,e^*,i^*)-\lambda I_3]=0$ that is

$$det[J(s^*,e^*,i^*)-\lambda I_3]=det\begin{bmatrix}-\beta\,i-\mu-\lambda & 0 & -\beta\,s\\ \beta\,i & -\sigma_E-\mu-\lambda & \beta\,s\\ 0 & \sigma_E & -\sigma_I-\mu-\lambda\end{bmatrix} \tag{20}$$

To find eigenvalues, characteristic equation will be considered as

$$\lambda^3-S_1\lambda^2+S_2\lambda-det[J(s^*,e^*,i^*)]=0$$

where S_1 =Trace of $J(s^*,e^*,i^*)=-(3\mu+\beta\,i+\sigma_E+\sigma_I)$, $S_2=$ sum of minors of diagonal elements of

$$J(s^*,e^*,i^*)=(\sigma_E+\mu)\,(\sigma_I+\mu)-\beta\,s\,\sigma_E+(\beta\,i+\mu)(\sigma_E+2\,\mu+\sigma_I),$$

$$det[J(s^*,e^*,i^*)]=-(\beta\,i+\mu)(\sigma_E+\mu)\,(\sigma_I+\mu)+\beta\,\mu\,s\,\sigma_E.$$

Thus, Characteristic equation is

$$\lambda^3+(3\mu+\beta\,i+\sigma_E+\sigma_I)\,\lambda^2+[(\sigma_E+\mu)\,(\sigma_I+\mu)-\beta\,s\,\sigma_E+(\beta\,i+\mu)(\sigma_E+2\,\mu+\sigma_I)]\lambda$$
$$+[(\beta\,i+\mu)(\sigma_E+\mu)\,(\sigma_I+\mu)-\beta\,\mu\,s\,\sigma_E]=0.$$

Now, compare with $\lambda^3 + a_1\lambda^2 + a_2\lambda + a_3 = 0$, we get

$$a_1 = (3\mu + \beta\, i + \sigma_E + \sigma_I)$$

$$a_2 = [(\sigma_E + \mu)(\sigma_I + \mu) - \beta\, s\, \sigma_E + (\beta\, i + \mu)(\sigma_E + 2\,\mu + \sigma_I)]$$

$$a_3 = [(\beta\, i + \mu)(\sigma_E + \mu)(\sigma_I + \mu) - \beta\, \mu\, s\, \sigma_E].$$

Threfore, from lemma (4.1), EE is stable if $a_1 > 0, a_2 > 0, a_3 > 0, a_1 a_2 - a_3 > 0$.

Now, we have to calculate basic reproductive number (R_0) and discuss stability according to that

- **Basic Reproductive Number** R_0

The basic reproductive number (R_0) is define as the number of secondary infectious that one infectious individual create over the duration of the infectious period, provided that every one else is susceptible.

The biological interpretation of R_0 is that if

$$R_0 < 1 \;\Rightarrow\; \text{Infection dies out.}$$

$$R_0 > 1 \;\Rightarrow\; \text{Infection persist.}$$

To compute basic reproductive number R_0 of our model, we employ the NGM as applied by Diekmann et. al.[19]. We will refer the second and third equations of (17) as the linearized infection subsystem as it only describe the production of new infected and changes in the states of already existing infected. The matrix

$$F = \begin{bmatrix} 0 & \beta \\ \sigma_E & 0 \end{bmatrix} \tag{21}$$

corresponding to transmissions and the matrix

$$V = \begin{bmatrix} -\sigma_E - \mu & 0 \\ 0 & -\sigma_I - \mu \end{bmatrix} \tag{22}$$

to transitions. Thus

$$V^{-1} = \begin{bmatrix} \frac{-1}{\sigma_I + \mu} & 0 \\ 0 & \frac{-1}{\sigma_E + \mu} \end{bmatrix} \tag{23}$$

$$FV^{-1} = \begin{bmatrix} 0 & \frac{-\beta}{\sigma_E+\mu} \\ \frac{-\sigma_E}{\sigma_I+\mu} & 0 \end{bmatrix} \tag{24}$$

Therefore, $det[FV^{-1} - \lambda] = 0 \Rightarrow \lambda^2 - \frac{\beta\,\sigma_E}{(\sigma_E+\mu)(\sigma_I+\mu)} = 0.$

As per the NGM, R_0 is the dominant eigenvalue of matrix FV^{-1}, hence

$$R_0 = \sqrt{\frac{\beta\,\sigma_E}{(\sigma_E+\mu)(\sigma_I+\mu)}}.$$

By using values of $\beta = 1.7$, $\sigma_E = \frac{1}{14} = 0.07142857$, $\sigma_I = \frac{1}{5} = 0.2$, $\mu = 0.00001956$, we obtain

$$R_0 = 2.92$$

According to theory, infection persist as $R_0 > 1$, which result in Pandemic situation in India. So authors will recommend to the government to increase measures for reducing R_0 (i.e. < 1) which control Pandemic situation. This is possible by reducing contact rate between peoples through effective social distancing, lockdown, by taking safety measures.

5. Numerical Simulations

In this section, we obtain the solution of fractional SEI model (2) by Adomian Decomposition Method as discussed in previous section.

Consider the series solution of system (2) as

$$u_i = \sum_{j=0}^{\infty} u_{i,j}$$

where $u_1 = S$, $u_2 = E$, $u_3 = I$

Thus

$$u_i = u_i(0) + I^{\alpha}[G_i(t, u_1, u_2, u_3)]$$

Consider

$$G_1(t, u_1, u_2, u_3) = -\frac{\beta}{N} u_1 u_3 + \mu N - \mu u_1$$

$$G_2(t, u_1, u_2, u_3) = \frac{\beta}{N} u_1 u_3 - (\sigma_E + \mu) u_2$$

$$G_3(t, u_1, u_2, u_3) = \sigma_E u_2 - (\sigma_I + \mu) u_3.$$

By using (14), we obtain the Adomian polynomial as follow

$$
\begin{aligned}
A_{10} &= -\frac{\beta}{N} u_{10}u_{30} + \mu N - \mu u_{10}, \\
A_{11} &= -\frac{\beta}{N} [u_{10}u_{31} + u_{11}u_{30}] - \mu u_{11} \\
A_{12} &= -\frac{\beta}{N} [u_{10}u_{32} + u_{11}u_{31} + u_{12}u_{30}] - \mu u_{12} \\
A_{20} &= \frac{\beta}{N} u_{10}u_{30} - (\sigma_E + \mu)u_{20} \\
A_{21} &= \frac{\beta}{N} [u_{10}u_{31} + u_{11}u_{30}] - (\sigma_E + \mu)u_{21} \\
A_{22} &= \frac{\beta}{N} [u_{10}u_{32} + u_{11}u_{31} + u_{12}u_{30}] - (\sigma_E + \mu)u_{22} \\
A_{30} &= \sigma_E u_{20} - (\sigma_I + \mu)u_{30} \\
A_{31} &= \sigma_E u_{21} - (\sigma_I + \mu)u_{31} \\
A_{32} &= \sigma_E u_{22} - (\sigma_I + \mu)u_{32}.
\end{aligned}
$$

The Adomian decomposition series given in (10), leads to following result

$$
\begin{aligned}
u_{10} &= 1300000000,\, u_{1(n+1)} = I^{\alpha}[A_{1n}] \\
u_{20} &= 1300,\, u_{2(n+1)} = I^{\alpha}[A_{2n}] \\
u_{30} &= 44,\, u_{3(n+1)} = I^{\alpha}[A_{3n}].
\end{aligned}
$$

We obtain, the first three iterations of the solution of fractional SEI model of COVID-19 for India as follows

$$S = u_1 = 1300000000 - 74.80\frac{t^{\alpha}}{\Gamma(\alpha+1)} - 142.89421783\frac{t^{2\alpha}}{\Gamma(2\alpha+1)} + 15.39024526\frac{t^{3\alpha}}{\Gamma(3\alpha+1)} + \cdots$$

$$E = u_2 = 1300 - 18.082569\frac{t^{\alpha}}{\Gamma(\alpha+1)} + 144.18763805\frac{t^{2\alpha}}{\Gamma(2\alpha+1)} - 20.53981631\frac{t^{3\alpha}}{\Gamma(3\alpha+1)} + \cdots$$

$$I = u_3 = 44 + 84.05628036\frac{t^{\alpha}}{\Gamma(\alpha+1)} + -18.10451226\frac{t^{2\alpha}}{\Gamma(2\alpha+1)} + 6.96018669\frac{t^{3\alpha}}{\Gamma(3\alpha+1)} + \cdots$$

Next, We have analysed the above model by considering the assumptions given below and further estimating or fitting various parameters given by table

(i) $\mu_I = \mu_0 = \mu$ that is the emigration from the population is equal to emigration into population.

(ii) $\frac{1}{D_E} = \sigma_E$ and $\frac{1}{D_I} = \sigma_I$.

(iv) Average exposed(Incubation) period is 14 days and average infection period is 5 days [24].

(vi) Initial case are only from emigrated people (i.e. persons having foreign travel history).

(vii) Initial rate of transmission is 1.7

Parameter	Description	Value	Reference
S	Susceptible population	1300000000	[36]
E	Exposed population	1300	Fitted
I	Infected population	44	Fitted
β	Infection rate	1.7	Fitted
σ_E	Reciprocal of average exposed period	0.07142857	Estimated
σ_I	Reciprocal of average infected period	0.2	Estimated
μ	rate of emigration	0.00001956	Estimated

TABLE 1. The parametric values for Fractional SEI model of COVID-19 for India.

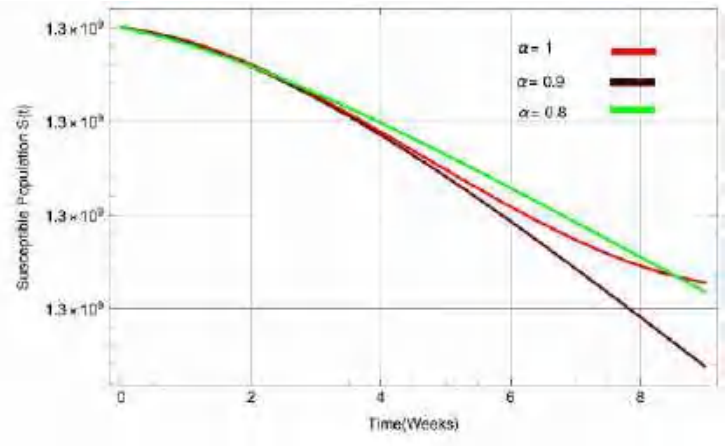

FIGURE 2. $S(t)$ for $\alpha(= 1, 0.9, 0.8)$

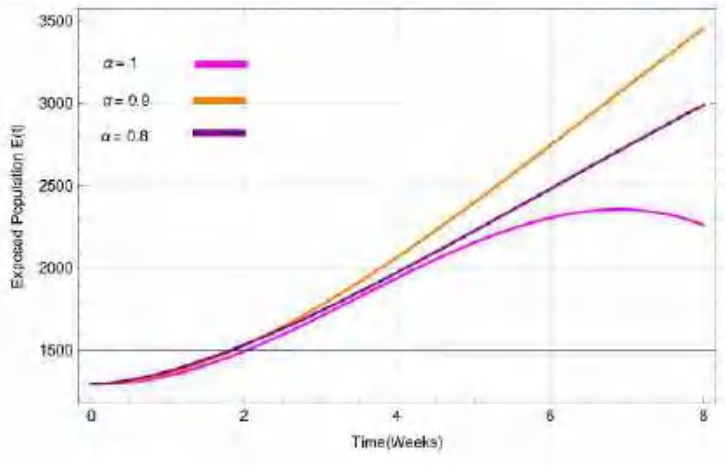

FIGURE 3. $E(t)$ for $\alpha(=1, 0.9, 0.8)$

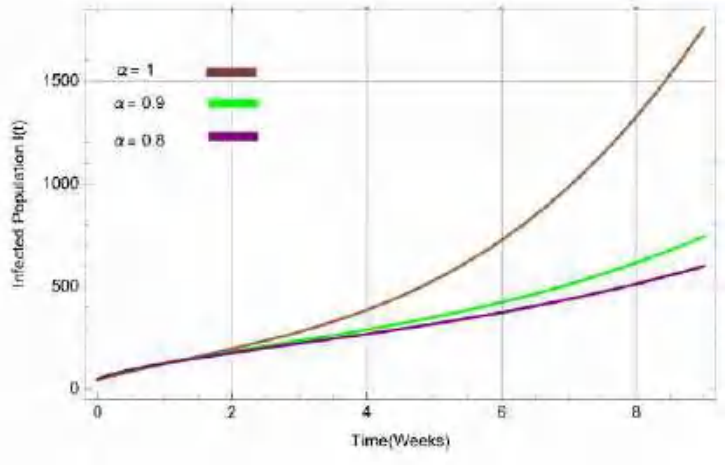

FIGURE 4. $I(t)$ for $\alpha(=1, 0.9, 0.8)$

Figs. 2, 3 and 4 shows the graphical representation of suspectable population $S(t)$, exposed population $E(t)$ and infected population $I(t)$ for various values of $\alpha(=1, 0.9, 0.8)$ using Adomian Decomposition method which predicts that this method can foresee the conduct of said variables precisely for the considered region. We observe that infection dies out slowly as value of α decreases. Hence, the non-integer order has a significant effect on the dynamics of SEI model of COVID-19 for India.

6. CONCLUSIONS

In this work, we have developed fractional SEI mathematical models and analysed dynamics of COVID-19, which is Pandemic throughout the world. Further, we have obtained series solutions of this model by Adomian Decomposition Method. We found basic reproduction number for this disease is $R_0 = 2.92$, which is unstable because it is greater than one. We also observe that R_0 is depend upon β and μ(note that σ_E and σ_I are constant). Results of above mathematical model are agree with recommendation of WHO that "It is still possible to interrupt virus spread, provided that countries put in place strong, measures to direct disease only". To keep $R_0 < 1$ that is asymptotically stable, we have to control β specially. This can be done by promoting social distancing measures, avoid large social gatherings, applying lock down and travel ban. To control μ, we may increasing effectiveness of passenger screening at airports. To stop spread of virus Indian government has already suspended all commercial passenger flight from 23^{rd} March 2020. Also, declare lock down from 25^{th} March 2020. This steps will help to reduce β and μ and hence R_0. We further Also, we represented solution graphically by Mathematica software. However, the result obtained above is depends on the limited data available in various research paper and note that real situation at initial stage of transmission is may be different.

CONFLICT OF INTERESTS

The author(s) declare that there is no conflict of interests.

REFERENCES

[1] A. Al-Omari, H.-B. Schuttler, J. Arnold, T. Taha, Solving nonlinear systems of first order ordinary differential equations using a Galerkin finite element method, IEEE Access. 1 (2013), 408–417.

[2] H. Wang, Z. Wang, Y. Dong, R. Chang, et al. Phase-adjusted estimation of the number of Coronavirus Disease 2019 cases in Wuhan, China, Cell Discov. 6 (2020), 10.

[3] H. Jafari, V. Gejji, Solving a system of nonlinear differential equations using Adomian Decomposition, J. Comput. Appl. Math. 196 (2006), 644-651.

[4] G. Hojjati, M.Y. Rahimi Ardabili, S.M. Hosseini, A-EBDF: an adaptive method for numerical solution of stiff systems of ODEs, Math. Computers Simul. 66 (2004), 33–41.

[5] https://www.mohfw.gov.in/

[6] I. Podlubny, Fractional Differential equation, Academic Press, San Diago (1999).

[7] J. Biazar, E. Barbolian, R. Islam, Solution of system of ordinary differential equations by Adomian decomposition Method, Appl. Math. Comput. 147 (2004), 713-719.

[8] K. B. Oldham, J. Spanier, The Fractional Calculus, Academic Press, New York (1974).

[9] K. Rock, S. Brand, J. Moir, M.J. Keeling, Dynamics of infectious diseases, Rep. Prog. Phys. 77 (2014), 026602.

[10] D. Kumar, J. Singh, D. Baleanu, S. Rathore, Analysis of a fractional model of the Ambartsumian equation, Eur. Phys. J. Plus. 133 (2018), 259.

[11] D. Kumar, F. Tchier, J. Singh, D. Baleanu, An efficient computational technique for fractal vehicular traffic flow, Entropy. 20 (2018), 259.

[12] M. Ozair, U. Saeed, T. Hussain, Frcational order SEIRS model, Adv. Stud. Biol. 6 (2014), 47-56.

[13] M.A. Khan, A. Atangana, Modeling the dynamics of novel coronavirus (2019-nCov) with fractional derivative, Alexandria Eng. J. 59 (2020), 2379–2389.

[14] M.I. Syam, M. Al-Refai, Fractional differential equations with Atangana–Baleanu fractional derivative: Analysis and applications, Chaos Solitons Fractals: X. 2 (2019), 100013.

[15] N.E. Mastorakis, Numerical solution of non-linear ordinary differential equations via collocation method (finite elements) and genetic algorithms, WSEAS Trans. Inf. Sci. Appl. 2 (2005), 467-473.

[16] N. Dogan, O. Akin, Series solution of epidemic model, TWMS J. APP. Engg. Math. 2 (2012), 238-244.

[17] N. Ozalp, E. Demirci, A fractional order SEIR model with vertical transmission, Math. Computer Model. 54 (2011), 1–6.

[18] S. Narjes, B. S. Alshakhoury, Mathematical modelling and control of MERS-COV epidemics, Thesis, Texas Woman's University (Dec. 2017).

[19] O. Diekmann, J.A.P. Heesterbeek, M.G. Roberts, The construction of next generation matrices for compartmental epidemic model, J. R. Soc. Interface, 7 (2010), 873-885.

[20] B. Padma, Study of some mathematical models in population dynamics and epidemiology, Thesis, Birla Institute of Technology and Science Pilani, (2008).

[21] R. Singh, R. Adhikari, Age-structured impact of social distancing on the COVID-19 epidemic in India, ArXiv:2003.12055 [Cond-Mat, q-Bio]. (2020).

[22] S.G. Samko, A.A. Kilbass, O.I. Marichev, Fractional Integrals and Derivatives: Theory and Applications. Gordon and Breach, Langhorne (1993).

[23] A. Shaikh, A. Tassaddiq, K.S. Nisar, D. Baleanu, Analysis of differential equations involving Caputo–Fabrizio fractional operator and its applications to reaction–diffusion equations, Adv. Differ. Equ. 2019 (2019), 178.

[24] N. Shawagfeh, D. Kaya, Comparing numerical methods for the solutions of systems of ordinary differential equations, Appl. Math. Lett. 17 (2004), 323-328.

[25] B.R. Sontakke, A. Shaikh, Approximate solutions of time fractional Kawahara and modified Kawahara equations by fractional complex transform, Commun. Numer. Anal. 2 (2016), 218-229.

[26] B.R. Sontakke, A.S. Shaikh, K.S. Nisar, Approximate solutions of a generalized hirota-satsuma coupled KdV and a coupled mKdV systems with time fractional derivatives, Malays. J. Math. Sci. 12 (2018), 173-193.

[27] T.-M. Chen, J. Rui, Q.-P. Wang, Z.-Y. Zhao, J.-A. Cui, L. Yin, A mathematical model for simulating the phase-based transmissibility of a novel coronavirus, Infect Dis Poverty. 9 (2020), 24.

[28] V.A. Okhuese, Mathematical prediction for COVID-19 as a global pandemic, medRxiv 2020.03.19.20038794. (March 2020).

[29] Y. Bai, L. Yao, T. Wei, F. Tian, D.-Y. Jin, L. Chen, M. Wang, Presumed asymptomatic carrier transmission of COVID-19, JAMA. 323 (2020), 1406.

[30] S. Yuzbasi, An exponential collocation method for the solutions of the HIV infection model of CD4+ T cells, Int. J. Biomath. 9 (2016), 885-893.

[31] S. Yuzbasi, M. Karacayir, An exponential Galerkin method of HIVinfection model of CD4+ T-cells Comput. Bio. Chem. 67 (2017), 205-212.

[32] D. Kumar, F. Tchier, J. Singh, D. Baleanu, An efficient computational technique for fractal vehicular traffic flow, Entropy, 20 (2018), 259.

[33] D. Kumar, J. Singh, D. Baleanu, S. Rathore, Analysis of a fractional model of the Ambartsumian equation, Eur. Phys. J. Plus. 133 (2018), 259.

[34] B.R. Sontakke, A.S. Shaikh, K.S. Nisar, Approximate solutions of a generalized Hirota-Satsuma coupled KdV and a coupled mKdV systems with time fractional derivatives, Malays. J. Math. Sci. 12 (2018), 173-193.

[35] B.R. Sontakke, A. Shaikh, Approximate solutions of time fractional Kawahara and modified Kawahara equations by fractional complex transform, Commun. Numer. Anal. 2 (2016), 218-229.

[36] https://www.mohfw.gov.in/

UGC-CARE List

UGC-CARE List

You searched for **"journal of advanced scientific research"**. Total Journals : 1

Search:

Sr No	Journal Title	Publisher	ISSN	E ISSN	UGC CARE coverage years	Details
1	Journal of Advanced Scientific Research	Scienssage	NA	0976-9595	from June - 2019 to January - 2022	Discontinued from Jan. 2022

Showing 1 to 1 of 1 entries

Previous 1 Next

Modern Research in Chemical Studies

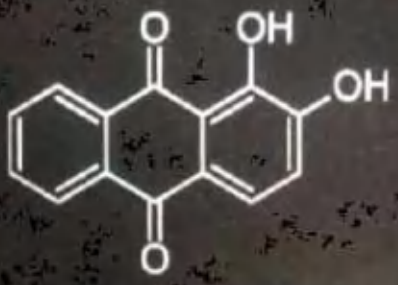

CHIEF EDITOR -
DR. DHONDIRAM TUKARAM SAKHARE

Volume - 1

Scripown
Publications

Published by
Scripown Publications,
2nd Floor, 304 and 305,
Pocket - 4 Sector - 22, Rohini,
Delhi, 110086, India
Email: scripownbooks@gmail.com

Kanpur Philosophers ISSN 2348-8301
International Journal of Humanities, Law and Social Sciences
Published Biannually by New Archaeological & Genological Society
Kanpur India

Vol. IX, Issue II (III) 2022

ROLE OF GOVERNMENT SCHEMES IN INDIA FOR RURAL DEVELOPMENT

Dr. Subhash Ramchandra Bhosale

Asst. Professor, Dept. Of Economics, Gokhale Education Society' S, RNC Arts, JDB Commerce and NSC Science College, Nashik Road. Nashik M.S. (India) 422101

Email: subhashbhosale1982@gmail.com

ABSTRACT

Rural development has garnered attention on a worldwide scale, in particular among nations on the path to industrialization, and it is of critical importance for a nation like India. The improvement of rural economies, particularly those parts of rural economies that are plagued by severe poverty, is the primary focus of rural development, and its primary objective is to raise those economies' overall levels of productive capacity. In addition to this, it highlights the necessity of addressing several urgent problems facing village economies, which are a barrier to growth and improvement in these places. The government of India has initiated a variety of programs aimed at fostering growth in the country's rural areas. The rural areas of India are plagued with a number of significant issues, the most significant of which are a lack of housing, a lack of infrastructure in villages, a lack of connectivity between towns and villages via all-weather roads, and a lack of employment opportunities in villages.

Keywords: Government schemes, rural development.

INTRODUCTION

There are a number of factors that reduce the amount of land that is suitable for farming, including buildings, roads, canals, parks, and other public locations. All of this is being done in order to provide accommodations for the country's rapidly expanding population. The challenge of the next century will be to increase biological yields to feed the ever-increasing population without causing damage to the ecological basis, despite the fact that land is becoming scarcer and water supplies are becoming depleted. This will have to be accomplished despite the fact that water supplies are becoming depleted and land is

becoming scarcer (Goyal et al., 2014). Therefore, this challenge shouldn't be considered as a demand or an imposition imposed on farmers by society, for which farmers would be accountable to shoulder the expense, but rather as a requirement and a plan to also protect their welfare and revenue. This is because: India possesses the resources necessary to properly address these challenges in a timely manner. This promise has the potential to be fulfilled through the implementation of government policies and the deployment of funds for infrastructure, as well as through the formation of proactive synergies among the many industries that play important roles in agricultural and rural development. [Citation needed] (MoRD, 2012). There is a tremendous amount of growth potential in Indian agriculture that has not yet been realized, and the National Policy on Agriculture seeks to realise this potential by, Increasing rural infrastructure to support faster agricultural development, encouraging value addition, accelerating agrobusiness growth, creating jobs in rural areas, ensuring a fair standard of living for farmers and agricultural workers and their families, preventing migrant labor, and ensuring a fair standard of living for farmers and agricultural workers and their families are just a few of the objectives. (Braun et al., 2005).

The population of India as a whole was counted in 2011, and the results showed that 68.8 percent of the population lives in rural regions. This is equivalent to around 83.25 crore people living in the world. There is widespread agreement that in order for rural development projects to effectively combat rural poverty, they need to be both comprehensive and long-term in nature (IDFCRDN, 2014). It is anticipated that the Ministry of Rural Development would get Gross Budgetary Support (GBS) of Rs. 44,3261 crore during the XII Five Year Plan (2012-2017), which is an increase from the XI Plan's allocation of Rs. 29,1682 crore. This computation took into account the Top Priorities established by the Ministry (Prabha et al., 2015). Despite the fact that agriculture only accounts for 14% of GDP at this point, there are still a great number of individuals living in rural areas that rely on it as their primary source of income. For this reason, significant agricultural expansion is very necessary in order to increase participation. There are indications that the sector's performance is getting better as a direct result of the significant structural adjustments that are now being implemented (Sarkar, 2014). Since the implementation of the X Plan, agricultural expansion has quickened, and measures to diversify farming are making significant progress (GOI, 2012).

Out of India's total land area of 328.7 million hectares, 140.8 million hectares were reported as the net sown area, and 195.2 million hectares were the gross cropped area with a cropping intensity of 138.7%, according to the Ministry of Agriculture, Government of India (2014). India now has 328.7 million hectares of land in total. India's overall land area is therefore estimated to be 328.7 million hectares. These numbers were arrived at by analyzing the data from 2011-12. The amazing size of the nation may be assessed in terms of its landmass, which totals 328,7 million hectares in the country's whole. It is projected that there are 65,300,000,000 hectares of land that are irrigated actively. During the fiscal year 2013-2014 in India, it is projected that the Agriculture and Allied Sector was responsible for producing 13.9% of the country's Gross Domestic Product (GDP) (using prices from 2004-2005). To wit: (CSO-MoSPI, 2014). The proportion of the Agriculture and Allied Sector to the Gross

Domestic Product (GDP) at the prices of 2004-2005 has continuously fallen, going from 14.6% in 2010-11 to 13.9% in 2013-14. It is realistic to anticipate a fall in agriculture and associated industries' proportion of GDP in an economy that is fundamentally changing while also undergoing significant growth.

OTHER IMPORTANT SCHEMS AND PROGRAMS :

1. Rastriya Krishi Vikas Yojana (RKVY): During the meeting that took place on the 29th of May, 2007, the National Development Council (NDC) came to the conclusion that an additional Central Assistance Scheme called RKVY should be initiated. The National Democratic Congress passed a resolution that the Central Government and the governments of the individual states should come up with a plan to revitalize agriculture, and that agricultural development strategies should be reoriented to meet the needs of farmers. The NDC reaffirmed its commitment to achieving annual growth in the agricultural sector of 4% during the XIth plan.

2. Mission on Seed and Planting Material: In order to accommodate the new circumstances with the current plan, significant adjustments are required. The following is a list of some of the reasons why the current system needs to be restructured and why it should be launched in the form of a Mission:

There are nine sub-strategies under the present strategy. It is necessary to modify preexisting components of the scheme due to the ever-changing nature of the seed industry and the knowledge gained through the course of its implementation. Embracing these changes is essential for survival in the modern world. Changes are needed to the standards for seed storage, processing, and laboratories, among other things, as well as the "Seed Village Program" and the "Assistance for Boosting Seed Production in Private Sector." The pattern of assistance in a couple of the other parts also needs to be modified. With the 2005-2006 school year, the strategy that has been in the works for some time will finally be put into effect. Transgenics, tissue culture, soil-less agriculture, and other methods of altering the genetic makeup of plants to increase crop yield are just a few examples of the rapidly developing technologies that are altering the methods traditionally used to produce seeds. The interests of farmers are being safeguarded by a renewed emphasis on seed quality certification. Because of these changes, the country's social and economic climate has also undergone significant shifts. The private sector is increasingly involved in many areas of the economy, including agriculture, thanks to the extensive liberalization of the economy.

The Submission on Seed and Planting Material will incorporate the ongoing Central Sector Plan Schemes for the XI plan, I These two initiatives have been given the names Development and Strengthening of Infrastructure Facilities for Production and Distribution of Quality Seeds (DSIS) and (ii) Implementation of PVP Legislation, respectively. Both of these initiatives are being carried out in conjunction with one another (PPVFRA). As a direct consequence of this, there will be 26 new components added to the seed business, and another 6 are being proposed for the protection of plant varieties and the rights of farmers. These 26 additions can be sorted into 10 categories: seed planning, seed production, varietal

replacement, specific interventions for public seed producing organisations, quality control with 2 new additions and 2 existing ones, contingency planning, public-private partnerships (PPPs) in the seed sector, funding for international treaty implementation, national campaigns, and capacity building. The Protection of Plant Varieties and Farmers' Rights Act (PPVFRA) Implementation Scheme, which under the XI Plan consisted of a total of 12 separate parts, is currently in the process of being expanded to include a total of 18 distinct components.

Division-wise Programs and Schemes

The Integrated Scheme for Agricultural Marketing is a component of the program known officially as the Agricultural Marketing (Central Sector Schemes) program. On April 1, 2014, the strategy was put into action with the objective of achieving the goals of establishing an environment that is user- and investment-friendly as well as streamlining the process. The several programs from the VI plan that were continued into the age of the XI plan were combined into a single program that was given the name "Integrated Scheme for Agricultural Marketing" in order to facilitate the accomplishment of this purpose. Its goals are to I encourage the implementation of Agri market reforms; (ii) connect farmers with potential buyers; (iii) expand farmers' access to Agri market information; and (v) back the quality certification of agricultural products. I. Its goals are to encourage agrimarketing by facilitating the development of marketing and agribusiness infrastructure, including cold storage. (ii) Its goals are to connect farmers with potential buyers. (iii) Its goals are to In order to accomplish these goals, it will be required to set up a marketing and agriculture infrastructure. ISAM was given a total of Rs. 4548.00 crore as part of the XII Plan.

A deeper inspection of the ISAM system shows each of its five components, which are as follows: The objective of the Agricultural Marketing Infrastructure (AMI) program is to strengthen the basis of the agricultural market via the construction of infrastructure projects such as storage facilities and value chain projects. [the Agricultural Marketing Infrastructure, Grading, and Standardization (AMIGS) project and the Grameen Bhandaran Yojana (GBY) project have been integrated into a single AMI program] Choudhary Charan Singh was the leader. (iii) Agri-Business Development (ABD) via Project Development Facility (PDF) and Enhanced Agmark Grading Facilities (SAGF); (iv) Enhanced Agmark Grading Facilities (SAGF); and (v) Training, Research, and Consultation. These are the five components that make up the National Institute of Agriculture Marketing. The second one is the Network for the Research and Sharing of Data in the Marketing Industry. (MRIN) (CCSNIAM).

Gramin Bhandaran Yojana (also known as Rural Godown Schemes, or RGS)

The program was active from the 1st of April in 2001 through the 31st of March in 2014. To meet the demands of farmers for cold storage of farm goods, cold processing of farm goods, cold storage of consumer goods, and cold storage of agricultural inputs; to encourage the grading, standardization, and quality control of agricultural products to improve their marketability; the provision of the pledge financing facility to farmers to prevent them from being forced to sell their crops at a loss as soon as they are harvested all of these things are

done to increase the marketability of such produce. These are the primary objectives of the program. Other objectives include: to meet the demands of farmers for cold storage of farm goods, cold processing of farm

With the goal of building scientific storage capacity and supporting facilities in geographically isolated locations, a scheme named "Rural Godowns" has been devised. In order to accomplish this objective, we will provide incentives to the public, private, and cooperative sectors all over the country to increase their investments in the development of storage infrastructure. As part of the plan, a subsidy equal to 25 percent of the total costs of the project will be provided retroactively. When we narrow our focus to just the communities of the NE States, Tribal and Hilly regions, and SC and ST states, this number jumps to 33.3%. Individuals, groups of individuals, partnerships, proprietary firms, Agricultural Produce Marketing Committees, Marketing Boards, Agro Processing Corporations, and Corporations are all examples of prospective promoters for the development of rural godowns. Other possible promoters include corporations and cooperatives.. These advocates might be able to get financial support from the Ministry of Rural Development.

OBJECTIVE OF THE STUDY

1. To study government schemes in India.
2. To study rural development.

METHODOLOGY

The data used in this investigation came from a variety of different sources, including primary and secondary ones. Information was gathered from secondary sources such as government agencies, the ministries of Human Resource Development and Agriculture, the papers of the five-year plan, the National Sample Surveys Organization (NSSO), reports and publications from the government, a variety of magazines and other printed content, and so on are some examples. The information was utilized in the process of making judgments on policy. In order to analyze the secondary data, appropriate statistical methods, such as percentages and averages, amongst others, and those that are tailored to the requirements of the study have been utilized.

The primary data came from in-depth interviews carried out with locals living in Haryana's myriad of different districts. The selection of the samples to be used in the analysis of the field research data was carried out with the application of the following criteria.

DATA ANALYSIS

Socio-Economic Profile of Sample Household

Table 1 displays the distribution of the grantees by gender. There are around 67.6% males and 32.5% females involved in SGSY programs . However, men make up 73.5% of SGRY scammers compared to women's 26.5%. In both plans, it is safe to generalize that men make up 70.5% of the population and women 29.5%.

35 and 45% of our respondents were classified as illiterate, respectively, in Table 1. And somewhere between 27% and 30% of them had never even finished elementary school. A very low fraction of them (between 9% and 8.10%) had completed intermediate-level schooling, whereas the vast majority had only completed fifth through tenth grade (28.5 percent and 15 percent respectively). This means that most recipients in the sample come from low-income backgrounds and have poor levels of education, which is a key source of their economic insecurity and lack of work. This has led to suggestions that efforts to improve schooling in rural regions receive more resources than they deserve.

Figures from Table 1 show that 54.5% of SGSY recipients were from scheduled castes, 27.0% were from backward castes, and 18.5% were from upper castes. Whereas 58% of SGRY residents self-identified as SC, 27.5 % as BC, and 14.5 % as upper caste, none of these categories applied to those living in SGY. This proves that a respectable amount of care was put into picking winners. Finally, it was established that 56.25% of beneficiaries are SC, 27.25% are BC, and 14% are general.

Table 1: Income and Education Levels of Representative Family Current Social and Economic Status Distribution of SGSY and SGRY Recipients

Socio-Economic Status		SGSY	SGRY	TOTAL
Gender Status	Male	6(67.1)	8 (73.5)	4 (70.6)
	Female	3 (32.5)	6 (26.5)	5(29.4)
Education Status	Illiterate	8(35)	3 (45)	4(40.0)
	Primary	4 (27.5)	4 (30)	3 (28.9)
	Middle	5 (28.5)	3 (15)	4(21.8)
	Above 10^{th}	4 (9)	5 (10)	7 (9.5)
Social Status	SC	5 (54.5)	4 (58)	8 (56.25)
	OBC	3 (27)	5(27.5)	5(27.25)
	General	4 (18.5)	4(14.5)	3 (14.24)
Economic Status (by types of Ration card)	APL	3 (31.5)	3 (28)	4 (29.75)
	BPL	5 (69.5)	5 (72)	3 (70.25)
Total		50 (100)	50 (100)	50 (100)

Table 1 provides a breakdown of SGSY and SGRY recipients by ration card number. A little over a third of SGSY's beneficiaries are in the APL range, while the remaining 69% are in the BPL range. As an alternative, under SGRY schemes, 28% of beneficiaries come from APL and 72% come from BPL. In the end, we can say that 30% of the beneficiaries across both schemes fall into the category of APL, while 70% fall into the category of BPL.

Table 6.2: Reasons we provide loans through the SGSY

pian	Dairy	Tailoring	Khachar rahadi	Shop	Other	Total
SGSY	5(70)	8 (7)	10 (4)	15 (7.5)	12 (11.5)	50(100)

In Table 6.2, you can see the various ways that credit under schemes is put to use. A quick glance at the data shows that there is no SGRY loan available because the plan is only for salary employees.

The dairy industry receives 74% credit, the tailoring industry receives 7% credit, and the khachar raddi industry receives 5% credit all thanks to SGSY initiatives. Because the interest rates for dairy loans are higher than those for stores and other uses (7.5 percent versus 6.5 percent), borrowers in SGSY schemes tend to favor the dairy category.

CONCLUSION

The Indian government has recently introduced a number of brand new programs , the most notable of which are Such government programs include the Pradhan Mantri Awaas Yoiana Gramin (PMAY-G) plan to supply housing, the Mahatma Gandhi National Rural Employment Guarantee Act (MGNREGA), and the Pradhan Manthi Gram Sadak Yoiana (PMGSY) program to build roads in rural areas. These programs are all aimed at helping India's rural people. These three programs are making major contributions to rural development in India and are thus deserving of your attention. According to the study, 44.54 lakh homes were constructed in the 2017-2018 fiscal year as a direct result of the Pradhan Mantri Awaas Yoiana Gramin (PMAY-G) program. Building 1.00 crore new homes by March of 2019 serves as a point of reference. In the 2017–18 fiscal year, PMGSY roads averaged 134 kilometers per day, breaking the previous record of 73 kilometers per day achieved between 2011 and 2014. The result is a 93% improvement in productivity on the building site. During the 2017–2018 fiscal year, MGNREGA helped produce more than 234,25 crore person days of wage employment across more than 177 lakh positions, delivering income for more than 5.12 crore households. A strong educational foundation may be an effective weapon in the struggle to eliminate social problems like these.

REFERENCES

[1]. D. Gangopadhyay, A.K. Mukhopadhyay & Pushpa Singh (2008),‘ Rural Development: A Strategy for Poverty Alleviation in India’, S & T for Rural Development and Inclusive Growth, India, Science and Technology.

[2]. Dr. C. Chandramouli (2011), ‘Rural Urban Distribution of Population’, Ministry of Home Affairs, Census of India 2011, New Delhi, 15th July, 2011.

[3]. Dey, S., & Bedi, A. (2010), ‘The National Rural Employment Guarantee Scheme in Birbhum’, Economic and Political Weekly, VolXLV, Issue - 41, pp-19-25.

[4]. Farooq Ahmad Ganiee (2014), ‘Transforming Rural India (2018-19), Ministry of Rural Development, Government of India’, International Journal of English Language, Literature and Humanities, Vol-1, Issue –V, Feb 2014.

[5]. London; George Allen and Unwin Ltd., (1954), ‘Economic Development with unlimited supplies of labour’, in the Manchester School 22 May; pp-139-32

[6]. Nandini Francis (2015), ‘Sustainable Rural Development through Agriculture: An Answer to Economic Development in India’, International Journal of Current Research, Vol.7, Issue-03, pp-13614 – 13618, March 2015.

[7]. Shah, M. (2004), 'National Rural Employment Guarantee Act: A Historic opportunity', Economic and Political Weekly, Vol-XXX, Issue - 39, PP-5287-5291

[8]. Surbhi Agrawal (2016), 'Pre- Post Rural Development', International Journal of Socio – Legal Analysis and Rural Development, Vol2, Issue – 1, PP-97-106.

[9]. Ministry of rural development, Govt. of India, Chapter VII- Rural Development, pp. 88-99.

[10]. Planning Commission, Govt. of India, Eleventh five year plan (2007-2012) Vol. I, Inclusive growth.

[11]. Overview of the National Conference of Ministers of State Governments of Rural Development, Panchayati Raj and Rural Roads, 27- 28 January, 2003, New Delhi.

[12]. Arora, R.C. (1986). Integrated Rural Development, S. Chand & Com. New Delhi, 34 p.

ScienSage

Journal of Advanced Scientific Research

Available online through http://www.sciensage.info

ISSN
0976-9595
Research Article

NOVEL [DBN][HSO_4] MEDIATED FACILE AND EFFICIENT SYNTHESIS OF DIHYDROPYRIMIDO [*4, 5-D*]PYRIMIDINE DERIVATIVES

Vishal U. Mane[1,2], Dhananjay V. Mane*[2,3]

[1]*Department of Chemistry, RNC Arts, JDB Commerce &NSC Science College, Nashik, Maharashtra, India*

[2]*Department of Chemistry, Shri Chhatrapati Shivaji College, Omerga, Dist. Osmanabad, Maharashtra, India*

[3]*Yashwantrao Chavan Maharashtra Open University, Nashik, Maharashtra, India*

**Corresponding author: dvmane11@gmail.com, mane_dv@ycmou.digitaluniversity.ac*

ABSTRACT

A [DBN][HSO_4] bronsted acidic ionic liquid promoted condensation followed by cyclization protocol has been developed for the first time by a successive reaction of aldehydes, barbituric acid and urea to afford dihydropyrimido [*4,5-d*] pyrimidine derivatives in high to excellent yields under microwave irradiation (MW=240W). The ionic liquid provided the capability to allow a variability of functional groups, easy workup, short reaction times, and recyclability of the catalyst, high yields and solvent-free conditions, thus providing economic and environmental advantages.

Keywords: [DBN][HSO_4], Environmentally benign, Dihydropyrimido [*4,5-d*] pyrimidine, Multicomponent reactions, Microwave irradiation.

1. INTRODUCTION

1,4-Dihydropyridine (DHP) motif represents the heterocyclic unit of significant pharmacological competence [1]. Dipyrimido-dihydropyridines having DHPs as privileged pharmacophore provide imperative ligands for biological receptors [2]. These compounds, although described for the first time more than a century ago, have recently been recognized as vital drugs such as felodipine and amlodipine (Fig. 1) as antihypertensive
and calcium channel blockers. Moreover, DHPs also act as nicotinamide adenine dinucleotide (NADH) mimics for the reduction of carbonyl compounds and their derivatives [3]. In human body, the main metabolic route of dihydropyridine drugs involves their oxidation to pyridines catalyzed by cytochrome P450 in liver [4]. Pyrimidines represent one of the most biologically, and pharmaceutically active *N*-containing class of compounds [5]. Pyrimidine derivatives serve as antineoplastic [6], antibacterial [7], anti-HIV [8], antibiotic [9], antifungal [10], and antitubercular agents [11]. Pyrimidine bases like thymine, cytosine, and uracil are the essential building blocks of nucleic acids. Many established drugs containing a pyrimidine nucleus are reported in the literature, namely 5-fluorouracil as an anticancer drug [12], idoxuridine as an antiviral drug [13] etc. When this pyrimidine moiety is fused with different heterocycles, it results in hybrid scaffolds with improved activity. Pyrido [*2,3-d*] pyrimidines are such pyrimidine based hybrid scaffolds, which have attracted considerable attention due to their broad biological and medicinal applications [14].

Barbituric acid is one of the most important nitrogen-containing heterocyclic systems; it is found in various natural and synthesized compounds of anti-inflammatory, analgesics, anesthetics, drugs, anticancer drugs, anxiolytics, HIV/AIDS protease inhibitors, and others [15a]. Phenobarbital and Riboflavin (vitamin B_2) are vital molecules in the market having barbituric acid as one of the pharmacophores (Fig. 1) [15b]. Thus, the extension of synthetic route for the construction of this molecule using an reusable, economical, nontoxic and mild catalyst is of massive importance from the academic and industrial points of view. Even though various modes have been reported in the literature, these reactions can be accomplished under a variability of tentative conditions, and several improvements have been reported in recent years, such as Zn_2þ@KSF [16a], Fe_3O_4@SiO_2 [16b], SiO_2 composite [17] and L-proline [18] as catalysts which usually requires forcing conditions, long reaction times and complex synthetic pathways. Therefore, there is a need to develop more efficient and sustainable chemical process for the synthesis of pyrimido [4,5-d] pyrimidines.

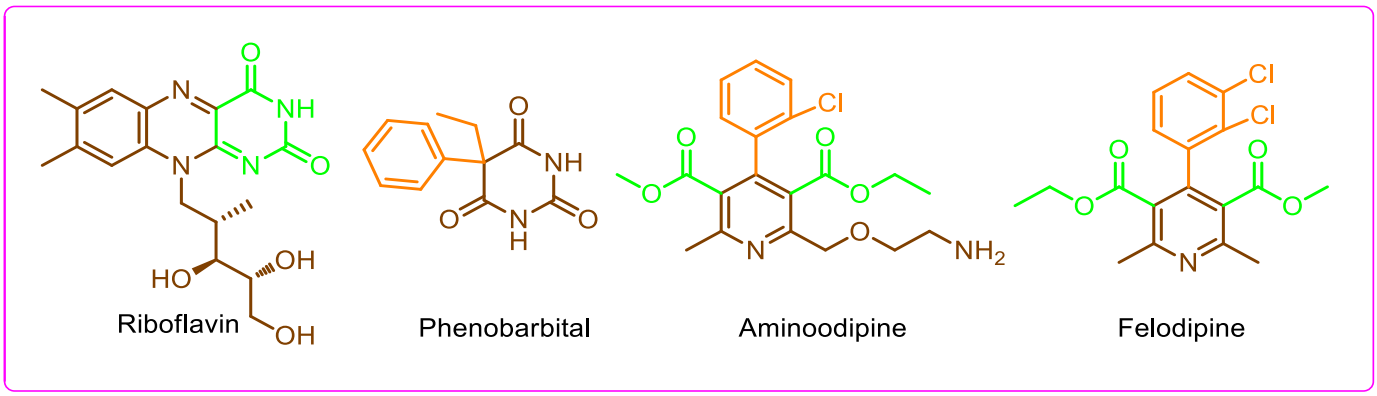

Fig. 1: Dihydropyrimido[*4,5-d*]pyrimidine incorporated bioactive molecules

Multicomponent reactions (MCRs) have received increasing attention due to their simplicity, efficiency, atom economy, short reaction times and the possibility for diversity-oriented synthesis [19]. Moreover, the incorporation of solvent-free methods in MCRs makes the process cleaner, safer and easier to perform [20]. Thus, the utilization of MCRs coupled with environmentally benign solvent-free condition is highly desirable. Owing to an extensive range of MCRs applications in different areas like the preparation of different structural scaffolds and the detection of new drugs, these types of reactions have drawn considerable attention in organic synthesis and pharmaceutical chemistry [21]. Besides, Ionic liquids (ILs) have taken the attention of the chemical community all over the globe as a green alternative option to traditional ecofriendly media for catalysis, synthesis, separation, and other several chemical tasks [22-27]. ILs include numerous exclusive properties, such as extensive liquid range, nonvolatility, low toxicity, high thermal stability, noncombustible, excellent solubility, and recyclability [28]. ILs act as "neoteric solvents" for a wide range of industrial and chemical processes. In recent times, ILs have been originating to be valuable as environmental friendly media for countless organic revolutions [29, 30]. Recently, DBN was widely used as catalysts in different research area. The combination of DBN with cation gives the formation of novel ionic liquids [31]. The large number of functionalized ILs has been considered for diverse purposes [32].

The use of microwave irradiation in combination with ILs, which has very high heat capacity, high polarity and no vapor pressure, and their high potentiality to absorb microwaves and convert them into heat energy, may accelerate the reaction very quickly. The synergy of microwave and ionic liquid in catalyst-free methodologies for the synthesis of heterocyclic compounds has attracted much interest because of the shorter reaction time, milder conditions, reduced energy consumption and higher product selectivity and yields [33].

As per our investigation, the existential of this work is to begin a rapid and efficient synthetic protocol for obtaining dihydropyrimido [*4,5-d*] pyrimidine derivatives under ecofriendly conditions. As an extension of emerging economic and efficient strategy to develop pharmaceutically and biologically significant molecules, herein, we reported synthesis of library of dihydro-pyrimido [*4,5-d*] pyrimidine derivatives promoted by synergistic effect of ionic liquid without any added catalyst in good to excellent yields.

2. EXPERIMENTAL

2.1. Material and methods

All the chemicals and solvents were purchased with high purities and used without further purification. The progress of the reaction was monitored by gas chromatography (GC) with a flame ionization detector (FID) with a capillary column (30 m 0.25 mm 0.25 lm) and thin layer chromatography (using silica gel 60 F-254 plates). The products were visualized with a 254 nm UV lamp. Products were purified by column chromatography on 100-200 mesh silica gel. The 1H NMR spectra were recorded on 400 MHz spectrometers using tetramethylsilane (TMS) as an internal standard. The ^{13}C NMR spectra were recorded at 100 MHz and chemical shifts were reported in parts per million (d) relative to tetramethylsilane (TMS) as an internal standard. Coupling constant (J) values were reported in hertz (Hz). The splitting patterns of the proton are described as s (singlet), d (doublet), dd (doublet of doublet), t (triplet), and m (multiplet) in

1H NMR spectroscopic analysis. The products were confirmed by ^{1}H and ^{13}C NMR spectroscopy analysis.

2.2. Preparation of [DBN][HSO_4]

General Procedure for the Synthesis of [DBN][HSO_4] are given in supporting information.

2.3. General Procedure for Synthesis of dihydropyrimido [4,5-d] pyrimidine derivatives (4a-l)

A mixture of aryl aldehyde (**1a**) (100 mg), barbituric acid (**2a**) (120 mg), urea (**3**) (56 mg) and ionic liquid [DBN][HSO_4] 20 mol% were kept under microwave irradiation at 280 W for 7 min. The progress of the reaction was monitored by thin layer chromatography (*n*-Hexane/EtOAc 8:2). Further, addition of ice cold water (10mL) was added and stirred for 15 min and filtered. The obtained solid was filtered, washed with cold water to remove the ionic liquid. The obtained crude compounds were recrystallized using ethanol. The synthesized compound is confirmed by MP, ^{1}H NMR and ^{13}C NMR spectra.

2.3.1. Characterization of 5-phenyl-5,6-dihydro-pyrimido[4,5-d]pyrimidine-2,4,7(1H,3H, 8H)-trione (4a)

The compound **4a** was synthesized from condensation reaction **1a, 2** and **3** as white solid; Mp: 243-244 °C; Yield 93%; 1H NMR (400 MHz, CDCL3, ppm): 11.36 (s, 1H, NH), 11.20 (s, 1H, NH), 10.25 (s, 1H, NH), 8.38 (s, 1H, NH), 7.20 (t, J = 7.8 Hz, 2H), 7.14-7.00 (m, 3H), 5.38 (s, 1H). ^{13}C NMR (101 MHz, $CDCl_3$) δ 163.01 (C=O), 158.32 (C=O), 154.24 (C=O), 142.2 (C=C), 136.1 (Ar-C=C), 128.5 (Ar-C=C), 126.5 (Ar-C=C), 122.70 (Ar-C=C), 90.22 (Ar-C=C) and 45.36 (Ar-C).

2.3.2. Characterization of 5-(m-tolyl)-5,6-dihy-dropyrimido[4,5-d]pyrimidine-2,4,7 (1H, 3H,8H)-trione (4b)

The compound **4b** was synthesized from condensation reaction **1b, 2** and **3** as white solid; Mp: 202-204 °C; Yield: 86%; ^{1}H NMR (400 MHz, CDCl3) δ 11.50 (s, 1H, NH), 11.28 (s, 1H, NH), 10.10 (s, 1H, NH), 8.32 (s, 1H, NH), 7.12-6.94 (m, 3H), 6.82 (d, J = 6.8 Hz, 1H), 5.20 (s, 1H) and 2.25 (s, 3H); ^{13}C NMR (101 MHz, $CDCl_3$) δ 165.1 (C=O), 159.24 (C=O), 153.26 (C=O), 141.34 (C=C), 138.25 (Ar-C=C), 128.30 (Ar-C=C), 127.54 (Ar-C=C), 123.52 (Ar-C=C), 91.35 (C=C), 52.14 (Ar-C) and 23.5 (Ar-Me).

2.3.3. Characterization of 5-(p-tolyl)-5,6-dihy-dropyrimido[4,5-d]pyrimidine-2,4,7(1H, 3H,8H)-trione (4c)

The compound **4c** was synthesized from condensation reaction **1c, 2** and **3** as white solid; Mp: 254-256 °C; Yield: 91%; ^{1}H NMR (400 MHz, CDCl3) δ 11.28 (s, 1H, NH), 11.15 (s, 1H, NH), 10.21 (s, 1H, NH), 8.24 (s, 1H, NH), 7.08 (d, J = 7.6 Hz, 2H), 6.90 (d, J = 7.5 Hz, 2H), 5.68 (s, 1H), 2.21 (s, 3H); ^{13}C NMR (101 MHz, $CDCl_3$) δ 166.10 (C=O), 158.62 (C=O), 154.78 (C=O), 140.52 (C=C), 138.60 (Ar-C=C), 129.48 (Ar-C=C), 127.74 (Ar-C=C), 124.51 (Ar-C=C), 93.42 (C=C), 50.41 (Ar-C) and 22.12 (Ar-Me).

2.3.4. Characterization of 5-(3-methoxyphenyl)-5,6-dihydropyrimido[4,5-d]pyrimidine-2,4,7(1H,3H,8H)-trione (4d)

The compound **4d** was synthesized from condensation reaction **1d, 2** and **3** as white solid; Mp: 232-234 °C; Yield: 85%; ^{1}H NMR (400 MHz, CDCL3) δ 11.35 (s, 1H, NH), 11.08 (s, 1H, NH), 10.02 (s, 1H, NH), 8.21 (s, 1H, NH), 7.05 (t, J = 8.4 Hz, 1H), 6.79 (d, J = 6.8 Hz, 2H), 6.61 (d, J = 7.0 Hz, 1H), 5.42 (s, 1H), 3.64 (s, 3H); ^{13}C NMR (101 MHz, $CDCl_3$) δ 169.34 (C=O), 158.20 (C=O), 153.78 (C=O), 140.68 (C=C), 138.60 (Ar-C=C), 127.75 (Ar-C=C), 125.34 (Ar-C=C), 91.30 (C=C), 55.4 (Ar-OMe) and 54.0 (Ar-C).

2.3.5. Characterization of 5-(4-methoxyphenyl)-5,6-dihydropyrimido[4,5-d]pyrimidine-2,4,7 (1H,3H,8H)-trione (4e)

The compound **4e** was synthesized from condensation reaction **1e, 2** and **3** as yellow solid; Mp: 282-284 °C; Yield: 93%; ^{1}H NMR (400 MHz, $CDCl_3$) δ 11.45 (s, 1H, NH), 11.18 (s, 1H, NH), 9.95 (s, 1H, NH), 8.31 (s, 1H, NH), 7.20-7.14 (m, 2H), 7.74-7.72 (m, 2H), 5.63 (s, 1H), 3.71 (s, 3H); ^{13}C NMR (101 MHz, $CDCl_3$) δ 167.01 (C=O), 157.91 (C=O), 154.21 (C=O), 140.52 (C=C), 139.41 (Ar-C=C), 128.25 (Ar-C=C), 127.63 (Ar-C=C), 93.21 (C=C), 55.60 (Ar-OMe) and 52.1 (Ar-C).

2.3.6. Characterization of 5-(3,4-dimethoxy-phenyl)-5,6-dihydropyrimido[4,5-d] pyri-midine-2,4,7(1H,3H,8H)-trione (4f)

The compound **4f** was synthesized from condensation reaction **1f, 2** and **3** as yellow solid; Mp: 224-226 °C;

Yield: 90%; ^{1}H NMR (400 MHz, $CDCl_3$) δ 11.27 (s, 1H, NH), 11.19 (s, 1H, NH), 10.15 (s, 1H, NH), 8.18 (s, 1H, NH), 6.95 (s, 1H), 6.79 (td, *J* = 8.4, 4.5 Hz, 2H), 5.82 (s, 1H), 3.81 (s, 3H), and 3.76; ^{13}C NMR (101 MHz, $CDCl_3$) δ 167.54 (C=O), 158.61 (C=O), 155.84 (C=O), 140.64 (C=C), 139.64 (Ar-C=C), 129.24 (Ar-C=C), 127.67 (Ar-C=C), 89.54 (C=C), 55.45 (Ar-OMe) and 53.71 (Ar-C).

2.3.7. Characterization of 5-(3-nitrophenyl)-5,6-dihydropyrimido[4,5-d]pyrimidine-2,4,7 (1H,3H,8H)-trione (4g)

The compound **4g** was synthesized from condensation reaction **1g, 2** and **3** as red solid; Mp: 194-196 °C; Yield: 83%; ^{1}H NMR (400 MHz, $CDCl_3$) δ 11.29 (s, 1H, NH), 11.24 (s, 1H, NH), 10.28 (s, 1H, NH), 8.14 (s, 1H, NH), 8.04-7.82 (m, 2H), 7.77 (d, *J* = 6.8 Hz, 1H), 7.39 (d, *J* = 7.8 Hz, 1H), 5.78 (s, 1H); ^{13}C NMR (101 MHz, $CDCl_3$) δ 169.91 (C=O), 159.63 (C=O), 154.23 (C=O), 140.54 (C=C), 139.61 (Ar-C=C), 130.5 (Ar-C=C), 127.51 (Ar-C=C), 92.35 (C=C) and 50.3 (Ar-C).

2.3.8. Characterization of 5-(4-nitrophenyl)-5,6-dihydropyrimido[4,5-d]pyrimidine-2,4,7 (1H,3H,8H)-trione (4h)

The compound **4h** was synthesized from condensation reaction **1h, 2** and **3** as red solid; Mp: 218-220 °C; Yield: 78%; ^{1}H NMR (400 MHz, $CDCl_3$) δ 11.31 (s, 1H, NH), 11.21 (s, 1H, NH), 10.35 (s, 1H, NH), 8.21 (s, 1H, NH), 7.41 (d, *J* = 7.8 Hz, 1H), 7.31 (d, *J* = 7.6 Hz, 1H), 6.86 (t, *J* = 7.8 Hz, 1H) and 5.54 (s, 1H); ^{13}C NMR (101 MHz, $CDCl_3$) δ 167.81 (C=O), 158.42 (C=O), 152.36 (C=O), 140.89 (C=C), 139.71 (Ar-C=C), 128.01 (Ar-C=C), 126.65 (Ar-C=C), 89.56 (C=C) and 50.3 (Ar-C).

2.3.9. Characterization of 5-(3-iodophenyl)-5,6-dihydropyrimido[4,5-d]pyrimidine-2,4,7 (1H,3H,8H)-trione (4i)

The compound **4i** was synthesized from condensation reaction **1i, 2** and **3** as white solid; Mp: 208-210 °C; Yield: 87%; ^{1}H NMR (400 MHz, $CDCl_3$) δ 11.52 (s, 1H, NH), 11.29 (s, 1H, NH), 10.08 (s, 1H, NH), 8.21 (s, 1H, NH), 7.32 (d, *J* = 6.8 Hz, 2H), 7.18 (d, *J* = 6.8 Hz, 2H) and 5.62 (s, 1H). ^{13}C NMR (101 MHz, $CDCl_3$) δ 168.45 (C=O), 157.88 (C=O), 153.23 (C=O), 141.10 (C=C), 139.21 (Ar-C=C), 129.15 (Ar-C=C), 126.53 (Ar-C=C), 91.24 (C=C) and 49.5 (Ar-C).

2.3.10. Characterization of 5-(4-bromophenyl)-5,6-dihydropyrimido[4,5-d]pyrimidine-2,4,7(1H,3H,8H)-trione (4j)

The compound **4j** was synthesized from condensation reaction **1j, 2** and **3** as pale yellow solid; Mp: 212-214 °C; Yield: 90%; ^{1}H NMR (400 MHz, $CDCl_3$) δ 11.47 (s, 1H, NH), 11.29 (s, 1H, NH), 10.00 (s, 1H, NH), 8.11 (s, 1H, NH), 7.28 (d, *J* = 8.4 Hz, 2H), 7.14-7.08 (m, 2H), 5.84 (s, 1H); ^{13}C NMR (101 MHz, $CDCl_3$) δ 167.44 (C=O), 157.89 (C=O), 152.32 (C=O), 141.81 (C=C), 136.52 (Ar-C=C), 128.41 (Ar-C=C), 127.14 (Ar-C=C), 90.42 (C=C) and 51.5 (Ar-C).

2.3.11. Characterization of 5-(4-chlorophenyl)-5,6-dihydropyrimido[4,5-d]pyrimidine-2,4,7(1H,3H,8H)-trione **(4k)**

The compound **4k** was synthesized from condensation reaction **1k, 2** and **3** as red solid; Mp294-296 °C; Yield: 88%; ^{1}H NMR (400 MHz, $CDCl_3$) δ 11.37 (s, 1H, NH), 11.29 (s, 1H, NH), 10.09 (s, 1H, NH), 8.14 (s, 1H, NH), 7.28 (s, 1H), 7.10 (d, *J* = 7.8 Hz, 2H), 6.58 (d, *J* = 7.8 Hz, 2H), 5.69 (s, 1H); ^{13}C NMR (101 MHz, $CDCl_3$) δ 168.44 (C=O), 157.76 (C=O), 153.67 (C=O), 140.52 (C=C), 134.41 (Ar-C=C), 128.24 (Ar-C=C), 122.63 (Ar-C=C), 88.56 (C=C) and 50.3 (Ar-C).

2.3.12. Characterization of 5-(4-hydroxyphenyl)-5,6-dihydropyrimido[4,5-d]pyrimidine-2,4,7(1H,3H,8H)-trione (4l)

The compound **4l** was synthesized from condensation reaction **1l, 2** and **3** as white solid; Mp: 208-210 °C; Yield: 81%; ^{1}H NMR (400 MHz, $CDCl_3$) δ 11.37 (s, 1H, NH), 11.29 (s, 1H, NH), 9.90 (s, 1H, NH), 8.14 (s, 1H, NH), 7.88 (d, *J* = 7.8 Hz, 2H), 7.55 (d, *J* = 7.8 Hz, 2H), 5.46 (s, 1H); ^{13}C NMR (101 MHz, $CDCl_3$) δ 167.51 (C=O), 158.52 (C=O), 154.21 (C=O), 141.56 (C=C), 139.24 (Ar-C=C), 130.74 (Ar-C=C), 128.98 (Ar-C=C), 92.41 (C=C) and 50.3 (Ar-C).

3. RESULTS AND DISCUSSION

3.1. Chemistry

To achieve optimized conditions protocol based on the reaction of benzaldehyde (**1a**), barbituric acid (**2**) (1 mmol) and urea (**3**) (1 mmol) as model reaction (**Scheme 1**), we checked temperatures and solvents, catalyst loading and the results of this study are summarized in Table 1.

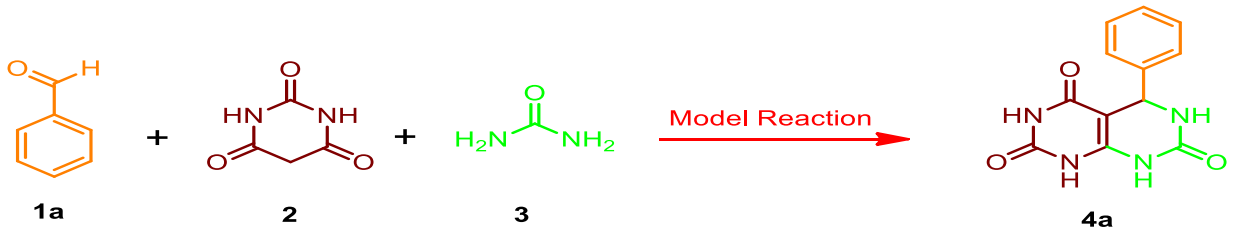

Scheme 1: Standard model reaction

It was found that when the reaction was carried out in the nonappearance of the catalyst in ethanol, lower yield of product was perceived, after 20 min (Table 1, entry 1). To obtain the preferred product (**4a**), we tested the reaction using different catalysts such as *p*-TSA, Sulfamic acid, Sulfanilic acid, Boric acid, Citric acid, Phosphotungstic acid, Xanthan sulfuric acid, Silica sulfuric acid, CSA and [DBN][HSO_4] (Table 1, entries 2-11). Thus, room-temperature [DBN][HSO_4] as the pre-eminent catalyst was tested for this reaction. In the presence of [DBN][HSO_4], compound **4a** was isolated in 95% yield after only 8 min under the microwave irradiations. Therefore, it can be thought that [DBN][HSO_4] is green and a superior solvent and catalyst compared to the others shown in Table 1.

Table 1: Efficiency Comparison of Various Catalysts for the Synthesis of dihydro-pyrimido[*4,5-d*]pyrimidine derivatives (4a).[a]

entry	catalyst	Time (min)	Yield[b] (%)
1	-	20	35
2	*p*-TSA	20	61
3	Sulfamic acid	20	64
4	Sulfanilic acid	20	50
5	Boric acid	20	59
6	Citric acid	20	62
7	Xanthan sulfuric acid	20	57
8	Phosphotungstic acid	20	62
9	CSA	20	64
10	Silica sulfuric acid	20	8
11	[DBN][HSO_4]	7	93

*[a]Reaction conditions: benzaldehyde **1a** (100 mg), barbituric acid **2** (120 mg), urea **3** (56 mg) and [DBN][HSO_4] (20 mol%) stirred at under microwave irradiation (MW = 280 W) [b] Isolated yields. Bold values are for highlighting the good result.*

In the next step we examine the efficiency of ionic liquid [DBN][HSO_4] for the synthesis of pyrimido [4,5-d] pyrimidine derivatives. When change in concentration of [DBN][HSO_4] on model reaction suggest that much more effect on yield of final product. The catalyst loading study suggest that 20 mol% of [DBN][HSO_4] catalyst are best for the synthesis of final product in 93% yields (Table 2).

Furthermore, we also studied the power level of microwave effect on model reactions according to these study better results of the desired product when reaction carried at 280 W (Table 3, entry 3). Detailed reaction conditions are shown in Table 3.

Table 2: Effect of catalyst concentration[a]

Entry	Catalyst (mol %)	Time (min)	Yield[b] (%)
1	5	20	61
2	10	15	71
3	15	12	84
4	20	7	93
5	25	7	93

*[a]Reaction conditions: **1a** (100 mg), **2** (120 mg), (**3**) (56 mg) and [DBN][HSO_4] under microwave irradiation. [b]Isolated yield.*

Table 3: Optimization of reaction condition for the synthesis of 4a under microwave set up[a]

Entry	Power levels in Watt	Time[b] (min)	Yield[c]
1	140	20	54
2	210	15	70
3	240	10	83
4	280	7	93
5	350	7	93

*[a]Reaction conditions: **1a** (100 mg), **2** (120 mg) and **3** (56 mg) in the presence of [DBN][HSO_4] 20 mol% under microwave irradiation. [b]Reaction progress monitored by TLC. [c]Isolated yield.*

A. extremely superlative method to economic and greener preparation is recovery and recyclability of a ionic liquid. Therefore we have to check the efficiency of catalyst after recover from the reaction media during the work-up procedure. When reaction is completed, then reaction mass was pour on ice cold water to obtained fine crystal of final 2-Amino-4H-pyrans

derivatives. In the last step removal H_2O from filtrate using reduced pressure to gave viscous liquid, which is on cooling to give pure ionic liquid. Recovered catalysts were reused for next four repeated cycles without considerable loss in catalytic efficiency (Table 4).

Table 4: Reusability of [DBN][HSO_4] ionic liquid for model reaction

Entry	Run	Time[a] (min)	Yield[b]
1	fresh	7	93
2	2	7	93
3	3	7	85
4	4	7	83
5	5	7	80

[a]*Reaction progress monitered by TLC.* [b]*Isolated yield.*

The structure of the titled product **4a** was confirmed by ^{1}H NMR and ^{13}C NMR. In ^{1}H NMR spectra of compound **4a** exhibit four singlet bands for four -NH groups at δ 8.38, 10.25, 11.20 and 11.36 ppm suggest that NH group present in the dihydropyrimido [*4,5-d*] pyrimidine compound. The aliphatic -CH proton was shown at δ 5.38 ppm suggests that formation of cyclic ring in our final compound. In the ^{13}C NMR spectrum of compound **4a**, distinct -C=O carbonyl group observed at δ 163.01, 158.32 and 154.24 ppm. The CH peak observed at δ 45.36 ppm confirmed that formation of compound **4a**.

3.2. Plausible Reaction Mechanism

Reaction mechanism cycle for the preparation of dihydropyrimido [*4,5-d*] pyrimidine analogues employing [DBN][HSO_4] is catalyst. In first step barbituric acid activated [DBN][HSO_4] ionic liquid followed by nucleophilic attack on electron deficient benzaldehyde results in formation of intermediate **II**. In the next step, removal of water molecules from intermediates **II** with the help of [DBN][HSO_4] takes place to give intermediates **III**. In the third step intramolecular cyclization occur to give intermediates **IV**. In the last step, formation of final product **4a** achieved *via* removal of H_2O molecule and regeneration of catalyst. Detailed reaction mechanism is presented in Scheme 4.

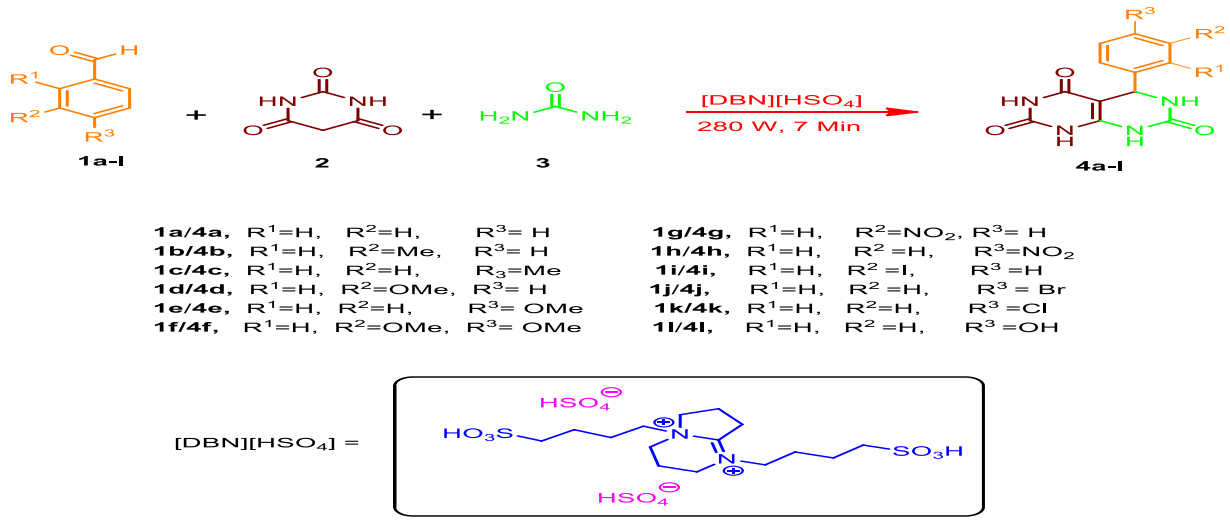

Scheme 2: Synthesis of pyrimido[4,5-d]pyrimidine derivatives (4a-l)

Table 5: [DBN][HSO_4] catalyzed synthesis of dihydropyrimido[*4,5-d*]pyrimidine derivatives[a]

Entry	Aryl aldehyde	Xanthene	Time (min)	Yield (%)[b]	Mp (°C)[c]	
					Observed	Reported
1	benzaldehyde	5-phenyl-5,6-dihydropyrimido [4,5-d]pyrimidine-2,4,7(1H,3H,8H)-trione	7	93	243-244	244-246 [34]
2	3-methyl benzaldehyde	5-(m-tolyl)-5,6- dihydro-pyrimido[4,5-d]pyrimidine-2,4,7(1H,3H,8H)-trione	7	86	202-204	-

3	4-methylbenzaldehyde	5-(p-tolyl)-5,6-dihydro-pyrimido[4,5-d]pyrimidine-2,4,7(1H,3H,8H)-trione	7	91	254-256	255-257 [35]
4	3-methoxybenzaldehyde	5-(3-methoxyphenyl)-5,6-dihydropyrimido[4,5-d]pyrimidine-2,4,7(1H,3H,8H)-trione	7	85	232-234	-
5	4-methoxybenzaldehyde	5-(4-methoxyphenyl)-5,6-dihydropyrimido[4,5-d]pyrimidine-2,4,7(1H,3H,8H)-trione	7	93	282-284	284-286 [34]
6	3,4-dimethoxybenzal-dehyde	5-(3,4-dimethoxyphenyl)-5,6-dihydropyrimido[4,5-d]pyrimidine-2,4,7(1H,3H,8H)-trione	7	90	224-226	-
7	3-nitrobenzaldehyde	5-(3-nitrophenyl)-5,6-dihydropyrimido[4,5-d]pyrimidine-2,4,7(1H,3H,8H)-trione	7	83	194-196	196-198 [36]
8	4-nitrobenzaldehyde	5-(4-nitrophenyl)-5,6-dihydropyrimido[4,5-d]pyrimidine-2,4,7(1H,3H,8H)-trione	7	78	218-220	-
9	3-iodobenzaldehyde	5-(3-iodophenyl)-5,6-dihydropyrimido[4,5-d]pyrimidine-2,4,7(1H,3H,8H)-trione	7	87	208-210	-
10	4-bromobenzaldehyde	5-(4-bromophenyl)-5,6-dihydropyrimido[4,5-d]pyrimidine-2,4,7(1H,3H,8H)-trione	7	90	212-214	210-212 [34]
11	4-chlorobenzaldehyde	5-(4-chlorophenyl)-5,6-dihydropyrimido[4,5-d]pyrimidine-2,4,7(1H,3H,8H)-trione	7	88	294-296	296-298 [37]
12	4-hydroxybenzaldehyde	5-(4-hydroxyphenyl)-5,6-dihydropyrimido[4,5-d]pyrimidine-2,4,7(1H,3H,8H)-trione	7	81	208-210	210-212 [34]

[a]*Reaction conditions: aldehydes (**1a-l**) (100 mg), barbituric acid (**2**) (120 mg), urea (**3**) (56 mg) in [DBN][HSO$_4$] 20 mol % stirred under microwave irradiations at 280 W;* [b]*isolated yields,* [c]*melting points are in good contact with those reported in the literature [34-37].*

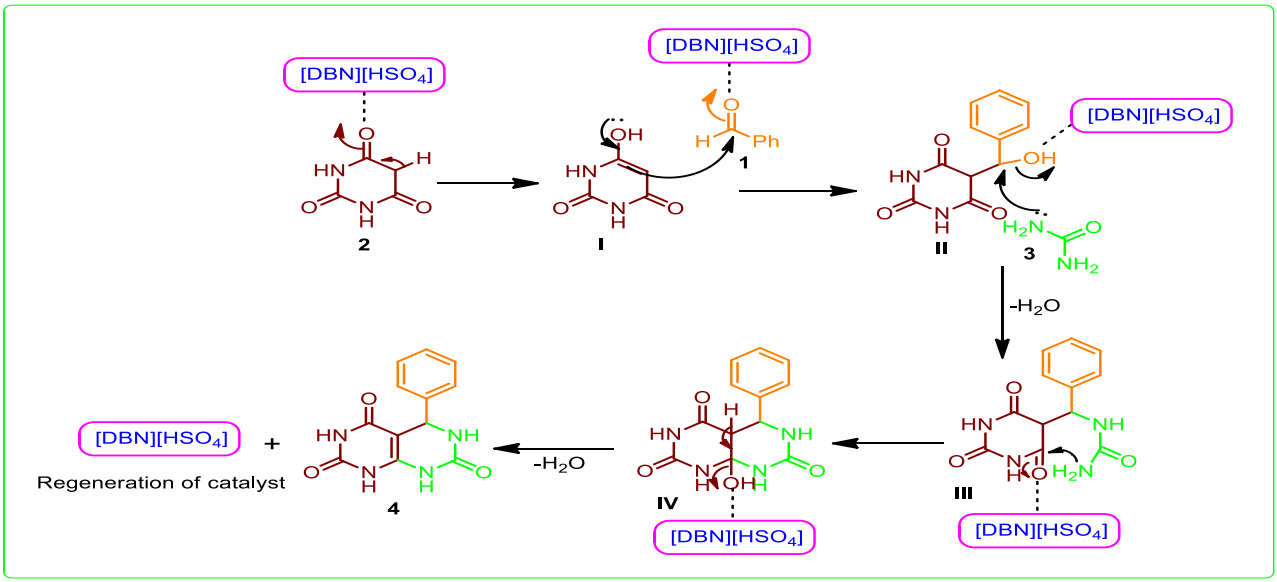

Scheme 4: Reaction mechanism cycle for the preparation of compounds 4a

4. CONCLUSION

In conclusion, an environmental friendly and highly efficient green methodology has been established for the synthesis of functionalized dihydropyrimido [*4,5-d*] pyrimidine derivatives using an inexpensive and recoverable [DBN][HSO_4] under microwave irradiation at 280 W for 7 min. This, to the best of our knowledge, has no examples. This reaction scheme exposes a number of advantages, such as uniqueness, high atom efficiency, mild reaction conditions, clean reaction profiles, easy workup procedure and ecofriendliness. Using [DBN][HSO_4] green protocol offers advantages such as excellent yields of products, shorter reaction time period, simple procedure, preparation of catalyst and reusability of the catalyst.

Conflict of Interest

The authors declare no conflict of interest, financial or otherwise.

5. ACKNOWLEDGEMENTS

The authors are very much grateful to authority of Department of Chemistry, Dr Babasaheb Ambedkar Marathwada University Aurangabad for providing laboratory facility. The authors are also thankful to the Principal, Shri Chhatrapati Shivaji College, Omerga and Principal R.N.C. Arts, J.D.B. Commerce & N.S.C. Science College, Nashik-Road, Nashik for providing support and all the necessary research facilities during my research.

6. REFERENCES

1. Mielcarek J, et al. *J. Pharm. Biomed. Anal.,* 1997; **15**: 681-686.
2. Shelat AA, Guy RK et al. *Nat. Chem. Biol.,* 2007; **3**:442-446.
3. Vo D, Matowe WC, Ramesh M, Iqbal N, Wolowyk MW, Howlett SE, Knaus EE, et al. *J. Med. Chem*., 1995; **38**:2851-2859.
4. Rueping M, Antonchick AP, et al. *Angew. Chem. Int. Ed.,* 2006; **45:**3683-3686.
5. Undheim K, Benneche T, et al. In Comprehensive Heterocyclic Chemistry II, ed. Katritzky AR, Rees CW, Scriven EVF, et al. *Pergamon Press, London,* 1996; **2:**93-231.
6. Gineinah MM, Nasr MNA, Badr SMI, El-Husseiny WM, et al. *Med. Chem. Res.,* 2013; **22:** 3943-3952.
7. Pandeya SN, Shriram D, Nath G, Clercq ED, et al. *Farmaco*, 1999; **54:**624-628.
8. Kim J, Kwon J, Lee D, Jo S, Park DS, Choi J, et al. *Bioorg. Med. Chem. Lett.,* 2014; **24:**5473-5477.
9. Moukha-chafiq O, Reynolds RC, et al. *ACS Comb. Sci.,* 2014; **16:**232-237.
10. Chen Q, Zhu X, Jiang L, Liu Z, Yang G, et al. *Eur. J. Med. Chem.,* 2008; **43:**595-603.
11. Gupta RA, Kaskhedikar SG, *Med. Chem. Res.,* 2013; **22:**3863-3880.
12. Longley DB, Harkin DP, Johnston PG, et al. *Nat. Rev. Cancer,* 2003; **3:**330-338.
13. Smolin G, Okumoto M, Feiler S, Condon D, et al. *Am. J. Ophthalmol.,* 1981; **91:**220-225.
14. Buron F, Merour JY, Akssira M, Guillaumet G, Routier S, et al. *Eur. J. Med. Chem.,* 2015; **95:** 76-95.
15. (a) Neumann DM, Cammarata A, Backes G, Palmer GE, Jursic BS, et al. *Bioorg. Med. Chem.,* 2014; **22:**813; (b) Ilangaratne NB, Mannakkara NN, Bell GS, Sander JW, et al. *Bull. World Health Organ,* 2012 **90**:871-871.
16. (a) Mahmoodi NO, Ramzanpour S, Pirbasti FG, et al. *Arch. Pharm. Chem. Life Sci.,* 2015; **348:**275-282; (b) Dam B, Nandi S, Pal AK, et al. *Tetrahedron Lett.,* 2014; **55:**5236-5240.
17. Affeldt RF, Benvenutti EV, Russowsky D, et al. *New J. Chem.,* 2012; **36:**1502-1511.
18. Jiang H, Mai R, Cao H, Zhu Q, Liu X, et al. *Org. Biomol. Chem.,* 2009; **7:**4943-4953.
19. Cioc RC, Ruijter E, Orru RVA, et al. *Green Chem*., 2014; **16:**2958-2975.
20. Isambert N, Duque MMS, Plaquevent JC, Genisson Y, Rodriguez J, Constantieux T, et al. *Chem. Soc. Rev*., 2011; **40:**1347-1357.
21. Norouzi F, Javanshir S, et al. *BMC Chem.,* 2020; **14:**1.
22. Welton T, et al. *Green Chem*., 2011; **13**:225-225.
23. Wang C, Guo L, Li H, Wang Y, Weng J, Wu L, et al. *Green Chem.,* 2006; **8:**603-607.
24. Wang C, Zhao W, Li H, Guo L, et al. *Green Chem.,* 2009; **11:**843-847.
25. Weng J, Wang, C.; Li, H.; Wang, Y. *Green Chem.,* 2006; **8:**96-99.
26. Dupont J, de Souza RF, Suarez PAZ, *Chem. Rev.,* 2002; **102:**3667-3692.
27. Sheldon R, et al. *Chem. Commun.,* 2001; **23:**2399-2407.
28. Dolzhenko AV, Dolzhenko AV, et al. *Green Synthetic Approaches for Biologically Relevant Heterocycles. Elsevier: Perth*, WA, Australia, 2015; 101-139.
29. Jiang T, Gao H, Han B, Zhao G, Chang Y, Wu W, Gao L, Yang G, et al. *Tetrahedron Lett.,* 2004; **45:** 2699-2701.
30. Wilkes JS, et al. *Green Chem.,* 2002; **4:**73-80.
31. Zhu X, Song M, Xu Y, et al. *ACS Sustain. Chem., Eng.,* 2017; **9:**8192-8198.

32. Carta A, Loriga M, Zanetti S, Sechi LA, *Farmaco.,* 2003; **58:**1251-1255.
33. Shi H, Zhu W, Li H, Liu H, Zhang M, Yan Y, Wang Z, et al. *Catal. Commun.,* 2010; **11:** 588-591.
34. Jadhav C, Khillare LD, Bhosle MR, et al. *Synt. Commu.,* 2018; **48:**233-246.
35. Rostamizadeh S, Nojavan M, Aryan R, Azad M, et al. *Catal Lett*., 2014; **144:**1772-1783.
36. Shinde SV, Jadhav WN, Karade NN, et al. *Oriental Journal of Chemistry,* 2010; **26:**307-317.
37. Kidwai M, Singhal K, Kukreja S, et al. *Naturforsch.,* 2007; **62b:**732-736.

Journal of Advanced Scientific Research
Available online through https://sciensage.info
ISSN 0976-9595
Research Article

[NMP][HSO_4]-MEDIATED ENVIRONMENTALLY BENIGN SYNTHESIS OF 4-THIAZOLIDINONE DERIVATIVES

Vishal U. Mane[1,2], Satish M. Chavan[1], Waseem A. Beg[1], Dhananjay V. Mane*[2,3]
[1]Department of Chemistry, RNC Arts, JDB Commerce & NSC Science College, Nashik, Maharashtra, India
[2]Department of Chemistry, Shri Chhatrapati Shivaji College, Omerga, Dist. Osmanabad, Maharashtra, India
[3]Yashwantrao Chavan Maharashtra Open University, Nashik, Maharashtra, India
*Corresponding author:dvmane11@gmail.com

Received: 07-09-2021; Revised: 12-02-2022; Accepted: 17-02-2022; Published: 31-03-2022
 https://doi.org/10.55218/JASR.202213202

ABSTRACT
A *N*-methyl-2-pyrrolidonium hydrogensulfate [NMP][HSO_4] bronsted acidic ionic liquid-promoted cyclocondensation-cyclization pathway has been established using one pot reaction of anilines, aldehydes and mercaptoacetic acid to give 4-thiazolidinone derivatives in good to promising yields using microwave irradiation. Applications for this protocol are easy workup, high yields, short reaction times, variability of functional groups, recyclability and solvent-free conditions.

Keywords:[NMP][HSO_4], Environmentally benign, Multicomponent reactions, 4-Thiazolidinones.

1. INTRODUCTION

Ionic liquids (ILs) are environment-friendly solvents because of their interesting properties and alternative to the harmful organic solvent. Furthermore, these are useful in the catalytic reaction [1], organic synthesis [2], because of their unique properties make them superior media for increasing selectivity, reactivity and recyclability. Various ionic liquids have been significantly used in heterocyclic synthesis as a solvent or catalyst [3].

Multicomponent reactions (MCRs) have been widely used for the synthesis of a wide range of heterocycles. As heterocyclic fragments are present in the majority of natural products and drug-like compounds, efficient synthesis of diverse heterocyclic compounds remains a key issue until now. MCR is one of the most effective synthetic techniques for the development of various heterocyclic compounds, applying subsequent trans-formation, cyclization and functionalization, leading to a diversity-oriented synthesis [4]. Thus, various medical chemists have been attracted by the development of multi-component reaction protocols for the synthesis of heterocyclic compounds.

4-Thiazolidinones and its derivatives have drawn considerable attention of the researchers in the recent years due to their medicinal properties. 4-Thiazoli-dinones is a medicinally significant pharmacophore with wide range of remarkable pharmacological activity such as anti-convulsant [5], anti-inflammatory [6], anti-microbial [7], anti-viral [8], antitumor [9], antidiabetic [10], antituberculosis [11], antiparasitic [12], analgesic [13], antidiarrhoeal [14], antiarthritic [15], cardio-vascular activity [16], anti-HIV [17] and FSH agonist [18]. Furthermore, 4-thiazolidinones conjugates also exhibit prominent cancer activity against several cancer cell lines such as antiproliferative activity against Reh and Nalm6 cells [19], antiapoptotic biocomplex (Bcl-XL-BH3) [20], breast cancer JSP-1 inhibitor [21], Cyclin B/CDK1 inhibitor [22], MCF-7 [23], integrin avb3 receptor [24], HT29 colon cancer cell line [25] and tumor necrosis factor (TNFα) [26]. Structures of representative bio-active 4-thiazolidinone motifs are disclosed in Fig. 1.

Due to the wide range of biological activities of 4-thiazolidinones, several synthetic pathways have been established for the synthesis of 4-thiazolidinone conjugates. Because of wide range of pharmacological activities, numerous catalytic routes have been established including, acetic acid [27], ammonium persulfate [28], acid catalysed [29], Bi[SCH_2COOH]$_3$ [30], Cd-Zr_4- [PO_4]$_6$ [31], DIPEA [32], DBSA [33], montmorillonite K-10 [34], *N*-methyl pyridinium tosylate [35], nano-Fe_3O_4@SiO_2 [36], silica gel [37], silica supported $CoFe_2O_4$@SiO_2/$PrNH_2$ [38], $SnCl_2$

[39], ionic liquid [bmim]OH [40] and Y[OTf]$_3$ [41]. However, the above well developed protocols have some drawbacks such as hazardous solvent, extended heating, separation, recycling of catalyst and tedious work-up procedure.

In addition, many of these processes employ organic solvents act as the reaction media. Hence, this protocol which overcomes these limitations requests a lot of interest for the scientist. Hence, the improvement toward fashionable reaction with reusability of catalyst, easy isolation of product, no waste is highly attractive. Recently, [NMP][HSO_4] was widely used as catalysts in different research areas. Reaction of HSO_4 with cation gives novel NMP based ionic liquids [42]. The large number of functionalized ILs has been considered for diverse purposes. Due to this wide range of applications, they are used as a suitable solvent for wide array of synthetic protocols [38]. The synthesis of NMP is based on ionic liquid *via* assembling the zwitterionic precursors to these functionalized acidic-SO_3H ionic liquid [43]. As per our study, the existential of this work is to begin efficient and rapid synthetic protocol for the synthesis of 4-thiazolidinone derivatives under ecofriendly conditions. As an extension of emerging efficient and economic strategy to expand biologically considerable active compounds, herein, we disclose first time microwave assisted solvent free synthesis of 4-thiazolidinone derivatives using NMP-based acidic ionic liquid to give good to prominent yields.

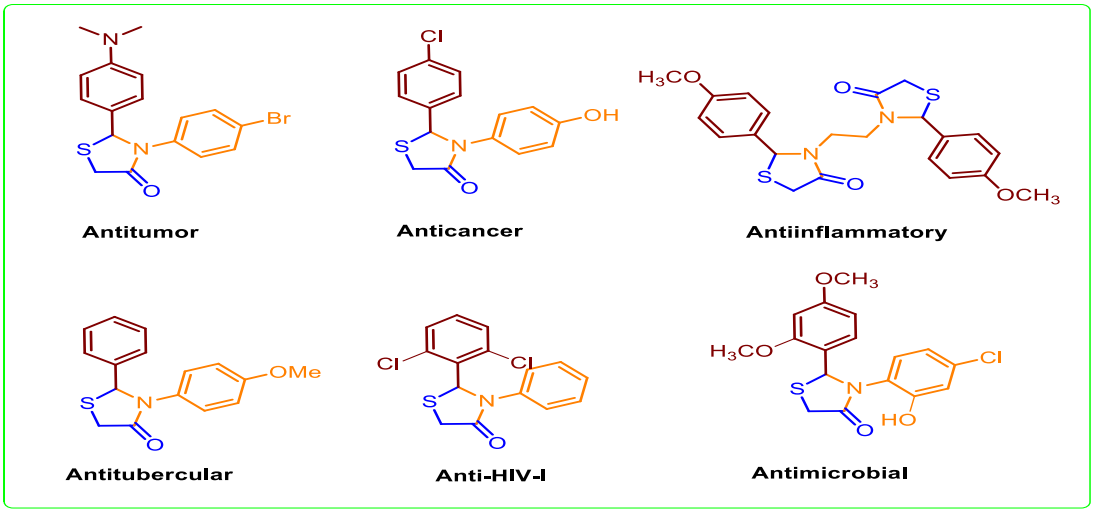

Fig. 1:Structure of bio-active 4-thiazolidinones conjugates

2. EXPERIMENTAL

2.1. Preparation of [NMP][HSO_4]

1-Methyl-2-pyrolidone (0.2mol) was charged into a 250-mL three-necked flask containing a magnetic stirrer. Then an equimolar amount of concentrated sulfuric acid (98 wt %) was added dropwise slowly into the flask at 80°C for 12 h. The mixture was washed by ether three times to remove non-ionic residues and dried under vacuum by a rotary evaporator to obtain the viscous clear [NMP][HSO_4] compound. The pH of the resulted ionic liquid (10% w/v) was determined and the obtained pH was equal to 1.2. Reaction details are shown in Scheme 1.

2.2. General Procedure for Synthesis of 4-thiazolidinone derivatives (4a-l)

A mixture of anilines (**1a**) (1 mmol), aryl aldehyde (**2a**) (1 mmol), mercaptoacetic acid (**3**) (1 mmol) and [NMP][HSO_4] 20 mol% was kept under microwave irradiation at 240 W for 8 min. The progress of the reaction was monitored by thin layer chromatography (*n*-Hexane/EtOAc 8:2). Further, ice cold water (10 mL) was added, stirred for 10 min. The obtained solid was filtered, washed with cold water to remove the ionic liquid. The obtained crude compounds were recrystallized using ethanol. The synthesized compound is confirmed by MP, ^{1}H NMR and ^{13}C NMR spectra.

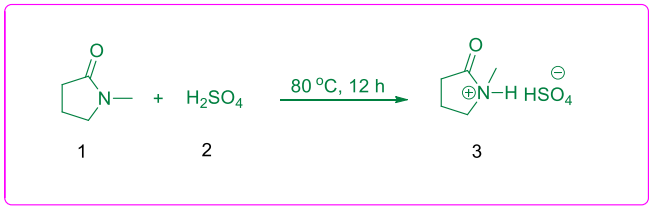

Scheme 1:Synthesis of [NMP][HSO_4] ionic liquid

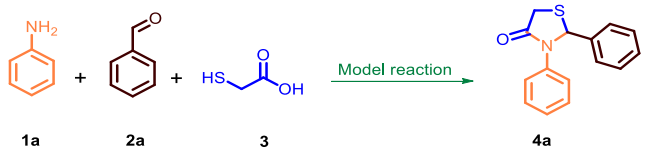

Scheme 2:Model reaction

3. RESULTS AND DISCUSSION

3.1. Characterization of compounds

3.1.1. 2,3-Diphenylthiazolidin-4-one (4a)

The **4a** was observed *via* cyclocondensation of **1a**, **2a** and **3** as white solid; Mp:130-132°C (lit.[46] 128-130°C); Yield:91%; ^{1}H NMR (400 MHz, $CDCl_3$, δ ppm):3.83 (d, 1H, *J* = 16 Hz), 3.97 (d, 1H, *J* = 16 Hz), 6.09 (s, 1H, S-CH-N), 7.20 (d, *J* = 7.9 Hz, 3H) and 7.22 (dd, *J* = 9.6, 4.9 Hz, 7H).

3.1.2. 2-phenyl-3-(p-tolyl)thiazolidin-4-one (4b)

The **4b** was observed *via* cyclocondensation of **1b**, **2a** and **3** as white solid; Mp:110-112°C (lit.[47] 110-112°C); Yield:89%; ^{1}H NMR (400 MHz, $CDCl_3$, δ ppm):2.27 (s, 3H, CH_3), 3.89 (d, 1H, *J* = 16 Hz), 3.99 (d, 1H, CH_2, *J* = 16 Hz), 6.05 (s, 1H, S-CH-N), 7.16 (m, 2H), 7.23 (d, *J* = 8.3 Hz, 2H) and 7.38-7.26 (m, 5H).

3.1.3. 3-(4-fluorophenyl)-2-phenyl thiazolidin-4-one (4c)

The **4c** was observed *via* oxidative cyclocondensation of **1c**, **2a** and **3** as white solid; Mp:115-116°C (lit.[48] 115-116°C); Yield:84%; ^{1}H NMR (400 MHz, $CDCl_3$, δ ppm):3.72 (d, 1H, *J* = 16 Hz), 3.82 (d, 1H, CH_2, *J* = 16 Hz), 6.05 (s, 1H, S-CH-N), 6.96 (dd, *J* = 24.1, 6.9 Hz, 2H) and 7.21-7.04 (m, 7H).

3.1.4. 3-(4-Chlorophenyl)-2-phenylthiazolidin-4-one (4d)

The **4d** was observed *via* cyclocondensation of **1d**, **2a** and **3** as white solid; Mp:110-112°C (lit.[48] 110-112°C); Yield:86%; ^{1}H NMR (400 MHz, $CDCl_3$, δ ppm):3.82 (d, 1H, *J* = 16 Hz), 3.89 (d, 1H, CH_2, *J* = 16 Hz), 5.98 (s, 1H, S-CH-N), 7.17-7.02 (m, 5H), 7.31-7.27 (m, 2H) and 7.41-7.26 (m, 2H).

3.1.5. 3-(4-bromophenyl)-2-phenylthiazolidin-4-one (4e)

The **4e** was observed *via* cyclocondensation of **1e**, **2a** and **3** as white solid; Mp:114-115°C (lit.[48] 115-116°C); Yield:85%; ^{1}H NMR (400 MHz, $CDCl_3$, δ ppm):3.86 (d, 1H, *J* = 16 Hz), 3.97 (d, 1H, CH_2, *J* = 16 Hz), 6.07 (s, 1H, S-CH-N), 7.12 (dd, *J* = 6.6, 4.7 Hz, 2H) and 7.38-7.18 (m, 7H).

3.1.6. 2-(4-chlorophenyl)-3-(p-tolyl)thiazolidin-4-one (4f)

The **4f** was observed *via* cyclocondensation of **1f**, **2b** and **3** as yellow solid; Mp:164-166°C; Yield:88%; ^{1}H NMR (400 MHz, $CDCl_3$, δ ppm):2.28 (s, 3H, CH_3), 3.84 (d, 1H, *J* = 16 Hz), 3.98 (d, 1H, CH_2, *J* = 16 Hz), 6.04 (s, 1H, S-CH-N), 7.01 (dd, *J* = 8.2, 2.8 Hz, 2H), 7.09 (d, *J* = 6.2 Hz, 2H) and 7.26 (dd, *J* = 8.0, 4.4 Hz, 4H); ^{13}C NMR (101 MHz, cdcl$_3$) δ 20.31, 32.70, 64.30, 124.95, 128.37, 129.19, 133.88, 134.00, 136.11, 137.44 and 170.16.

3.1.7. 3-Phenyl-2-(p-tolyl)thiazolidin-4-one (4g)

The **4g** was observed *via* cyclocondensation of **1a**, **2c** and **3** as brown solid; Mp:118-120°C (lit.[46] 116-118°C); Yield:91%; ^{1}H NMR (400 MHz, $CDCl_3$, δ ppm):2.29 (s, 3H, CH_3), 3.89 (d, 1H, *J*= 16 Hz), 4.02 (d, 1H, CH_2, *J* = 16 Hz), 6.05 (s, 1H, S-CH-N), 7.05 (dt, *J* = 6.4, 5.1 Hz, 4H) and 7.40-7.22 (m, 5H).

3.1.8. 3-(4-Chlorophenyl)-2-phenylthiazolidin-4-one (4h)

The **4h** was observed *via* cyclocondensation of **1d**, **2c** and **3** as white solid; Mp:110-112°C (lit.[46] 110-112°C); Yield:88%; ^{1}H NMR (400 MHz, $CDCl_3$, δ ppm):3.98 (d, 1H, CH_2, *J* = 16 Hz), 2.25 (s, 3H, CH_3), 3.89 (d, 1H, *J* = 16 Hz), 6.13 (s, 1H, S-CH-N), 7.16-6.93 (m, 4H), 7.45 (d, *J* = 8.2 Hz, 2H), 8.13 (d, *J* = 8.5 Hz, 2H).

3.1.9. 3-(4-chlorophenyl)-2-(4-nitrophenyl)thiazolidin-4-one (4i)

The **4h** was observed *via* cyclocondensation of **1d**, **2d** and **3** as white solid; Mp:150-152°C; Yield:79%; ^{1}H NMR (400 MHz, $CDCl_3$, δ ppm):3.94 (d, 1H, *J* = 16 Hz), 4.04 (d, 1H, CH_2, *J* = 16 Hz), 6.17 (s, 1H, S-CH-N), 7.14 (d, *J* = 8.0 Hz, 2H), 7.34 (d, *J* = 8.1 Hz, 2H), 7.55 (d, *J* = 8.6 Hz, 2H) and 8.16 (d, *J* = 8.2 Hz, 2H).

3.1.10. 3-(4-methoxyphenyl)-2-phenylthiazolidin-4-one (4j)

The **4j** was observed *via* cyclocondensation of **1a**, **2g** and **3** as yellow solid; Mp:62-64°C (lit.[48] 61-62°C); Yield:95%; ^{1}H NMR (400 MHz, $CDCl_3$, δ ppm):3.82 (d, 1H, *J* = 16 Hz), 3.86 (s, 3H, , CH_3), 3.96 (d, 1H, CH_2, *J* = 16 Hz), 6.10 (s, 1H, S-CH-N), 7.24-7.12 (m, 5H), 7.47 (d, *J* = 8.4 Hz, 2H) and 7.82 (d, *J* = 8.2 Hz, 2H).

3.1.11. 2,3-di-p-tolylthiazolidin-4-one (4k)

The **4k** was observed *via* cyclocondensation of **1b**, **2c** and **3** as white solid; Mp:122-124°C (lit.[48] 121-123°C); Yield:90%; ^{1}H NMR (400 MHz, $CDCl_3$, δ ppm):2.30 (s, 6H, CH_3), 3.84 (d, 1H, *J*=16 Hz), 3.95 (d, 1H, CH_2, *J* = 16 Hz), 6.14 (s, 1H, S-CH-N), 7.54 (d, *J* = 8.1 Hz, 4H) and 7.84 (d, *J* = 8.2 Hz, 4H).

3.1.12. 2-(4-methoxyphenyl)-3-phenylthiazolidin-4-one (4l)

The **4l** was observed condensation of **1b**, **2c** and **3** as white solid; Mp:98-100°C (lit.[48] 97-99°C); Yield:92%; ^{1}H NMR (400 MHz, $CDCl_3$, δ ppm):3.83 (s, 3H, -OCH_3), 3.97 (d, 1H, *J* = 16 Hz), 4.12 (d, 1H, CH_2, *J* = 16 Hz), 6.10 (s, 1H, S-CH-N), 7.40-7.26 (m, 5H), 7.64 (d, *J* = 8.3 Hz, 2H) and 7.88 (d, *J* = 8.1 Hz, 2H).

3.2. Chemistry

To attain optimized reaction conditions procedure based on the reaction of aniline (1a), benzaldehyde (2a) (1 mmol) and mercaptoacetic acid (3) (1 mmol) as representative reaction (Scheme 1), we screened solvents, catalyst loading, temperatures and the details of this study are illustrated in Table 1.

Table 1:Screening study for the Synthesis of 4-Thiazolidinone (4a)[a]

Entry	Catalyst	Time (min)	Yield[b] (%)
1	-	30	42
2	*p*-TSA	30	71
3	Sulfamic acid	20	62
4	Sulfanilic acid	30	55
5	Boric acid	20	62
6	Citric acid	30	56
7	Phosphotungstic acid	30	51
8	Xanthan sulfuric acid	20	58
9	Silica sulfuric acid	20	69
10	CSA	30	71
11	[NMP][HSO_4]	8	95

*[a]Reaction conditions:aniline **1a** (1 mmol), benzaldehyde **2a** (1 mmol), mercaptoacetic acid **3** (1 mmol) and [NMP][HSO_4] (20 mol%) under microwave (MW = 240 W). [b]Isolated yields*

When the reaction was performed without using catalyst it gives lower yield of titled product after 30 min (Table 1, entry 1). We perform model reaction for the synthesis of compounds 4a using different catalysts such as Boric acid, Citric acid, CSA, Sulfanilic acid, Sulfamic acid, *p*-TSA, Phosphotungstic acid, Silica sulfuric acid, [NMP][HSO_4] and Xanthan sulfuric acid (Table 1, entries 2-11). Thus, [NMP][HSO_4] catalyst was screened for model reaction at room temperature to give 40% yield. When the reaction was performed using [NMP][HSO_4] under microwave it gives 95% yield of final product 4a (Table 1, entries 11). Therefore, above results suggest that [NMP][HSO_4] act as a green and excellent catalyst for the synthesis of 4-thiazolidinones and results are disclose in Table 1.

Further, we examine the efficiency of bronsted acidic [NMP][HSO_4] ionic liquid for the synthesis of 4-thiazolidinones derivatives. Using different loading of [NMP][HSO_4] catalyst on model reaction results change in the yield of 4-thiazolidinone **4a**. Catalyst concentration study suggest that 20 mol% of [NMP][HSO_4] catalyst is effective for synthesis of 4-thiazolidnone and results are disclose in (Table 2, entry 4).

Table 2:Effect of [NMP][HSO_4] Catalyst Loading[a]

Entry	Catalyst (mol %)	Time (min)	Yield[b] (%)
1	5	20	60
2	10	15	70
3	15	12	80
4	20	8	95
5	25	8	95

*[a]Reaction conditions:aniline **1a** (1 mmol), benzaldehyde **2a** (1 mmol), thioglycolic acid **3** (1 mmol) and [NMP][HSO_4] under microwave irradiation. [b]Isolated yield*

Next, we examine effect of microwave power on the model reactions. This examination results suggest that 240 W power levels effective for the synthesis of 4-thiazolidnone **4a** and results are disclosed (Table 3, entry 3).

Table 3:Effect of microwave power levels for the synthesis of 4a[a]

Entry	Power levels in Watt	Time[b] (min)	Yield[c]
1	140	12	68
2	210	10	85
3	240	8	95
4	280	8	95

*[a]Reaction conditions:aniline **1a** (1 mmol), benzaldehyde **2a** (1 mmol), thioglycolic acid **3** (1 mmol) in the presence of [NMP][HSO_4] 20 mol% under microwave irradiation. [b]Reaction progress monitored by TLC. [c]Isolated yield*

Enormously excellent protocol to greener and economic synthesis is recyclability and recovery of catalyst. Due to this, we screen the recyclability and

recovery of catalyst. This recyclability and recovery study results confirm that our NMP-based bronsted acidic ionic liquid is promising for the synthesis of 4-thiazolidnone without loosing its catalyst efficiency and results are disclosed in (Table 4, entry 2-5).

Table 4:Recovery and Reusability of bronsted acidic [NMP][HSO_4] catalyst for model reaction

Entry	Run	Time[a] (min)	Yield[b]
1	fresh	8	95
2	2	8	95
3	3	8	84
4	4	8	82
5	5	8	80

[a]*Reaction progress monitered by TLC.* [b]*Isolated yield*

We also examine the comparative study [NMP][HSO_4] catalyst with other reported protocol for the synthesis of 4-thiazolidinones. The study suggests that [NMP][HSO_4] is prominent catalyst for the efficient and facile synthesis of 4-thiazolidnones and results are disclosed (Table 5, entry 9).

The structural elucidation of synthesize **4f** compound was confirmed by ^{1}H and ^{13}C NMR analysis. In ^{1}H NMR spectra, the peak was observed at 2.28 δ ppm for the CH_3 group. The peak observed at doublet of a doublet 4.00-3.86 ppm due to the presence of -CH_2 protons in titled compound. The C-H proton of the 4-thiazolidinone ring was observed at singlet at δ 6.04 ppm. In ^{13}C NMR spectra, peak observed at 32.70, 64.30 and 170.1 ppm for the CH, CH_2 and C=O bond present in synthesized compounds.

Table 5: Comparative study of [NMP][HSO_4] with Reported Catalysts

Entry	Catalyst	Time (min)	Yield (%)	condition	Ref.
1	[bmim][PF_6]	9 h	80	80°C	[44]
2	[bmim][BF_4]	1.7 h	82	80°C	[44]
3	[MOEMIM]TFA	9 h	90	80°C	[44]
4	$HClO_4$-SiO_2	5 h	85	PhMe/100	[45]
5	TfOH-SiO_2	5 h	72	PhMe/100	[45]
6	H_2SO_4-SiO_2	5 h	55	PhMe/100	[45]
7	Silica gel, DCM	6 h	96	DCM/RT	[37]
8	$Bi(SCH_2COOH)_3$	2 h	90	70°C	[40]
9	[NMP][HSO_4]	8 min	95	240W	Present work

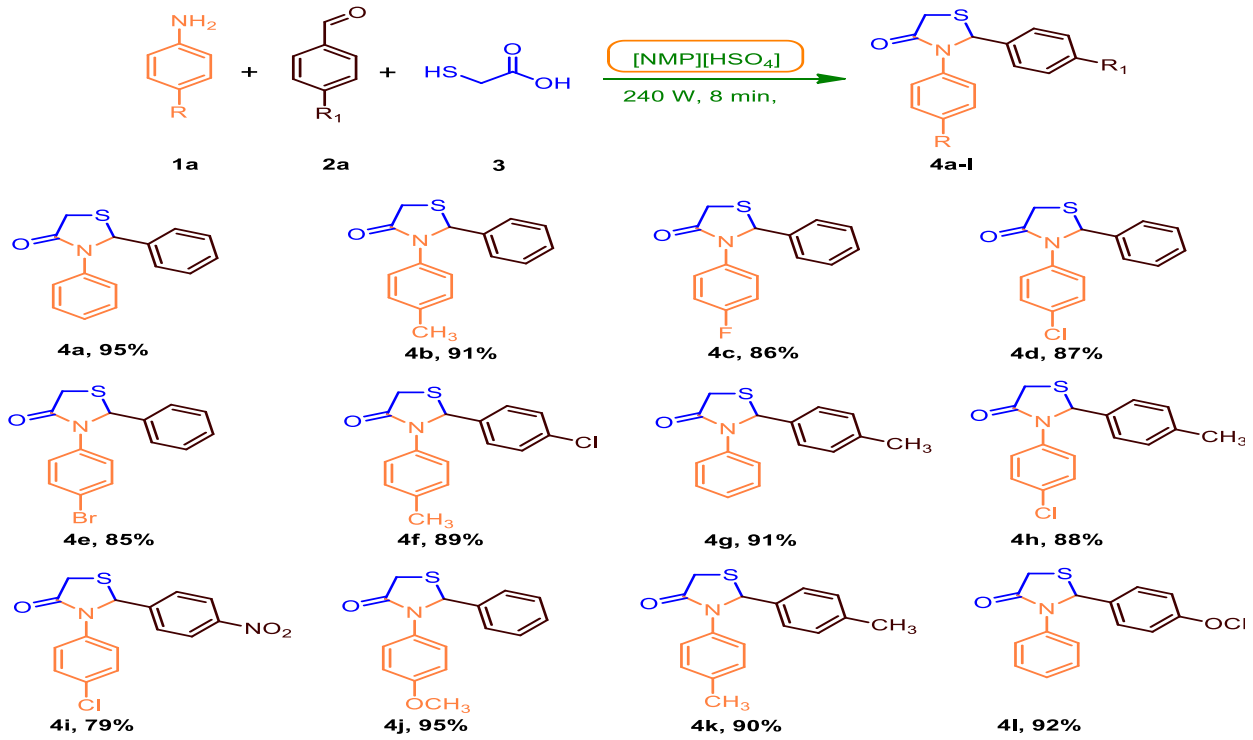

Scheme 3: Substrate scope for the synthesis of 4-Thiazolidinones using [NMP][HSO_4] catalyst

3.3. Plausible Reaction Mechanism

Reaction mechanism for the synthesis of 4-thiazolidinones employing [NMP][HSO_4] is catalyst. In first step, benzaldehyde is activated followed by nucleophilic substitution of aniline which results formation of **I** intermediate. In next step, removal of water molecules from intermediates **I** with the help of [NMP][HSO_4] gives imine product **II**. In the third step, intermediate **III** reacts with **3** and afforded cycloaddition product **IV**. Further, intramolecular cyclization occurs to form final product **4a** *via* removal of H_2O molecule and regeneration of catalyst. Detailed reaction mechanism is disclosed in Scheme 4.

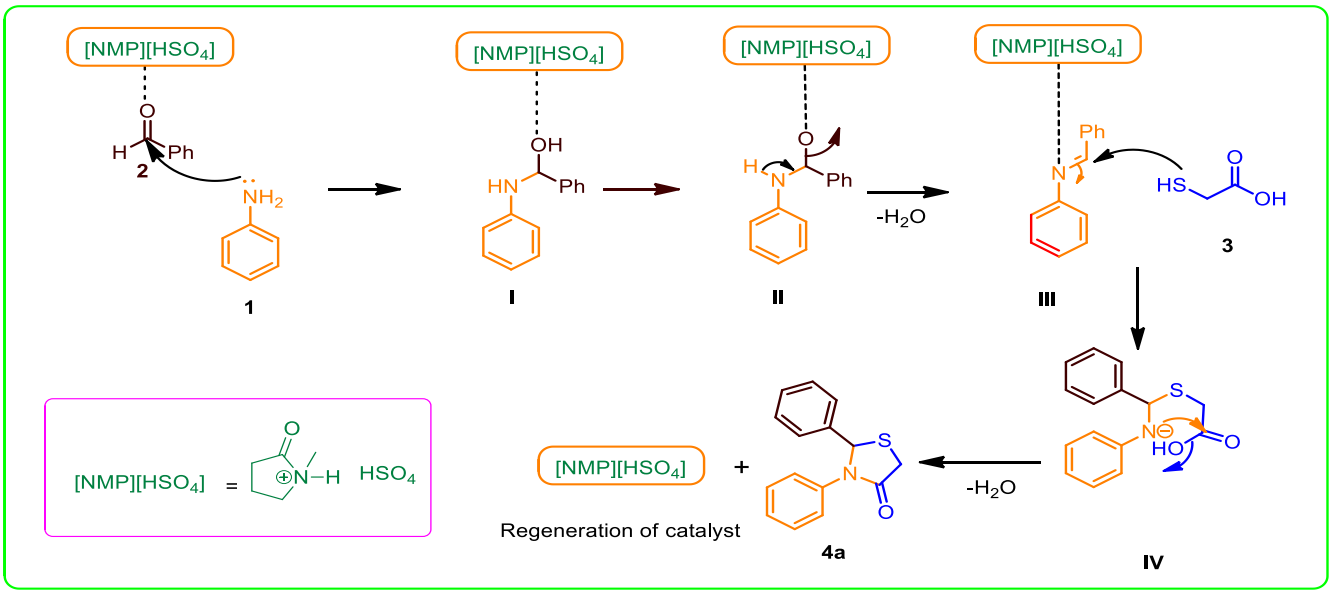

Scheme 4: Reaction mechanism for the synthesis of compound 4a

4. CONCLUSION

A highly efficient and environmentally benign protocol has been developed for the synthesis of 4-thiazolidinones using an recoverable and inexpensive [NMP][HSO_4] under microwave irradiation at 240 W for 8 min. This reaction protocol has many more advantages, such as uniqueness, high atom efficiency, clean reaction profiles, mild reaction condition, ecofriendliness, simple workup and without using any hazardous solvents.

Declaration of Competing Interest

The authors declare that they have no known competing financial interests or personal relationships that could have appeared to influence the work reported in this paper.

5. ACKNOWLEDGEMENTS

The author V.U.M. is very much grateful to Authority of Department of Chemistry, Dr Babasaheb Ambedkar Marathwada University Aurangabad for providing laboratory facility. The authors are also thankful to the Principal, Shri Chhatrapati Shivaji College, Omerga and Principal R.N.C. Arts, J.D.B. Commerce & N.S.C. Science College, Nashik-Road, Nashik for providing support and necessary all research facilities during my research.

6. REFERENCES

1. Greaves, TL, Drummond CJ, et al. *Chem. Rev.*, 2008; **108**:206-237.
2. Rub C, Konig B, et al. *Green Chem.*, 2012; **14**:2969-2982.
3. Martins MAP, Frizzo CP, Tier AZ, Moreira DN, Zanatta N, Bonacorso HG, et al. *Chem. Rev.*, 2014; **114**:1-70.
4. Brauch S, van Berkel SS, Westermann B. *Chem. Soc. Rev.*, 2013; **42**:4948-4962.
5. Amin KM, Rahman DE, Al-Eryani YA, et al. *Bioorg. Med. Chem.*, 2008; **16**:5377-5388.
6. Vigorita MG, Ottana R, Monforte F, Maccari R, Trovato A, Monforte MT, et al. *Bioorg. Med. Chem. Lett.*, 2001; **11**:2791-2794.
7. Pansare DN, Mulla NA, Pawar CD, Shende VR, Shinde DB, et al. *Bioorg. Med. Chem. Lett.*, 2014; **24**:3569-3573.

8. Barreca ML, Chimirri A, De Luca L, Monforte AM, Monforte P, Rao A, et al. *Bioorg. Med. Chem. Lett.,* 2001; **11**:1793-1796.
9. Joy MJ, Jacob N, Kutty NG, *Indian Drugs,* 2005; (**42**):47-51.
10. Ottana R, Maccari R, Giglio M, Del Corso A, Cappiello M, Mura U, et al. *Eur. J. Med. Chem.,* 2011; **46**:2797-2806.
11. Aridoss G, Amirthaganesan S, Kim MS, Kim JT, Jeong YT, et al. *Eur. J. Med. Chem.,* 2009; **44**: 4199-4210.
12. Carlson EE, May JF, Kiessling LL, et al. *Chem. Biol.,* 2006; (**13**):825-837.
13. Taranalli AD, Thimmaiah NV, Srinivas S, Saravanan E, Bhat AR, et al. *Asian J. Pharm. Clin. Res.,* 2009; **2**:79-83.
14. Mazzoni O, di Bosco AM, Grieco P, Novellino E, Bertamino A, Borrelli F, et al. *Chem. Biol. Drug Des.,* 2006; **67**:432-436.
15. Panico AM, Vicini P, Geronikaki A, Incerti M, Cardile V, Crasci L, et al. *Bioorg. Chem.,* 2011; **39**:48-52.
16. Bhandari SV, Bothara KG, Patil AA, Chitre TS, Sarkate AP, Gore ST, et al. *Bioorg. Med. Chem.,* 2009; **17**:390-400.
17. Barreca ML, Balzarini J, Chimirri A, Clercq ED, Luca LD, Holtje HD, et al. *J. Med. Chem.,* 2002; **45**:5410-5413.
18. Wrobel J, Jetter J, Kao W, Rogers J, Di L, Chi J, et al. *Bioorg. Med. Chem.,* 2006; **14**:5729-8741.
19. Kumar KSS, Hanumappa A, Vetrivel M, Hegde M, Girish YR, Byregowda TR, et al. *Bioorg. Med. Chem. Lett.,* 2015; **25**:3616-3620.
20. Degterev A, Lugovskoy A, Cardone M, Mulley B, Wagner G, Mitchison T, et al. *Nat. Cell Biol.,* 2001; **3**:173-182.
21. Cutshall NS, O'Day C, Prezhdo M, et al. *Bioorg. Med. Chem. Lett.,* 2005; **15**:3374-3379.
22. Chen S, Chen L, Le NT, Zhao C, Sidduri A, Lou JP, et al. *Bioorg. Med. Chem. Lett.,* 2007; **17**:2134.
23. Carter PH, Scherle PA, Muckelbauer JA, Voss ME, Liu RQ, Thompson LA, et al. *Proc. Natl. Acad. Sci. USA,* 2001; **98**:11879-11884.
24. Dayam R, Aiello F, Deng J, Wu Y, Garofalo A, Chen X, et al. *J. Med. Chem.,* 2006; **49**:4526-4534.
25. Ottana R, Carotti S, Maccari R, Landini I, Chiricosta G, Caciagli B, et al. *Bioorg. Med. Chem. Lett.,* 2005; **15**:3930-3933.
26. Sala M, Chimento A, Saturnino C, Gomez-Monterrey IM, Musella S, Bertamino A, Campiglia et al. *Bioorg. Med. Chem. Lett.,* 2013; **23**:4990-4995.
27. Thakare MP, Kumar P, Kumar N, Pandey SK, et al. *Tetrahedron Lett.,* 2014; **55:**2463-2466.
28. Ghomi JS, Navvab M, Alavi HS, et al. *Ultrason Sonochem.,* 2015; **31**:102-106.
29. Wei L, Cheng W, Xia Y, et al. *Chin. J. Chem.,* 2018; **36**:293-298.
30. Zhu X, Song M, Xu Y, et al. *ACS Sustain. Chem. Eng.,* 2017; **9**:8192-8198.
31. Foroughifar N, Ebrahimi S, et al. *Chin Chem.*, 2013; **24**:389-391.
32. Sharma R, Veera G, Devi B, Reddy KS, Reddy MV, Kondapi AK, et al. *Hetero Commun.*, 2015; **21**:187.
33. Prasad D, Preetam A, Nath M, et al. *RSC Adv.,* 2012; **2**:3133-3140.
34. Azgomi N, Mokhtary M, et al. *J Mol Cat Chem.*, 2015; **398**:58-64.
35. Liaras K, Fesatidou M, Geronikaki A, et al. *Molecules*, 2018; **23:**685.
36. Apotrosoaei M, Vasincu IM, Dragan M, Buron F, Routier S, Profire L, et al. *Molecules*, 2014; **19**:13824-13847.
37. Gautam D, Gautam P, Chaudhary RP, et al. *Chin Chem Lett.*, 2012; **23**:1221-1224.
38. Carta A, Loriga M, Zanetti S, Sechi LA, et al. *Farmaco.,* 2003; **58**:1251-1255.
39. Ghomi JS, Navvab M, Alavi HS, et al. *J Sulfur Chem.*, 2016; **37**:601.
40. Sadou N, Bouzroura SA, Nechak R, Kolli BN, Morizur V, Martini SP, et al. *Polycycl Aromat Comp.,* 2016; **36**: 1-11.
41. Shaterian HR, Aghakhanizadeh M, et al. *Res Chem Intermed.,* 2013; **39**:3877-3885.
42. Wei L, Cheng W, Xia Y, et al. *Chin. J. Chem.,* 2018; **36**:293-298.
43. Cole AC, Jensen JL, Ntai I, Tran KLT, Weave KJ, et al. *J. Am. Chem. Soc.,* 2002; **124**:5962-5963.
44. Kumar D, Sonawane M, Pujala B, Jain VK, Bhagat S, Chakraborti AK, et al. *Green Chem.,* 2013; **15**:2872-2884.
45. Yadav AK, Kumar M, Yadav T, Jain R, et al. *Tetrahedron Lett.,* 2009; **50:**5031-5034.
46. Carpentier J, Lamonier JF, Siffert S, Zhilinskaya EA, Aboukais A, et al. *Appl. Catal. A Gen.*, 2002; **234**:91-101.
47. Yu JJ, Jiang ZL, Zhu ZP. Hao ZP, Xu A, et al. *J. Phys. Chem. B*, 2006; **110**:4291-4300.
48. Alejandre A, Medina F, Salagre P, Correig X, Sueiras JE, et al. *Chem. Mater.*, 1999; **11**:939-948.